

# Open Research Online

---

The Open University's repository of research publications and other research outputs

## Transplantation of Pancreatic Islet in an Immunoisolation Device

### Thesis

How to cite:

Cornolti, Roberta (2009). Transplantation of Pancreatic Islet in an Immunoisolation Device. PhD thesis The Open University.

For guidance on citations see [FAQs](#).

© 2009 The Author

Version: Version of Record

---

Copyright and Moral Rights for the articles on this site are retained by the individual authors and/or other copyright owners. For more information on Open Research Online's [data policy](#) on reuse of materials please consult the policies page.

---

[oro.open.ac.uk](http://oro.open.ac.uk)

UNRESTRICTED

The Open University, UK

— Advanced School of Pharmacology —  
Dean, Enrico Garattini M D

Mario Negri Institute for  
Pharmacological Research

17/03/2009

# TRANSPLANTATION OF PANCREATIC ISLET IN AN IMMUNOISOLATION DEVICE

Thesis submitted by

**Cornolti Roberta, Dr. Eng.**

for the degree of

**Doctor of Philosophy**

Discipline of Life and Biomolecular Sciences

Open University Research School, London

“Mario Negri” Institute for Pharmacological Research

Submission date: 29 September 2008

Date of award: 17 March 2009

ProQuest Number: 13837700

All rights reserved

INFORMATION TO ALL USERS

The quality of this reproduction is dependent upon the quality of the copy submitted.

In the unlikely event that the author did not send a complete manuscript and there are missing pages, these will be noted. Also, if material had to be removed, a note will indicate the deletion.



ProQuest 13837700

Published by ProQuest LLC (2019). Copyright of the Dissertation is held by the Author.

All rights reserved.

This work is protected against unauthorized copying under Title 17, United States Code  
Microform Edition © ProQuest LLC.

ProQuest LLC.  
789 East Eisenhower Parkway  
P.O. Box 1346  
Ann Arbor, MI 48106 – 1346

**Transplantation of pancreatic islet in an immunoisolation device**

**Abstract**

Background: Type-1 diabetes is caused by autoimmune destruction of insulin-producing  $\beta$ -cells in the pancreas. Today, transplantation of whole pancreas or islets is the only treatment that can restore endogenous insulin production. Within the past 20 years, pancreatic islet transplantation has become a clinical reality and an option in diabetes treatment. However, large use of this therapy is limited by shortage in organ donations and use of immunosuppressive drugs. Immunoisolation potentially allows elimination of immunosuppressive drugs and use of xenogenic tissue solving the problem of a shortage in organ donation.

Aims: The present work was designed to ameliorate isolation of islets from different species and encapsulation of islets in immunoisolation devices (hollow fibres and microcapsules). Moreover, a mathematical model for immunoisolation membrane selection was developed.

Results and conclusions: The application of the automated method allows significant increase in the number of islets obtained. These islets were then used for *in vitro* or *in vivo* studies of immunoisolation devices, tested in different protocols. Experimental results indicate that islet transplantation using alginate gel microcapsule in the peritoneal cavity successfully control glycaemia in diabetic animals. However, it is not possible to translate in human application for the implantation site. An alternative strategy was developed based on membrane device to be used in the subcutaneous space. Despite permeability properties have been proved to be adequate, the *in vivo* functional response of transplanted



islet in hollow fibre device was only temporary, probably for development of fibrotic tissue around the device.

*Future work:* The use of theoretical model allows evaluation and selection of new membrane materials for islet immunoisolation. Efficacy of new devices would be determined by performing allo- or xeno- transplantations into diabetic recipients, exploring new sites of implantation that minimize surgical procedures and reduce implant failure.

## Acknowledgement

This thesis was performed at the Department of Bioengineering, Mario Negri Institute, Bergamo, Italy.

I would like to express my sincere gratitude to:

Dr. Eng. Andrea Remuzzi, my director of the study and supervisor, for introducing me to bioengineer research and for sharing with me his great interest in islets, transplantation and immunoisolation. His never ending support and enthusiasm for research kept me on track and are vital for the work presented in this thesis.

Prof. Catherine Sarraf, my external supervisor, for sharing her great knowledge in science and immunology, for good criticism of my work, and many corrections.

Ph.D Chiara Arrigoni, Dr. Marina Figliuzzi, Dr. Lorena Micali, Dr. Matteo Trudu, Irene Cattaneo and Dr. Barbara Bonandrini for their kindness and skilful assistance and for creating a pleasant and encouraging atmosphere both inside and outside the Institute.

It would not have been possible for me to complete this work without the help of my husband, Filippo and son, Diego, who have been a great emotional support for me. Finally, I would like to express my deep gratitude to my parents for continuous support and timely encouragement throughout the course of this thesis.

# Table of Contents

Abstract	I
Acknowledgements	III
Table of contents	IV
List of Figures	X
List of Tables	XIV
Chapter 1. Introduction	2
1.1 Pathophysiology of diabetes mellitus	4
1.1.1 <i>Anatomy and function of the pancreas</i>	4
1.1.2 <i>Insulin</i>	7
1.1.3 <i>Diabetes Mellitus</i>	9
1.1.4 <i>Diabetes complications</i>	10
1.2 Conventional treatment for type-1 diabetes	19
1.2.1 <i>Conventional therapy</i>	19
1.2.2 <i>Intensive therapy</i>	20
1.2.3 <i>Insulin pump therapy</i>	21
1.3 Alternative treatment for type-1 diabetes	24
1.3.1 <i>Pancreas transplantation</i>	24
1.3.2 <i>Stem cell therapy</i>	27
1.3.3 <i>Islet transplantation</i>	33
1.4 Immunoisolation	38
Overview of the thesis and aims	41
References	43

---

Chapter 2.	Set-up of methods for islet isolation	49
2.1	Rat islet isolation	51
2.1.1	<i>Manual procedure – materials and methods</i>	51
2.1.2	<i>Automatic procedure - materials and methods</i>	54
2.1.3	<i>Islet viability</i>	58
2.1.4	<i>Results</i>	59
2.2	Bovine islet isolation	61
2.2.1	<i>Manual procedure – materials and methods</i>	62
2.2.2	<i>Automatic procedure - materials and methods</i>	65
2.2.3	<i>Results</i>	68
2.3	Human islet isolation	69
2.3.1	<i>Manual procedure – materials and methods</i>	70
2.3.2	<i>Automatic procedure - materials and methods</i>	72
2.3.3	<i>Results</i>	75
	References	77
Chapter 3.	<i>In vivo</i> functionality of the islets: syngenic, allogenic and xenogenic free islet transplantation	80
3.1	Materials and methods	81
3.2	Results	84
3.2.1	<i>Syngenic free islet transplantation</i>	84
3.2.2	<i>Allogenic free islet transplantation</i>	87
3.2.3	<i>Xenogenic free islet transplantation</i>	89
	Conclusion	90
	References	91

---

Chapter 4.	<i>In vivo</i> evaluation of encapsulation: syngenic, allogenic and xenogenic immunoisolated islet transplantation	93
4.1	Microcapsules	100
4.1.1	<i>Materials and methods</i>	100
4.1.2	<i>Results</i>	102
4.2	Hollow fibers devices	107
4.2.1	<i>Materials and methods</i>	107
4.2.2	<i>Results</i>	112
	References	120
Chapter 5.	<i>In vitro</i> evaluation of encapsulation: oxygen consumption rate (OCR) measurements	125
5.1	Experimental set-up for OCR determination	128
5.2	OCR measurements and results	131
	Conclusion	135
	References	138
Chapter 6.	<i>In vivo</i> evaluation of glycaemic control in transplanted islets using CGMS	141
6.1	Intraperitoneal glucose tolerance test	143
6.1.1	<i>Materials and methods</i>	143
6.1.2	<i>Results</i>	146
6.2	Pharmacokinetic model and fitting of experimental data	148
6.2.1	<i>Materials and methods</i>	149
6.2.2	<i>Results</i>	150

---

	Conclusion	153
	References	154
Chapter 7.	Design of an immunoisolation device for islet transplantation	158
7.1	Determination of solute diffusivity	159
7.1.1	<i>Solute diffusivity in porous membrane</i>	159
7.1.2	<i>Solute diffusivity in alginate gel</i>	162
7.2	Mathematical model of an immunoisolation device for islet transplantation	163
7.2.1	<i>Simulation of glucose transport</i>	170
7.2.2	<i>Simulation of insulin transport</i>	172
7.2.3	<i>Simulation of immunoglobulin (IgG) transport</i>	175
	Discussion and conclusion	179
	References	187
Chapter 8.	Conclusions	189
8.1	Goals achieved	191
8.1.1	<i>Islet isolation</i>	191
8.1.2	<i>Islet transplantation by immunoisolation</i>	192
8.2	Future perspective	195
	References	196
Appendix	A. MatLab codes for simulation of glucose, insulin and IgG	197
	B. Standard Operating Procedure for Human Islet Isolation	203
	C. Project of Islet Laboratory	231

## List of Figures

- 1.1 Numbers of people with diabetes (in millions) for 2000 and 2010
- 1.2 Human pancreas
- 1.3 Different cells in a pancreatic islet
- 1.4 Processing of pre-pro-insulin to active insulin
- 1.5 Abnormal growth of blood vessels in retinopathy
- 1.6 Normal and diabetic kidney
- 1.7 Cumulative incidence of a sustained change in nephropathy and retinopathy in patients with IDDM
- 1.8 Insulin pump
- 1.9 Different approaches for generating insulin-producing cells
- 1.10 Improvements in clinical outcome with high rates of insulin independence with patients treated in the Edmonton Protocol
- 1.11 Increase in clinical islet transplant activity
- 1.12 Future milestones in clinical islet transplantation
  
- 2.1 Rat pancreas perfusion
- 2.2 Schematic representation of the automated circuit for pancreas digestion
- 2.3 Modified digestion chamber of stainless steel 316
- 2.4 Islet number *per* rat pancreas obtained utilizing manual or automatic procedure
- 2.5 Optical imaging of islets isolated using manual or automatic procedure
- 2.6 Propidium iodide (red) – acridine orange (green) staining of islets isolated by manual or automatic procedures

- 
- 2.7 Purification step carried out by density-gradient separation of islets
  - 2.8 Islet equivalent *per* gram of pancreas obtained utilizing manual or automatic procedure
  - 2.9 Scheme and photograph of the air-filtered room for human islet isolation
  - 2.10 Human pancreas perfusion with peristaltic pump
  - 2.11 Human islets before and after purification
  - 2.12 Islets *per* gram of human pancreas obtained utilizing manual or automatic procedures
  
  - 3.1 The kidney capsule incised with the tip of a needle and a small PE50 catheter inserted. Islets injected with a Hamilton syringe under the kidney capsule
  - 3.2 A- Average non-fasting blood glucose level after islet implantation in 14 rats  
B- Average non-fasting blood glucose level after islet implantation in rat with nephrectomy
  - 3.3 A and B- Islet beneath the kidney capsule positive for insulin (immunofluorescence, insulin in red and nuclei in blue) also 3 or 4 months after transplantation (A low magnification and B high magnification). C - Islet beneath the kidney capsule. Histology of the preserved structure (haematoxylin and eosin staining)
  - 3.4 Averages of non-fasting blood glucose levels after allogeneic islet implantation in rats treated with cyclosporine (blue line) or without (red line)
  - 3.5 Histology of cellular infiltrations beneath the kidney capsule at low and high magnification
  - 3.6 Averages, non-fasting blood glucose levels after xenogenic islet implantation in rats treated with a high dose of cyclosporine



- 4.1 Different kinds of immunoisolation devices.
- 4.2 The TheraCyte® device
- 4.3 Biocompatible implantable steel and PTFE device.
- 4.4 Foreign body reaction is normal when an implanted synthetic material is implanted into a living, vascular tissue
- 4.5 Droplet generator and light microscopy of microcapsules
- 4.6 Average of non-fasting blood glucose levels after microencapsulated syngeneic islet implantation in diabetic rats
- 4.7 Light microscopy (hematoxylin-eosin staining) of islets contained in microcapsules recovered from 200 day old rat after syngeneic implantation
- 4.8 Average of non-fasting blood glucose levels after microencapsulated allogeneic islet implantation in diabetic rats
- 4.9 Light microscopy (hematoxylin-eosin staining) of islets contained in microcapsules 100 days after allogeneic transplantation
- 4.10 Average of non-fasting blood glucose levels after microencapsulated xenogeneic islet implantation in diabetic rats with or without cyclosporine
- 4.11 Light microscopy (hematoxylin-eosin staining) of xenogenic islets contained in microcapsules with cyclosporine or without
- 4.12 Schematic representation of the device: a parallel array of hollow fibres held together with a weaving
- 4.13 Representative SEMs of membrane thickness of Fresenius , Spectrum and Amicon hollow fibres
- 4.14 Non-fasting blood glucose level after islet implantation in Fresenius, Spectrum and Amicon hollow fibre devices beneath the skin in diabetic rats

- 4.15 Light microscopy (hematoxylin-eosin staining) of islets contained in Fresenius, Spectrum and Amicon devices recovered from rats 2 weeks after implantation. Representative morphology of an islet encapsulated in a hollow fibre device 2 weeks after implantation, showing central necrosis
- 4.16 Light microscopy (hematoxylin-eosin staining) of fibrotic overgrowth around Fresenius, Spectrum and Amicon device recovered from MWF rats 2 weeks after implantation
- 4.17 Histological evaluation revealed the presence of a large number of macrophages, notably near membrane of devices containing islets (A, ED1+, in red) but only few lymphocytes (B, CD8+, in red) in the fibrotic capsule.
- 4.18 Non-fasting blood glucose level (black) and body weight (red) after islet implantation in Fresenius hollow fibre devices beneath the skin in diabetic rats
- 4.19 Light microscopy (haematoxylin-eosin staining) of fibrotic overgrowth and of islets contained in Fresenius devices recovered from rats 2 weeks after implantation. Representative morphology of an islet encapsulated in a hollow fibre device 2 weeks after implantation, showing central necrosis
- 4.20 Histological evaluation revealed the presence of a large number of macrophages ED1+ on membranes of devices contained islets or in empty devices.
- 5.1 Global view of the system used for OCR measurements
- 5.2 Thermostated chamber
- 5.3 Schematic of Clark's electrode. Pt cathode, Ag anode, insulating material and the teflon membrane
- 5.4 OCR calculated by linear regression
- 5.5 Representative experiment of OCR vs. time

- 
- 5.6 Islets encapsulated in microcapsules or in hollow fibres
  - 5.7 OCR of free islets measured the day of islet isolation (0), 24 h after the isolation process (1) and 48 h after (2).
  - 5.8 OCR in free islets measured the day after the isolation process exposed to low or high glucose concentration \* $p < 0.01$  low glucose vs. high glucose
  - 5.9 OCR in free islets, islets in microcapsules and islets in hollow fibres measured 24 h after the isolation process or 48 h after
  
  - 6.1 Medtronic continuous subcutaneous glucose monitoring system
  - 6.2 Photograph of the system inserted on the back of the rats with all the components specified
  - 6.3 Two compartments model with first order absorption
  
  - 7.1 Solute diffusivity of molecules of radius ( $a$ ) in pores of a membrane with radius
  - 7.2 SEM of the nanoporous polycarbonate membrane
  - 7.3 One-dimension model of the device
  - 7.4  $x$ - $t$  region covered by a grid of rectangles of side  $dx$ ,  $dt$
  - 7.5 Demonstration that  $r > 0.5$  is a critical point
  - 7.6 Glucose concentrations in  $x = x_{step}$
  - 7.7 Family of curves  $C(x,t)$  in function of  $x$  at different times
  - 7.8 Family of curves  $C(x,t)$  in function of  $x$  at different times
  - 7.9 Quantity of mass insulin mass in function of time
  - 7.10 Family of curves  $C(x,t)$  in function of  $x$  at different times
  - 7.11 IgG concentrations in  $x = L_{mstep} + 1$

- 7.12 Time at which 90% of glucose reach the centre of device in function of pore density
- 7.13 Time at which quantity of mass reach the maximum value (in minutes) in function of pore density
- 7.14 Time at which the value of IgG concentration just after the membrane (in  $x=L_{mstep}+1$ ) reached 10% in function of pore density

## List of Tables

- 4.1 Advantages and limitations of different immunoisolation approaches
  
- 5.1 OCR,  $\Delta$ OCR and % increase in preparation of free islets exposed to low and high glucose concentration
  
- 6.1 Values of non-fasting blood glucose concentration for the three experimental groups
- 6.2 Values of AUC for the three experimental groups. \* $p < 0.05$  vs. kidney capsule and microcapsules
- 6.3 Values of  $k_a$ ,  $k_{pl}$  and  $k_{tot}$  for the three experimental groups
  
- 7.1 Glucose diffusivity in different cases ( $\text{mm}^2/\text{sec}$ )
- 7.2 Time at which 90% of glucose reach the centre of device (in seconds)
- 7.3 Insulin diffusivity in different cases ( $\text{mm}^2/\text{h}$ )
- 7.4 Time at which quantity of mass reach the maximum value (in minutes)
- 7.5 IgG diffusivity in different cases ( $\text{mm}^2/\text{h}$ )
- 7.6 Time at which the value of IgG concentration just after the membrane (in  $x = L_{mstep} + 1$ ) reached 10% (in minutes)

## Chapter 1

### Introduction

#### 1.1 Pathophysiology of diabetes mellitus

*1.1.1 Anatomy and function of the pancreas*

*1.1.2 Insulin*

*1.1.3 Diabetes Mellitus*

*1.1.4 Diabetes complications*

#### 1.2 Conventional treatment for type-1 diabetes

*1.2.1 Conventional therapy*

*1.2.2 Intensive therapy*

*1.2.3 Insulin pump therapy*

#### 1.3 Alternative treatment for type-1 diabetes

*1.3.1 Pancreas transplantation*

*1.3.2 Stem cell therapy*

*1.3.3 Islet transplantation*

#### 1.4 Immunoisolation devices

Overview of the thesis and aims

References

## Introduction

Diabetes mellitus (DM), long considered a disease of minor significance to world health, is now taking its place as one of the main risks to human health in the 21st century. The past two decades have seen an explosive increase in the number of people diagnosed with diabetes. Significant changes in the human environment and in human behaviour and lifestyle, have accompanied globalization and these have resulted in escalating rates of both obesity and diabetes. There are two main forms of diabetes. Type 1 diabetes is due primarily to autoimmune-mediated destruction of  $\beta$ -cells of pancreatic islets, resulting in absolute insulin deficiency. People with type 1 diabetes must take exogenous insulin for survival to prevent development of ketoacidosis. Its frequency is low relative to type 2 diabetes, which accounts for over 90% of cases globally. Type 2 diabetes is characterized by insulin resistance and/or abnormal insulin secretion, either of which may predominate. People with type 2 diabetes are not dependent on exogenous insulin, but may require it for control of blood glucose levels if this is not achieved with diet alone or with oral hypoglycaemic agents.

The global figure of people with diabetes is set to rise from the current estimate of 150 million to 220 million in 2010, and 300 million in 2025, as shown in Figure 1.1 modified from (1). Most cases will be of type 2 diabetes, which is strongly associated with a sedentary lifestyle and obesity. This trend of increasing prevalence of diabetes and obesity has already imposed a huge burden on health-care systems and this will continue to increase in the future.

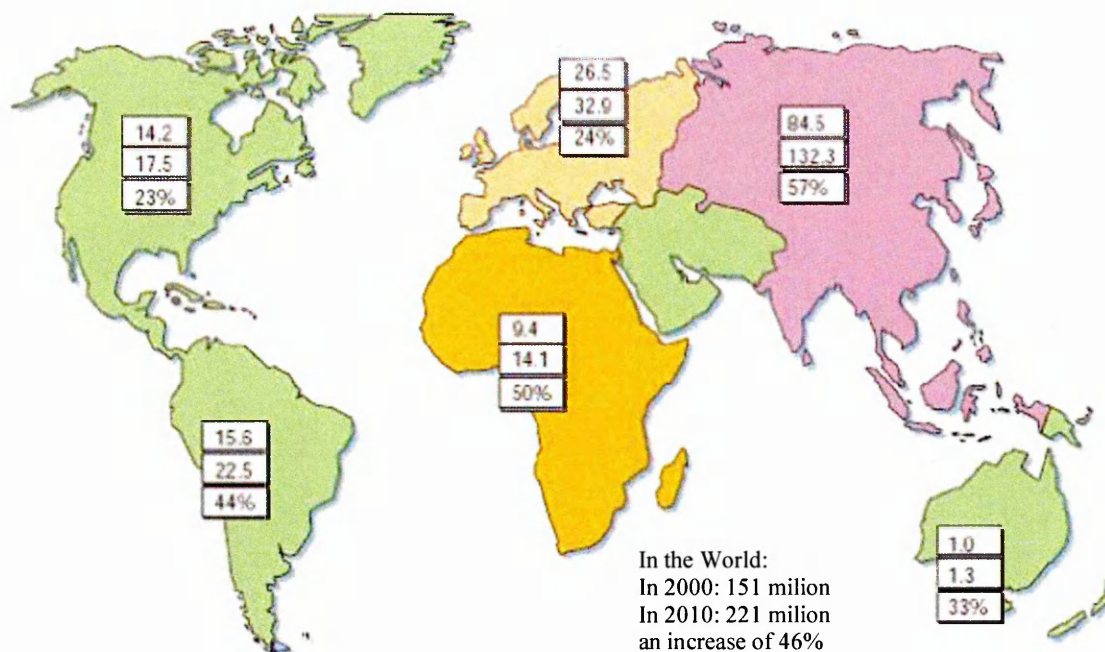


Figure 1.1 Numbers of people with diabetes (in millions) for 2000 and 2010 (top and middle values, respectively), and the percentage of the increase (1).



## **1.1 Pathophysiology of diabetes mellitus**

Diabetes mellitus is a disease that causes abnormally high levels of glucose in the blood due either to insulin deficiency or to resistance of the body's cells to action of insulin. Glucose level in blood is usually between 60-120 mg/dl. When we eat, glucose gets absorbed into the bloodstream and circulates to each of the cells of the body to provide them with energy. The cell membrane separates a cell from the external medium. Hence blood glucose cannot just enter into the cell body to provide energy. The main function of insulin, a protein produced by the pancreas, is to allow glucose to cross the lipid bilayer and get into the cell.

### ***1.1.1 Anatomy and function of the pancreas***

The pancreas is located deep in the abdominal cavity behind the stomach. It is formed of a large dense portion, the head, that is in contact with the duodenum, a middle portion, the body and a final portion the tail (Figure 1.2) (2).

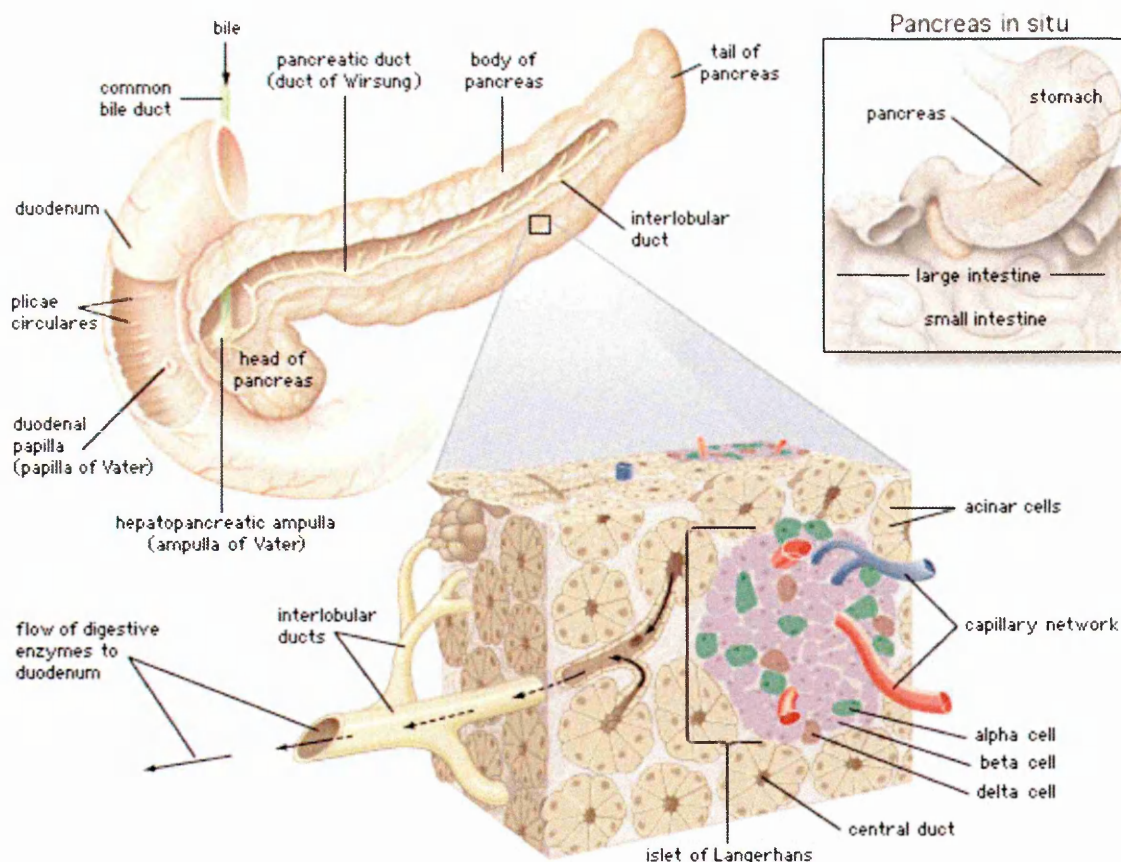


Figure 1.2 Human pancreas. The pancreas is attached to the duodenum, the upper portion of the small intestine. A large main duct, the duct of Wirsung, collects pancreatic juice and empties into the duodenum. Enzymes active in digestion of carbohydrates, fat, and protein continuously flow from the pancreas through the duct (2).

The human pancreas is composed of two different functional cell populations. The large portion of pancreatic tissue approximately more than 95%, is exocrine tissue, which produces a range of powerful digestive enzymes and pro-enzymes for fats, starches and proteins. These digestive enzymes flow in pancreatic ducts into the small intestine where they process ingested food. The enzymes split foodstuffs into simpler substances, which are absorbed into the bloodstream and transported throughout the body for immediate use by tissues or for later use. The smaller portion is endocrine tissue, which is composed of

islets of Langerhans; the name is that of a student, who in 1869 discovered them.

Pancreatic islets contain different kind of cells (Figure 1.3 (3)):

- $\alpha$  cells produce and release glucagon, which raises the blood glucose level, exactly the opposite function of insulin. There is a proper balance in secretion of insulin and glucagon, which is very important in maintaining the appropriate blood glucose level
- $\beta$  cells produce, store and release insulin for the blood stream as *per* demand. The product of these cells determines blood glucose levels within seconds and responds to how much insulin needs to be secreted
- $\delta$  cells produce somatostatin that probably mediates on behalf of insulin by blocking the action of glucagon
- $\varphi$  cells produce further minor pancreatic polypeptide hormones

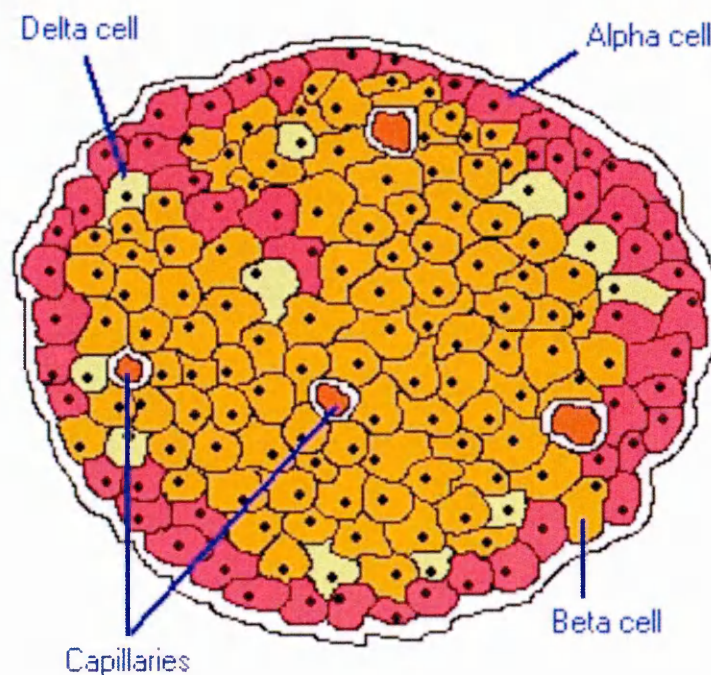


Figure 1.3 Different cells in a pancreatic islet: schematic figure showing exocrine and endocrine parts of the pancreas, specifying the cells contained in an islet (3).

A human pancreas has more than one million pancreatic islets and each islet contains 1,000 to 2,000  $\beta$  cells that can communicate with one another through gap junctions that allow transmission of chemical and electrical signals.

$\beta$  cells occupy the central portion of the islet and are surrounded by a band of  $\alpha$  and  $\delta$  cells. Aside from insulin, glucagon and somatostatin, a number of other minor hormones have been identified as products of pancreatic islet cells.

Islets are richly vascularized, allowing their secreted hormones ready access to the blood circulation. Although islets comprise only 1-2% of the mass of the pancreas, they receive about 10 to 15% of pancreatic blood flow. Additionally, they are innervated by parasympathetic and sympathetic neurons, and nervous signals clearly modulate secretion of insulin and glucagon.

### ***1.1.2 Insulin***

Insulin is a rather small protein, with a molecular weight of 5,734 Da. It is composed of two peptide chains referred to as the A chain and B chain. A and B chains are linked together by two disulphide bonds. In most species, the A chain consists of 21 amino acids and the B chain of 30 amino acids. The amino acid sequence is highly conserved among vertebrates and insulin from one mammal almost certainly is biologically active in another.

Insulin is synthesized in significant quantities only in  $\beta$  cells in the pancreas. Insulin mRNA is translated as a single chain precursor called preproinsulin, and removal of its signal peptide during insertion into the endoplasmic reticulum generates proinsulin. Proinsulin consists of three domains: an amino-terminal B chain, a carboxy-terminal A chain and a connecting peptide in the middle known as C peptide. Within the endoplasmic

reticulum, proinsulin is exposed to several specific endopeptidases that excise C peptide, thereby generating the mature form of insulin (Figure 1.4 (4)). Insulin and free C peptide are packaged in the Golgi apparatus into secretory granules that accumulate in the cytoplasm. When the  $\beta$  cell is appropriately stimulated, insulin is secreted from the cell by exocytosis and diffuses into islet capillary blood. C peptide is also secreted into blood, but has no known biological activity.

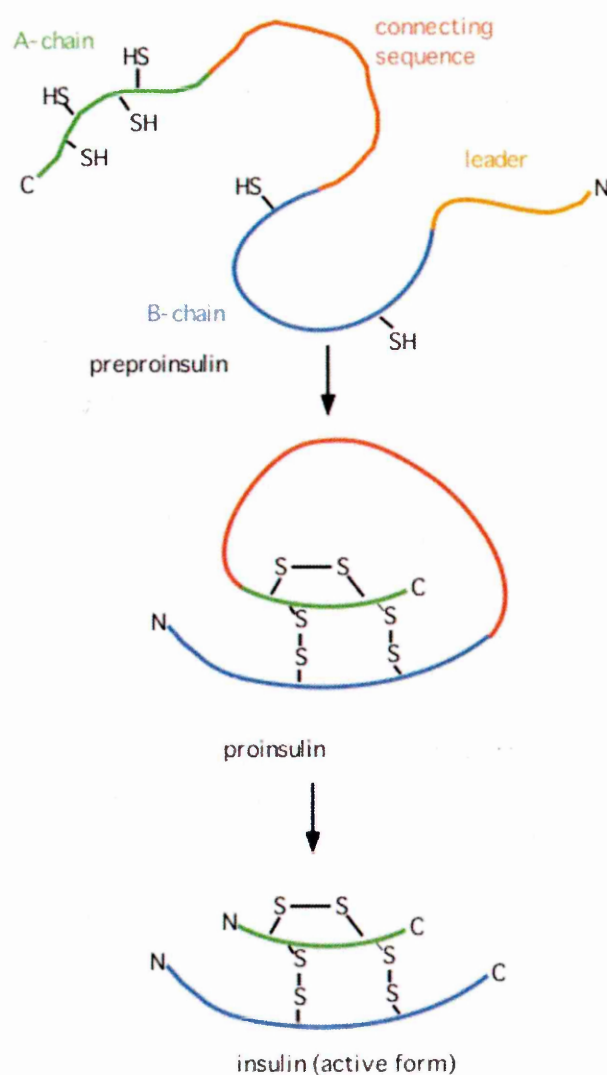


Figure 1.4 Processing of pre/pro/insulin to active insulin: pre/pro/insulin is synthesized as a random coil on membrane-associated ribosomes; after membrane-transport the leader sequence (yellow) is cleaved off by a protease and the resulting pro-insulin folds into a stable conformation. The connecting sequence (red) is cleaved off to form the mature and active insulin molecule. (4)

Insulin is secreted primarily in response to elevated blood glucose concentrations. Some neural stimuli (e.g. sight and taste of food) and increased blood concentration of other fuel molecules, including amino acids and fatty acids, also promote insulin secretion. Most cells of the body have insulin receptors that bind insulin from the circulation. When a cell has insulin attached to it, the cell activates other receptors designed to absorb glucose from the blood stream into the cell. Cells use glucose as a source of energy for movement, growth, repair, and all other functions.

Despite long intervals between meals or the occasional consumption of meals with a substantial carbohydrate load, human blood glucose levels normally remain within a remarkably narrow range. In most people this varies from around 70 mg/dl to perhaps 110 mg/dl (3.9 to 6.1 mmol/l), except shortly after eating when blood glucose level rises temporarily.

Insulin is required for all animal life. In humans, insulin deprivation due to removal or destruction of the pancreas leads to death in days or at most, weeks. Failure to make insulin or to respond to it, is clinically called diabetes mellitus.

### ***1.1.3 Diabetes mellitus***

Diabetes mellitus, the most important metabolic disease of man, is a state of insulin deficiency. The World Health Organization recognizes three main forms of diabetes mellitus:

- Type 1 or insulin-dependent diabetes mellitus is the result of frank deficiency of insulin. The onset of this disease typically is in childhood. It is due to destruction of pancreatic  $\beta$  cells, by T-cell mediated autoimmune attack. Many of the acute effects of this disease can be controlled by insulin replacement therapy. Maintaining tight control of blood glucose concentration by monitoring, treatment with insulin and dietary management minimizes

long-term adverse effects of this disorder on blood vessels, nerves and other organ systems, allowing healthy life.

- Type 2 diabetes mellitus is due to insulin resistance or reduced insulin sensitivity, combined with reduced insulin secretion. Defective responsiveness of body tissues to insulin almost certainly involves insulin receptors in cell membranes. In the early stage, the predominant abnormality is reduced insulin sensitivity, characterized by elevated levels of insulin in the blood. Typically, the onset of this disease is in adulthood. The nature of the defect has been difficult to ascertain, in some patients the insulin receptor is abnormal, in others, one or more aspects of insulin signalling is defective, and in others, no defect has been identified. Because there is not, at least initially, an inability to secrete adequate amounts of insulin, insulin injections are not useful for therapy. Rather the disease is controlled through dietary therapy and hypoglycaemic agents.

- Gestational diabetes mellitus resembles type 2 diabetes in several aspects, involving a combination of inadequate insulin secretion and responsiveness. It occurs in about 2%–5% of all pregnancies and may improve or disappear after delivery. Gestational diabetes is fully treatable but requires careful medical supervision throughout the pregnancy. About 20%–50% of affected women develop type 2 diabetes later in life. Even though it may be transient, untreated gestational diabetes can damage the health of the foetus or mother.

#### ***1.1.4 Diabetes complications***

Diabetes is associated with increased risk of a number of serious, sometimes life-threatening complications. Diabetes involves damage to the heart, blood vessels, eyes, kidneys, and nerves, although the subject may not know that damage is taking place. It's important to diagnose and treat diabetes early, because it can cause damage even before it makes someone feel ill.

How diabetes causes long-term problems is unclear. However, changes in small blood vessels and nerves are common. These changes may be the first step toward many problems that diabetes causes. Many people are not even aware that they have diabetes until they develop one of its complications

- *Retinopathy*

Damage to the eye is the most feared complication of diabetes. Total blindness in diabetes is uncommon since just under 2% of people with type 1 diabetes actually suffer total vision loss. Loss of vision occurs largely through blood vessel damage (5). With high blood sugars, damage can occur to blood vessels throughout the body in three ways:

- Leakage: high levels of blood sugars cause damage to individual cells and later is associated with as damage to structures like capillaries. Endothelial cells, which form a very smooth surface on the inner walls of blood vessels, and helper cells, called pericytes, are especially damaged by excess sugar. These cells lose the electrical charge normally found at their surface, due to inactivation of mineral transporting enzymes and to depletion of energy resources in the high blood sugar environment. As damage progresses, the blood vessel walls starts to become porous, letting proteins and other materials leak out abnormally.

- Blood vessel blockage: high blood sugars cause partial and total blockages within existing blood vessels. Blockage of capillaries is found in background retinopathy, but a more serious form of blockage of arterioles occurs in pre-proliferative and proliferative retinopathy. Arteriolar blockage slows delivery of oxygen and other nutrients that are required to maintain cell health. The oxygen deficit in turn can trigger release of growth factors.



- Abnormal growth: as blood vessels become blocked and oxygen deprivation begins, excess growth factors start to be released to promote growth of new blood vessels, or neovascularization. Proliferative diabetic retinopathy can be seen in the eye with an ophthalmoscope, as neovascularization. Neovascularization appears as a twisted collection of blood vessels and is quite dangerous because these vessels grow abnormally out of the retina into the clear vitreous gel. This abnormal growth of blood vessels can be seen in the center of the Figure 1.5. Right above the center is an example of the vessels growing out of the retina.

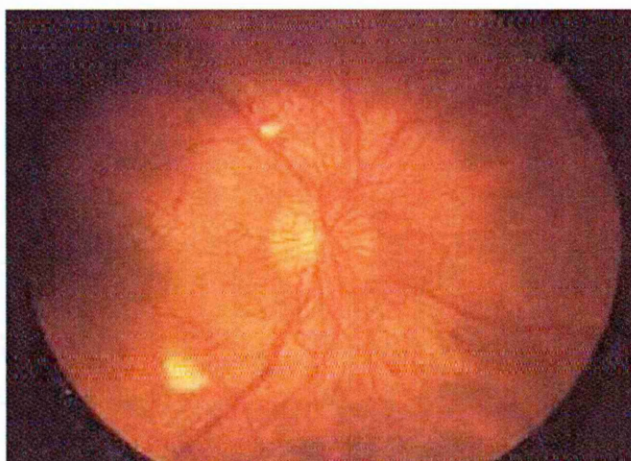


Figure 1.5 Abnormal growth of blood vessels in retinopathy (5)

Because vessels grow beyond the supporting structure of the retina, they are very prone to bleeding, especially when they occur near the area where blood vessels and nerves enter the eye. Any jerking motion or even a rise in blood pressure can lead to a rupture of one of these abnormal vessels and cause an hemorrhage. Before bleeding occurs, someone who has neovascularization will usually not be aware they have these abnormal blood vessels. But they can be detected at an early stage with regular eye examination, laser treatment at this stage will often prevent bleeding from occurring.

- *Nephropathy*

Diabetic nephropathy, also known as Kimmelstiel-Wilson syndrome and intercapillary glomerulonephritis, is a progressive kidney disease caused by angiopathy of capillaries in kidney glomeruli. It is characterized by nephrotic syndrome and nodular glomerulosclerosis. It is due to longstanding diabetes mellitus, and is a prime cause for the requirement of dialysis (6).

During diabetic nephropathy the kidney becomes damaged and more protein than normal collects in the urine. As the disease progresses, more of the kidney is destroyed (Figure 1.6). Over time, the kidney's ability to function starts to decline, which may eventually lead to chronic kidney failure.

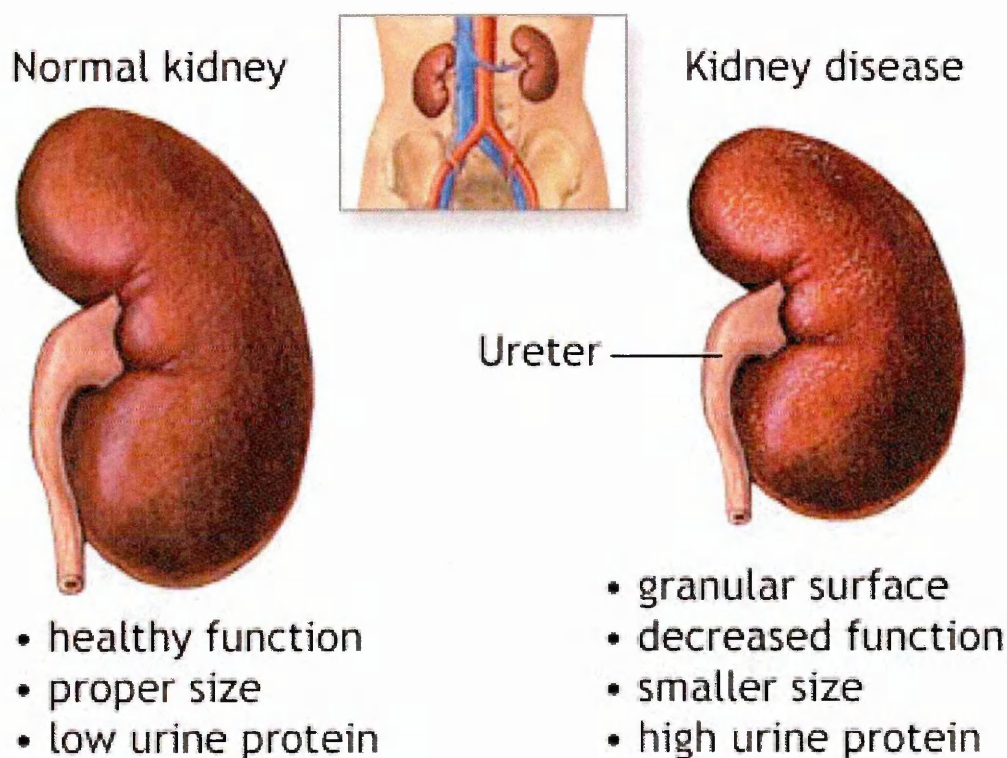


Figure 1.6 Normal and diabetic kidney (7)

Each kidney is made of hundreds of thousands of units called nephrons. Each nephron includes a cluster of blood vessels and epithelial cells called a glomerulus. The function of the glomerulus is to filter blood and form urine, which drains *via* the ureter.

The earliest histologically detectable change in the course of diabetic nephropathy is congestion in the glomerulus. At this stage, the kidney may start allowing more albumin than normal to enter urine, and this can be detected by sensitive tests for albumin. This stage is called microalbuminuria.

As diabetic nephropathy progresses, increasing numbers of glomeruli are destroyed. Now, amounts of albumin being excreted in the urine increase, and may be detected by ordinary urinalysis techniques. Now at kidney biopsy diabetic nephropathy changes are evident.

Protein may appear in the urine for 5 to 10 years before other symptoms develop. High blood pressure often accompanies diabetic nephropathy. Over time, the kidney's ability to function starts to decline, and diabetic nephropathy may eventually lead to chronic kidney failure. The disorder continues to progress toward end-stage kidney disease, often within 2 to 6 years after the appearance of high protein in the urine (proteinuria).

Treatment for diabetic nephropathy attempts to manage and slow the progression of the disease. Aggressive blood pressure control is by far the most important factor in protecting kidney function, regardless of the stage of the diabetic nephropathy.

Angiotensin-converting enzyme (ACE) inhibitors protect the kidneys more effectively than other types of high blood pressure medication. A new class of blood pressure regulators known as angiotensin-receptor blockers (ARBs) may also offer compatible protection.

- *Neuropathy*

Diabetic neuropathies comprise a family of nerve disorders caused by diabetes. People with diabetes can, over time, have damage to nerves throughout the body. Neuropathies lead to numbness and sometimes pain and weakness in hands, arms, feet, and legs. Problems may also occur in every organ system, including the digestive tract, heart, and sex organs. People with diabetes can develop nerve problems at any time, but the longer a person has diabetes, the greater the risk. An estimated 50 percent of those with diabetes have some form of neuropathy, but not all with neuropathy have symptoms. The highest rates of neuropathy are among people who have had the disease for at least 25 years (8).

Diabetic neuropathy also appears to be more common in people who have had problems controlling their blood glucose levels, in those with high levels of blood fat and blood pressure, in overweight people, and in people over the age of 40 (8).

The causes of these complaints are probably different for different varieties of diabetic neuropathy. Researchers are studying the effect of glucose on nerves to discover exactly how prolonged exposure to high glucose causes neuropathy. Nerve damage is likely to be due to a combination of factors: metabolic factors, such as high blood glucose level, long duration of diabetes, possibly low levels of insulin, abnormal blood fat levels, neurovascular factors, leading to damage to blood vessels that carry oxygen and nutrients to the nerves, autoimmune factors that cause inflammation in nerves, mechanical injury to nerves (such as carpal tunnel syndrome) inherited traits that increase susceptibility to nerve disease and lifestyle factors such as smoking or alcohol use.

Diabetic neuropathies can be classified as peripheral, autonomic, proximal, and focal. Each affects different parts of the body in different ways. Peripheral neuropathy causes either pain or loss of feeling in the toes, feet, legs, hands, and arms. Autonomic neuropathy causes changes in digestion, bowel and bladder function, sexual response, and

perspiration. It can also affect nerves that serve the heart and control blood pressure. Autonomic neuropathy can also cause hypoglycaemia (low blood sugar) unawareness, a condition in which people no longer experience the warning signs of hypoglycaemia. Proximal neuropathy causes pain in the thighs, hips, or buttocks and leads to weakness in the legs. Focal neuropathy results in the sudden weakness of one nerve, or a group of nerves, causing muscle weakness or pain. Any nerve in the body may be affected.

- *Cardiopathy*

Diabetic cardiopathy is a disorder with involvement of myocardial, interstitial, coronary, and neural structures. Patients with diabetes mellitus have a heightened rate of cardiovascular mortality. Cardiovascular complications are now the leading cause of diabetes related morbidity and mortality. It is generally appreciated that the major ones include enlarged arteries, epicardial coronary arteries, and damage to the microvasculature. It is also now widely appreciated that the mortality after acute myocardial infarction is greater in patients with diabetes mellitus, both at 30 days and one year after infarction. Stress hyperglycaemia, with and without diabetes mellitus, is associated with increased risk of in-hospital mortality of patients with acute myocardial infarction.

The incidence of coronary occlusion in persons with clinical diabetes has been estimated at from 8-17% with diabetic adults having heart disease death rates 2 to 4 times as high as the general population; risk of stroke is also found to be 2 to 4 times higher in people with diabetes. Arteriosclerosis obliterans in the lower extremities, a form of peripheral vascular disease, may produce disturbances in sensation, decrease in muscular endurance, intermittent claudication on effort, absence of peripheral pulses in the lower legs and feet and gangrene, ultimately leading to amputation of the extremity.

- *Ketoacidosis*

Another acute complication more likely to occur in DM is ketoacidosis, a condition caused by a lack of insulin leading to a build-up of ketoacids. Chemical compounds called ketones are one of the natural by-products of fat metabolism. Excessive ketones are formed by biochemical imbalance in uncontrolled or poorly managed diabetes. The condition known as diabetic ketoacidosis can directly cause an acute life-threatening event, a diabetic coma. Diabetic ketoacidosis is a life-threatening medical emergency with a mortality rate just under 5% in individuals under 40 years of age, but with more serious prognosis in the elderly, who suffer mortality rates over 20%. Before the discovery of insulin treatment and other intravenous injections, acidosis was the chief cause of death among diabetics. Today diabetics can use a simple urine dipstick at home to measure the level of excreted ketoacids in their urine (9).

Complications of ketoacidosis are hyperglycaemia and ketoacidaemia, due to insulin lack, hyperglucagonaemia, and elevated levels of the stress hormones catecholamines, cortisol, and growth hormone.

- Hyperglycaemia results from increased hepatic production of glucose as well as diminished glucose uptake by peripheral tissues. Hepatic glucose output is a consequence of increased gluconeogenesis resulting from insulinopenia as well as from associated hyperglucagonaemia.

- Ketoacidaemia represents the effect of insulin lack at multiple enzyme loci. Insulin lack associated with elevated levels of growth hormone, catecholamines, and glucagon contributes to an increase in lipolysis from adipose tissue and in hepatic ketogenesis.

- Fluid and electrolyte depletion. Hyperglycaemia results in osmotic diuresis and dehydration secondary loss of electrolytes. Ketonuria similarly causes loss of water and electrolytes. Balance studies during withdrawal of insulin and treatment in patients with

type 1 diabetes show that on average water depletion is about 5 L; sodium, 300-500 mmol; potassium, 270-400 mmol; chloride, 100-400 mmol *per* day. Drowsiness is fairly common but frank coma only occurs in about 10% of patients. There is correlation between degree of depression of sensorium and extracellular osmolarity. When serum hyperosmolality exceeds 320-330 mosm/L, central nervous system depression or coma may ensue. Coma in a diabetic patient with a low osmolality should urgently prompt a search for cause of coma other than hyperosmolality.

## 1.2 Conventional treatment for type-1 diabetes

Insulin was the first, and remains the primary means of treatment for type 1 diabetes; it is administered by subcutaneous injection. This method is necessary since insulin is destroyed by gastric secretions when it is taken by mouth.

### *1.2.1 Conventional therapy*

Conventional insulin injection therapy requires a strict daily schedule to keep glucose levels correct. This means not only taking the same doses of insulin at the same times every day, but also eating and exercising at the same levels at the same times each day. Insulin injections must be balanced with meals and daily activities, and glucose levels must be closely monitored through frequent blood sugar testing. Many diabetics need to inject insulin only once a day; others require two or more injections. It typically needs a mixture of short-acting insulin (to cover breakfast and dinner) and intermediate-acting insulin (to regulate glucose between meals and at night).

- Short-acting insulin is used to control blood sugar peak that occurs at mealtimes (bolus insulin).
- Intermediate-acting insulin is used to provide an insulin effect all day long or to control blood sugar through the night (basal insulin).
- Long-acting insulin has a slow onset and virtually no peak. It lasts for up to 36 hours, and can be used as basal insulin.

Negative aspects of this kind of therapy are linked to the standard of life that the patient must follow. If the patient introduces any variation into his/her life-style, the therapy must be modified to avoid hypo and hyperglycaemia.



### ***1.2.2 Intensive therapy***

A DCCT (diabetes control and complications trial) was a large diabetes study sponsored by the National Institute of Health of the USA that ran for 10 years. It began in 1983, with randomly assigned 1441 patients with type 1 diabetes to receive either intensive therapy or conventional therapy:

- Patients in the intensive therapy group took three or more injections of insulin *per* day or used an insulin pump and checked their blood glucose at least four times *per* day. They were given a blood glucose target level of between 3.9 mmol/L and 6.7 mmol/L before meals and less than 10 mmol/L after meals
- Patients in the conventional therapy group took one or two injections of insulin *per* day and had no glucose goals other than avoiding hyperglycaemia or hypoglycaemia.

Study participants were between 13 and 40 years of age at the start of the study and were followed up for an average of six and a half years. The study showed that intensive diabetes therapy with tight glycaemic control continued to protect against cardiovascular, eye, and kidney complications of diabetes over the long term of diabetes. The results were so striking that patients in the conventional group were urged to switch to intensive therapy, and most of them did so. Thus, intensive therapy has become the recommended treatment for all adults and teens with type 1 diabetes (10). More than 10 years after the end of this study comparing intensive and conventional therapy, participants who originally received intensive therapy showed a very significant reduction in the risk of kidney failure (Figure 1.7), high blood pressure, heart attack, stroke, or death from cardiovascular disease. Cardiovascular disease being a leading cause of death and disability among people with diabetes, plus those who develop kidney complications being at greatest risk of this. Intensive diabetes therapy has long-term beneficial effects on the risk of cardiovascular disease in patients with type 1 diabetes (11).

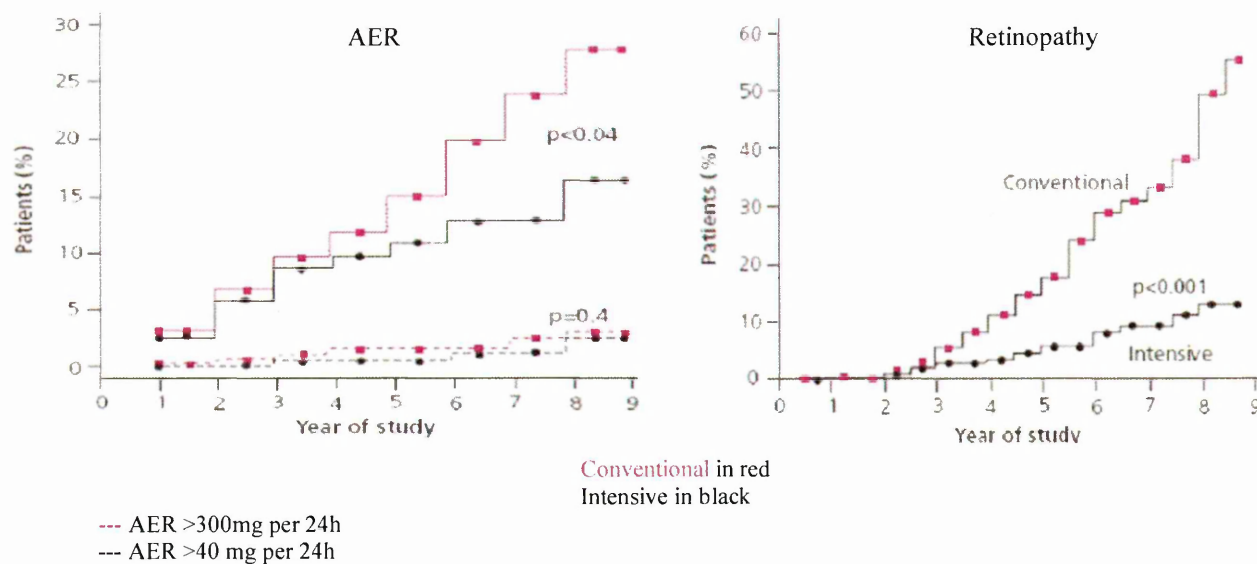


Figure 1.7: Cumulative incidence of a sustained change in nephropathy (urinary albumin excretion - AER) and retinopathy in patients with IDDM, receiving intensive or conventional therapy (modified from (11)).

Maintenance of glucose level near to the physiological one, using intensive insulin therapy, could be a way to block progression of diabetic complications. This requires precision and care from patients and from their doctor to avoid reduction of glucose concentration thus a hypoglycaemic state (under 65 mg/dl).

The scientific community is searching for a way to administer insulin to the diabetic patient, avoiding continuous injection and trying to obtain best glucose control, minimizing hypo- and hyperglycaemic episodes.

### 1.2.3 Insulin pump therapy

An insulin pump is a small mechanical device, a little larger than a pager that is worn outside the body, often on a belt or in a pocket. It delivers fast-acting insulin into the body via a thin plastic tube ending in a small, flexible plastic cannula or a very thin needle. The

cannula is inserted beneath the skin at the infusion site, usually in the abdomen or upper buttocks.

The insulin pump is a computer-driven device that delivers fast-acting insulin in precise amounts at pre-programmed times, but wearing the insulin pump might require more compliance on the part of the patient than traditional injection therapy, especially if the patient is not used to checking blood sugar several times a day (Figure 1.8).

Pump therapy may not be suitable for everyone. It is however being successfully used by children, teenagers and adults, including women during pregnancy. Cases are also increasing of pump therapy being used with infants and babies, including those that are premature. The key to successful use of pump therapy is motivation. Those most suited must have received structured education, have a good knowledge and understanding of diabetes and of how insulin, exercise and food intake affect blood glucose levels. They must be willing to take significant responsibility for their day-to-day diabetes management or in the young have reliable adult supervision. This requires commitment to regular testing of blood glucose levels and confidence in acting on results.

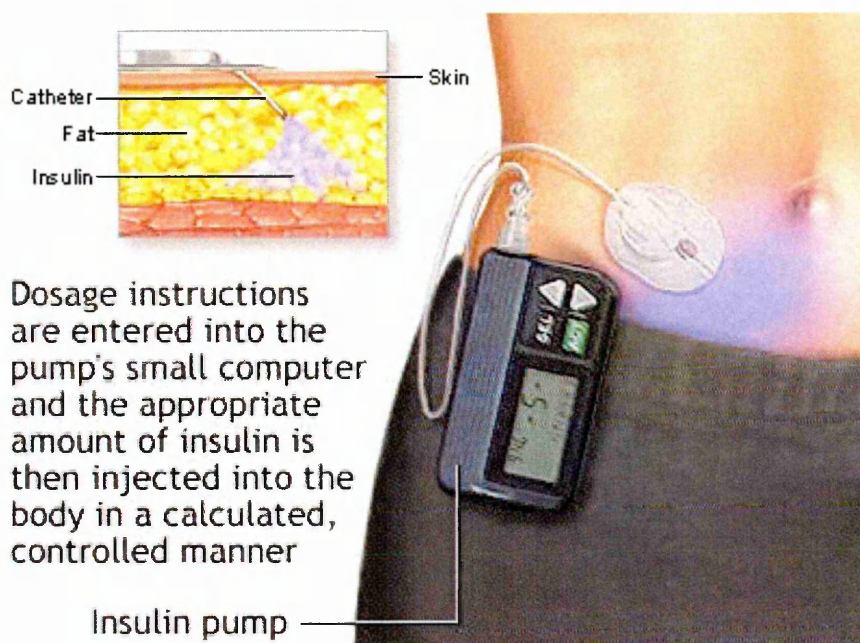


Figure 1.8 Insulin pump. The catheter at the end of the insulin pump is inserted through a needle into the abdominal fat of a person with diabetes. Dosage instructions are entered into the pump's small computer and the appropriate amount of insulin is then injected into the body in a calculated controlled manner (12).

But this kind of therapy presents many problems: difficulty in using a computer for aged people, large dimension of the pump and infections at the infusion site. Moreover, these systems are not totally safe and precise, as they need to have a security system that would block the pump should malfunction occur.

### 1.3 Alternative treatment for type-1 diabetes

#### *1.3.1 Pancreas transplantation*

Whole pancreas transplantation, first performed in 1966 in combination with a kidney transplant in diabetic patients suffering from end-stage renal failure, demonstrated that a euglycaemic state could be obtained without the need for exogenous insulin. Early procedures however, were complicated by a high morbidity rate. Improvements in transplant techniques, immunosuppression therapies and post-transplant monitoring of graft function and rejection has resulted in a dramatic improvement in patient morbidity and graft survival. With the improved outcomes and demonstrated efficaciousness in controlling the diabetic glycaemic state, whole pancreas transplantation is now recognized by the American Diabetes Association as an acceptable therapeutic alternative to continued insulin therapy in diabetic patients with imminent or established end-stage renal disease who have had, or plan to have, kidney transplantation.

Pancreas transplantation may be considered as a group of three separate, clinical entities: simultaneous pancreas and kidney transplantation (SPK), pancreas after kidney transplantation (PAK) and transplantation of the pancreas alone (PTA). Each form of transplantation is characterized by its own indications, risks and outcomes.

- Simultaneous pancreas and kidney transplantation. Diabetes is a major cause of renal disease and it is associated with approximately 40% of new cases of end-stage renal failure (ESRF) in the US, who will subsequently require renal dialysis or kidney transplantation. When a diabetic patient develops ESRF and requires a kidney transplant, consideration is now commonly given to whether the patient would also benefit from receiving a pancreas as well. SPK transplantation is the most common form of pancreas transplantation performed, accounting for 60% of the total number of pancreas transplants

performed each year in the US (approximately 900/year). The annual number of SPK transplants has remained stable over the last 10 years, however this may reflect increasing interest in the option of PAK transplantation (living donor kidney transplantation) by the patient in ESRF with IDDM.

When SPK transplantation is performed, the patient undergoes only one operation and following the surgery may be managed on the same (or very similar) immunosuppressive drugs they would have received for a renal transplant alone. The combined procedure offers excellent patient and pancreatic graft survival, producing a sustained euglycaemic state for exogenous insulin or oral hyperglycaemic agents. The renal transplant provides an effective method of surveillance of both grafts for acute rejection (creatinine clearance, biopsy) and may in part explain the improved one-year and long-term pancreatic graft survival rates when compared to pancreas transplantation without a donor-matched kidney transplant. There also has been no evidence that pancreas transplantation may have a deleterious effect on the simultaneously transplanted kidney.

- Pancreas after kidney transplantation. As the number of patients with ESRF has increased in the past decade, demand for renal transplantation has outpaced the supply of cadaveric kidneys available. By 2000, the number of living donor kidney transplants performed in the US exceeded the number of cadaveric donor transplants. Whereas SPK transplantation is usually restricted to the use of cadaveric organs only, PAK transplantation offers the option of using a living donor kidney, and in doing so both expands the number of kidneys available for transplantation and allows the diabetic patient the opportunity to benefit early from living donor kidney transplant (better long term outcome, avoidance of dialysis). With improved surgical techniques, better immunosuppressive drugs and rejection monitoring, outcomes for solitary pancreas procedures have improved such that PAK transplantation is now routinely considered. The

kidney transplant recipient is required to demonstrate stable renal function and minimal post-procedure complications to be acceptable for subsequent pancreas transplantation. PAK transplant option requires the patient to undergo two major operations, however post-transplantation immunosuppression and care are similar to those for kidney transplantation alone.

- Pancreas transplantation alone. PTA is offered to diabetic patients in some centers when there has been difficulty in management of diabetes and the person has suffered severe hypoglycaemic episodes (often with hypoglycaemic unawareness), so long as there is little or no evidence of renal disease. As with PAK transplantation, improvements in PTA graft survival have improved significantly in recent years, although the question of whether or not the procedure may have an adverse long-term affect on recipients' renal function (calcineurin antagonist-based immunosuppression) has not been resolved. Normalizing blood glucose levels after pancreas transplantation may offer this patient group the possibility of long-term improvement in renal function. The American Diabetes Association's 2006 Position Statement on pancreas and islet transplantation recommends "In the absence of indications for kidney transplantation, pancreas-alone transplantation should only be considered a therapy in patients who exhibit these three criteria: history of frequent, acute and severe metabolic complications (hypoglycaemia, marked hyperglycaemia, ketoacidosis) requiring medical attention; clinical and emotional problems with exogenous insulin therapy that are so severe as to be incapacitating; and consistent failure of insulin-based management to prevent acute complications" (13). Since 2001, PTA has accounted for approximately 12% of pancreas transplants performed annually in the US.

The complexity of the whole pancreas transplant procedure, along with likelihood of pre-existing disease secondary to their IDDM, exposes the recipient to a variety of significant

operative and post-operative risks. The extent of the post-operative problems is likely to be limited to widespread acceptance of pancreas transplantation in the early era of its development. Serious surgical complications following the procedure include: thrombosis of graft vessels, intra-abdominal haemorrhage, anastomotic leak (enteric or bladder), graft pancreatitis, pancreatic fistula formation and intra-abdominal sepsis, all of which may require re-laparotomy and possibility of graft loss. In recent years, with improvements in donor and recipient selection criteria, surgical technique, immunosuppression protocols (reduced incidence of early, acute rejection) and prophylactic regimes (anti-viral, anti-bacterial and antithrombotic), there has been a significant decrease in overall incidence of serious complications and rate of re-laparotomy.

### ***1.3.2 Stem cell therapy***

In developing potential stem cell therapy for patients with diabetes, researchers hope to achieve a system that meets several criteria. Ideally, the stem cells should be able to multiply in culture and reproduce themselves exactly. A stem cell has the ability to divide for many times in culture and to be able to differentiate into specialized cells. This should also be possible *in vivo* to produce a desired cell phenotype. For diabetes therapy, it is not clear whether it would be desirable to produce only  $\beta$ -cells or whether other types of pancreatic islet cell are also necessary (14). Studies by Bernat Soria and colleagues (15), have indicated that isolated  $\beta$ -cells are less responsive to changes in glucose concentration than intact islet clusters made up of all islet cell types. Islet cell clusters typically respond to higher-than-normal concentrations of glucose by releasing insulin in two phases: a quick release of high concentration insulin and a slower release of lower concentrations. In this manner  $\beta$ -cells would be able to fine-tune their response to glucose. Extremely high concentrations of glucose may require that more insulin be released quickly, while



intermediate concentrations of glucose could be handled by a balance of quickly and slowly released insulin.

Many workers believe that it would be preferable to develop a system in which stem or precursor cell types could be cultured to produce all the cells of the islet cluster in order to generate a population of cells that would be able to coordinate release of the appropriate amount of insulin to the current physiologically relevant concentrations of glucose in the blood stream (Figure 1.9 modified from (16)).

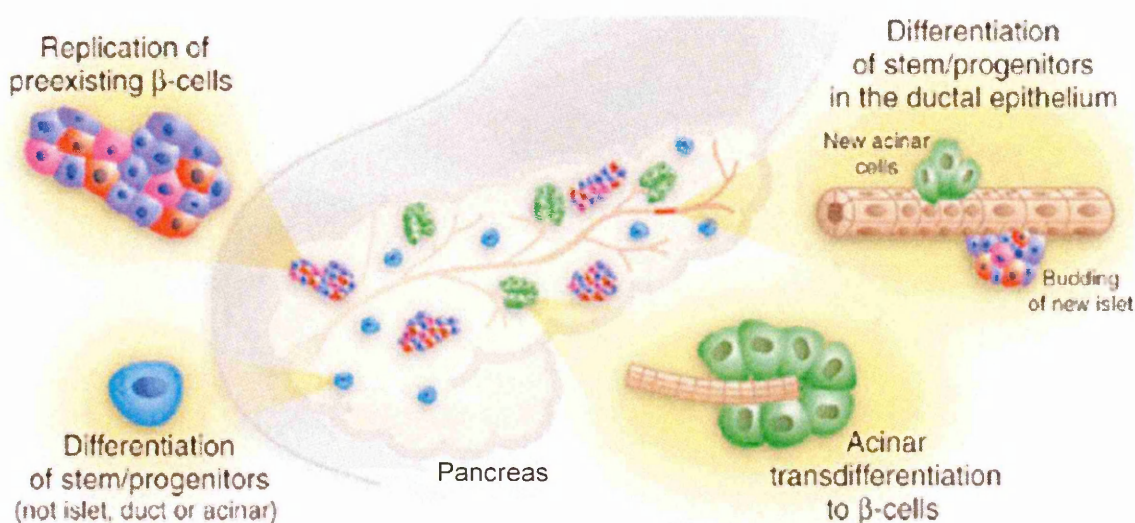


Figure 1.9 Different approaches for generating insulin-producing cells (16)

### *Foetal tissue as source of islet cells*

Several groups are investigating the use of foetal tissue as a potential source of islet progenitor cells. For example, using mice as recipients, insulin content of implants from several sources of stem cells, fresh human foetal pancreatic tissue, purified human islets, and cultured islet tissue have been compared (17). It was found that insulin content was initially higher in fresh tissue and purified islets. However, with time, insulin concentration decreased in the whole grafts, while it remained the same in purified islet grafts. When cultured islets were implanted, their insulin content increased over the course

of three months. It was concluded that precursor cells within the islets were able to proliferate and differentiate into functioning islet tissue, but that purified islet cells alone could not further proliferate when grafted. Importantly, it was found that it was also difficult to expand cultures of foetal islet progenitor cells (18).

#### *Adult tissue as source for islet cells*

Many groups have focused on culturing islet cells from human adult cadavers for use in developing transplantable material. Although differentiated beta cells are difficult to make proliferate and thus to culture, some have had success in engineering such cells to do this. F. Levine and his colleagues at the University of California, San Diego, have engineered islet cells isolated from human cadavers by adding to the cells' DNA special genes that stimulate cell proliferation (19). However, once such cells that could proliferate in culture were established, they no longer produced insulin. The cell lines were further engineered to express the islet beta cell gene, PDX-1, which stimulates expression of the insulin gene. Such cell lines have been shown to propagate in culture and can be induced to differentiate to cells that produce insulin. When transplanted into immunodeficient mice, the cells secreted insulin in response to glucose. This group is currently investigating whether these cells would be able to reverse diabetes in an experimental diabetes model in mice (20). These investigators report that their cells do not produce as much insulin as normal islet beta cells, but it is within one order of magnitude below.

The major problem in dealing with these cells is maintaining the delicate balance between cell population growth and differentiation. Cells that proliferate well do not produce insulin efficiently, and those that do produce insulin do not proliferate well. According to the study, the major issue was developing technology to be able to grow large numbers of these cells that would produce normal amounts of insulin reproducibly (21).

Another promising source of islet progenitor cells lies in cells that line pancreatic ducts. Some believe that multipotent (capable of forming cells from more than one embryonic germ layer) stem cells are normally found intermingled with mature, differentiated duct cells, while others believe that mature duct cells themselves can undergo differentiation, or a reversal of differentiation to a less mature type of cell, which could then differentiate into insulin-producing islet cells (22). S. Bonner-Weir and her colleagues have reported that when ductal cells isolated from adult human pancreatic tissue were cultured, they could be induced to differentiate into clusters that contained both ductal and endocrine cells. Over the course of three to four weeks in culture, the cells secreted low amounts of insulin when exposed to low concentrations of glucose, and higher amounts of insulin when exposed to higher glucose concentrations. It was determined by immunochemistry and ultrastructural analysis that these clusters contained all types of endocrine cells of the islet. In principle it might be possible to perform a biopsy and remove duct cells from a patient's own pancreas, and then proliferate them in culture to give the patient back his or her own islet cells. This could work for patients with type 1 diabetes and who lack functioning beta cells, but with pancreatic duct cells still intact. However, autoimmune destruction might still be a problem and potentially lead to destruction of these autologous transplanted cells (23). Type 2 diabetes patients too might benefit from transplantation of cells expanded from their own duct cells since they would not need any immunosuppression. Many believe that if there is a genetic component to the death of beta cells, then beta cells derived from ductal cells of the same individual would also be susceptible to autoimmune attack.

J. Habener has also looked for islet-like stem cells from adult pancreatic tissue. He and his colleagues discovered a population of stem-like cells within both adult pancreatic islets and pancreatic ducts (24). These cells did not express any marker typical of ductal cells, so

would be unlikely to be such. Instead, they expressed a marker, nestin, which is typically found in developing neural cells. Nestin-positive cells do not express markers typically found in mature islet cells. However, depending upon growth factors added, cells differentiated into different phenotypes, including liver, neural, exocrine pancreas, and endocrine pancreas, judged by the markers they expressed. These could be maintained in culture for up to eight months.

### *Embryonic stem cells*

The discovery of methods to isolate and grow human embryonic stem cells, since 1998, renewed hopes of doctors, researchers, and diabetes patients and their families, that a cure for type 1 diabetes, and perhaps type 2 diabetes as well, may be within striking distance (25). In theory, embryonic stem cells can be cultured and coaxed into developing into insulin-producing islet cells of the pancreas. With a ready supply of cultured stem cells at hand, the theory is that a line of embryonic stem cells could be grown, as needed for anyone requiring cell transplantation. The cells would be engineered to avoid immune rejection. Before transplantation, they could be placed into non-immunogenic material so that they would not be rejected and the patient would avoid the devastating effects of immunosuppressant drugs. There is also some evidence that differentiated cells derived from embryonic stem cells might be less likely to cause immune rejection (26). Although having a replenishable supply of insulin-producing cells for transplantation into humans may be a long way off, researchers have been making remarkable progress in their quest for it.

Since their discovery, several teams have been investigating the possibility that human embryonic stem cells could be developed for a therapy for treating diabetes. Recent studies in mice show that embryonic stem cells can be initiated into differentiating into

insulin-producing beta cells, and new reports indicate that this strategy may be possible using human embryonic cells as well (27).

Recently, workers in Spain have reported using mouse embryonic stem cells that were engineered to allow cells to be selected that were differentiating into insulin-producing cells (28). Soria *et al.* at the Universidad Miguel Hernandez in San Juan, Alicante, Spain, added DNA containing part of the insulin gene, to embryonic cells from mice. This gene was linked to a further one that rendered the mice resistant to a certain antibiotic drug. By growing cells in the presence of the antibiotic, only those that were activating the insulin promoter were able to survive. The cells were cloned and then cultured under varying conditions. Cells cultured in the presence of low concentrations of glucose differentiated and were able to respond to changes in glucose concentration by increasing insulin secretion nearly sevenfold. The cells were then implanted into spleens of diabetic mice and it was found that symptoms of diabetes were reversed.

Recently Kim *et al.* described a series of experiments in which they induced mouse embryonic cells to differentiate into insulin-secreting structures that resembled pancreatic islets (29). They started with embryonic stem cells and let them form embryoid bodies, an aggregate of cells containing cells of all three embryonic germ layers. They then selected a population of cells from the embryoid bodies that expressed the neural marker nestin. Using a sophisticated five-stage culturing technique, they were able to induce the cells to form islet-like clusters that resembled those found in native pancreatic islets. The cells responded to normal glucose concentrations by secreting insulin, although insulin amounts were lower than those secreted by normal islet cells. When the cells were injected into diabetic mice, the cells survived, although they did not reverse the symptoms of diabetes. A potential advantage in use of embryonic cells is that, in theory, they could be engineered

to express genes appropriate to allowing them to escape or reduce detection by the immune system.

Before any cell-based therapy to treat diabetes arrives at the clinic, many safety issues must be addressed. A major consideration is whether any precursor or stem-like cells transplanted into the body might revert to a more pluripotent state and induce formation of tumours. These risks would seemingly be lessened if fully differentiated cells were used to be for transplantation.

However, before any kind of human islet-precursor cells could be used therapeutically, a renewable source of human stem cells must be developed. Although many progenitor cells have been identified in adult tissue, few of them could be cultured for multiple generations. Embryonic stem cells show the greatest promise for generating cell lines free of contaminants that can also self renew. Most researchers agree that until a therapeutically useful source of human islet cells is developed, all avenues of research should be exhaustively investigated, including both adult and embryonic sources of tissue.

### ***1.3.3 Islet transplantation***

The Diabetes Control and Complications Trial Research Group reported improved glycaemic control through intensive insulin therapy, delaying onset and slowing progression of diabetic complications (10). Improved glycaemic control however, was hard to sustain and associated with intense insulin therapy was a significant increase in severe hypoglycaemic episodes. Whole pancreas transplantation is capable of producing a sustained, euglycaemic state, reducing incidence of hypoglycaemia and offering the possible benefit of reducing microvascular, macrovascular and neurologic complications. Pancreas transplantation however, is a major, complex surgical procedure associated with significant risk and cost that may limit its general acceptability, especially when a

potential diabetic recipient has yet little evidence of renal impairment and does not need a combined kidney/pancreas transplant.

Within the past 20 years, pancreatic islet transplantation has become a clinical reality and an option in the treatment of diabetes. Islet transplantation has a distinct advantage over whole pancreas transplantation with regard to reduced peri-procedure morbidity. The procedure avoids major surgery and the risk of associated post-operative complications, re-laparotomy and acute (vascularized) graft loss. Islet transplantation, with its ability to be cultured for a period of time prior to transplantation, also offers the future possibility of reducing immunogenicity (both allo- and auto-) of the graft so that little or no immunosuppression would be required (30).

Early efforts to treat diabetic patients with pancreatic islet transplantation were mostly unsuccessful. Although the first human pancreatic islet allografts were performed in 1974, it wasn't until 1991 that a pancreatic islet transplant recipient achieved sustained euglycaemia off insulin (for 1 year). In 2000, the Edmonton group reported 7 consecutive islet transplant recipients achieving exogenous insulin independence (Figure 1.10). All recipients received islets from 2 pancreas donors (one received islets from 4 donors), and were maintained on a glucocorticoid-free immunosuppression protocol using Sirolimus and low-dose Tacrolimus (31).

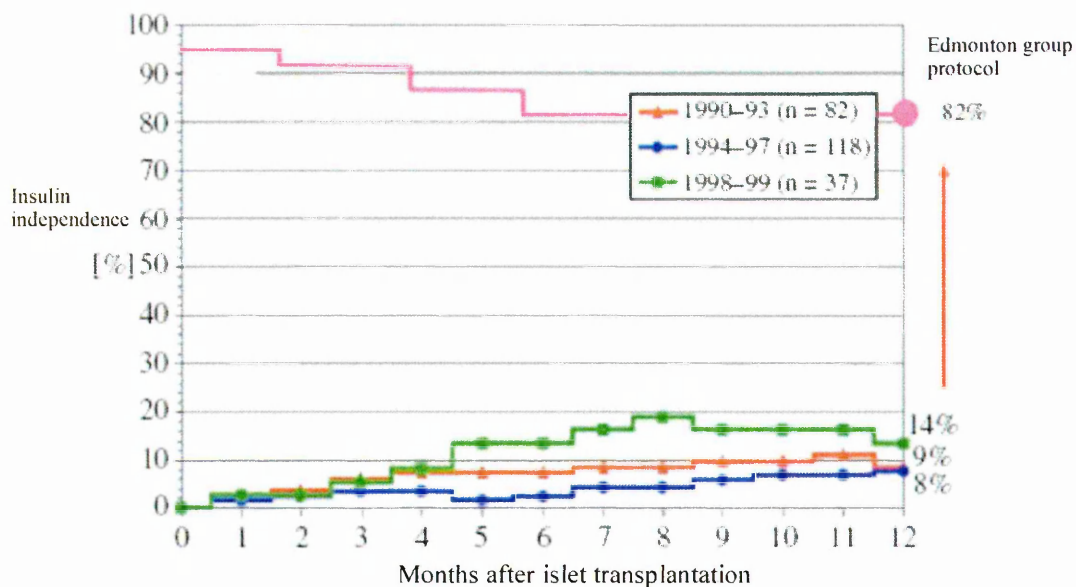


Figure 1.10 Improvements in clinical outcome with high rates of insulin independence with patients treated using the Edmonton Protocol, compared to previous reports in the international Islet Transplant Registry.

The success of the Edmonton program has led to general acceptance that islet transplantation is a clinically feasible therapy, which may be considered for the treatment of patients with diabetes, especially when accompanied by severe hypoglycaemia. Since the report of success from Edmonton, interest has grown in islet transplantation and now more than 20 centers in North America and many more worldwide are performing this procedure (32) (Figure 1.11).



## International Islet Transplant Activity (1999-2004)

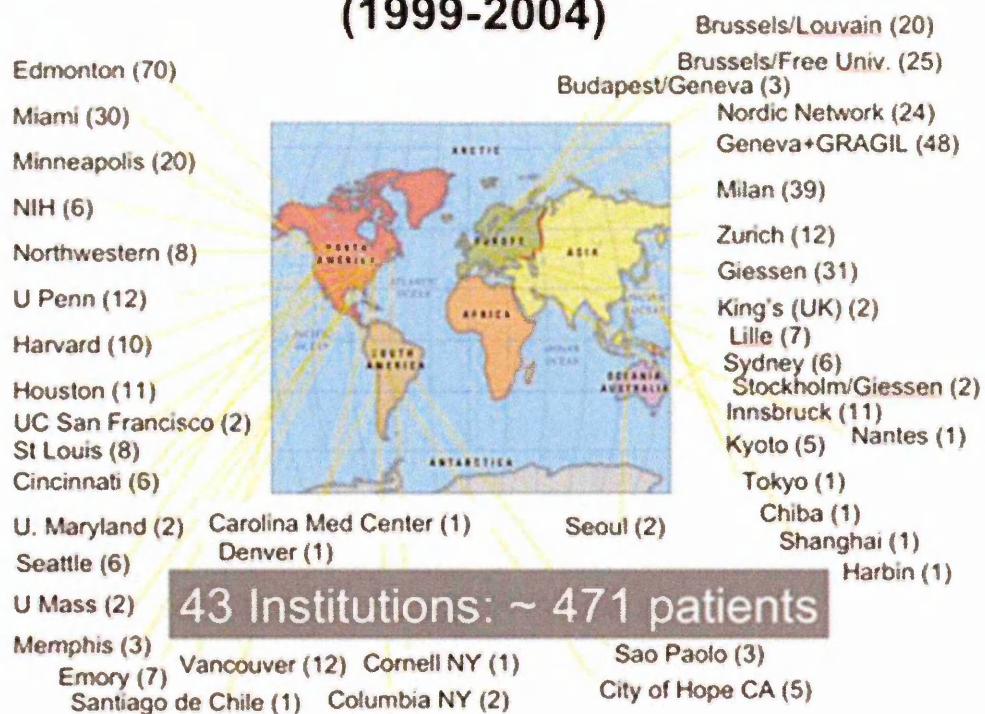


Figure 1.11 Increase in clinical islet transplantation activity, with 471 patients transplanted at 43 international institutions (modified from (32)).

Pancreatic islet transplantation, in general, has been restricted to patients with diabetes who suffer from hypoglycaemic unawareness or metabolic instability, or have early evidence of secondary complications due to their diabetes. The patients require long-term, calcineurin-based immunosuppression and thus are subjected to risks from these agents, such as nephrotoxicity, infection and malignancy. The patient may also become sensitized due to their alloimmune response to the transplant, potentially interfering with subsequent transplantation. Patients with evidence of significant diabetic renal impairment are excluded from islet transplantation until they either require or have undergone a kidney transplant. To improve the likelihood of attaining euglycaemia of insulin, most transplant programs and clinical trials will restrict islet transplantation therapy to patients weighing

less than 70 kg, a body mass index (BMI) < 27 and not requiring an excessive amount of daily insulin for glycaemic control (33) (34).

As islet transplantation techniques move forward, one of the first challenges is to achieve reliably insulin independence with single-donor grafts. Moreover, future milestones for clinical islet transplantation imply xenotransplantation (immunoisolating the islets and treating the patient with immunosuppressive drugs), gene therapy and stem cell technology. (Figure 1.12). (15)

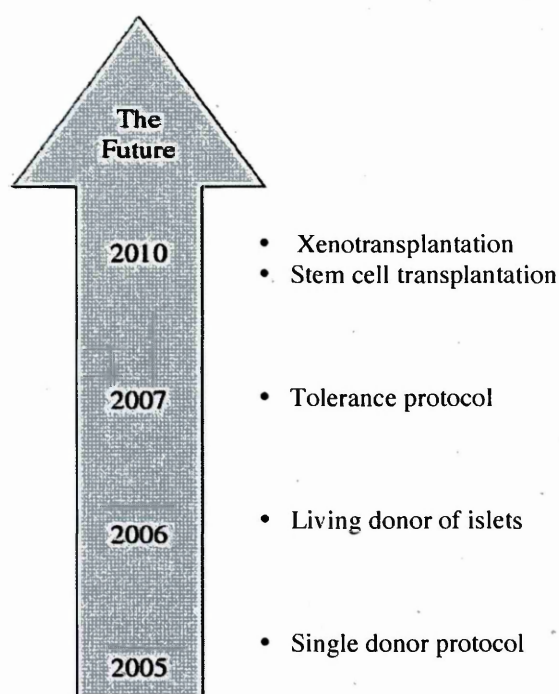


Figure 1.12 Future milestones in clinical islet transplantation

### 1.4 Immunoisolation

Routine application of islet transplantation would be tremendously enhanced by an unlimited supply of donor tissue, a standard implantation procedure and the ability to maintain transplanted tissue without requirement of immunosuppressive drugs. To achieve these goals, immunoisolation of islet cells has been proposed to protect cells from attack by the host immune system. The term “immunoisolation” refers to encapsulation of a graft in a selectively permeable membrane. To support the graft, low molecular weight substances, such as oxygen, glucose and other nutrients, should be exchanged across the membrane while protection against rejection requires that immune cells and other humoral factors detrimental to graft survival should be excluded (35). Clearly, one prerequisite for a therapeutic effect is that the cell products, such as insulin, are also exchanged across the membrane and are taken up by surrounding microcirculation. Development of immunoisolation techniques, by separation of implanted cells from the host immune system has been recognized for a long time as an experimental strategy to prevent immunorecognition and rejection (35).

Using immunoisolation of islets, chronic administration of immunosuppressive drugs could theoretically be eliminated or minimized, as transplanted cells are separated from the host immune system by a biocompatible and semipermeable membrane. Moreover, immunoisolation of pancreatic islet cells for transplantation into patients with diabetes theoretically permits grafting of xenogenic islets, thus expanding a potential supply of donor islet tissue. Hence, immunoisolation could open up the possibility of using islets harvested from animals, or insulin-producing cells engineered from stem cells without a requirement of immunosuppression of transplant recipients. Porcine and bovine insulin

amino acid sequences have considerable sequence homology with human insulin, and therefore pigs and cows are considered attractive as options for xenogeneic donors.

Immunoisolation of xenogeneic cells requires stringent biological and physical criteria to be met. The immunological response to a xenograft has various features that distinguish it from an alloresponse. The first difference depends on the species cross, in that the recipient may have natural cytotoxic antibodies against xenoantigens of the donor tissue. In addition, the major mechanism of recognition of xenoantigens is *via* an indirect pathway, in which xenoantigen is processed and presented by host antigen-presenting cells (APCs), to immune T cells. The reaction to xenogeneic cells is very complex and involves not only cells and antibodies, but also complement and cytokines, which can inflict cell damage (36).

Devices produced from synthetic membranes and loaded with viable cells are being developed as substitutes in case of failing organ or tissue dysfunction (37). Thus immunoisolation of islets for transplantation may have two potential benefits. First, it may permit allo-islet transplantation without the use of pharmacological immunosuppression. Secondly, encapsulation may facilitate transplantation of islets from non-human species (xenografts) thereby giving access to an unlimited source of insulin-producing tissue. Two main types of encapsulation technique have been used so far: micro- and macroencapsulation. In microencapsulation, a single islet or small groups of islets are encapsulated in a gel capsule usually consisting of alginate. In macroencapsulation a large number of islets is entrapped in a chamber surrounded by semipermeable membrane.

There is evidence in the literature that xenotransplantation of islets encapsulated within hollow fibres, macrobeads or planar diffusion devices can restore normoglycaemia mostly in diabetic mice, when implanted in the peritoneal cavity (38). However, this implantation site is not ideal in clinical conditions because it requires invasive procedures (39) (40).

Subcutaneously has been regarded as a more adequate site for transplantation of a bioartificial pancreas, since islets can be implanted with minimally invasive surgical procedures, if even it may be less vascularized and has more fibrotic reaction.

## Overview of the thesis and aims

Below, find a summary of each chapter, with the principal aims and methods used to obtain successful results.

Chapter 2 deals in greater detail with the process of islet isolation and the method set-up is described. The chapter discusses differences between manual methods of islet isolation plus the automated procedure. It also shows the application of manual and automatic methods for three species of pancreas: rat, bovine and human.

Chapter 3 explains and evaluates the method of islet functionality *in vivo* using syngeneic, allogeneic and xenogenic free islet transplantation. It documents results obtained after implanting islets in diabetic rats and discusses the limits of these protocols, offering an alternative to ameliorate functionality.

Chapter 4 describes the application of an immunoisolation device in experimental settings. It systematically analyzes the results obtained to be able to categorize important observations. Also, here appear published (41) results obtained using the immunoisolation device in a xenotransplantation model.

Chapter 5 illustrates the set-up and measurement system used to evaluate oxygen consumption rate in the tissue. It explains how the data were collected and were elaborated to be able to measure free or encapsulated islet viability and functionality. Results obtained using this method are planned to be published on *Cell Transplantation: The*

*Regenerative Medicine Journal* (Authors: Cornolti R., Figliuzzi M. and Remuzzi A. Title: Effect of Micro and Macro Encapsulation on Oxygen Consumption by Pancreatic Islets).

Chapter 6 reveals the *in vivo* method used to continuously monitor glycaemia in transplanted rats, using a Medtronic® continuous glucose monitoring system; after intraperitoneal tolerance test for glucose, responses of syngeneic transplanted islets in microcapsules or those placed under recipient kidney capsules were monitored. These results are currently being prepared for publication.

Chapter 7 discusses the project development and design of an ideal immunoisolation device. Geometric properties of a polymeric membrane used for immunoisolation were experimentally determined and a mathematical model explaining kinetics of molecular and metabolite diffusion through the membrane was developed. These results also are currently being prepared for publication.

Chapter 8 develops and summarizes goals achieved in this study and presents future work to be performed in order to further test and improve the immunoisolation device proposed.

Finally, one appendix is presented and divided in three parts. Appendix A is the MatLab® code for the mathematical model developed in chapter 7. Appendix B contains the standard operating procedure for human islet isolation and Appendix C is a plan of the Islet Laboratory.

---

## References

1. Zimmet P, Alberti KG, Shaw J. Global and societal implications of the diabetes epidemic. *Nature* 2001;414:782-787.
2. [www.britannica.com/EBchecked/topic-art/22980/68636/Structures-of-the-pancreas](http://www.britannica.com/EBchecked/topic-art/22980/68636/Structures-of-the-pancreas). Date of access: 2008, 1 July.
3. [http://www.elm.manchester.ac.uk/pub\\_projects/2000/mnby71c2/pancreas.htm](http://www.elm.manchester.ac.uk/pub_projects/2000/mnby71c2/pancreas.htm). Date of access: 2008, 9 July.
4. [http://bass.bio.uci.edu/~hudel/bs99a/lecture26/lecture7\\_3.html](http://bass.bio.uci.edu/~hudel/bs99a/lecture26/lecture7_3.html). Date of access: 2008, 15 June.
5. [http://diabetesnet.com/diabetes\\_complications](http://diabetesnet.com/diabetes_complications). Date of access: 2008, 15 June.
6. Standards of medical care in diabetes-2008. *Diabetes Care* 2008;31 Suppl 1:S12-54.
7. <http://www.nlm.nih.gov/medlineplus/ency/imagepages/19713.htm>. Date of access: 2008, 25 June.
8. <http://diabetes.niddk.nih.gov/dm/pubs/neuropathies>. National Institute of Diabetes and Digestive and Kidney Diseases. Diabetic Neuropathies: The Nerve Damage of Diabetes. Date of access: 2008, 9 July
9. Masharani U. Diabetic coma diabetic ketoacidosis. Diabetic ketoacidosis. American Medical Network 2006.
10. The effect of intensive treatment of diabetes on the development and progression of long-term complications in insulin-dependent diabetes mellitus. The Diabetes Control and Complications Trial Research Group. *N Engl J Med* 1993;329:977-986.



11. Nathan DM, Cleary PA, Backlund JY, Genuth SM, Lachin JM, Orchard TJ *et al.* Intensive diabetes treatment and cardiovascular disease in patients with type 1 diabetes. *N Engl J Med* 2005;353:2643-2653.
12. <http://www.nlm.nih.gov/medlineplus/ency/imagepages/18035.htm>. Date of access: 2008, 28 June
13. Wiseman ACG, Peter. Transplant therapies for diabetes: a review of outcomes and indications for kidney, pancreas and islet transplantation. *Diabetes and the endocrine pancreas II. Current Opinion in Endocrinology & Diabetes* 2006;13:338-343.
14. National Institute of Health. *Stem Cells: Scientific Progress and Future Research Directions*. 2001; Chapter 7.
15. Nanji SA, Shapiro AM. Advances in pancreatic islet transplantation in humans. *Diabetes Obes Metab* 2006;8:15-25.
16. Bonner-Weir S, Weir GC. New sources of pancreatic beta-cells. *Nat Biotechnol* 2005;23:857-861.
17. Beattie GM, Otonkoski T, Lopez AD, Hayek A. Functional beta-cell mass after transplantation of human fetal pancreatic cells: differentiation or proliferation? *Diabetes* 1997;46:244-248.
18. Humphrey RK, Bucay N, Beattie GM, Lopez A, Messam CA, Cirulli V *et al.* Characterization and isolation of promoter-defined nestin-positive cells from the human fetal pancreas. *Diabetes* 2003;52(10):2519-2525.
19. de la Tour D, Halvorsen T, Demeterco C, Tyrberg B, Itkin-Ansari P, Loy M *et al.* Beta-cell differentiation from a human pancreatic cell line in vitro and in vivo. *Mol Endocrinol* 2001;15:476-483.

20. Itkin-Ansari P, Demeterco C, Bossie S, de la Tour DD, Beattie GM, Movassat J *et al.* PDX-1 and cell-cell contact act in synergy to promote delta-cell development in a human pancreatic endocrine precursor cell line. *Mol Endocrinol* 2000;14:814-822.
21. Kayali AG, Flores LE, Lopez AD, Kutlu B, Baetge E, Kitamura R *et al.* Limited capacity of human adult islets expanded in vitro to redifferentiate into insulin-producing beta-cells. *Diabetes* 2007;56:703-708.
22. Bonner-Weir S, Taneja M, Weir GC, Tatarkiewicz K, Song KH, Sharma A *et al.* In vitro cultivation of human islets from expanded ductal tissue. *Proc Natl Acad Sci USA* 2000;97:7999-8004.
23. Yatoh S, Dodge R, Akashi T, Omer A, Sharma A, Weir GC *et al.* Differentiation of affinity-purified human pancreatic duct cells to beta-cells. *Diabetes* 2007;56:1802-1809.
24. Zulewski H, Abraham EJ, Gerlach MJ, Daniel PB, Moritz W, Muller B *et al.* Multipotential nestin-positive stem cells isolated from adult pancreatic islets differentiate ex vivo into pancreatic endocrine, exocrine, and hepatic phenotypes. *Diabetes* 2001;50:521-533.
25. Mountford P, Nichols J, Zevnik B, O'Brien C, Smith A. Maintenance of pluripotential embryonic stem cells by stem cell selection. *Reprod Fertil Dev* 1998;10:527-533.
26. Roche E, Ensenat-Waser R, Vicente-Salar N, Santana A, Zenke M, Reig JA. Insulin-producing cells from embryonic stem cells experimental considerations. *Methods Mol Biol* 2007;407:295-309.
27. Boyd AS, Wu DC, Higashi Y, Wood KJ. A comparison of protocols used to generate insulin-producing cell clusters from mouse embryonic stem cells. *Stem Cells* 2008;26:1128-1137.

28. Soria B, Roche E, Berna G, Leon-Quinto T, Reig JA, Martin F. Insulin-secreting cells derived from embryonic stem cells normalize glycemia in streptozotocin-induced diabetic mice. *Diabetes* 2000;49:157-162.
29. Shim JH, Kim SE, Woo DH, Kim SK, Oh CH, McKay R *et al*. Directed differentiation of human embryonic stem cells towards a pancreatic cell fate. *Diabetologia* 2007;50:1228-1238.
30. Meloche RM. Transplantation for the treatment of type 1 diabetes. *World J Gastroenterol* 2007;13:6347-6355.
31. Shapiro AM, Lakey JR, Ryan EA, Korbitt GS, Toth E, Warnock GL *et al*. Islet transplantation in seven patients with type 1 diabetes mellitus using a glucocorticoid-free immunosuppressive regimen. *N Engl J Med* 2000;343:230-238.
32. Shapiro AM, Lakey JR, Paty BW, Senior PA, Bigam DL, Ryan EA. Strategic opportunities in clinical islet transplantation. *Transplantation* 2005;79:1304-1307.
33. Ryan EA, Paty BW, Senior PA, Bigam D, Alfadhli E, Kneteman NM *et al*. Five-year follow-up after clinical islet transplantation. *Diabetes* 2005;54:2060-2069.
34. Ryan EA, Bigam D, Shapiro AM. Current indications for pancreas or islet transplant. *Diabetes Obes Metab* 2006;8:1-7.
35. Kizilel S, Garfinkel M, Opara E. The bioartificial pancreas: progress and challenges. *Diabetes Technol Ther* 2005;7:968-985.
36. Desai TA, West T, Cohen M, Boiarski T, Rampersaud A. Nanoporous microsystems for islet cell replacement. *Adv Drug Deliv Rev* 2004;56:1661-1673.
37. Li RH. Materials for immunoisolated cell transplantation. *Adv Drug Deliv Rev* 1998;33:87-109.

38. Lanza RP, Jackson R, Sullivan A, Ringeling J, McGrath C, Kuhlreiber W *et al.* Xenotransplantation of cells using biodegradable microcapsules. *Transplantation* 1999;67:1105-1111.
39. de Vos P, Hamel AF, Tatarkiewicz K. Considerations for successful transplantation of encapsulated pancreatic islets. *Diabetologia* 2002;45:159-173.
40. Tatarkiewicz K, Hollister-Lock J, Quickel RR, Colton CK, Bonner-Weir S, Weir GC. Reversal of hyperglycemia in mice after subcutaneous transplantation of macroencapsulated islets. *Transplantation* 1999;67:665-671.
41. Figliuzzi M, Cornolti R, Plati T, Rajan N, Adobati F, Remuzzi G *et al.* Subcutaneous xenotransplantation of bovine pancreatic islets. *Biomaterials* 2005;26:5640-5647.

## Chapter 2

### Set-up of methods for islet isolation

#### 1.5 Rat islet isolation

*1.5.1 Manual procedure – materials and methods*

*1.5.2 Automatic procedure - materials and methods*

*1.5.3 Islet viability*

*1.5.4 Results*

#### 1.6 Bovine islet isolation

*1.6.1 Manual procedure – materials and methods*

*1.6.2 Automatic procedure - materials and methods*

*1.6.3 Results*

#### 1.7 Human islet isolation

*1.7.1 Manual procedure – materials and methods*

*1.7.2 Automatic procedure - materials and methods*

*1.7.3 Results*

### References

## Set-up of methods for islet isolation

The concept of transplanting islet tissue in diabetic patients is not new. The earliest case of transplanting a slice of sheep pancreas into the thigh of a dying diabetic child took place in 1893 (1), but the discovery of insulin in 1922 changed the treatment significantly (2). Many researchers began to believe that a cure for the disease had been found since deaths rate of diabetics reduced considerably. However, secondary complications resulting from diabetes are severe and now are the leading cause of morbidity and mortality; hence, a need to find a suitable alternative to the use of exogenous insulin injections is necessary. Many of the complications resulting from diabetes include blindness, kidney failure, male impotence, myocardial infarction, gangrene (and thus amputation) and death. Two events, which took place between 1965 and 1970, gave a boost to research in islet transplantation. Moskalewski published his preliminary work (3), which was followed by that of Lacy (4) in which methods to obtain islets using collagenase digestion were presented. Setting up a method to obtain islets that could be implanted into a diabetic patient minimizes the risk of infection due to exogenous injection. Avoiding non-function of the implant though, has to be the first step.

Before islets can be transplanted, important parameters such as islet yield, islet viability, islet purity and islet sterility need to be assessed. All these factors are mainly controlled by the islet isolation procedure. Transplantation of highly purified islets also has potential advantages of increased safety, reduced immunogenicity of the graft, and improved islet implantation. Presence of impurities adds to an immune response to the implant increasing chances of rejection. For these reasons, purity is an important factor in the final outcome; islet preparations with only the highest purity should be used for transplantation purposes.

Viability of islets is affected by many variables, such as procurement of suitable pancreas, separating enzymes used, digestion time, solutions used in the isolation process, islet purification solutions and forces that act upon them during the isolation process. Since viability is a measure of the cells' effectiveness and state outside the host, it is the main indication of how they will fare inside the host, thus a major factor in success of cell transplantation. It is crucial that isolated islets should not only be viable but also they should respond appropriately to glucose challenge.

A manual method for islet isolation has been first set-up in our laboratory. To improve the number of the islets obtained, an automated method was then introduced. The procedure applied meets the following requirements: 1) minimal traumatic injury to the islets, 2) continuous digestion in which islets progressively liberated could be saved from further enzymatic action, 3) minimal human intervention in the digestion process, and 4) high yield and purity of the isolated islets. Introduction of the automated method for islet isolation resulted in significantly higher yield.

## 2.1 Rat islet isolation

Initially, a manual procedure for digestion of rat pancreas was set up for islet isolation from one or two pancreata of Lewis rats (rat body weight 250-300g).

### *2.1.1 Manual procedure – materials and methods*

#### Solutions used

Collagenase solution: 30 ml collagenase P (0.3 mg/ml) in HBSS at 4°C

Foetal calf serum (heat-inactivated): 1 x 100 ml at 4°C

HBSS 1x + 10% foetal calf serum

HBSS 1x + 2% foetal calf serum

Dithizone solution: (25 ml at 4°C)

- a. 50 mg dithizone
- b. 5 ml DMSO
- c. 15 ml HBSS

Histopaque 1.077: 30 ml at 4°C,  $\delta = 1.077$

Cell culture medium: (1 x 500 ml)

- a. 45.5 ml RPMI 1640 + L-glutamine
- b. 5 ml FCS inactivated
- c. 0.5 ml penicillin/streptomycin



*Pancreas preparation (Figure 2.1)*

Rats weighing 200-215 g were anaesthetized with an intraperitoneal injection of sodium pentobarbital. After main bile duct location at its entrance into the gut, it was ligated with silk suture. The duct was cannulated with polyethylene tubing (PE 50) connected to a 22-gauge cannula and the rat was killed. The pancreas was distended by introduction of 10-12 ml of collagenase solution, was dissected free from the small bowel, stomach and spleen, removed and rinsed in a centrifuge tube containing 15 ml of cold HBSS

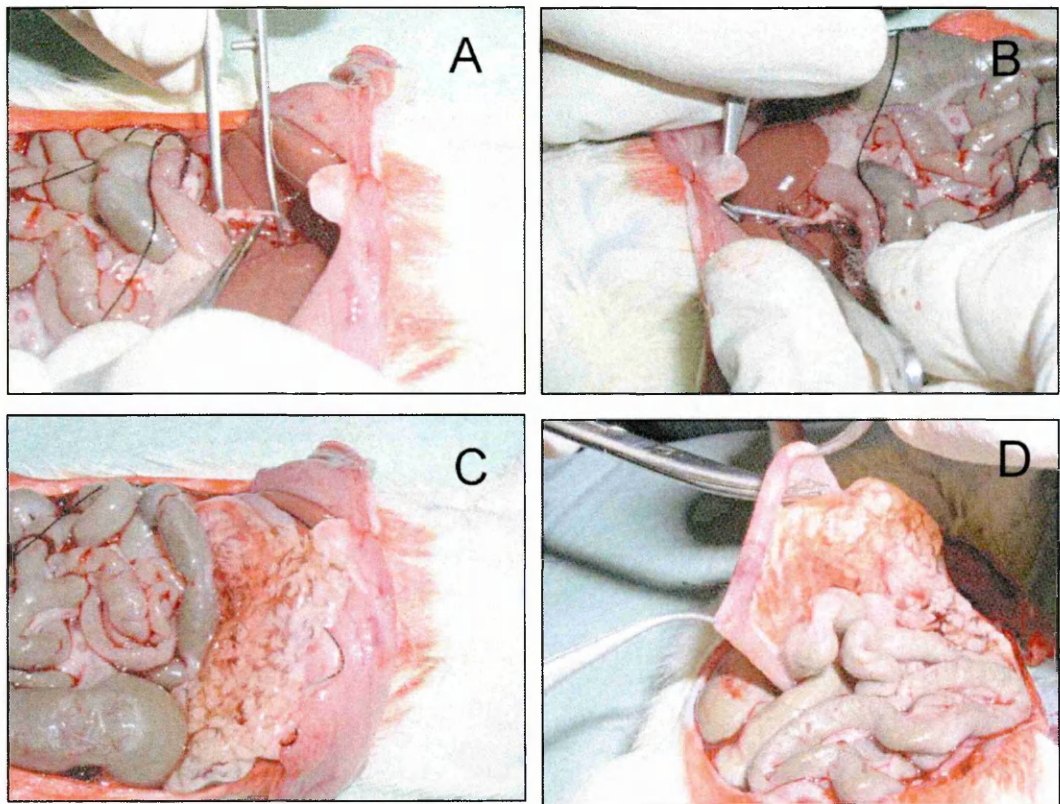


Figure 2.1 Pancreatic duct identified (A) and cannulated near the hilus of the liver (B). The main pancreatic duct was legated at the duodenal junction and 10 ml of cold collagenase was injected (C). The distended pancreas was dissected from the duodenum (D).

### Pancreas digestion

All manipulations were performed in a class 100 biological safety cabinet. The distended pancreas was cut into small pieces and these were loaded into the centrifuge tube containing collagenase solution and were incubated in a shaking water-bath at 37°C. Every four to five minutes the centrifuge tube was shaken for 5 seconds and 0.5 ml sample was put into 35 mm petri dish to monitor dissociation of the tissue, microscopically, after staining the samples with 0.5 ml of dithizone solution. Digestion was stopped by addition of ice cold HBSS containing 10% heat-inactivated foetal calf serum. A stainless steel mesh was inserted into the beaker (1L) on ice and digested tissue was passed through the stainless steel mesh and then collected into the cooled centrifuge tubes. Tubes were centrifuged for 2 min at 800 rpm at 4°C (digested tissue washing, 3 times).

### Islet purification

Pellets were collected and resuspended in 30 ml of Histopaque (1.077 density, 1 ml of pellet in 30 ml of Histopaque) and slowly 20 ml of HBSS containing 2% of FCS was added. The mixture was centrifuged for 5 minutes at 1800 rpm and 4°C.

Islets were situated in the interface between HBSS and Histopaque and purified islet fractions were centrifuged in 50 ml tubes containing cold HBSS + 2% FCS for 2 min at 1500 rpm at 4°C. Supernatant was discarded and washing was repeated for 2 min at 800 rpm at 4°C.

### Islet counting

Taking 200 µl samples of the islet suspension in triplicate, into 35 mm petri dishes, staining with 200 µl of dithizone was performed. Islets were counted using a microscope with an eyepiece containing a calibrated grid.

*Islet culture*

Islets were finally resuspended in 8 ml of cell culture medium and were plated in one untreated 25 cm<sup>2</sup> tissue culture flask. Then they were incubated overnight at 37°C in 5% CO<sub>2</sub>

**2.1.2 Automatic procedure – materials and methods**

To improve islet number obtained from a rat pancreas, a procedure was developed based on the automated method introduced by Ricordi and colleagues (Figure 2.2) (5), and has been used to process 10-14 pancreata of Lewis rats (rat body weight 250-300g).

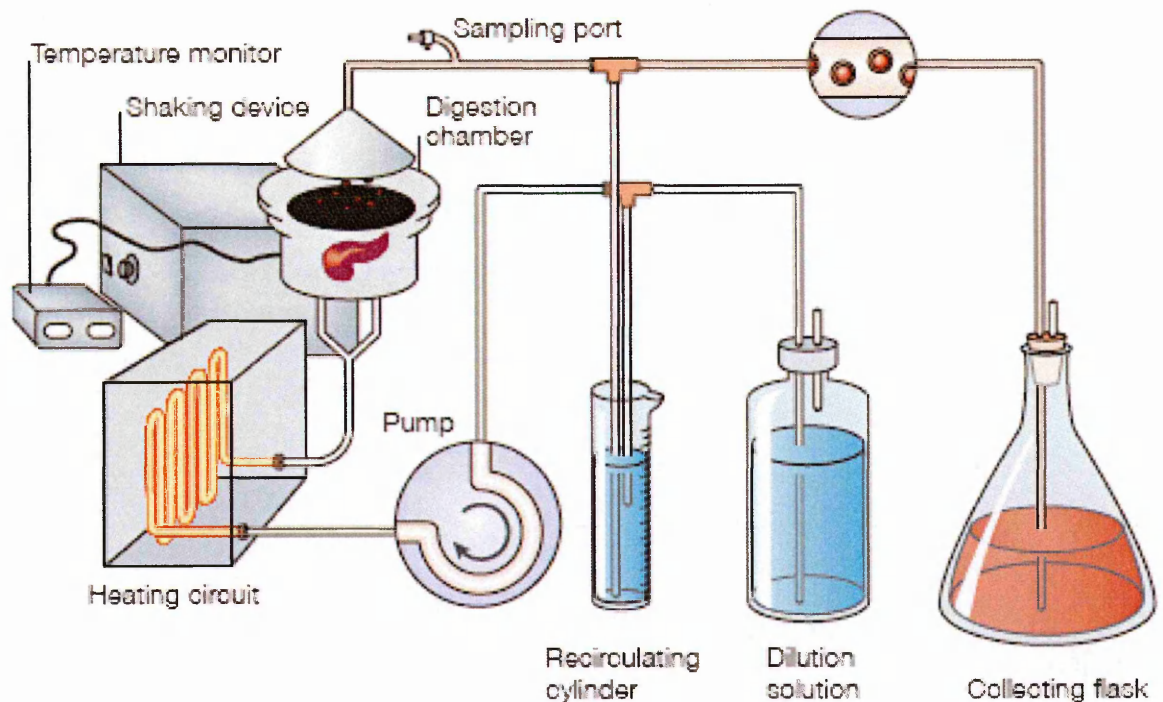


Figure 2.2 Schematic representation of the automated circuit for pancreas digestion and islet isolation, modified from (6)

To ameliorate enzyme perfusion and digestion of acinar pancreas, perfusion system and digestion chamber were modified. The components were designed and constructed.

Modification of the digestion chamber was made consisting of two holes on the base of the chamber inclined at  $45^\circ$  from each other, thus allowing good agitation of the solution and better digestion of the pancreas. A finite element model of the chamber for fluidodynamic simulation (Figure 2.3) was developed using CFD software (Fluent 6.1, FLUENT Inc.) (7).

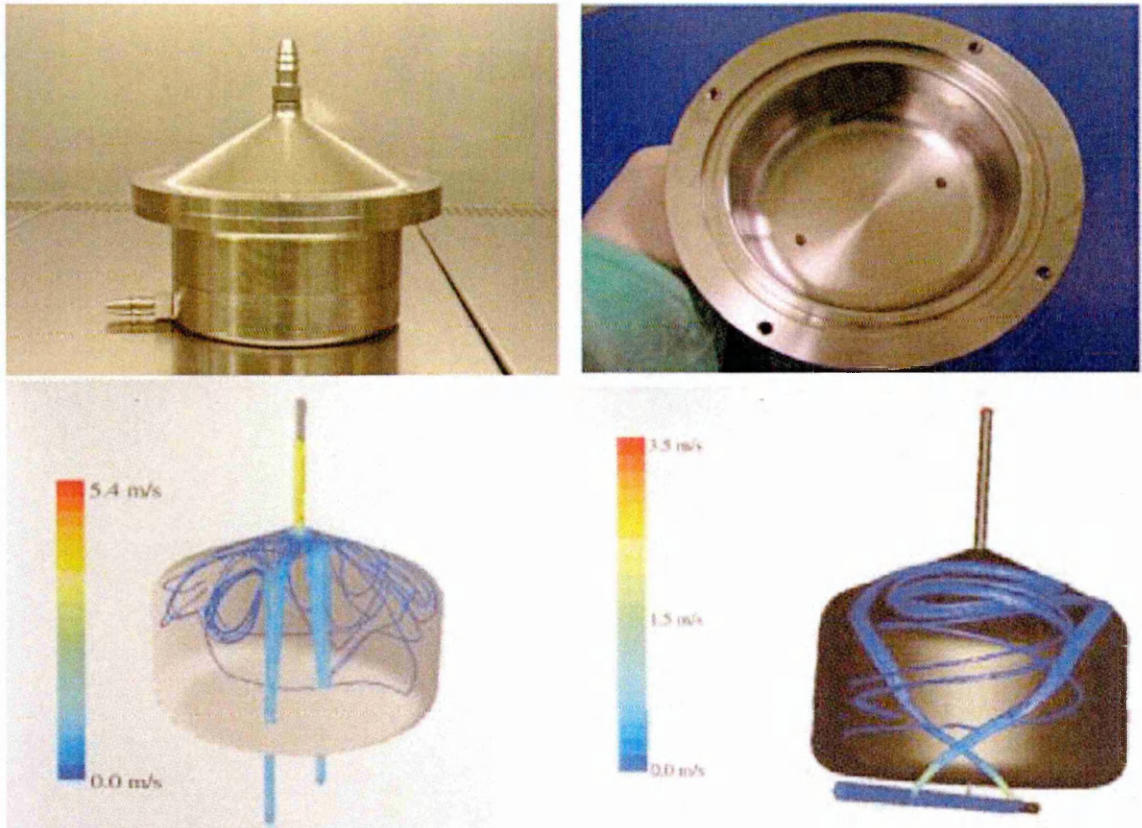


Figure 2.3 Modified digestion chamber of stainless steel 316. Comparison between finite element models of the chamber for fluidodynamic simulation of Ricordi's (5) chamber and the new one described here

### Solutions used

Collagenase solution: 750 ml collagenase P (0.3 mg/ml) in HBSS at  $4^\circ\text{C}$ ,

Eurocollins (500 ml)

Foetal calf serum (heat-inactivated): 1 x 100 ml at  $4^\circ\text{C}$



HBSS 1x + 10% foetal calf serum

HBSS 1x + 2% foetal calf serum

Dithizone Solution: (25 ml at 4°C)

- a. 50 mg dithizone
- b. 5 ml DMSO
- c. 15 ml HBSS

Histopaque 1.077: 30 ml at 4°C,  $\delta = 1.077$

Cell culture medium: (1 x 500 ml)

- a. 45.5 ml RPMI 1640 + L-glutamine
- b. 5 ml FCS inactivated
- c. 0.5 ml penicillin/streptomycin

### *Pancreas preparation*

Pancreas preparation was as described above for the manual procedure, page 52.

### *Pancreas digestion*

All manipulations were performed in a class 100 biological safety cabinet. Distended pancreas was cut into small pieces and since they leaked collagenase solution, four stainless steel ball bearings were loaded into the digestion chamber. A 500  $\mu\text{m}$  stainless steel mesh was inserted inside the chamber and the cover was closed. The peristaltic pump was activated with a flow rate of 410 ml/min and the system was filled with collagenase solution passing through a heating circuit to ensure a stable temperature of 35-37°C during the digestion process; collagenase solution recirculated continuously at 410 ml/min

Every four to five minutes the chamber was shaken for 5 seconds and 0.5 ml sample was put into 35 mm petri dish to monitor microscopically dissociation of tissue, after staining

the samples with 0.5 ml dithizone solution. Digestion continued until acinar tissue free of islets appeared in the samples, and when significant numbers of cleaved islets appeared digestion was ended. After opening the circuit, ice cold HBSS containing 10% heat-inactivated FCS was flushed through and digested tissue was collected, inserting the end of the outlet tube into cooled 250 ml conical tubes, until no more islets appeared in samples. Tubes filled with digested tissue were centrifuged for 2 min at 1000 rpm at 4°C (washing for three times)

*Islet purification and counting*

This method was as described above for the manual procedure, page 53.

*Islet culture*

Islets were finally resuspended in 25 ml of cell culture medium and were plated in one untreated 75 cm<sup>2</sup> tissue culture flask. Finally, they were incubated overnight at 37°C in 5% CO<sub>2</sub>

### ***2.1.3 Islet viability***

#### ***Staining solutions used***

Propidium iodide (PI) stock solution: 20.1 mg propidium iodide was dissolved in 200 ml PBS.

Acridine orange (AO) stock solution: 1 mg acridine orange was dissolved in 200 ml PBS.

1 part of PI and 1 part of AO were mixed.

#### ***Procedure***

10-50 islets were transferred together with 50  $\mu$ l culture medium into a well of a 96-well flat-bottom plate. 100  $\mu$ l propidium iodide/acridine orange staining solution was added. The plate was incubated for about 10 min at room temperature with occasional shaking. Islets were transferred to petri dishes with 5 ml culture medium, and then into a glass blood counting chamber. Using a fluorescence microscope, islets were illuminated with light from the rhodamine filter for red staining of nuclei of dead cells and light from the FITC-filter for green staining of cytoplasm of living cells.

### 2.1.4 Results

The number of islets isolated *per* rat pancreas significantly increased after introducing the automatic procedure (Figure 2.4). Moreover, manual islet isolation of 2 pancreata involved around half-one day's work, during which 12 pancreata could be isolated using the automatic procedure.

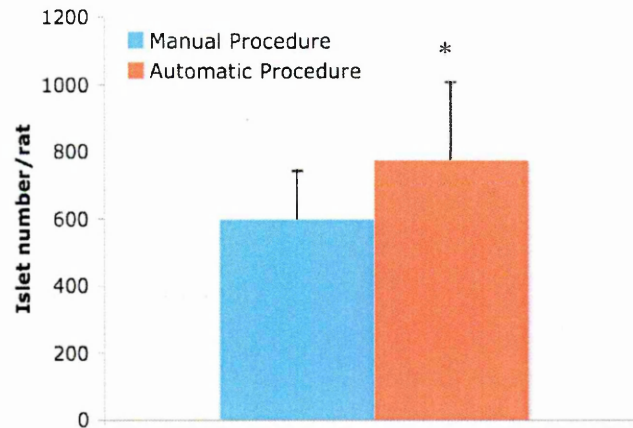


Figure 2.4 Islet number *per* rat pancreas obtained utilizing manual (blue) or automatic (red) procedure,

\*  $p < 0.01$

Considering morphology (microscopic appearance, Figure 2.5) and viability (propidium iodide - orange acridine staining, Figure 2.6) of islets obtained, there were no quality differences between the two alternative methods used.

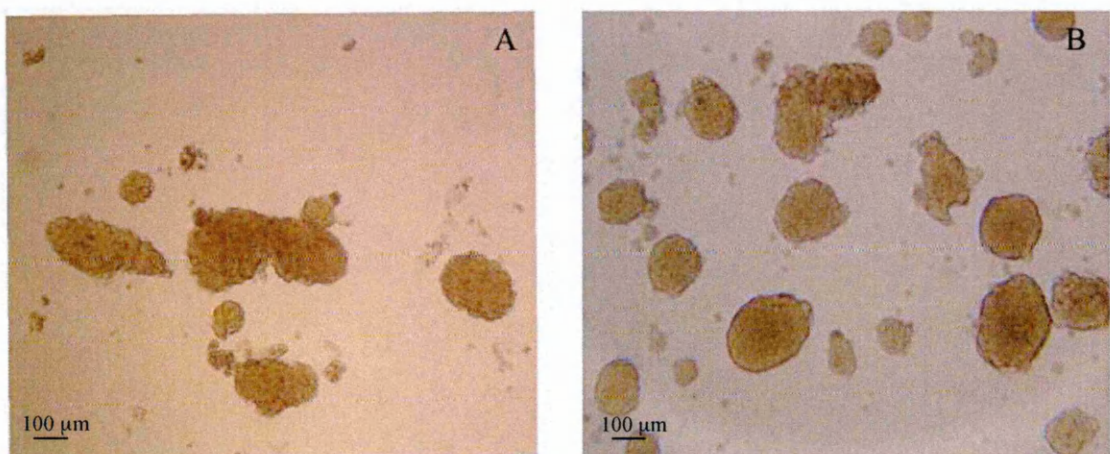


Figure 2.5 Optical imaging of islets isolated using manual (A) or automatic (B) procedures



For viability of islets, fluorescent dyes such as propidium iodide were used. It is excluded from intact cells but permeates through membranes of dead or dying cells, which bind and stain nucleic acids (red fluorescence) intensely. Living cell cytoplasm can be counterstained (green) using non-polar substances such as fluoresceine diacetate, calcein or others that are hydrolyzed and accumulate in living cells. Acridine orange, at high concentration stains nucleic acids orange, but at low concentration it is an excellent green stain for cytoplasm of living cells (Figure 2.6) (8).

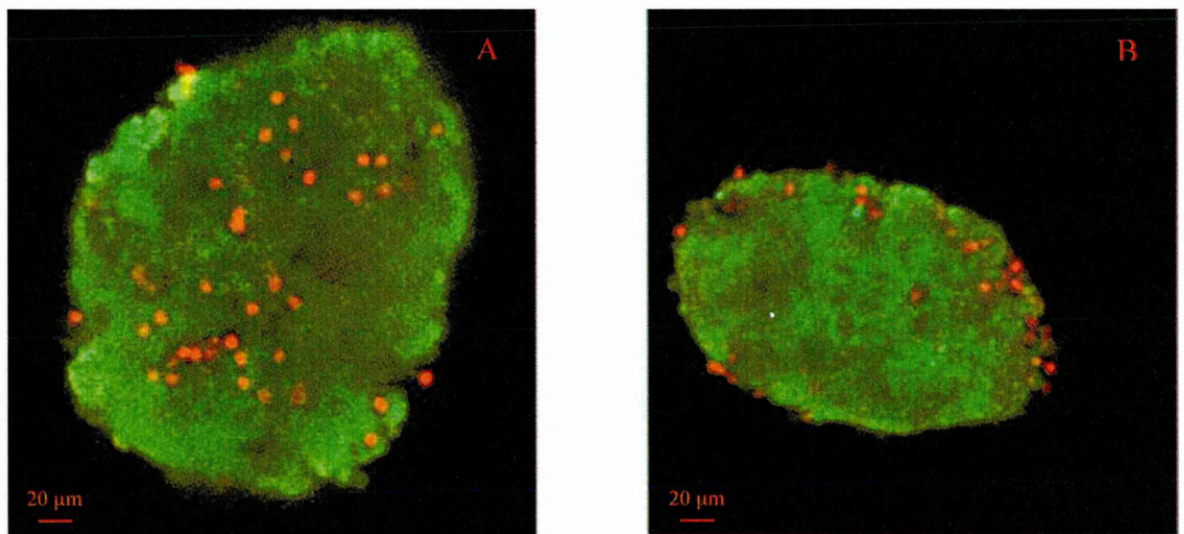


Figure 2.6 Propidium iodide (red) – acridine orange (green) staining of islets isolated by manual (A) or automatic (B) procedures

## 2.2 Bovine islet isolation

Islets were isolated from pancreas obtained from 6-month-old calves (9). Although porcine islets have been considered to be a good source for xenogenic transplantation, they have been shown in the laboratory to be fragile and their isolation is inconsistent because of loss of viability and islet fragmentation (10). Very recently, it has been shown that pancreas from the adult pig is more suitable for islet isolation and shows a higher degree of viability than that of piglets (11). It has also been shown previously that bovine islets can be isolated efficiently from pancreas and that they demonstrate satisfactory function *in vitro* and *in vivo* (12). The main advantage in using bovine pancreas is related to easier access to the organ. Thus, for porcine pancreas one must avoid conventional animal processing, at the slaughterhouse, that involves lengthy ischaemia time. On the contrary, harvesting bovine pancreas is feasible during conventional slaughtering with an acceptable time of ischaemia.

### ***2.2.1 Manual procedure – materials and methods***

The technique established in our laboratory is based on manual passage of the tissue through different sized stainless steel meshes.

#### ***Solutions used***

Collagenase solution: 800 ml collagenase P (2.7 U) in HBSS at 4°C

Eurocollins (500 ml)

Foetal calf serum (FCS heat-inactivated) at 4°C

HBSS 1x + 10% or 2% FCS

Histopaque 1.077: 30 ml at 4°C,  $\delta = 1.077$

Cell culture medium: (1 x 500 ml)

- a. 44.5 ml M199 1x 1640 + L-glutamine
- b. 5 ml FCS
- c. 0.5 ml penicillin/streptomycin

#### ***Pancreas preparation***

After pancreas explantation from 6-month-old calves at the slaughterhouse, it was taken as quickly as possible to the laboratory; there, all manipulations were performed in a class 100 biological safety cabinet. Its sterile bag was opened and the gland was removed from the transport solution. Peripancreatic fat, lymphnodes and vessels were removed. The organ was weighed and the major pancreatic duct was cannulated with an 18-23 gauge needle.

#### ***Pancreas distension and digestion***

After pancreas distension by intraductal injection of the collagenase P solution, it was cut into small pieces. Pancreas pieces and the leaked collagenase solution were loaded into an

airtight case and incubated in a shaking water-bath at 37°C. Every four to five minutes the centrifuge tube was shaken for 5 seconds and a 0.5 ml sample was put into a 35 mm petri dish to monitor dissociation of the tissue under the microscope. Digestion was stopped by addition of ice cold HBSS containing 10% FCS. Two stainless steel meshes (500 µm and 90 µm) were inserted one above the other. The digested tissue was passed through the stainless steel mesh and then collected from the 90 µm stainless steel meshes into cooled centrifuge tubes. Tubes were centrifuged for 2 min at 800 rpm at 4°C (digested tissue washed 3 times)

#### *Islet purification*

The pellet was resuspended in 30 ml of Histopaque (1.077 density, 1 ml of pellet in 30 ml of Histopaque) and slowly 20 ml of HBSS containing 2% of FCS was added. The mixture was centrifuged for 5 minutes at 1800 rpm at 4°C. Islets were situated in the interface between HBSS and Histopaque and purified islet fractions were centrifuged in a 50 ml tube containing cold HBSS + 2% FCS for 2 min at 1500 rpm at 4°C. Supernatant was discarded and washing was repeated for 2 min at 800 rpm at 4°C.

#### *Islet counting*

Taking 200 µl samples of islet suspension in triplicate, into 35 mm petri dishes, islets were counted under a microscope using an eyepiece containing a calibrated grid. Each counted islet was classified into size range according to mean estimated diameter. The islet equivalent number was calculated utilizing corresponding conversion factors (5). Islets smaller than 50 µm were not considered for counting.

<b>Islet diameter (range in <math>\mu\text{m}</math>)</b>	<b>Conversion factor</b>
50 – 100	0.16
100 – 150	0.66
150 - 200	1.7
200 - 250	3.5
250 - 300	6.3
300 - 350	10.4
> 350	15.8

### Islet culture

25,000 islet equivalents were finally resuspended in 25 ml of cell culture medium and were plated in one untreated 75 cm<sup>2</sup> tissue culture flask. Finally, they were incubated overnight at 37 °C in 5% CO<sub>2</sub>

### ***2.2.2 Automatic procedure – Materials and methods***

Overall strategy-governing optimization of the automated method for islet isolation began with the notion that islets must be liberated from surrounding exocrine tissues by enzymatic and not mechanical forces. To limit adverse effects on islets during the isolation protocol, processing time was minimized. The technique described readily allows three people to complete the procedure from arrival of the pancreas at the islet laboratory to time when islets were placed in culture.

#### ***Solutions used***

Collagenase solution: 800 ml collagenase P (2.7 U) in HBSS at 4°C

Eurocollins (500 ml)

University of Wisconsin solution (UW)

Foetal calf serum (FCS, heat-inactivated): 1 x 100 ml at 4°C

HBSS 1x + 10% FCS

HBSS 1x + 2% FCS

Histopaque 1.077: 30 ml at 4°C,  $\delta = 1.077$

Cell culture medium: (1 x 500 ml)

- a. 45.5 ml M199 1x 1640 + L-glutamine
- b. 5 ml FCS inactivated
- c. 0.5 ml penicillin/streptomycin

#### ***Pancreas preparation***

Preparation of the pancreas was as described above, page 62.

### Pancreas distension and digestion

After pancreas distension by intraductal injection of collagenase P solution, the pancreas was cut into small pieces. Pancreas pieces, the leaked collagenase solution and stainless steel ball bearings were loaded into the digestion chamber. Peristaltic pump was activated with a flow rate of 410 ml/min and the system was filled with collagenase solution passing through a heating circuit for a stable temperature of 35-37°C during the digestion process. Continuously collagenase solution recirculated at 410 ml/min. Every four to five minutes the chamber was shaken for 5 seconds and a 0.5 ml sample was put into a 35 mm petri dish to monitor dissociation of the tissue under the microscope. Digestion continued until acinar tissue free of islets appeared in the samples. When significant numbers of cleaved islets appeared the digestion was stopped. After opening the circuit, ice cold HBSS containing 10% FCS was flushed through. The digested tissue was collected inserting the end of the outlet tube into cooled 175 ml conical tubes, until no more islets appeared. Tubes filled with digest tissue were centrifuged for 2 min at 1000 rpm at 4°C (washing for three times). Pellets were resuspended in UW solution for 25-40 minutes.

### Islet purification

The UW pre-incubated tissue was centrifuged for 2 min at 1000 rpm at 4°C and then resuspended in 260 ml of Histopaque. Histopaque dissolved tissue was loaded at 40 ml/min into spinning COBE 2991 (blood cell processor, Figure 2.7). 140 ml of HBSS was added and spun for 5 min. 30 ml fractions of the gradient was collected in conical tubes on ice and centrifuged for 2 minutes at 1500 rpm. All fractions were pooled in a conical tube and resuspended in 100 ml of M199 + 10% FCS.

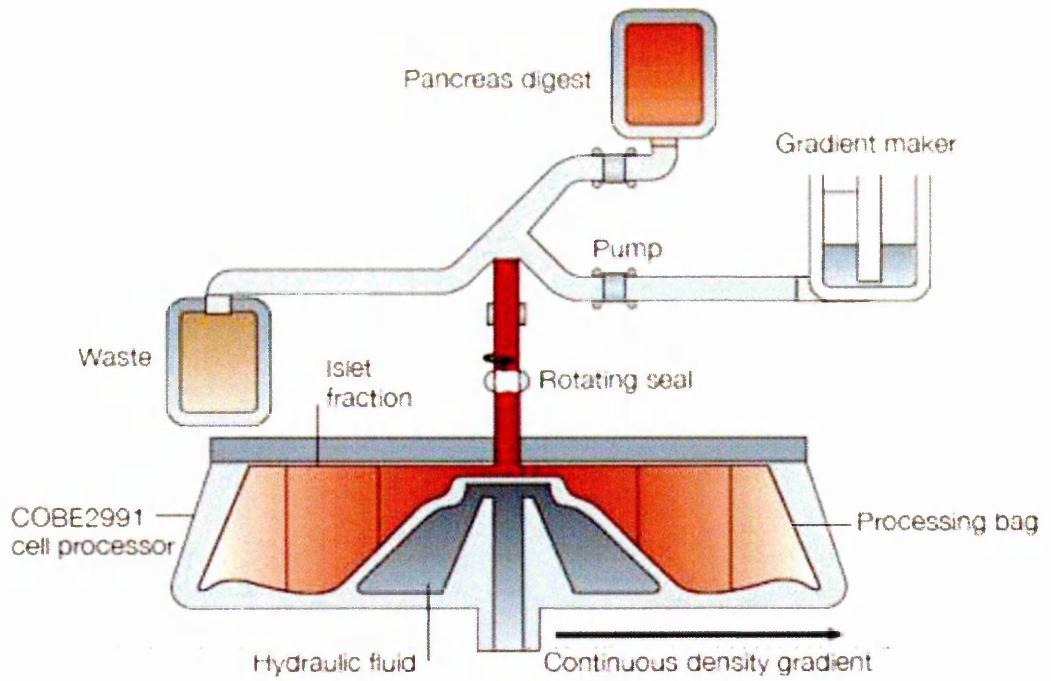


Figure 2.7 Purification carried out by density-gradient separation of islets, using a COBE 2991 cell processor

Islet counting and culture

Islet culture and counting were performed as described previously, page 63.



### 2.2.3 Results

The novel techniques introduced here improved the outcome of bovine islet isolation; numbers of islets isolated significantly increased with the automated procedure (Figure 2.8).

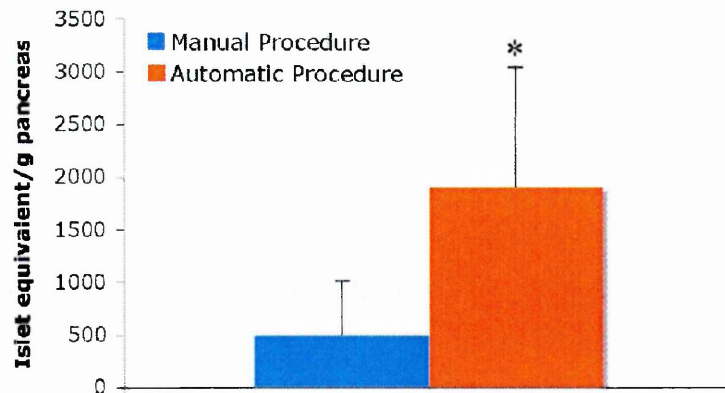


Figure 2.8 Islet equivalent *per gram* of pancreas obtained utilizing manual or automated procedure, \*  $p < 0.01$

These results opened the possibility of obtaining a large number of islets for implantation in diabetic models for studying, for example immunorejection. Moreover, such islets can be used for testing immunoisolation devices of xenotransplantation.

### 2.3 Human islet isolation

Interest in islet grafting as a potential alternative to whole-pancreas transplantation has been growing. There is an increase in the number of new centres, with at least 40 more sites currently in development in the world. In our laboratory, a programme of human islet allotransplantation has been initiated. The first phase of this has set-up a safe and secure method for islet isolation. An air-filtered room plus instruments dedicated to this particular procedure are used exclusively (Figure 2.9). A detailed description of the Standard Operating Procedure for the automatic process and a project of the Human Islet Laboratory are specified in Appendix B and C.

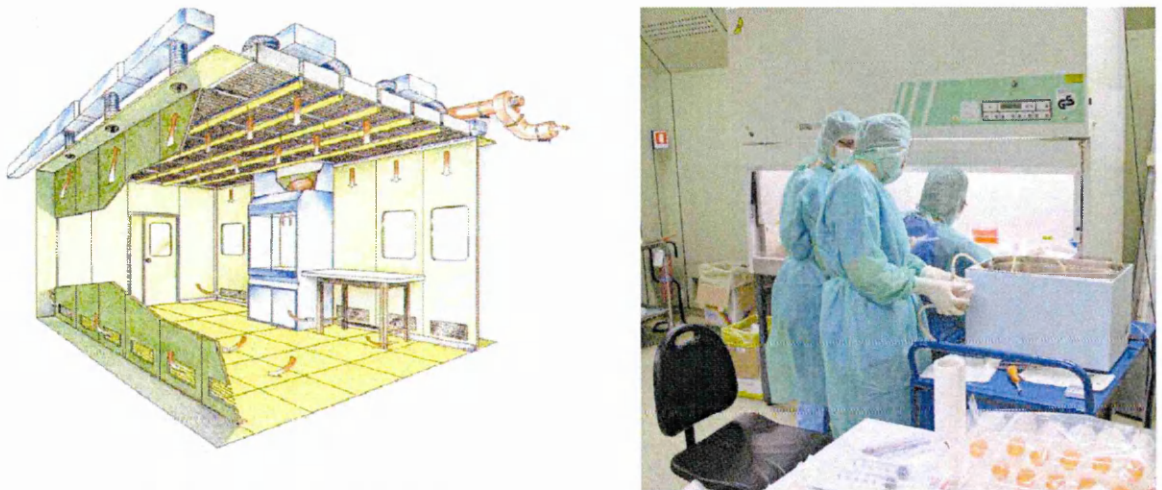


Figure 2.9 Scheme and photograph of the air-filtered room for human islet isolation

### ***2.3.1 Manual procedure – Materials and methods***

#### ***Solutions used***

Liberase solution: 800 ml Liberase P (3 U/mg) in HBSS at 4°C

Human serum albumin (HSA)

HBSS 1x + 10% HSA

HBSS 1x + 2% HSA

Histopaque 1.077: 30 ml at 4°C,  $\delta = 1.077$

Cell culture medium: (1 x 500 ml)

- a. 45.5 ml CMRL 1x + L-glutamine
- b. 5 ml HSA
- c. 0.5 ml penicillin/streptomycin

#### ***Pancreas preparation***

After pancreas explantation from the cadaveric donor at the hospital, tissue was taken as rapidly as possible to the laboratory. There, all manipulations were performed in a class 100 biological safety cabinet. Pancreas sterile bag was opened and the gland was removed from transport solution. Peripancreatic fat, lymph nodes and vessels were removed from the pancreas. Organ was weighted and the major pancreatic duct cannulated with a 18-23 gauge needle

### Pancreas distension and digestion

After pancreas distension by intraductal injection of the Liberase solution, pancreas was cut into small pieces. Pancreas pieces and the leaked collagenase solution were loaded into an airtight case and incubated in a shaking water-bath at 37°C. Every four to five minutes the centrifuge tube was shaken for 5 seconds and 0.5 ml sample was put into a 35 mm petri dish to monitor the dissociation of the tissue under the microscope, staining the samples with 0.5 ml of dithizone solution. Digestion was stopped by addition of ice cold HBSS containing 10% HAS. Two stainless steel meshes (500  $\mu\text{m}$  and 90  $\mu\text{m}$ ) were inserted one above the other. The digested tissue was passed through 500  $\mu\text{m}$  stainless steel mesh and then collected from the 90  $\mu\text{m}$  mesh into cooled centrifuge tubes. Tubes were centrifugated for 2 min at 800 rpm at 4°C (digested tissue washing 3 times)

### Islet purification

Pellets were resuspended in 30 ml of Histopaque (1.077 density, 1 ml of pellet in 30 ml of Histopaque) and slowly 20 ml of HBSS containing 2% of FCS was added. The mixture was centrifuged for 5 minutes at 1800 rpm and 4°C. Islets were situated in the interface between HBSS and Histopaque and purified islet fractions were centrifugated in 50 ml tube containing cold HBSS + 2% FCS for 2 min at 1500 rpm at 4°C. Supernatant was discarded and washing was repeated for 2 min at 800 rpm at 4°C.

### Islet counting

Taking 500  $\mu\text{l}$  samples in triplicate of the islet suspension into a 35 mm petri dish, islets were counted under a microscope with a calibrated grid in the eyepiece, staining samples with 0.5 ml of dithizone solution. Each counted islet was classified into size range according to its mean estimated diameter. The islet equivalent number was calculated

utilizing the corresponding conversion factor (13). Islets smaller than 50  $\mu\text{m}$  were not considered for counting.

Islet diameter (range in $\mu\text{m}$ )	Conversion factor
50 – 100	0.16
100 – 150	0.66
150 - 200	1.7
200 - 250	3.5
250 - 300	6.3
300 - 350	10.4
> 350	15.8

### Islet culture

25,000 islet equivalents were finally resuspended in 25 ml of cell culture medium and plated in one untreated 75  $\text{cm}^2$  tissue culture flask. Finally, they were incubated overnight at 37 °C in 5%  $\text{CO}_2$ .

### **2.3.2 Automatic procedure – Materials and methods**

#### Solutions used

Liberase solution: 350 ml Liberase in RPMI at 4°C

UW solution

HSA at 4°C

RPMI 1x + 10% or + 2% HSA

Biocoll 1.1: 250 ml at 4°C,  $\delta = 1.1$

Cell culture medium: (1 x 500 ml)

- a. 45.5 ml CMRL + L-glutamine
- b. 5 ml HSA
- c. 0.5 ml penicillin/streptomycin

### Pancreas preparation

Preparation of the pancreas was as described above, page 70.

### Pancreas distension and digestion

Pancreas was perfused by intraductal injection of the Liberase solution using the peristaltic pump at a pressure of around 80 mmHg, for 5 minutes, and then for an additional 5 minutes at 180 mmHg (Figure 2.10). After pancreas distension, it was cut into small pieces. The pancreas pieces, leaked Liberase solution and stainless steel ball bearings were loaded into the digestion chamber, inserting the 500  $\mu$ m stainless steel mesh inside, then the chamber cover was closed. The peristaltic pump was activated with a flow rate of 410 ml/min and the system was filled with RPMI solution passing through a heating circuit to achieve a stable temperature of 35-37°C during the digestion process.



Figure 2.10 Human pancreas perfusion using peristaltic pump

Continuously Liberase solution recirculated at 410 ml/min. Every four to five minutes the chamber was shaken for 5 seconds and 0.5 ml sample was put into 35 mm petri dish to monitor the dissociation of the tissue under the microscope, staining the samples with 0.5 ml of dithizone solution. Digestion continued until islet tissue free of acinar appeared in



the samples. When significant numbers of cleaved islets appear in the samples the digestion was stopped. After opening the circuit, ice cold RPMI containing 2% HSA was flushed through. Digested tissue was collected inserting the end of the outlet tube into the cooled 250 ml conical tubes, until no more islets appeared. Tubes filled with digested tissue were centrifuged for 2 min at 1000 rpm at 4°C (washing three times). Pellets were resuspended in UW solution and stored for 25-40 minutes

#### Islet purification

The UW pre-incubated tissue was centrifuged for 2 min at 1000 rpm at 4°C and then resuspended in 260 ml of Biocol 1.090. Using a gradient mixer, a linear gradient was created from 1.090 to 1.070, spinning for 5 min at 2700 rpm. 50 ml fractions of the gradient were collected in 250 ml tubes on ice and were centrifuged for 2 minutes at 1500 rpm. All fractions were pooled in a conical tube and were resuspended in 100 ml CMRL + 10% HSA and pooled all fractions in a conical tube

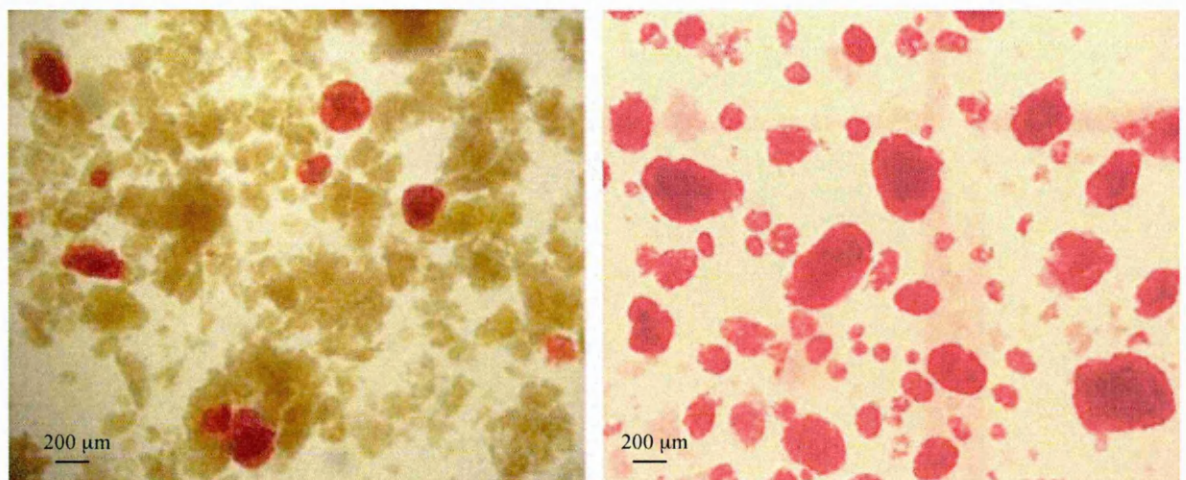


Figure 2.11 Human islets before and after purification (islet are stained in red by dithizone)

#### Islet counting and culture

Islet counting and culture were as described above, page 71-72.

### 2.3.3 Results

Also for human tissue, introduction of the automated procedure significantly improved the number of islets obtained from a pancreas (Figure 2.12).

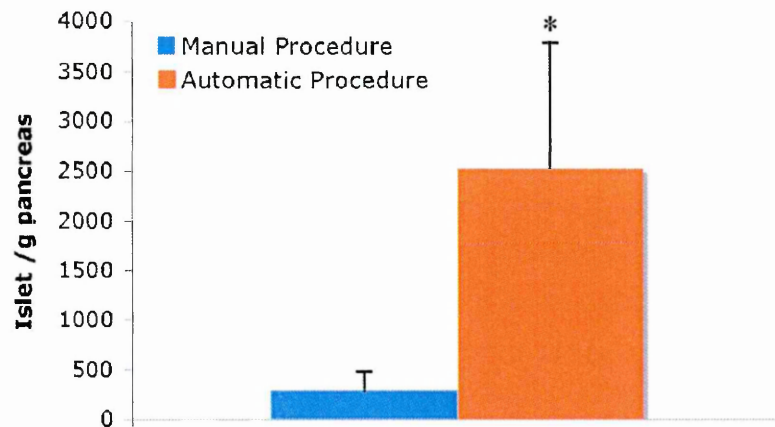


Figure 2.12 Islets per gram of human pancreas obtained utilizing manual or automated procedures, \*  $p < 0.01$

Despite initial enthusiasm concerning the use of islet transplantation as a cure for diabetes, the majority of patients with type 1 diabetes will still be more safely managed with repetitive insulin injections instead of facing potential risks of current anti-rejection therapies. Moreover clinical trials have shown that insulin independence does not exceed an average of 15 months and if compared to whole-pancreas transplantation, at 5 years only 10% of islet recipients are still insulin-independent compared with 90% of pancreas recipients (14). To achieve insulin independence, 850,000 islets were required in the Edmonton series of patients, suggesting that factors such as presence of autoimmunity and diabetogenic immunosuppression may have detrimental effects on islet engraftment and function. Additional drawbacks include complications of immunosuppression and nephrotoxicity with chronic treatment by Sirolimus and Tacrolimus therapy. However, clinical use of islet transplantation is limited by shortages in organ donation, need of immunosuppressive drugs and allosensitization of the patient. The need for relatively large



masses of insulin-producing cells to achieve insulin independence has led to the use of multiple donors (sequential or pooled islet preparations) *per* recipient. This may increase the risk for allosensitization to multiple anti-human leukocyte antigen (HLA) antibodies, limiting the possibility of future solid organ transplantation (15). For these reasons this procedure has been abandoned in our establishment, as being in the best interest of patients.

Development of immunoisolation techniques by separation of implanted cells from the host immune system has been recognized for a long time as an experimental strategy to prevent immunorecognition and rejection. Immunoisolation of islets for transplantation may have two potential benefits. First, it may permit allo-islet transplantation without the use of pharmacological immunosuppression and avoiding allosensitization of the patient. Secondly, encapsulation may facilitate transplantation of islets from non-human species (xenografts) thereby providing access to an unlimited source of insulin-producing tissue (16).

## References

1. Williams P. Notes on diabetes treated with extracts and grafts of sheep's pancreas. *British Medical Journal* 1894.
2. Banting FGBCH. The internal secretion of pancreas. *Journal of lab Clinical medicine* 1922.
3. Moskalewski S. Isolation and Culture of the Islets of Langerhans of the Guinea Pig. *Gen Comp Endocrinol* 1965;44:342-353.
4. Lacy PE, Kostianovsky M. Method for the isolation of intact islets of Langerhans from the rat pancreas. *Diabetes* 1967;16:35-39.
5. Ricordi C, Lacy PE, Finke EH, Olack BJ, Scharp DW. Automated method for isolation of human pancreatic islets. *Diabetes* 1988;37:413-420.
6. Ricordi C, Strom TB. Clinical islet transplantation: advances and immunological challenges. *Nat Rev Immunol* 2004;4:259-268.
7. Cattaneo E. Isole di Langerhans: ideazione e sviluppo di un dispositivo per la separazione ottimizzata delle isole pancreatiche. Milano: Politecnico di Milano; 2004.
8. Bank HL. Assessment of islet cell viability using fluorescent dyes. *Diabetologia* 1987;30:812-816.
9. Figliuzzi M, Zappella S, Morigi M, Rossi P, Marchetti P, Remuzzi A. Influence of donor age on bovine pancreatic islet isolation. *Transplantation* 2000;70:1032-1037.
10. Ricordi C, Finke EH, Lacy PE. A method for the mass isolation of islets from the adult pig pancreas. *Diabetes* 1986;35:649-653.

11. Brandhorst D, Brandhorst H, Hering BJ, Bretzel RG. Long-term survival, morphology and in vitro function of isolated pig islets under different culture conditions. *Transplantation* 1999;67:1533-1541.
12. Marchetti P, Giannarelli R, Cosimi S, Masiello P, Coppelli A, Viacava P *et al.* Massive isolation, morphological and functional characterization, and xenotransplantation of bovine pancreatic islets. *Diabetes* 1995;44:375-381.
13. Ricordi C. Islet isolation assessment. In: Company RGL, (ed). *Pancreatic islet cell transplantation*. Austin, 1992.
14. Ruggerenti P, Remuzzi A, Remuzzi G. Decision time for pancreatic islet-cell transplantation. *Lancet* 2008;371:883-884.
15. Cardani R, Pileggi A, Ricordi C, Gomez C, Baidal DA, Ponte GG *et al.* Allosensitization of islet allograft recipients. *Transplantation* 2007;84:1413-1427.
16. Narang AS, Mahato RI. Biological and biomaterial approaches for improved islet transplantation. *Pharmacol Rev* 2006;58:194-243.

## Chapter 3

*In vivo* functionality of the islets: syngeneic, allogeneic and xenogenic free islet transplantation

### 1.8 Materials and methods

### 1.9 Results

#### *1.9.1 Syngeneic free islet transplantation*

#### *1.9.2 Allogeneic free islet transplantation*

#### *1.9.3 Xenogenic free islet transplantation*

Conclusion

References

## ***In vivo* functionality of the islets:**

### **syngeneic, allogeneic and xenogenic free islet transplantation**

In the last chapter it was explained how islets can be obtained from a pancreas and the procedure for purify them from exocrine tissue. To test functionality of the islets, different procedures can be applied, *in vitro* and *in vivo*. Transplantation of islets into a syngeneic recipient is faster than any colorimetric procedure and is indicative of a real and consistent functionality. In our laboratory a chemically induced rat model of diabetes has been developed. In contrast to clinical studies in which islets are transplanted to patients with autoimmune type I diabetes mellitus, the majority of experimental islet transplantation studies have been performed on rats, whose native islet damage is induced chemically through administration of Streptozotocin® (STZ). STZ was first developed in 1963 as a broad spectrum antibiotic isolated from *Streptomyces achromiogenes* but was demonstrated to have beta-cell specific diabetogenic effects (1). It specifically and irreversibly destroys pancreatic beta cells by entering them and inducing degranulation, Golgi apparatus hypertrophy and DNA breaks, which ultimately result in beta cell pyknosis (2) (3). Upon injection of a toxic dose of STZ, animals experience initial hyperglycaemia due to inhibition of insulin release. This is followed by hypoglycaemia within 6-12 hours due to feedback increase in insulin secretion and beta cell degranulation. Permanent hyperglycaemia usually begins 24-48 hours following treatment and is a result of irreversible beta cell destruction. Following this, plasma insulin secretion is not detectable for more than 12 weeks following treatment. Permanence, rapid tempo, reproducibility, and specificity of diabetes induction by high-dose STZ treatment makes it

the optimal choice for long-term studies of islet isograft or allograft function with minimal concern for recovery of native pancreatic islet function.

In this model of diabetes syngeneic, allogeneic or xenogenic free islets were transplanted beneath the kidney capsule. For diabetes induction two different doses of STZ injected intravenously were used, on the basis of the species used: for Lewis rats 65 mg/kg and for Munich Wistar Fromter rats (MWF) 50 mg/kg.

### **3.1 Materials and methods**

#### *Islet preparation*

The day after islet isolation using the manual or the automated procedure, islets were resuspended in HBSS. After centrifugation, they were introduced into a polyethylene catheter with an internal diameter of 500  $\mu\text{m}$  (PE50), concentrated into pellets.

#### *Islet transplantation*

In the laboratory, rats were anaesthetized using Avertin (4) and when the anaesthetic had taken effect, the left flank of the rat was shaven. After kidney location (just inferior to the spleen), a small incision in the skin permitted peritoneal identification. Making a small incision into the peritoneum, the kidney was exposed and externalized. During the procedure the kidney was kept moist by showering it with saline. Using a 23 or 25 gauge needle, a small scratch was made on the right flank of the kidney, creating a nick in the kidney capsule. Into this, the PE50 tubing was carefully and slowly inserted beneath the capsule, making a small pocket (Figure 3.1–A). Using a Hamilton syringe, islets were slowly advanced into the desired location (Figure 3.1–B). The PE50 tubing was then slowly removed and carefully the nick was cauterized using low temperature. The kidney

was then gently replaced into the peritoneum, prior to closing the rat's epidermis with a suture and skin staples.

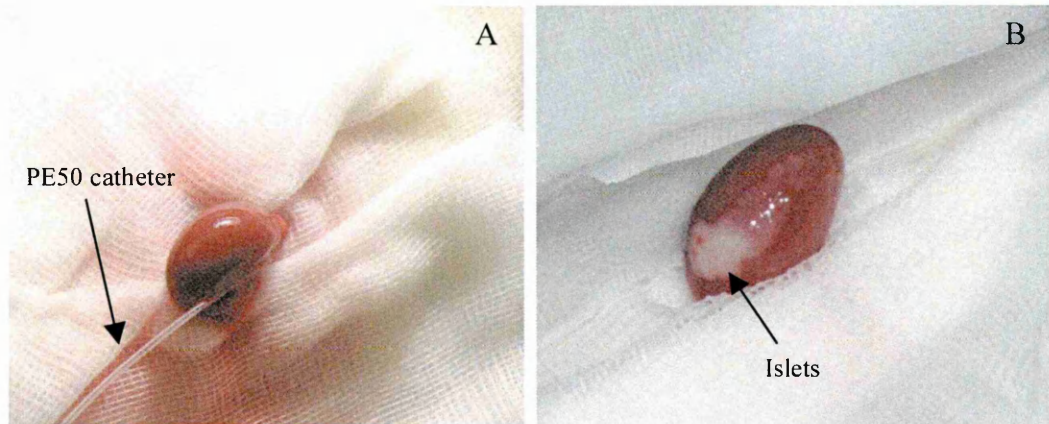


Figure 3.1 Kidney capsule incised using the tip of a needle and a small PE50 catheter inserted (A). Islets were injected using a Hamilton syringe beneath the kidney capsule (B).

#### *Islet functionality in vivo*

To verify whether glycaemic control was achieved after islet implantation, non-fasting blood glucose was measured daily from tail bleedings using the Glucocard Memory 2.

#### *Kidney plus islet retrieval*

Animal treatment was noted until functional failure of the grafts (measured as hyperglycaemia). Then the kidneys were retrieved under anaesthesia and animals were sacrificed.

#### *Morphological evaluation*

Kidneys, containing pancreatic islets, recovered from each animal were analyzed using tissue chromogens and a fluorescence microscope or a light microscope, to determine the presence of insulin and the structure of islets. After kidney removal, samples were fixed in paraformaldehyde solution or in Doubosque-Brazil solution, then embedded in OCT compound or in liquid paraffin wax. Samples in OCT compound were frozen and 4  $\mu$ m

sections were cut for immunohistochemical detection of insulin. Samples embedded in paraffin wax were used for examination using haematoxylin and eosin staining.

*Immunostaining with fluorescent secondary antibodies. Protocol for insulin*

Non-specific binding was blocked by incubation of sections with 3% bovine serum in PBS (block solution). After 1 hour, circles were drawn round dry sections, using PAP pen to prevent loss of antibody. Primary antibody was added (insulin rabbit anti-rat, dilution 1:100 in block solution). These were incubated for 2 hours at room temperature or overnight at 4°C. Sections were washed at least 3 times, and at least 5 minutes each wash, in PBS and then secondary antibody was applied (goat anti-rabbit, dilution 1:100 in block solution); this was incubated for 1hr at room temperature. Sections were washed for at least 3 times, at least 5 minutes each, in PBS and DAPI (4',6-Diamidino-2-Phenylindole, double stranded DNA staining) was applied. This stains nuclei with the DNA intercalating fluorescent dye DAPI, to be seen on a fluorescence microscope fitted with appropriate blue filters. After mounting with appropriate medium, slides were analysed using a fluorescence microscope.

*Morphological evaluation with haematoxylin and eosin staining*

Sections were taken to water (quickly twice) and then were placed in haematoxylin for 10 minutes. They were then washed in tap water (quickly twice) and placed in eosin for 5 minutes. Then they were washed once quickly and dehydrated in 100% alcohol, then after washing in toluene, sections were mounted on glass slides.



## 3.2 Results

### 3.2.1 Syngeneic free islet transplantation

Fourteen transplants were performed using 3,000 syngeneic free islets beneath the kidney capsule of Lewis diabetic rats; 10 rats normalized hyperglycaemia within 7 days after islet transplantation, as shown in Figure 3.2-A, and this state was maintained until rat sacrifice (in some cases for more than 200 days). In 5 of the fourteen animals, after 30 days post transplantation, nephrectomy was performed under anaesthesia to determine whether, after kidney and islet removal, a hyperglycaemic state was reached. In fact, in the 5-nephrectomized rats, a hyperglycaemic state was reached the day after kidney removal (Figure 3.2-B).

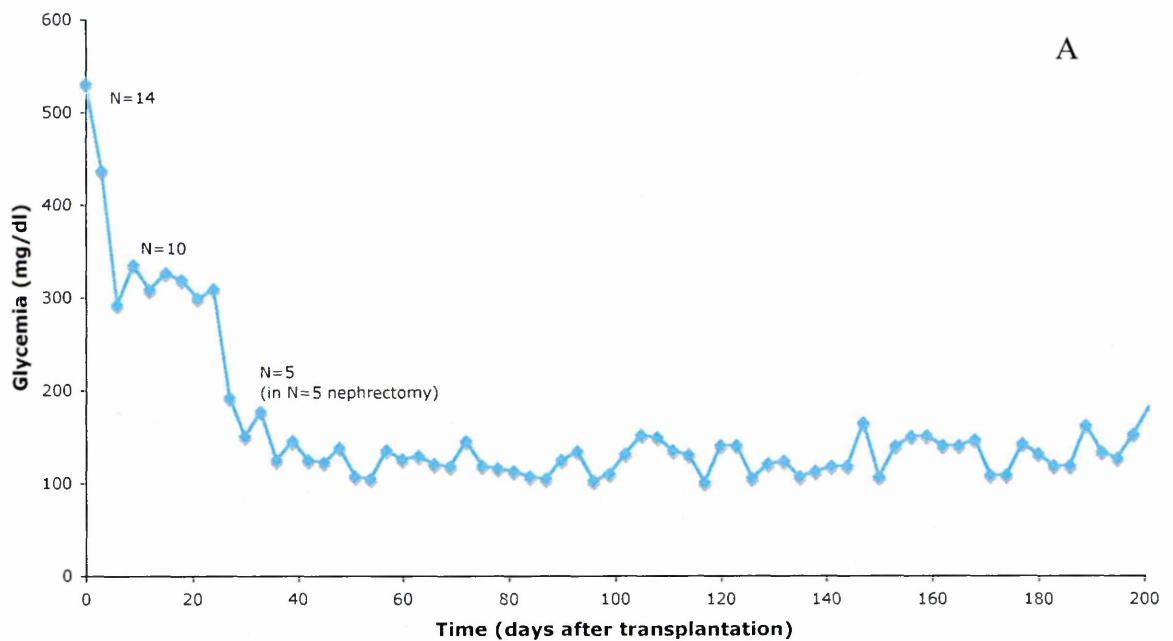


Figure 3.2-A Average non-fasting blood glucose level after islet implantation in 14 rats

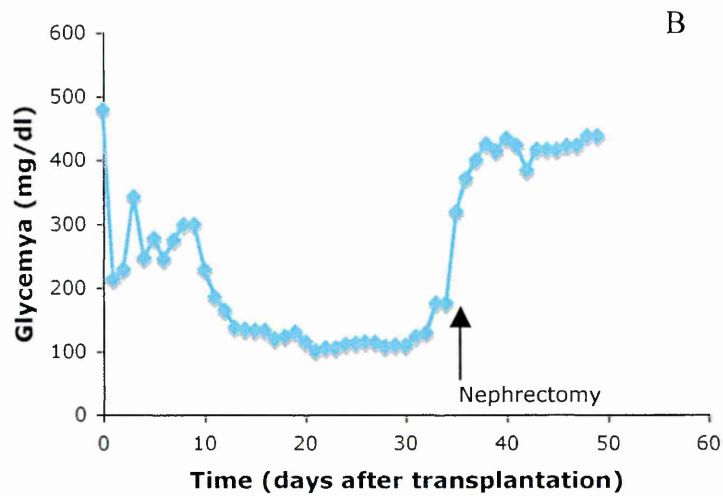


Figure 3.2-B Average non-fasting blood glucose level after islet implantation in rat with nephrectomy

In Figures 3.3-A and B it is shown that islet  $\beta$  cells beneath the kidney capsule still synthesised insulin (immunofluorescence, insulin red and nuclei blue) 3 or 4 months after transplantation. Equivalent histology is shown in Figure 3.3-C (haematoxylin and eosin staining), where preserved structure of the implanted islets is illustrated.

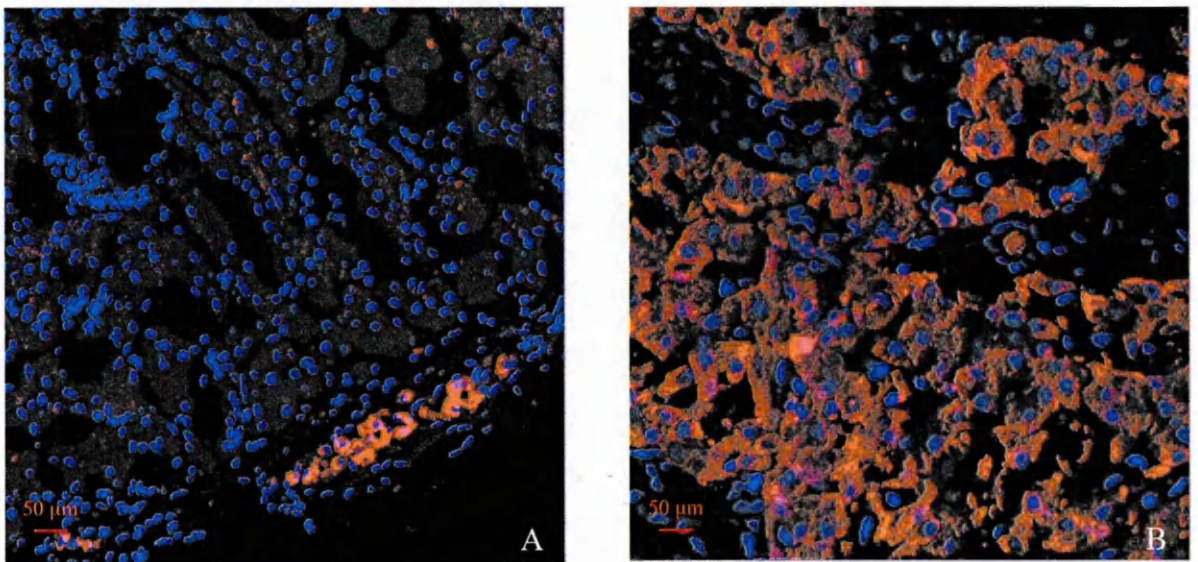


Figure 3.3-A and B Islet beneath the kidney capsule positive for insulin (immunofluorescence, insulin in red and nuclei in blue) also 3 or 4 months after transplantation (A low magnification and B high magnification).

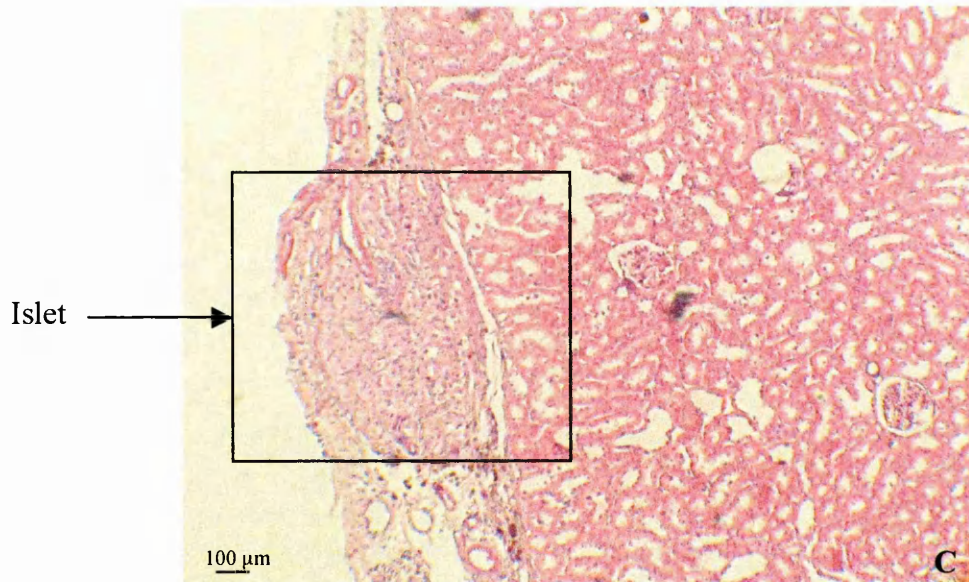


Figure 3.3-C Islet beneath the kidney capsule. Histology of the preserved structure (haematoxylin and eosin staining)

### 3.2.2 Allogeneic free islet transplantation

Seven transplants were performed of 3,000 allogeneic free islets beneath kidney capsules of diabetic rats (Lewis rats as donors and MWF diabetic rats as recipients). The day of transplantation and for the following 20 days, 3 rats were treated with cyclosporine (daily intramuscular injection, 5mg/kg), an immunosuppressant drug widely used in human post-allogeneic organ transplantation to reduce activity of the patient's immune system and thus to reduce the risk of organ rejection. Only rats treated with cyclosporine normalized hyperglycaemia within 2-3 days after islet transplantation, as shown in Figure 3.4, blue line, and this average state was maintained for 18 days. In the 4 rats in which there was no immunosuppression, the hyperglycaemic state was maintained with no glycaemic control, red line.

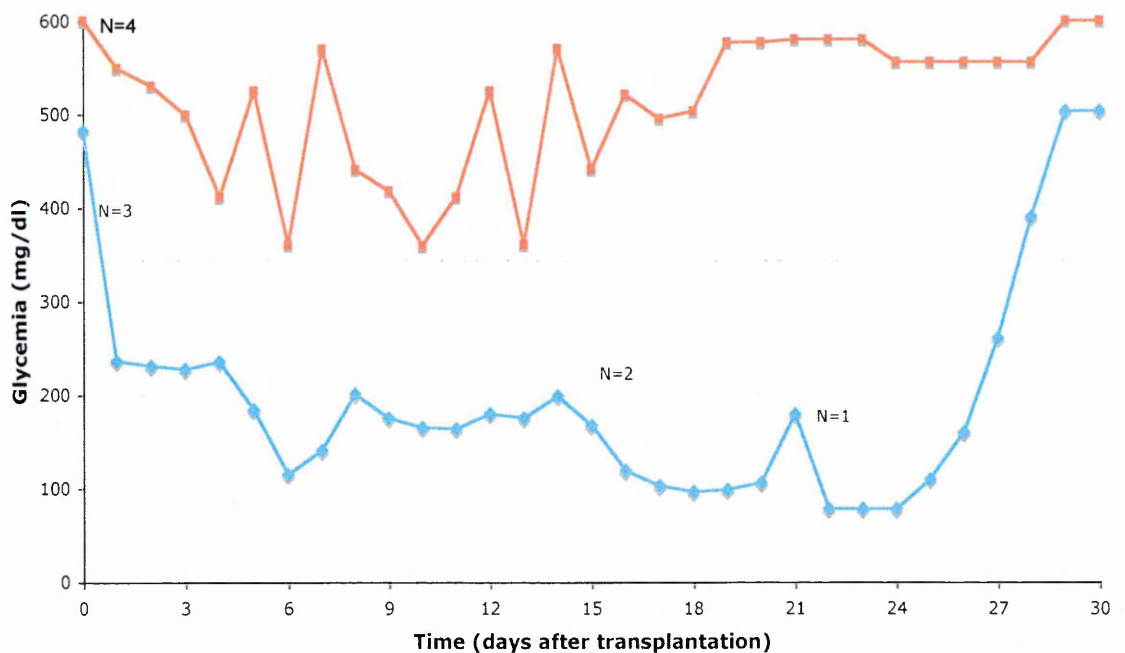


Figure 3.4 Averages of non-fasting blood glucose levels after allogeneic islet implantation in rats treated with cyclosporine (blue line) or without (red line)



When kidneys were removed after rat sacrifice, morphological evaluation using haematoxylin and eosin stained sections no intact islets could be found, only infiltration of cells of the host immunosystem (indicative of graft rejection), as shown in Figure 3.5.

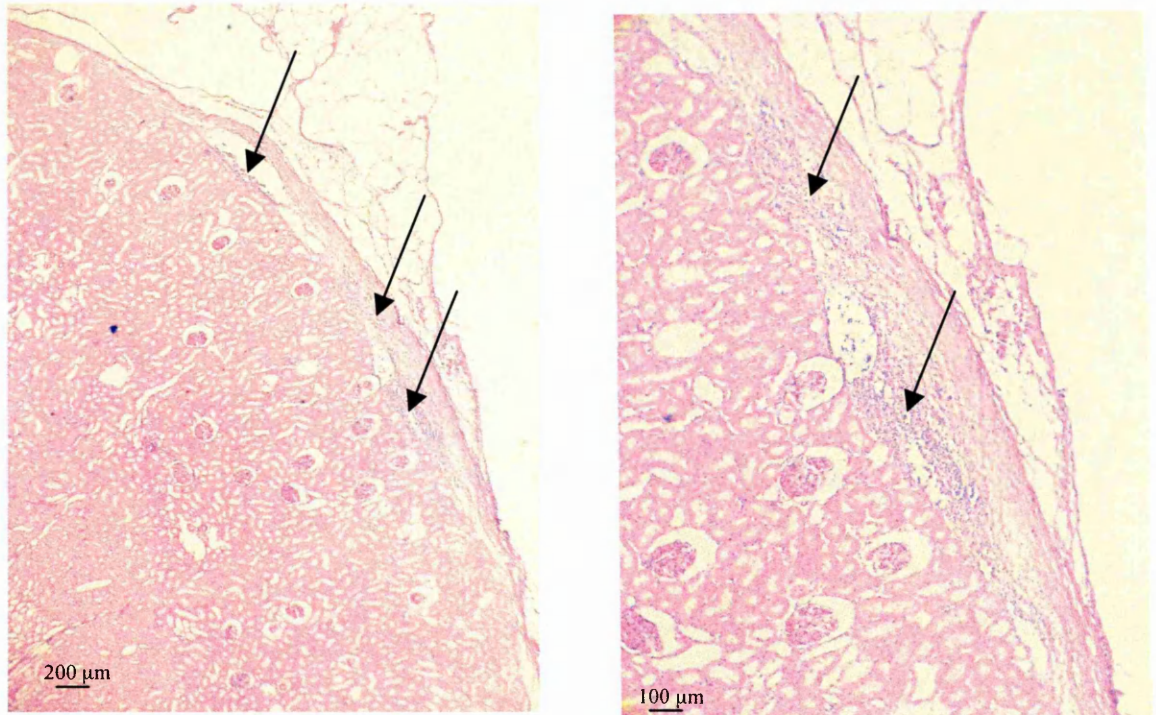


Figure 3.5 Histology of cellular infiltrations (indicated by arrows) beneath the kidney capsule at low and high magnification

### 3.2.3 Xenogenic free islet transplantation

Eleven transplants were performed with an average of 13,000 (from 7,000 to 24,000) xenogenic free islets, beneath the kidney capsule (bovine islets transplanted into Lewis or MWF diabetic rats). Seven of these animals were treated with a high dose of cyclosporine from the day of transplantation until sacrifice (daily intramuscular injection, 30 mg/kg) and the other 4 were treated with a low dose (daily intramuscular injection, 10 mg/kg). High dose of cyclosporine allowed normalization of glycaemia for an average of two days (range 1-5 days, Figure 3.6) while in low dose animals the hyperglycaemic state was maintained.

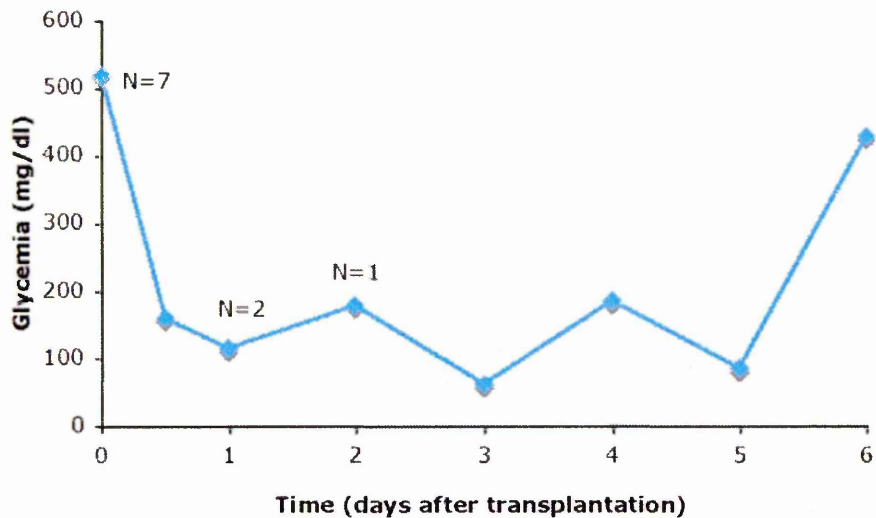


Figure 3.6 Averages, non-fasting blood glucose levels after xenogenic islet implantation in rats treated with a high dose of cyclosporine

## Conclusion

Several experiments with syngeneic, allogeneic and xenogenic islets were performed to determine a procedure for *in vivo* evaluation of the success of using transplanted islets. It was concluded that syngeneic islets functioned and allowed normalization of glycaemia to take place in diabetic rats. Considering allotransplantation, it was observed that only with use of an immunosuppressant like cyclosporine islet transplants could be successful for a short time be permitted, allowing a short-period of normalization of hyperglycaemia. Use of the immunosuppressant did not overcome xenogenic free islet acceptance, to control islet cell functionality. The use of immunoisolation of the islets is fundamental to test islet functionality and moreover to use xenogenic islets in experimental and clinical settings, avoiding the immunological response to the xenograft and the transfer of animals proteins to the host. Islets from other species used in humans could overcome the problem of organ shortage and, if not rejected, could provide successful therapy for diabetes.

## References

1. Rerup CC. Drugs producing diabetes through damage of the insulin secreting cells. *Pharmacol Rev* 1970;22:485-518.
2. Agarwal MK. Streptozotocin: mechanisms of action: proceedings of a workshop held on 21 June 1980, Washington, DC. *FEBS Lett* 1980;120:1-3.
3. Yamamoto H, Uchigata Y, Okamoto H. Streptozotocin and alloxan induce DNA strand breaks and poly(ADP-ribose) synthetase in pancreatic islets. *Nature* 1981;294:284-286.
4. Papaioannou VE, Fox JG. Efficacy of tribromoethanol anesthesia in mice. *Lab Anim Sci* 1993;43:189-192.



## Chapter 4

*In vivo* evaluation of encapsulation: syngeneic, allogeneic and xenogenic immunoisolated islet transplantation

### 4.1 Microcapsules

*4.1.1 Materials and methods*

*4.1.2 Results*

### 4.2 Hollow fibre devices

*4.2.1 Materials and methods*

*4.2.2 Results*

References

## ***In vivo* evaluation of encapsulation: syngeneic, allogeneic and xenogenic immunoisolated islet transplantation**

Previously, it was explained how islets can be obtained from a pancreas and how they can be tested in terms of functionality *in vivo*. It was concluded that there is need for an immunoisolation device to prevent inter-reactions between host and graft in allo- and xeno-transplanted islets.

The term “immunoisolation” refers to encapsulation of a graft in a selectively permeable membrane that allows exchange of only low molecular weight substances, such as oxygen, glucose, insulin and other nutrients. Moreover, this membrane would have to protect from host immune cells that cause rejection. Entries in the literature deeply analyze the possibility of using such membranes. The term “biohybrid artificial organs” indicates devices produced from synthetic membranes loaded with viable cells and these are being developed as substitutes in case of failing organ or tissue function (1). A number of studies are in progress on the use of such biohybrids for a wide variety of diseases for example in endocrine deficiencies such as diabetes (2) (3), hypoparathyroidism (4), treatment of neurodegenerative disorders such as Parkinson’s disease (5), Alzheimer’s disease (6) and amyotrophic lateral sclerosis (7). A bioartificial liver was assembled encapsulating porcine hepatocytes in a perfusion machine and used extra corporally for temporary treatment of patients with liver failure (8). The use of immunoisolation in islets for transplantation permits their allotransplantation and maybe even xenotransplantation without the use of pharmacological immunosuppression; this would provide access to an unlimited source of insulin-producing tissue. In the literature two main types of encapsulation can be found,

micro and macroencapsulation devices with intra- or extravascular implantation (Figure 4.1).

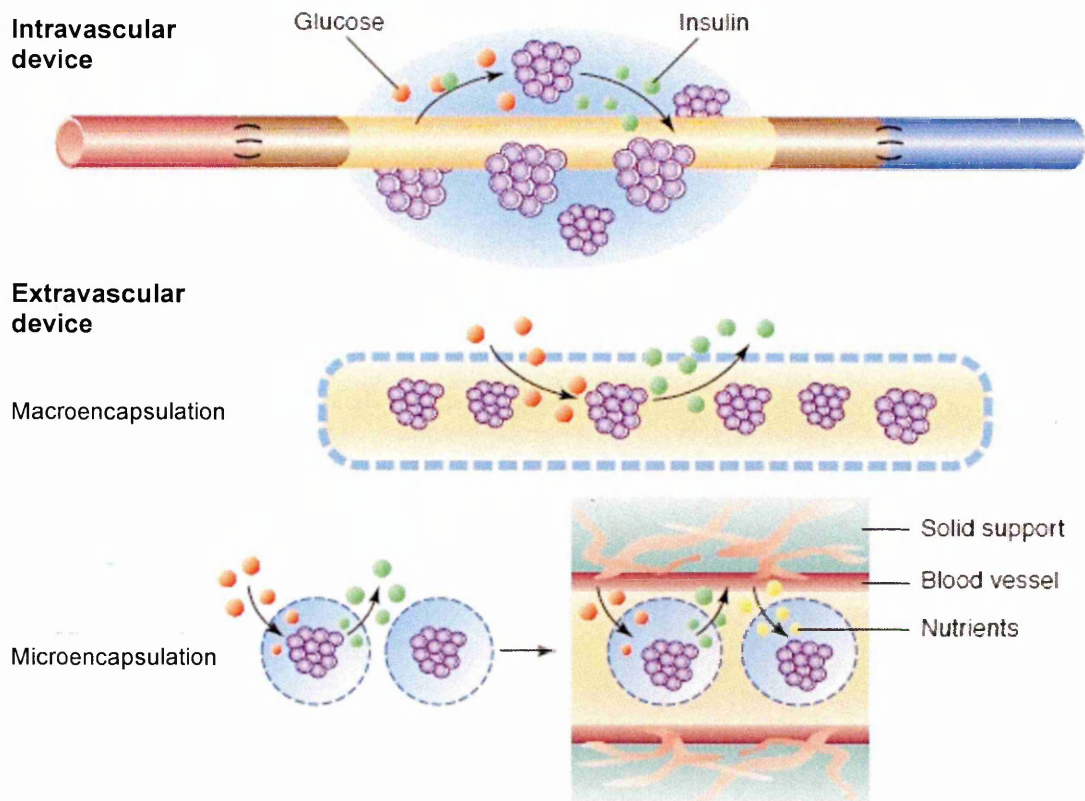


Figure 4.1 Different kinds of immunoisolation devices. In the intravascular device, islets can be distributed in a chamber surrounding a selectively permeable membrane. For the extravascular approach, islets are immunoisolated within membrane-diffusion chambers or enveloped in microcapsules, modified from (9)

In **microencapsulation** a small number of islets are encapsulated in an alginate matrix, sometimes covered with an outer layer of poly-L-lysine. This technique was first described in 1980 by Lim and Sun (10) where it was shown that microencapsulated islets, implanted intraperitoneally in diabetic rats, reversed diabetes for up to 3 weeks. Poor biocompatibility of the material used with the host, was the cause of graft failure. Many factors influence the success of capsule transplantation: type and purity of the alginate,

capsule size, wall thickness, mechanical strength, permeability and surface characteristics (11) (12) (13).

Recently, two clinical trials using encapsulated xenoislets (14) or alloislets (15) were reported but no patient became insulin-independent.

Another technique of immunoisolating islets is **macroencapsulation**. One kind of device is a perfusion chamber. This consists of a permselective tube connected to the recipient blood circulation as an Arterio-Venous (A-V) shunt. Housing is placed around the tube, creating a space in which the islets are placed (16) (3). This type of encapsulation aims to optimize diffusion of oxygen to the transplanted islets, however the system has several side effects such as thrombosis and occlusion of the device.

Another type is the diffusion chamber; this could have different geometry: planar sheets and hollow fibres. The functionality of this device is dependent on diffusion of nutrients and oxygen from implant sites (peritoneal cavity, omentum and subcutaneous space) to the islets. Lanza *et al* used allotransplantation of canine islets encapsulated in tubular diffusion devices. Twelve dogs served as recipients and three of them became insulin-free for 51 to >90 days (17). In 1993 the same group had studied long-term function of bovine, porcine and canine islet xenografts encapsulated in permselective acrylic membrane chambers and implanted into STZ-diabetic rats. Twelve months graft survival rates were 40%, 25% and 10%, respectively (18). A planar device with encapsulated rat islets in diabetic mice normalized fasting glycaemia up to 30 days and on histological examination, numerous macrophages were found to be adhered to the outer surface of the membrane. Many of the remaining islets showed histological signs of damage, and the authors concluded that this semipermeable membrane had only been partially efficient in protecting the xenoislets (19).

TheraCyte<sup>®</sup> is a diffusion chamber constructed from a bilateral polytetrafluoroethylene (PTFE) membrane the outer layer of which is 5  $\mu\text{m}$  PTFE; this induces neovascularization at the tissue-membrane interface (Figure 4.2).

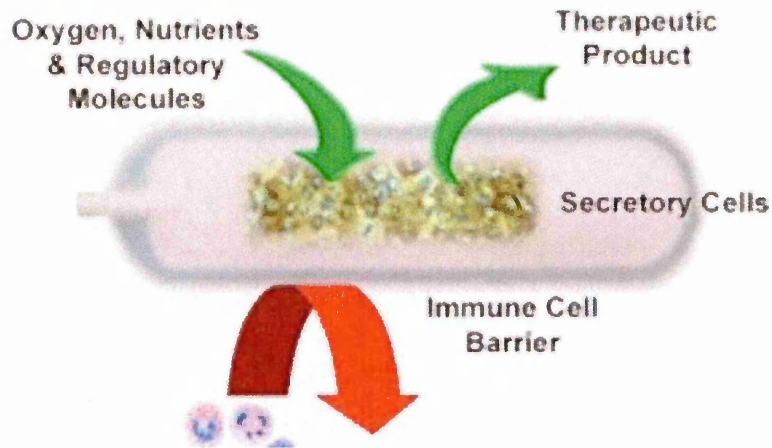


Figure 4.2 The TheraCyte<sup>®</sup> device

This vascularizing membrane has been glued on to a conventional immunoprotective PTFE membrane with a pore size of 0.45  $\mu\text{m}$ . Vascularization around this arrangement implanted subcutaneously in rats was evaluated by Sorenby *et al* (20). Tatarkiewicz K *et al* (21) showed reversal of diabetes in nude mice, using 1200 rat islets encapsulated in TheraCyte<sup>®</sup> and transplanted subcutaneously. Loudovaris *et al* have explored the possibility of using TheraCyte<sup>®</sup> for encapsulation of insulinoma cell lines instead of primary islets (22). This type of device has also been used in allotransplantation of islets in diabetic rats, but no glucose normalization was reached and only weight gain was observed with respect to controls (23).

Recently Pileggi *et al* showed reversal of diabetes by syngeneic mouse pancreatic islet transplantation into a subcutaneous device (Figure 4.3); this consists of a stainless-steel biocompatible mesh with removable PTFE stoppers on each end. At the time of implantation, one of the stoppers is replaced by a PTFE plunger which fills the lumen, in

order to prevent its occlusion by host connective tissue. The plunger is then removed at time of islet transplantation, and the device is sealed with a stopper. The strong outer frame protects the islets from physical damage and the stainless-steel biocompatible open mesh membrane promotes growth of blood vessels inside it, to nourish the islets with oxygen and nutrients. The host subcutaneous space is an easily-accessible implantation site, which might be of interest for many cell based reparative therapies (24) using this appliance.

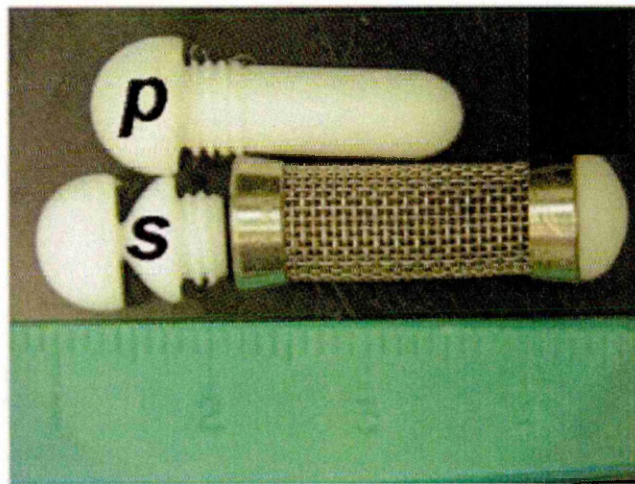


Figure 4.3 Biocompatible implantable steel and PTFE device. “s” PTFE stopper and “p” PTFE plunger.

Ruler indicates size in cm.

Despite promising results, a number of problems remain to be solved for successful use of such an immunoisolation device in clinical studies. When artificial material is implanted into a living body, also if it is biocompatible, it will cause acute and in some cases chronic inflammation (25) (26). Moreover, the foreign body reaction causes development of granulation tissue, foreign body multinucleate giant cells, macrophages and fibrosis (27) (Figure 4.4).



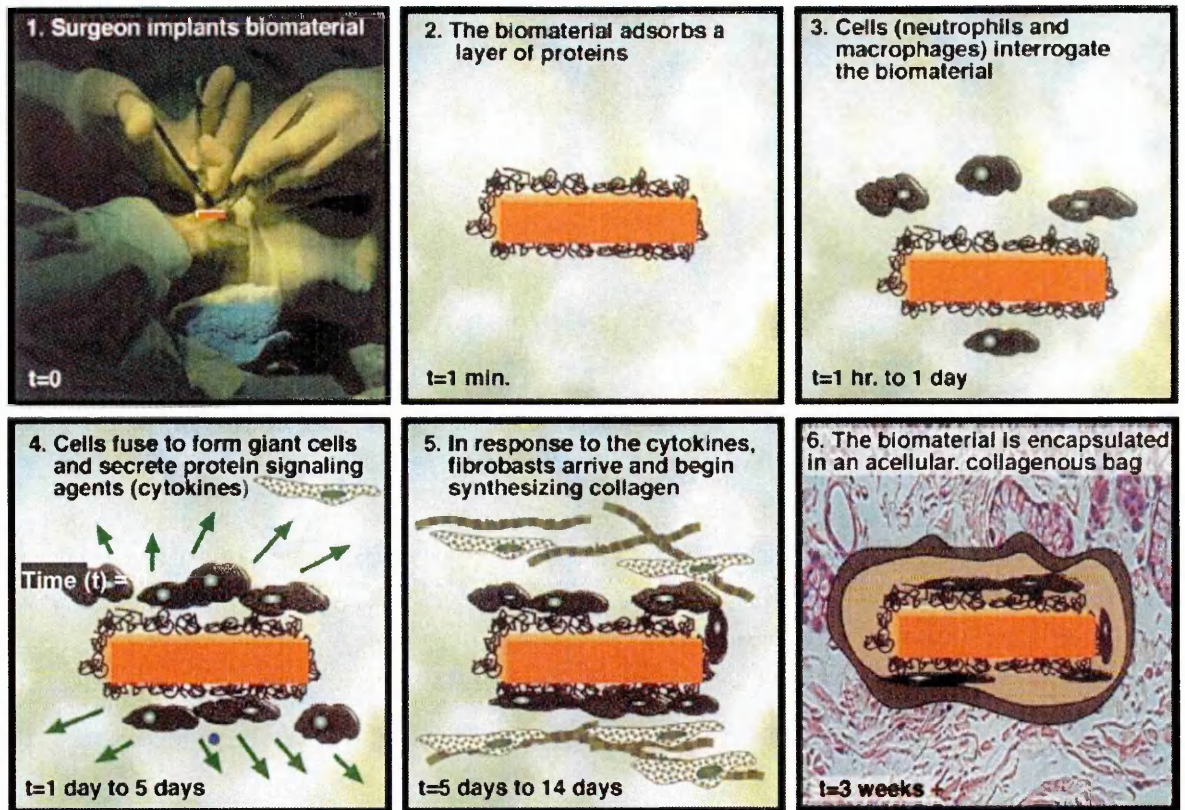


Figure 4.4 Foreign body reaction is normal when an implanted synthetic material is implanted into a living, vascular tissue. Diagram modified from (27)

The procedure for implantation of macroencapsulation devices and the surgical trauma also contribute to the inflammatory response of the host. Cytokines and other factors present in surrounding tissues during the acute phase may cross the protective membrane and destroy the cells inside. The avascular fibrotic capsule that develops around the implant and the immune cells, can compromise functionality and survival of the encapsulated cells. Different immunoisolation approaches offer advantages or limitations, linked to their geometry and the site of implantation (Table 4.1, (9))

<b>System</b>	<b>Advantages</b>	<b>Limitations</b>
Intravascular macrocapsule	Close contact with bloodstream	Thrombosis Infections Major implantation surgery
Extravascular macrocapsule	Minor implantation surgery Device can be retrieved	Large surface-to-volume ratio Low seeding density of cells
Extravascular microcapsule	Minor implantation surgery Optimal surface-to-volume ratio Implantation in several sites	Transplantation near blood vessels required for optimal longevity and function

Table 4.1 Advantages and limitations of different immunoisolation approaches

The importance of finding a suitable implantation site can be a problem especially for macroencapsulation devices. In most experiments, the epididymal fat pad, peritoneal cavity and subcutaneous tissue have been used for hollow fibre and diffusion devices.

Vascular chambers require access to large diameter major vessels such as the iliac artery or vein. The need to implant several of them, chronic treatment with anticoagulants and risks connected with vascular surgery (especially in diabetic patients) seem to limit their usefulness in a clinical setting. For microcapsules most groups prefer implantation in the peritoneal cavity so that volume of the graft does not constitute a problem (28). The major drawback here is the risk of inducing intraperitoneal adhesions. The subcutaneous site has poor blood supply but, on the other hand is safe and easily accessible for clinical use. As discussed above, physiological conditions inside the device will depend on the characteristics of the immunoisolating membrane and on properties of the surrounding tissue.

Two systems of immunoisolation have been developed in our laboratory: alginate microcapsules and hollow fibre systems. Methods for device construction and results of transplantations performed, follow.



## 4.1 Microcapsules

### 4.1.1 Materials and methods

#### Islet microencapsulation

As described above, islets were separated from pancreatic tissue and purified. After overnight culture, they were suspended in a solution of 1.7% sodium alginate (Manugel DMB, Monsanto plc, Surrey, United Kingdom) at a concentration of 3 IEQ/ $\mu$ l.

The islet–alginate mixture was extruded through an air jet droplet generator into a solution of 100mM  $\text{CaCl}_2$  solution. Resulting gel beads had diameters ranging from 800 to 950  $\mu$ m. After complete gelification, beads were washed in calcium-free Krebs–Ringer solution, then in Krebs–Ringer–Hepes 25mM, and then were cultured overnight once more in complete medium at 37°C.

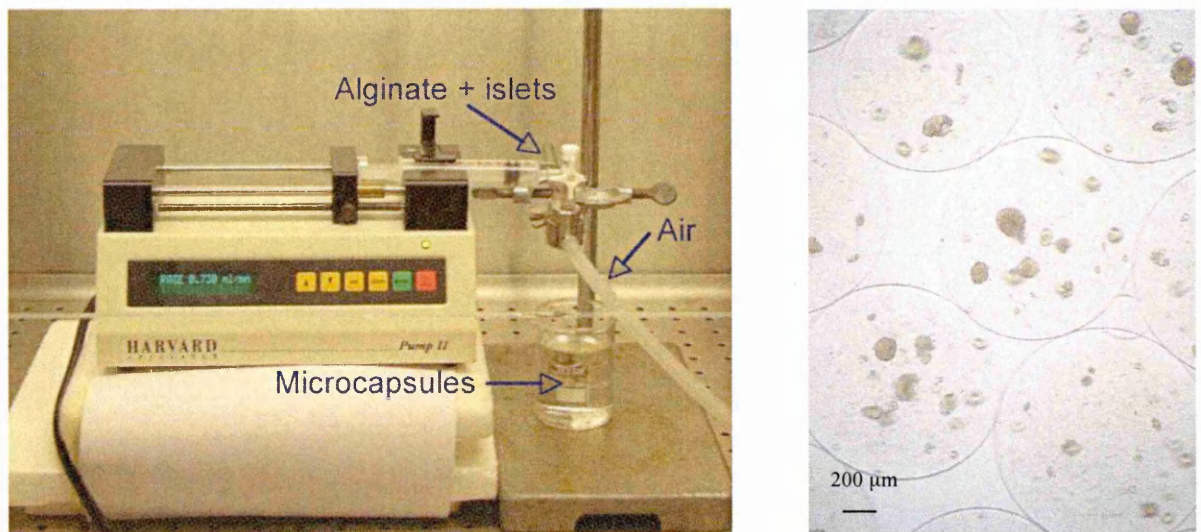


Figure 4.5 Droplet generator and light microscopy of microcapsules

#### Microcapsules implantation

Before transplantation, microcapsules were washed in saline solution to eliminate FCS in the medium and then were put into a syringe coupled with a Venflon IV canula (14

gauge). In the treatment facilities, rats were anesthetized with Avertin and when the anaesthetic had taken effect, the abdomen of the rats were shaven. A small incision in the skin permits view of the peritoneum. Making a small incision also in the peritoneum, the canula was inserted and microcapsules were infused; then the rats were closed up with sutures. To verify whether glycaemia control had been reached, after islet implantation, non-fasting blood glucose was measured daily by tail bleedings using the Glucocard Memory 2.

#### *Microcapsules explantation and morphological evaluation*

Animals were followed until functional failure of grafts, measured as hyperglycaemia, then microcapsules were retrieved under anaesthesia through peritoneal washing using saline solution and animals were then sacrificed.

Capsules recovered from each animal were analyzed using light microscopy to estimate percentage of capsules with fibrotic overgrowth. Samples of microcapsules were fixed in Bouin's solution and finally embedded in paraffin; 3 µm thick sections were mounted on glass slides and used for histological examination using haematoxylin and eosin.

#### *Morphological evaluation*

Sections were taken to water (quickly twice) and then were placed in haematoxylin for 10 minutes. They were then washed in tap water (quickly twice) and placed in eosin for 5 minutes. Then they were washed once quickly and dehydrated in 100% alcohol, then after washing in toluene, sections were mounted on glass slides.

### 4.1.2 Results

#### Syngeneic implantation

In order to assess islet functionality inside the microcapsules, avoiding the process of rejection of allotransplantation, 14 transplantations of 3000 syngeneic microencapsulated islets were performed into Lewis rats. After encapsulation, islets were transplanted intraperitoneally and glycaemia was monitored daily by tail bleedings, using the Glucocard Memory 2 system. As shown in Figure 4.6, diabetic rats normalized glycaemia for  $160 \pm 80$  days on average, bearing in mind that some of the rats were sacrificed when normoglycaemic.

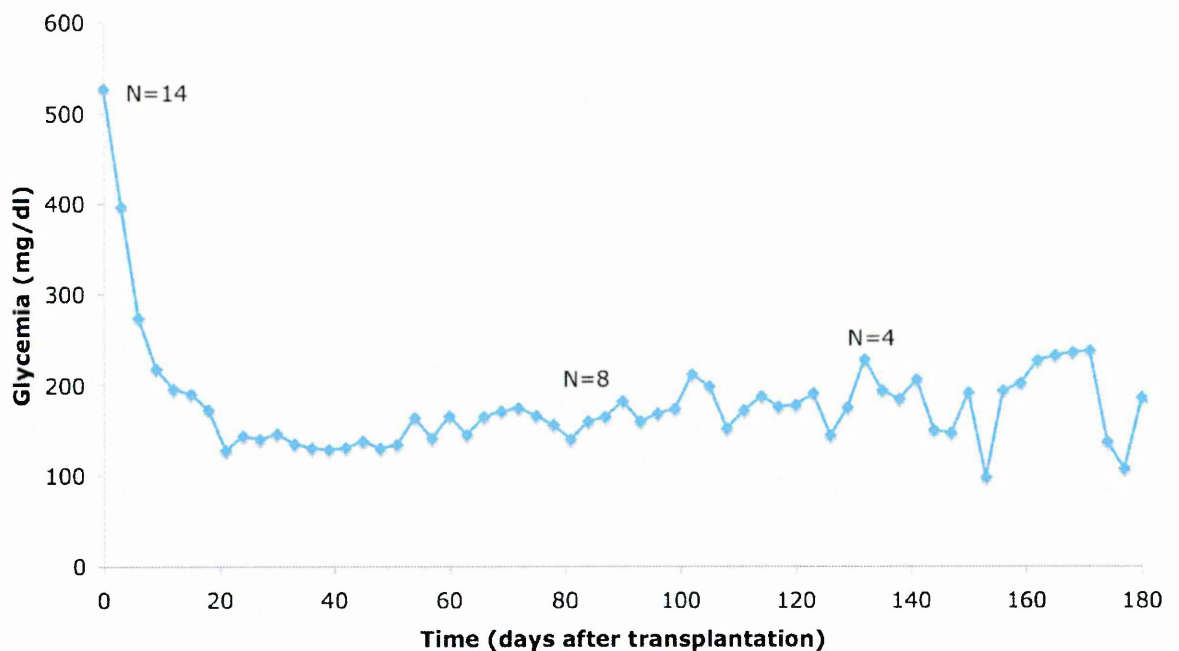


Figure 4.6 Average non-fasting blood glucose levels after microencapsulated syngeneic islets implanted into diabetic rats

These results demonstrate that this system of encapsulation did not damage the islets during the process of encapsulation and morphological appearance of encapsulated islet

cells being typical of healthy tissue (Figure 4.7); moreover the islets worked properly, allowing normoglycaemic control.

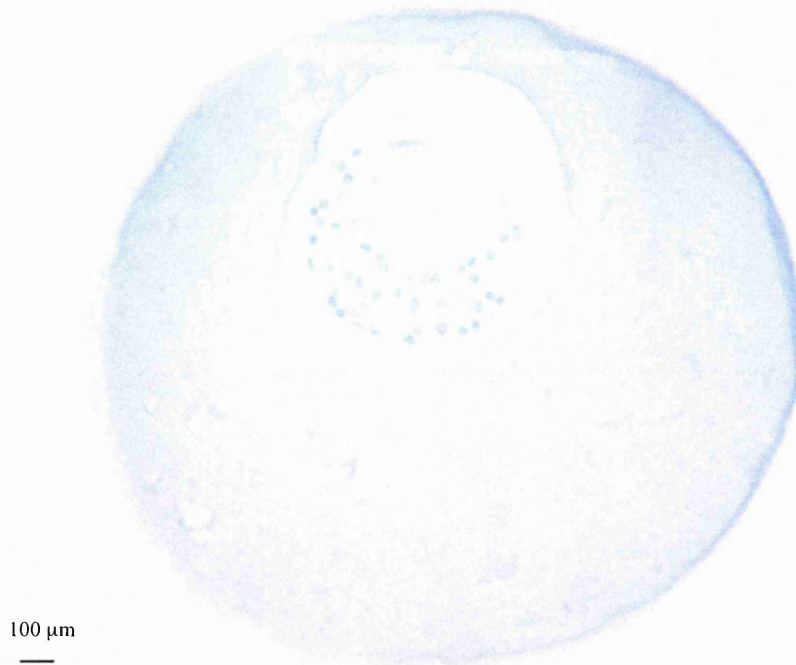


Figure 4.7 Light microscopy (haematoxylin-eosin staining) of islet contained in a microcapsule recovered from 200 day old rat after syngeneic implantation.

#### *Allogeneic implantation*

In order to assess microcapsule functionality, considering the process of rejection in islet allotransplantation, 4 transplantations of 3000 allogeneic microencapsulated islets were performed in Munich Wistar Fromter (MWF) rats using Lewis rats as donors. After encapsulation, islets were transplanted intraperitoneally and glycaemia was monitored daily by tail bleedings using the Glucocard Memory 2 system. On the day of transplantation and for the following 20 days, 2 rats were treated with cyclosporine (daily intramuscular injection, 5mg/kg), an immunosuppressant drug widely used in post-allogeneic organ transplantation to reduce activity of the patient's immune system and so to reduce the risk of organ rejection. All rats (with or without cyclosporine) normalized

hyperglycaemia within 2-3 days after islet transplantation, as shown in Figure 4.8, and this state was maintained for more than 100 days.

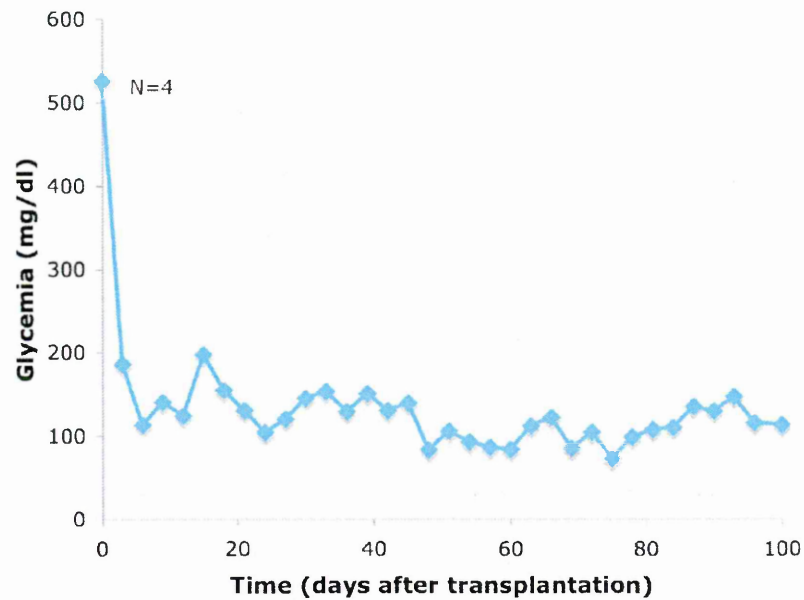


Figure 4.8 Average non-fasting blood glucose levels after microencapsulated allogeneic islet implantation in diabetic rats

Then, explanted microcapsules were processed and tissue sections were analyzed for morphological evaluation of islet structure (Figure 4.9). Sections showed that structure of islets was good also after 100 days.

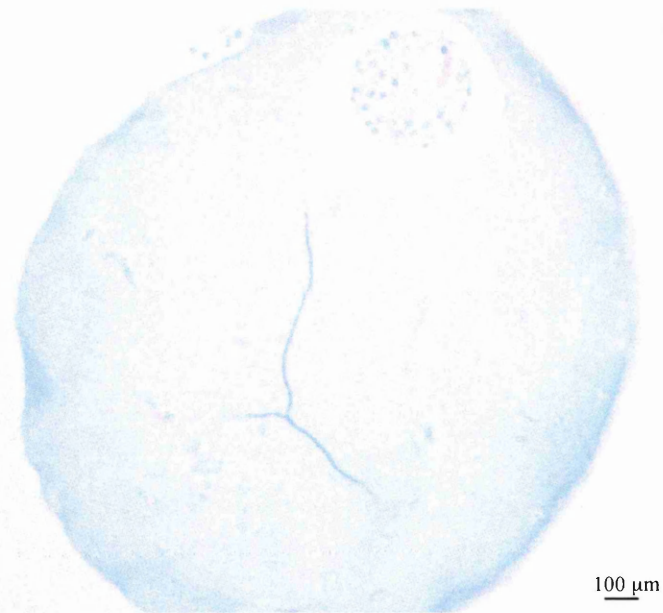


Figure 4.9 Light microscopy (hematoxylin-eosin staining) of islets contained in microcapsules 100 days after allogeneic transplantation

#### Xenogenic implantation

The results of using microcapsules were that they provided a good system of encapsulation and immunoisolation, thus the next step was to evaluate their functionality using bovine islets was performed. Forty-eight transplantations were performed using 16,000 xenogenic bovine microencapsulated islets into Munich Wistar Fromter (MWF) rats. After encapsulation, microcapsules were transplanted intraperitoneally and glycaemia was monitored daily by tail bleeding using the Glucocard Memory 2 system. The day of transplantation and for the following 20 days, 34 rats were treated with cyclosporine (daily intramuscular injection, 10 mg/kg), an immunosuppressant drug widely used in organ transplantation to reduce activity of a patient's immune system and thus to reduce the risk of organ rejection. 41 rats (with or without cyclosporine) normalized hyperglycaemia within 2-3 days after islet transplantation and this state was maintained in average for  $23 \pm 15$  days in rats with cyclosporine (Figure 4.10 in black), for  $9 \pm 4$  days in rats without cyclosporine (Figure 4.10 in red).



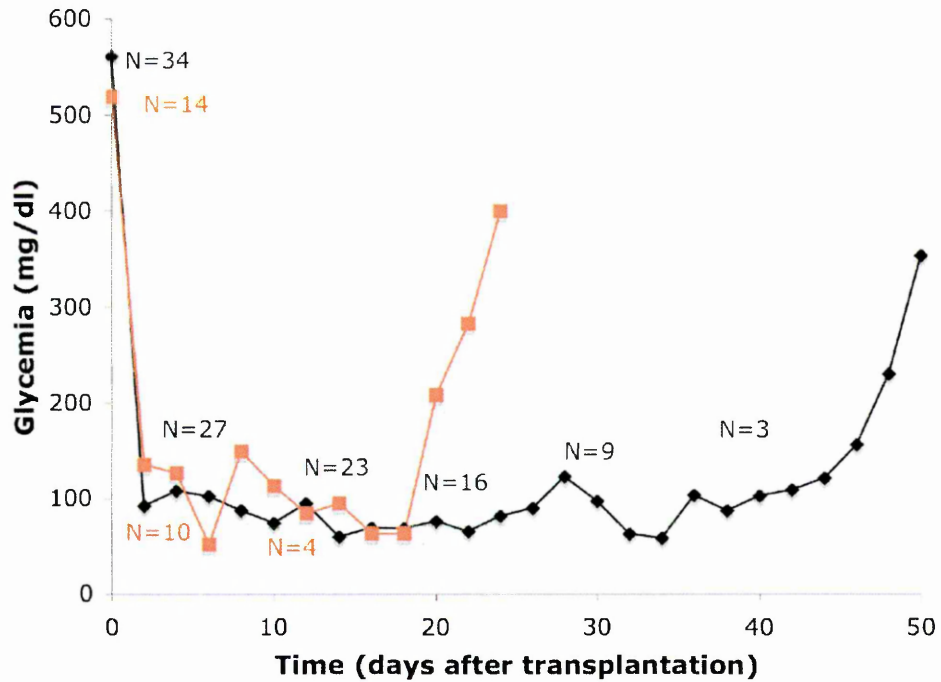


Figure 4.10 Average non-fasting blood glucose levels after microencapsulated xenogenic islet implantation into diabetic rats with (black) or without (red) cyclosporine

Also in this case, after explantation, microcapsules were fixed and then processed for microscopic evaluation of islet structure. In Figure 4.11 it can be seen that in microcapsules implanted into animals treated with cyclosporine, islet structure was maintained, but where cyclosporine had not been given, islets structure was destroyed.

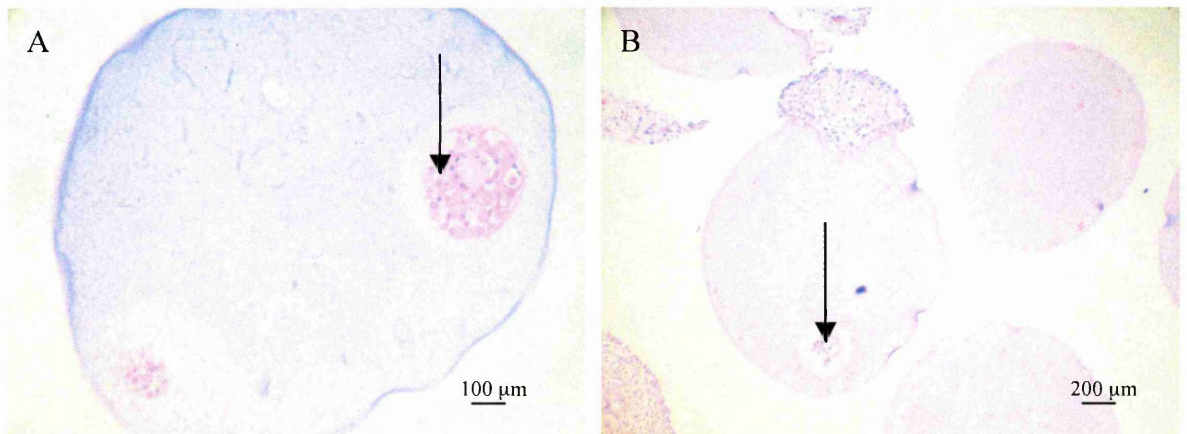


Figure 4.11 Light microscopy (haematoxylin-eosin staining) of xenogenic islets (indicated with arrows) contained in microcapsules with cyclosporine (A) or without (B)

## 4.2 Hollow fibre device

The subcutaneous site has been regarded as an adequate site for transplantation of bioartificial pancreas, as here islets can be implanted with minimally invasive surgical procedures. This site can be accessed easily for subsequent retrieval of non-functioning implanted material or to replace non-functioning cells with fresh islets within already implanted devices (21). However, there have been only a few reports describing successful transplantation of islets contained in immunoprotective devices into the subcutaneous space. Encouraging results were obtained by pioneering work of Lacy *et al* (2) that obtained normoglycaemia in diabetic mice after subcutaneous transplantation of rat islets encapsulated in hollow fibres. Tatarkiewicz *et al* (21) transplanted rat islets in TheraCyte chambers, subcutaneously, into diabetic nude mice. Mice returned to normoglycaemia within 3 weeks after transplantation and blood glucose levels were stable until 8 weeks after transplantation. Despite these encouraging results, no attempts have been found in the literature to extend this technique to larger and immunocompetent animals, even in the rat.

### 4.2.1 Materials and methods

#### Device construction

Device for subcutaneous implantation has been developed in our laboratory, with an internal volume of 270  $\mu$ l. This, schematically represented in Figure 4.12, is made as a planar and parallel array of hollow fibres of polyethersulphone that is 25mm wide and 62mm long.



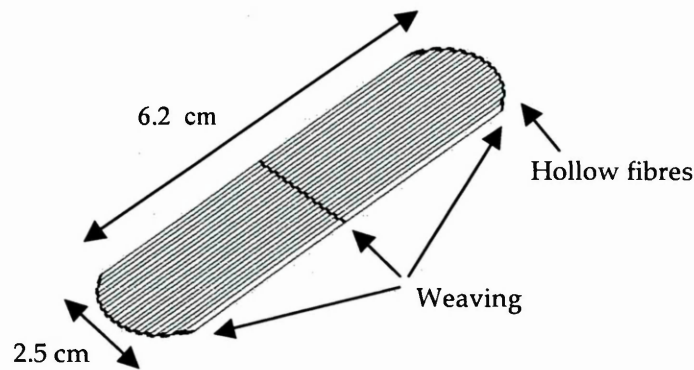


Figure 4.12 Schematic representation of the device: a parallel array of hollow fibres held together with a weaving

Three groups of devices were assembled with different polyethersulphone membranes. Group 1 with hollow fibres from Fresenius Medical Care (Bad Hamburg, Germany), 490  $\mu\text{m}$  internal diameter and 65  $\mu\text{m}$  membrane thickness, Group 2 from Spectrum Labs Inc. (Breda, Netherlands), 500  $\mu\text{m}$  internal diameter and 68  $\mu\text{m}$  membrane thickness, and Group 3 from Amicon WR Grace and Co. (Beverly, MA, USA), 570  $\mu\text{m}$  internal diameter and 80  $\mu\text{m}$  membrane thickness. Samples of hollow fibres used for device construction were processed for scanning electron microscopy (SEM) analysis. Samples were frozen in liquid nitrogen, broken and mounted on aluminium supports. Then they were gold coated and viewed on a Leica Stereoscan microscope (Leica, Cambridge, England) at 8 kVolt (Figure 4.13).

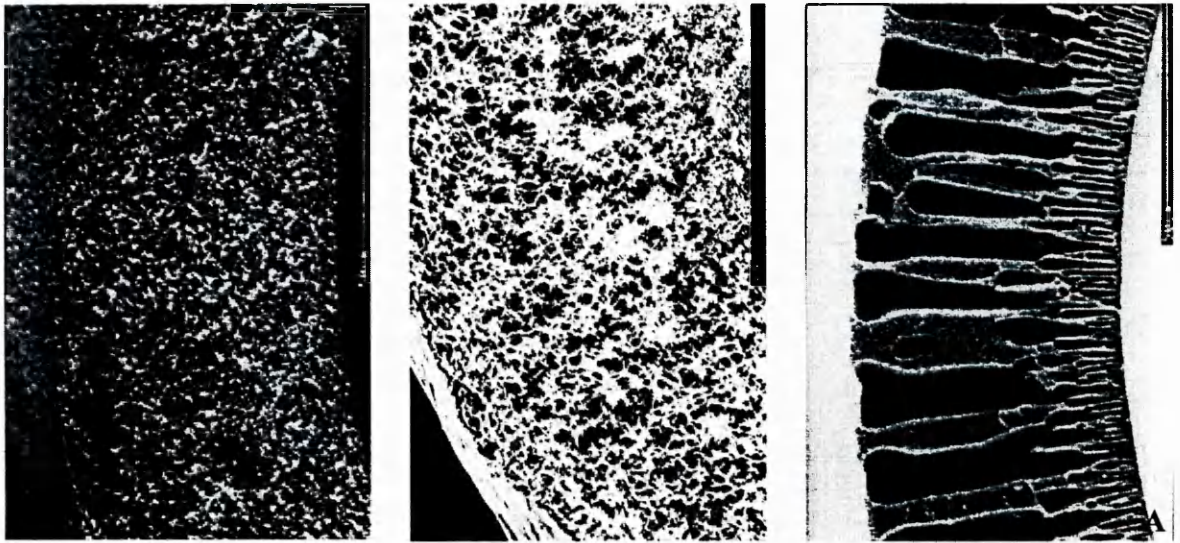


Figure 4.13 Representative SEMs of membrane thickness of Fresenius (F), Spectrum (S) and Amicon (A) hollow fibres.

Fresenius membrane was the most compact material with a selective layer near the inner surface. The Spectrum membrane also was of uniform porous material, but more open, and the Amicon membrane was characterized by columnar fenestrations that communicated with the outer surface but not with the inner one.

#### *Islet encapsulation*

After culture, islets were suspended in a solution of 1.7% sodium alginate (Manugel DMB) at a concentration of 30 IEQ/ $\mu$ l. In order to insert this solution into the fibres, a perfusion system that allows uniform loading of islet solution among the fibres was used. After perfusion, the device was immersed into 100mM CaCl<sub>2</sub> solution for 10 min for alginate gelification.

*Device implantation and retrieval*

Implantation of devices was performed under Avertin anaesthesia. A skin incision was made on the back of the animal, followed by preparation of two subcutaneous pockets, gently, with blunt dissection by forceps on the right and left sides; devices were inserted into the pockets. Animals were followed until functional failure of the grafts, measured as hyperglycaemia, then the devices were retrieved under anaesthesia and animals were sacrificed.

*Histological evaluation.*

Devices containing pancreatic islets recovered from each animal were analyzed using fluorescence microscopy or light microscopy to determine the presence and nature of cell overgrowth outside the membranes and to evaluate islet structure. To this purpose, after device removal, samples of hollow fibres (around 5 mm in length) were fixed in Bouin's solution or in paraformaldehyde solution. Segments of alginate gel containing islets were extruded from hollow fibre samples and were fixed in Bouin's solution. After 4 hours fixation in Bouin's solution samples were embedded in paraffin wax and samples in paraformaldehyde solution were embedded in OCT compound and frozen. Three  $\mu\text{m}$  thick sections were mounted on glass slides and were used for both histological examination using hematoxylin and eosin staining and immunohistochemical detection of macrophages and T lymphocytes.

*Immunostaining with fluorescent secondary antibodies. Protocol for macrophages and T lymphocytes*

Non-specific binding was blocked first by incubation of sections with 3% bovine serum in PBS (block solution) for 1 hour. To prevent loss of antibody, circles round dry section

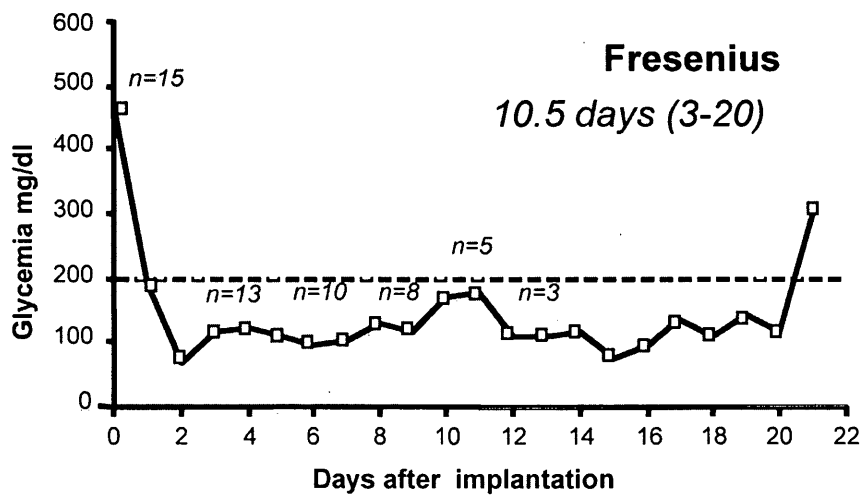
were drawn with PAP pen. Primary antibodies were added (mouse anti-rat mAb anti-monocyte/macrophage clone ED1, mouse anti rat mAb anti CD8a clone OX8, goat anti human mAb anti CD4 clone, dilution 1:100 in block solution); this incubated was for 2 hours at room temperature or overnight at 4°C. Sections were washed for at least 3 times, at least 5 minutes each time, in PBS. Secondary antibodies were then applied and incubated for 1 hour at room temperature. Sections were washed at least 3 times, for at least 5 minutes each time, in PBS. DAPI was applied and after mounting, slides were analyzed on a fluorescence microscope.

**4.2.2 Results**

For this experiment a high number of bovine islets was needed to be able to judge functionality in terms of normoglycaemia. With islets obtained from one bovine pancreas isolation different experiments were performed, comparing different hollow fibres, in order to select the best to use in an allogeneic protocol of transplantation.

Xenogenic implantation

A total of 54 devices containing bovine islets, were implanted under the skin of 27 diabetic rats to evaluate survival and function of implanted islets. Each device was assembled with 8000 IEQ. They were implanted into the subcutaneous site with minor surgery and were easily retrieved when required. All STZ-induced diabetic rats normalized hyperglycaemia within 1 to 2 days after device implantation, as shown in Figure 4.14. Rats implanted with islets contained in Fresenius and Spectrum fibres maintained normoglycaemia for 10.5 days on average (range from 3 to 20 days) and for 9.5 days on average (range from 6 to 17 days) respectively. The device made with Amicon fibres maintained normoglycaemia for shorter time periods, 5.8 days on average (range from 2 to 10 days).



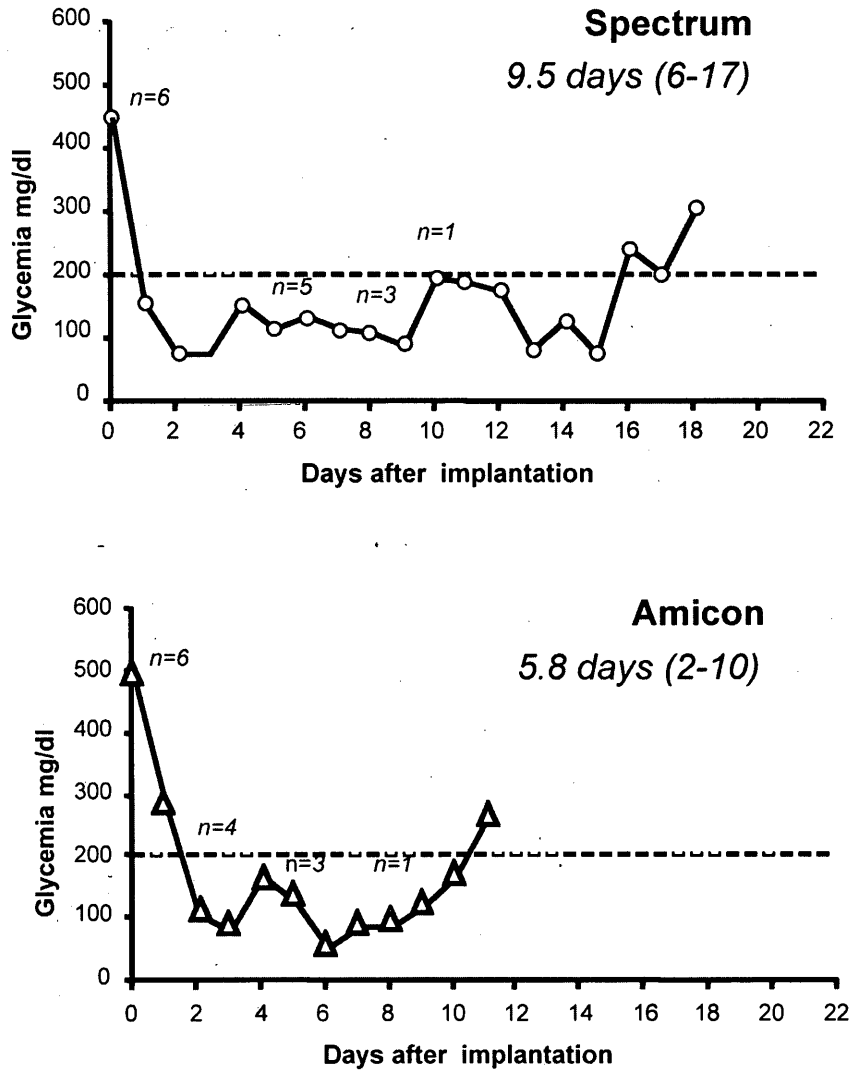


Figure 4.14 Non-fasting blood glucose levels after islet implantation into Fresenius, Spectrum and Amicon hollow fibre devices, beneath the skin of diabetic rats.

After hyperglycaemia was observed, all devices were removed. They appeared to be macroscopically intact and histological analysis at light microscopy showed that all devices were surrounded by a foreign-body inflammatory reaction.

Morphological appearance of most islets encapsulated in Fresenius and Spectrum hollow fibres was preserved from 14 to 28 days after implantation by which time hyperglycaemia

developed. Islets presented rather spherical structures and there was only limited islet destruction, as shown in Figure 4.15 (A and B). A central area affected by cell necrosis was occasionally observed, as shown in Figure 4.15 (D) that indicated probable local hypoxic damage. In contrast, islets encapsulated in Amicon fibres showed more pronounced lysis with only a few islets remaining intact. Most islets were fragmented inside the alginate gel as shown in Figure 4.15 (C).

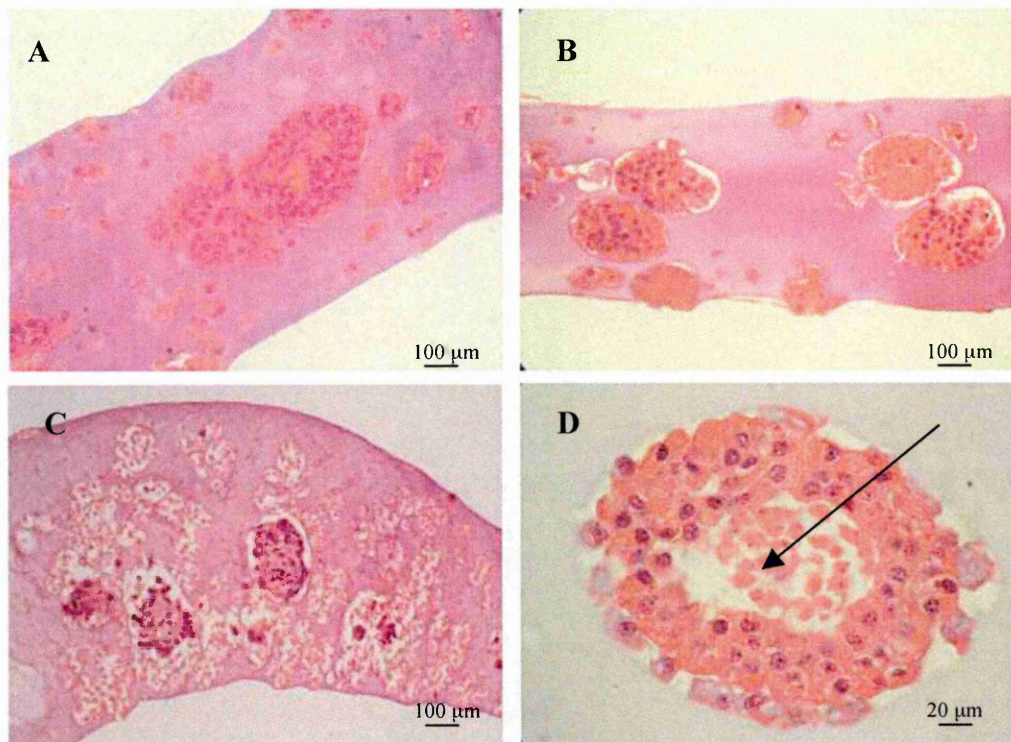


Figure 4.15 Light microscopy (haematoxylin-eosin staining) of islets contained in Fresenius fibre (A), Spectrum fibre (B) and Amicon fibre (C) devices, recovered from rats 2 weeks after implantation. Islets are entrapped inside alginate gel. Representative morphology (D) of an islet encapsulated in a hollow fibre device 2 weeks after implantation, showing central necrosis (arrow).

Moreover histological analysis at light microscopy showed that all devices were surrounded by a foreign-body inflammatory reaction (Figure 4.16).



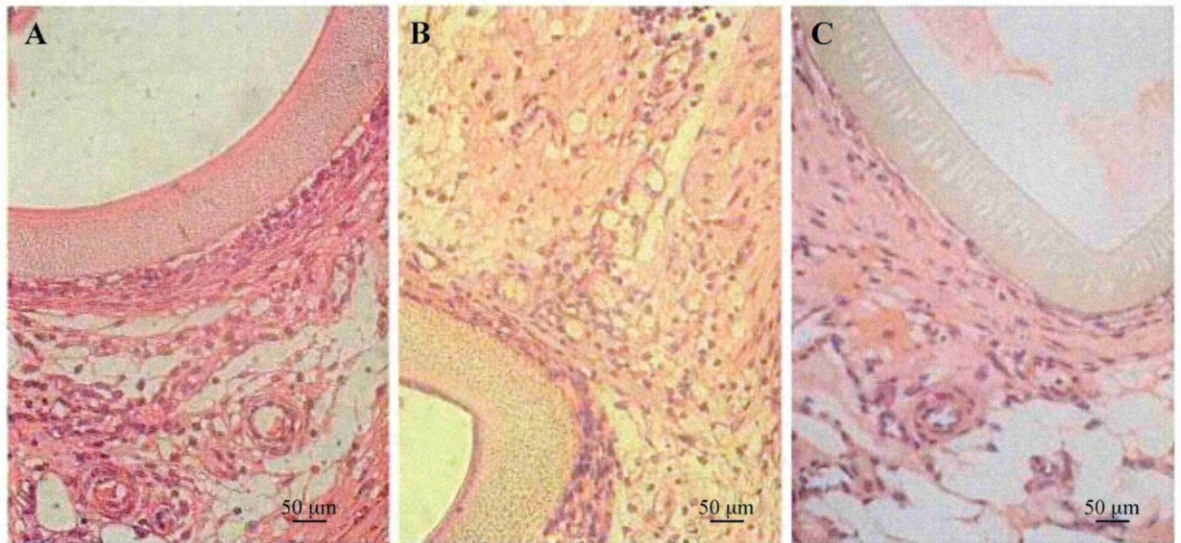


Figure 4.16 Light microscopy (hematoxylin-eosin staining) of fibrotic overgrowth around Fresenius fibre (A), Spectrum fibre (B) and Amicon fibre (C) device recovered from MWF rats 2 weeks after implantation

Immunohistochemical analysis revealed the presence of a large number of macrophages (A) but only few lymphocytes (B) in the fibrotic capsule around membrane devices (Figure 4.17). Cell composition of the fibrotic reaction was similar in all three groups.

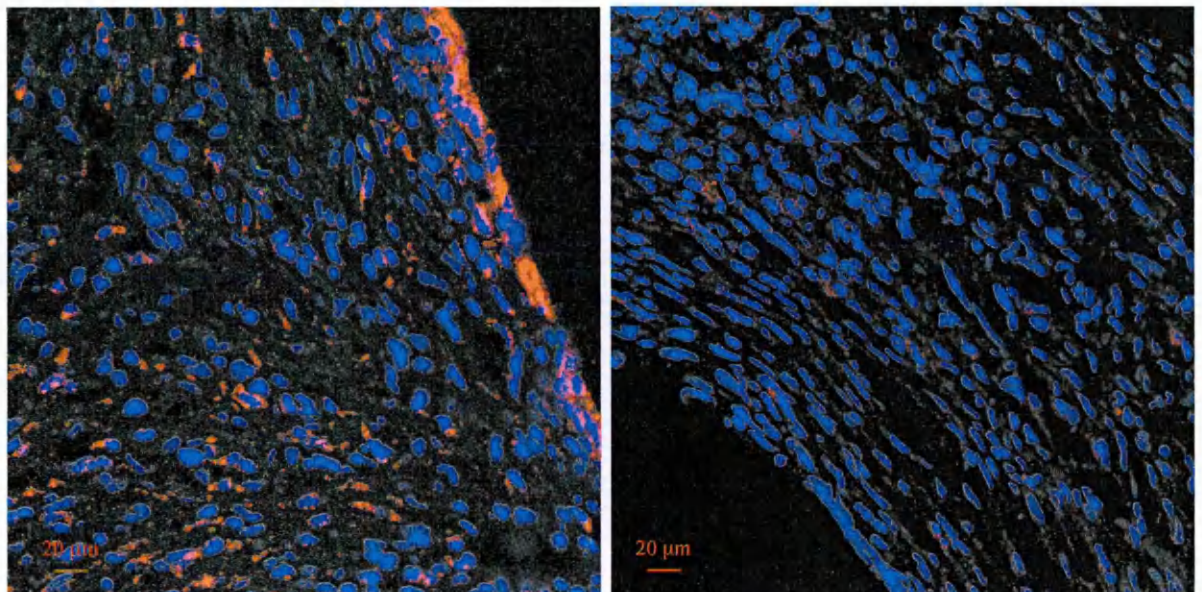


Figure 4.17 Histological evaluation revealed the presence of a large number of macrophages, notably near membrane of devices containing islets (A, ED1+, in red) but only few lymphocytes (B, CD8+, in red) in the fibrotic capsule



In conclusion, implantation of devices successfully normalized hyperglycaemia in diabetic rats and these results demonstrated that, at least in the first time period after implantation, the islets were functional, metabolites were effectively exchanged across membrane walls and membrane provided functional immunoprotection to the bovine islets. The reason for loss of islet function after a maximum of 20 days seemed independent of islet isolation. Thus, bovine islets embedded in alginate gel and transplanted into the peritoneal cavity of diabetic rats showed prompt normalization of blood glucose, and normoglycaemia was maintained for a long period of time. The reason for loss of function of islets within immunoisolation membranes must be related to the presence of the membrane material and/or cellular deposition outside the devices. Morphological analysis of the devices retrieved and processed, when animals returned to a hyperglycaemic condition, showed foreign body inflammatory reaction at the membrane-tissue interface that was comparable in all three fibres used. This reaction mainly consisted of a fibrotic capsule with predominant presence of macrophages, with only a minority of infiltrating cells, such as T lymphocytes. This indicates that the membranes effectively protected these bovine islets from xenorejection and that the cellular reaction was mainly related to implantation of artificial material.

Most of the islets retrieved from Amicon fibres were broken and fragmented, confirming *in vitro* and *in vivo* data of a shorter functional duration. In Fresenius and Spectrum devices, better preservation islets were noted. However, in islets that showed preserved structure frequently presented a central necrotic area. This is probably was caused by inadequate oxygenation when islets were isolated from the organ and transplanted. In normal physiological conditions, islets in the pancreas are highly vascularized and well oxygenated but, when inserted into the device, oxygen transmission is only related to

diffusion. Poor vasculature of the subcutaneous site may further contribute to this necrosis of implanted islets.

*Syngeneic transplantation*

Analyzing results obtained from the xenogenic protocol, it was decided to test syngeneic transplantation of devices made of Fresenius hollow fibres. These experiments were performed to understand whether transplantation site and immunoisolation membrane would allow normalization of glycaemia using syngeneic islets. First, it was implanted 3000 syngeneic islets (the same amount used in microcapsules) within devices beneath the skin of 5 diabetic rats. No normalization of glucose concentration was obtained but all five rats that received encapsulated islets showed prolonged weight gain (Figure 4.18).

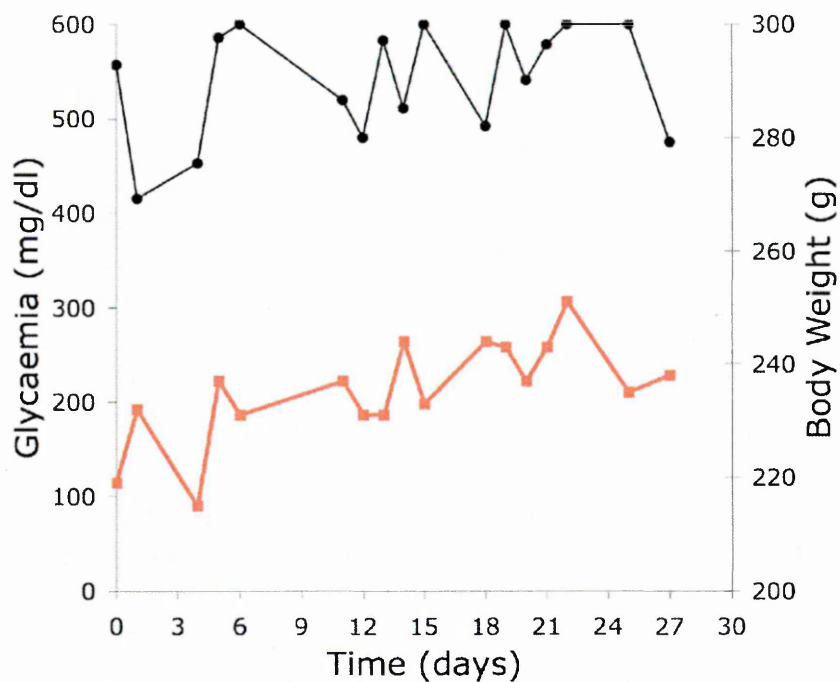


Figure 4.18 Non-fasting blood glucose levels (black) and body weight (red) after islet implantation in Fresenius hollow fibre devices beneath the skin of diabetic rats

Histological evaluation of islets inside the device showed that after 2 weeks islet structure was damaged and only few nuclei were seen. Moreover, histological analysis at light microscopy showed that all devices were surrounded by the foreign-body reaction, but less dense that seen after in xenogenic implantation (see Figure 4.19).

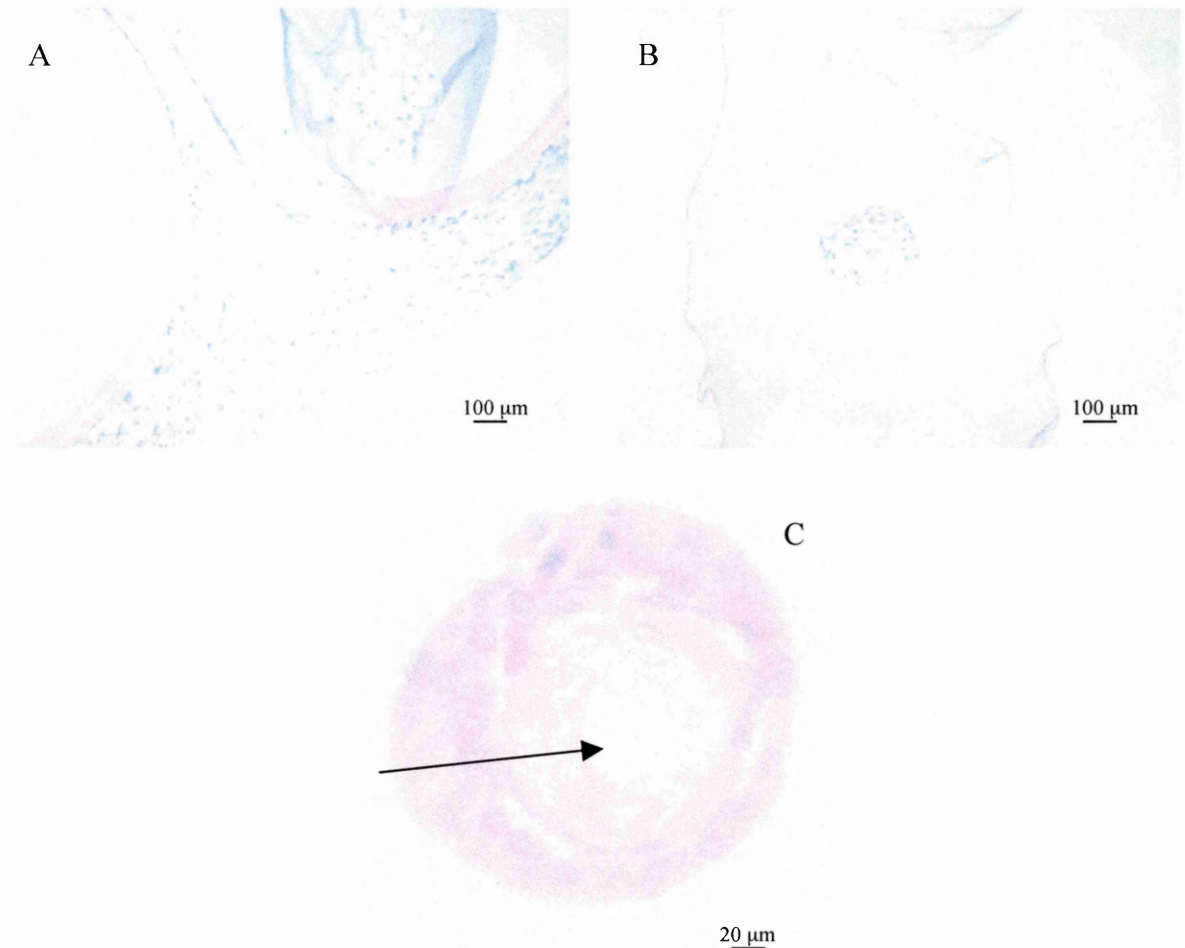


Figure 4.19 Light microscopy (haematoxylin-eosin staining) of fibrotic overgrowth (A) and of islets contained in Fresenius (B) devices recovered from rats 2 weeks after implantation. Representative morphology (C) of an islet encapsulated in a hollow fibre device 2 weeks after implantation, showing central necrosis (arrow)

Immunohistochemical analysis revealed the presence of a large number of macrophages but no lymphocytes in the fibrotic capsule around membrane devices. Cell composition of

the fibrotic reaction observed around implanted hollow fibres was similar, with or without the use of cells inside the device (Figure 4.20).

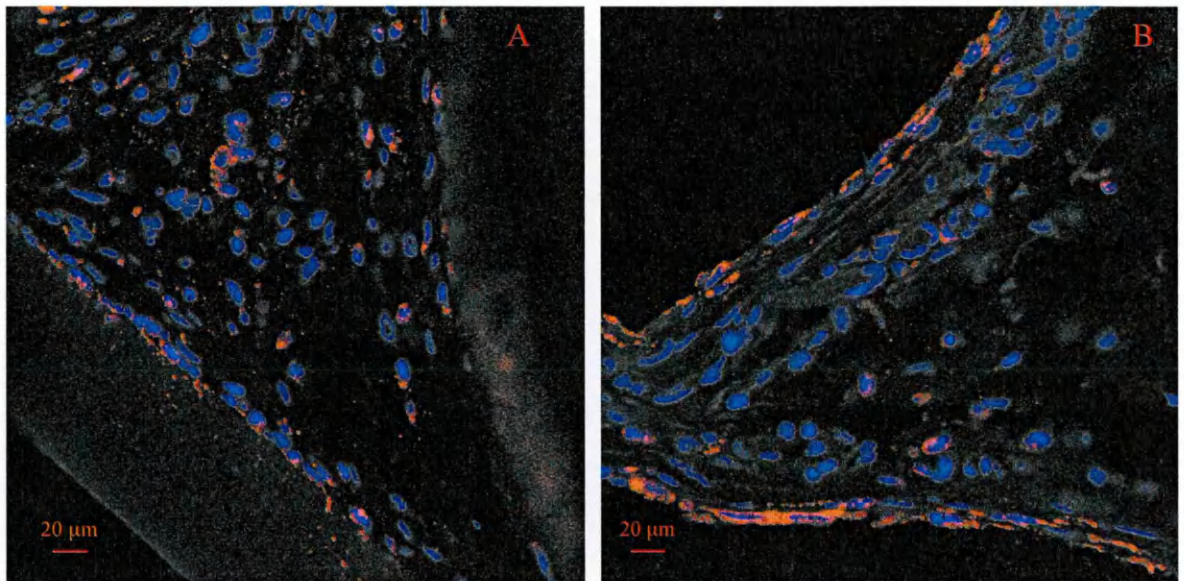


Figure 4.20 Histological evaluation revealed the presence of a large number of macrophages ED1+ (in red) on membranes of devices contained islets (A) or on empty devices (B).

These preliminary experiments demonstrate that material with permeability was needed that provides immunoprotection plus tissue nutrition is essential. Immunohistochemical detection of macrophages and lymphocytes demonstrated that in xenogenic and syngeneic islet transplantation the response was comparable, probably due to tissue response to the artificial material implanted and not to the cells inside the device. In both cases central necrosis was observed in islet explanted. Next finding a good material for device implantation, with ideal porosity and biocompatibility was required.

## References

1. Colton CK. Implantable biohybrid artificial organs. *Cell Transplant* 1995;4:415-436.
2. Lacy PE, Hegre OD, Gerasimidi-Vazeou A, Gentile FT, Dionne KE. Maintenance of normoglycemia in diabetic mice by subcutaneous xenografts of encapsulated islets. *Science* 1991;254:1782-1784.
3. Lanza RP, Chick WL. Immunoisolation: at a turning point. *Immunol Today* 1997;18:135-139.
4. Hasse C, Schrezenmeir J, Stinner B, Scharck C, Wagner PK, Neumann K et al. Successful allotransplantation of microencapsulated parathyroids in rats. *World J Surg* 1994;18:630-634.
5. Hara K, Uchida K, Fukunaga A, Toya S, Kawase T. Implantation of xenogenic transgenic neural plate tissues into parkinsonian rat brain. *Cell Transplant* 1997;6:515-519.
6. Winn SR, Hammang JP, Emerich DF, Lee A, Palmiter RD, Baetge EE. Polymer-encapsulated cells genetically modified to secrete human nerve growth factor promote the survival of axotomized septal cholinergic neurons. *Proc Natl Acad Sci U S A* 1994;91:2324-2328.
7. Aebischer P, Schlupe M, Deglon N, Joseph JM, Hirt L, Heyd B *et al.* Intrathecal delivery of CNTF using encapsulated genetically modified xenogenic cells in amyotrophic lateral sclerosis patients. *Nat Med* 1996;2:696-699.
8. Kanai N, Hagihara M, Nagamachi Y, Tsuji K. Beneficial effects of immunoisolated fetal and neonatal pig liver fragments on acute liver failure in a large animal. *Cell Transplant* 1999;8:413-417.

9. de Vos P, Marchetti P. Encapsulation of pancreatic islets for transplantation in diabetes: the untouchable islets. *Trends Mol Med* 2002;8:363-366.
10. Lim F, Sun AM. Microencapsulated islets as bioartificial endocrine pancreas. *Science* 1980;210:908-910.
11. Wang T, Lacik I, Brissova M, Anilkumar AV, Prokop A, Hunkeler D *et al.* An encapsulation system for the immunoisolation of pancreatic islets. *Nat Biotechnol* 1997;15:358-362.
12. De Vos P, Wolters GH, Fritschy WM, Van Schilfgaarde R. Obstacles in the application of microencapsulation in islet transplantation. *Int J Artif Organs* 1993;16:205-212.
13. De Vos P, De Haan BJ, Wolters GH, Strubbe JH, Van Schilfgaarde R. Improved biocompatibility but limited graft survival after purification of alginate for microencapsulation of pancreatic islets. *Diabetologia* 1997;40:262-270.
14. Elliot RP, Garkavenko O, Schroeder BA. No evidence of infection with porcine endogenous retrovirus in recipients of encapsulated porcine islet-cell xenograft. Abstract book, 7th World Congress of the IPITA 1999;229:143.
15. Calafiore R, Basta G, Luca G, Lemmi A, Montanucci MP, Calabrese G *et al.* Microencapsulated pancreatic islet allografts into nonimmunosuppressed patients with type 1 diabetes: first two cases. *Diabetes Care* 2006;29:137-138.
16. Lanza RP, Chick WL. Transplantation of encapsulated cells and tissues. *Surgery* 1997;121:1-9.
17. Lanza RP, Borland KM, Lodge P, Carretta M, Sullivan SJ, Muller TE *et al.* Pancreatic islet transplantation using membrane diffusion chambers. *Transplant Proc* 1992;24:2935-2936.

18. Lanza RP, Beyer AM, Staruk JE, Chick WL. Biohybrid artificial pancreas. Long-term function of discordant islet xenografts in streptozotocin diabetic rats. *Transplantation* 1993;56:1067-1072.
19. Jesser C, Kessler L, Lambert A, Belcourt A, Pinget M. Pancreatic islet macroencapsulation: a new device for the evaluation of artificial membrane. *Artif Organs* 1996;20:997-1007.
20. Sorenby A, Rafael E, Tibell A, Wernerson A. Improved histological evaluation of vascularity around an immunoisolation device by correlating number of vascular profiles to glucose exchange. *Cell Transplant* 2004;13:713-719.
21. Tatarkiewicz K, Hollister-Lock J, Quickel RR, Colton CK, Bonner-Weir S, Weir GC. Reversal of hyperglycemia in mice after subcutaneous transplantation of macroencapsulated islets. *Transplantation* 1999;67:665-671.
22. Loudovaris T, Jacobs S, Young S, Maryanov D, Brauker J, Johnson RC. Correction of diabetic nod mice with insulinomas implanted within Baxter immunoisolation devices. *J Mol Med* 1999;77:219-222.
23. Sweet IR, Yanay O, Waldron L, Gilbert M, Fuller JM, Tupling T *et al.* Treatment of Diabetic Rats with Encapsulated Islets. *J Cell Mol Med* 2008.
24. Pileggi A, Molano RD, Ricordi C, Zahr E, Collins J, Valdes R *et al.* Reversal of diabetes by pancreatic islet transplantation into a subcutaneous, neovascularized device. *Transplantation* 2006;81:1318-1324.
25. Brauker J, Martinson LA, Young SK, Johnson RC. Local inflammatory response around diffusion chambers containing xenografts. Nonspecific destruction of tissues and decreased local vascularization. *Transplantation* 1996;61:1671-1677.

26. Fritschy WM, de Vos P, Groen H, Klatter FA, Pasma A, Wolters GH *et al.* The capsular overgrowth on microencapsulated pancreatic islet grafts in streptozotocin and autoimmune diabetic rats. *Transpl Int* 1994;7:264-271.
27. Castner DG, Ratner BD. Biomedical surface science: Foundations to frontiers. *Surface Science* 2002;500:28-60.
28. Soon-Shiong P, Heintz RE, Merideth N, Yao QX, Yao Z, Zheng T *et al.* Insulin independence in a type 1 diabetic patient after encapsulated islet transplantation. *Lancet* 1994;343:950-951.



## Chapter 5

### *In vitro* evaluation of encapsulation: oxygen consumption rate (OCR) measurements

1.10 Experimental set-up for OCR determination

1.11 OCR measurements and results

Conclusion

References

## ***In vitro* evaluation of encapsulation: oxygen consumption rate (OCR) measurements**

In the previous chapters it has been explained how islets can be obtained from a pancreas and how they can be tested in terms of their functionality *in vivo*. Islet encapsulation in semipermeable matrices, such as alginate gel, or within membrane devices (1), have been studied in experimental as well as in clinical settings (2). An immunoisolation device has been described here that allows adequate diffusion of oxygen and nutrients to maintain islet viability and function yet at the same time, selective enough to prevent permeation of host immune proteins.

This chapter presents the rapid and quantitative experimental method by using which viability of encapsulated islets has been determined. Previous classical methods have been based on selective staining, thus being more qualitative than quantitative, and requiring long and often difficult procedures. Recent studies have shown a direct correlation between changes in mitochondrial activity and cell function as a whole (3), and according to these findings, metabolic follow-up would offer an alternative, valid way to quantify cellular activity.

Thus, it has been proposed to couple classical tests for cell viability to a device to measure oxygen catabolism of cell cultures (Figure 5.1). This combination allows more reliable, precise and indeed faster, measurements to be made. The device consists of:

- oximeter
- measurement chamber
- circulator
- magnetic stirrer

- data recorder/computer-assisted acquisition system

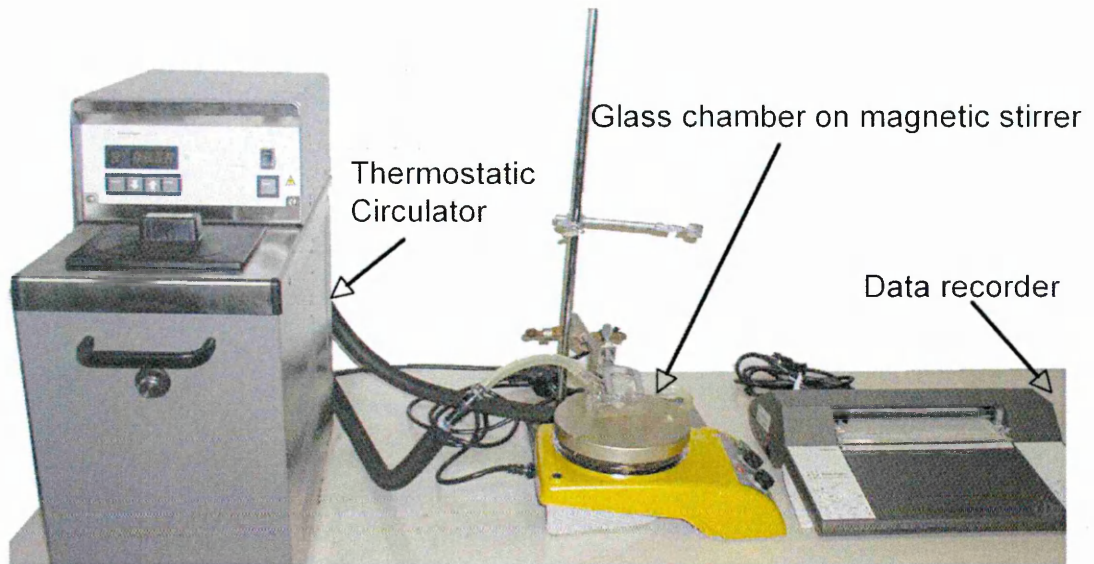


Figure 5.1 Global view of the system used for OCR measurements

The main component of the measurement device is the Clark's electrode (4). Measurements are based on the classical polarographic method, in which a potential difference is created in two half cells, one of platinum, the cathode, and one of silver, the anode (see page 129), permitting reduction of a chemical element, such as oxygen. This process results in generation of an electric current, which is converted into a tension signal before being sent to a data detection system. Data are subsequently elaborated using Excel software to provide an output, which is the oxygen consumption rate (OCR) *per* vital unit. The measurement chamber is made of two compartments, an internal one, in which the measurement is carried out, and an external one, the water jacket, which enables changes in the operative conditions to be made.

Adequate measurement of viability of pancreatic islets during the time elapsed between isolation and transplantation is crucial, in order to prevent transplantation of inefficient islets. Correlation between glycaemia and oxygen consumption is crucial in transplanted

islets, which are exposed to high glycaemic levels and might quickly undergo cell death as a response to hypoxia. Moreover, after the isolation process, the islets lack any blood supply but with this system they can gather sufficient nutrients thanks to the diffusion process alone. This implies that oxygen consumption of islets inside the immunoisolation device produces an oxygen gradient that regulates gas flux through the membrane, as *per* its diffusion coefficient, as stated in Fick's Law. Thus, whenever the diffusion coefficient is very low, the oxygen flux to the inner cells of the islet is inferior to oxygen consumption, resulting in hypoxia, and eventually in death of the islet cells.

This has been used to investigate the role of glucose in  $\beta$ -cell metabolism. Since insulin secretion depends directly on glucose haematic levels, a considerable increase in cellular activity, and therefore oxygen consumption, is registered in islets, in response to high glycaemic levels.

Therefore, precise measurement of cellular oxygen consumption using appropriate techniques is not only an efficient method to quantify the cells' viability, but it also offers a new way to explore the various factors influencing their functionality under different operational conditions.

### 5.1 Experimental set-up for OCR determination

For measurement of OCR, a thermostated chamber was designed (see Figure 5.2), made of two compartments, the inner, in which the measurements are carried out, and the external water jacket enabling temperature to be changed during operating conditions.

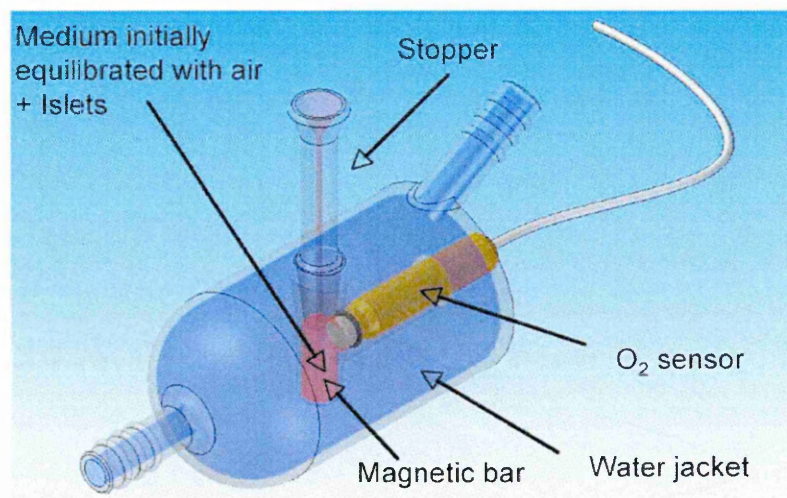


Figure 5.2 Thermostated chamber

A Clark oxygen electrode (4) is composed of the two half-cells separated by a salt bridge, the platinum electrode is separated from the solid silver by insulating material. The electrodes are immersed in a concentrated potassium chloride solution separated by a Teflon membrane, attached by an O-ring. The oxygen monitor holds a constant voltage difference across the two electrodes so that the platinum electrode is negatively charged with respect to the silver one (Figure 5.3). Platinum is a strong catalyst for the covalent dissociation or re-association of water; in the Clark electrode, electrons are released from it, combining with dissolved molecular oxygen and hydrogen ions to produce water. The rate at which electrons are liberated is proportional to the concentration of oxygen that is

available to combine with them. Movement of electrons produces the electrical current that is then converted to a voltage by the oxygen monitor circuitry.

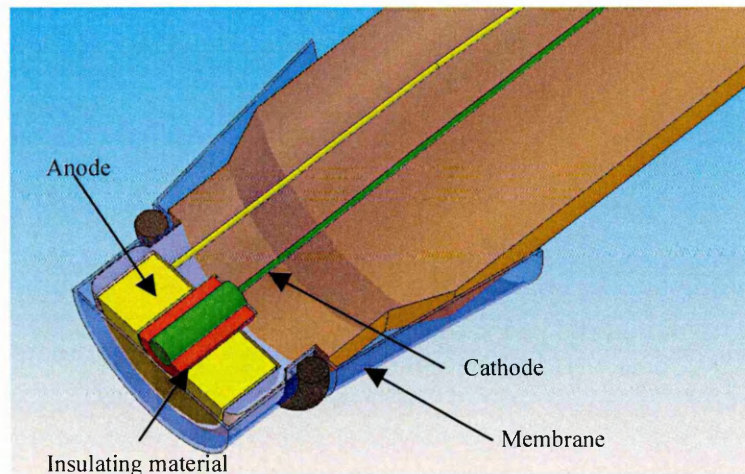


Figure 5.3 Schematic of Clark's electrode. Pt cathode (green), Ag anode (yellow), insulating material (red) and the Teflon membrane

The system was preliminarily calibrated using distilled water at 37°C in which atmospheric oxygen concentration was taken to be  $[O_2]=215 \mu\text{M}$  (5). Null  $O_2$  concentration was obtained by saturating the solution in the chamber using nitrogen gas. After 10 minutes recording was constant and taken to correspond to zero  $[O_2]$ . Oxygen consumption was calculated from the slope of oxygen concentration recording vs. time by linear regression analysis (as shown in Figure 5.4). OCR per islet equivalent was then calculated as

$$OCR = \frac{\Delta[O_2]}{\Delta T} \cdot \frac{V}{IEQ} \quad \left[ \frac{pmol}{IEQ \cdot min} \right]$$

where IEQ is the number of islet equivalents in the chamber and V the solution volume.



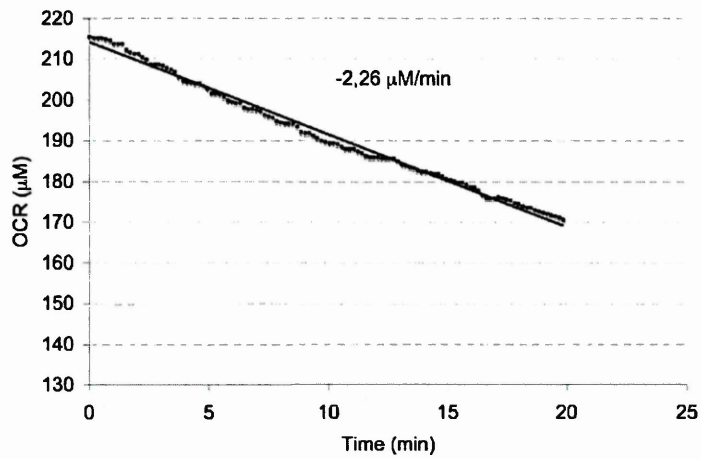


Figure 5.4 OCR calculated by linear regression

A representative experiment is reported in Figure 5.5, in which the  $[\text{O}_2]$  was recorded for up to complete consumption. As shown in the figure,  $[\text{O}_2]$  changes with time were close to constant even for the low levels of  $[\text{O}_2]$  that were reached in more than 160 minutes.

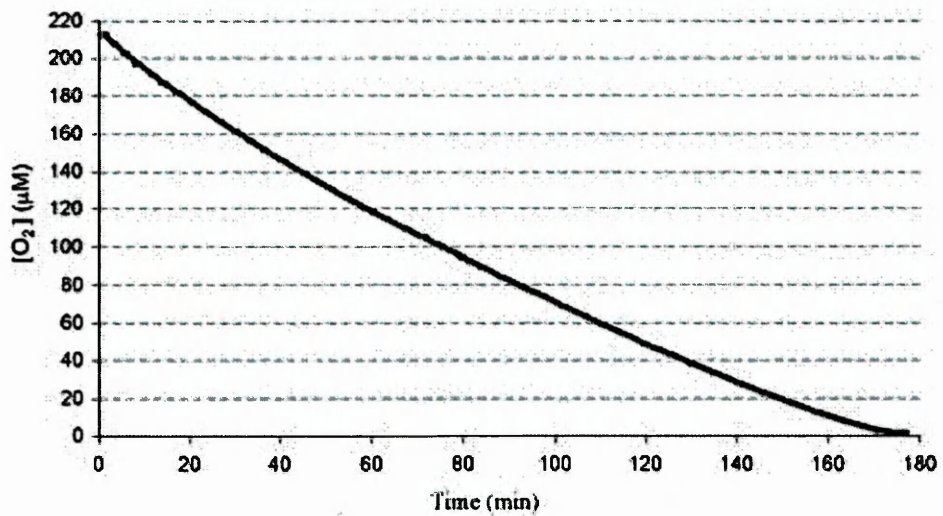


Figure 5.5 Representative experiment of OCR vs. time

## 5.2 OCR measurements and results

### *Islet encapsulation in microcapsules and in polysulphone hollow fibres*

After islet isolation and 24 hours in culture, for the production of capsules, islets were suspended in a solution of 1.7% sodium alginate (Manugel DMB, Monsanto plc, Surrey, United Kingdom) at a concentration of 3 islet equivalents (IEQ)/ $\mu\text{l}$ . The islet-alginate mixture was then extruded through an air jet droplet generator into a solution of 100 mM  $\text{CaCl}_2$  solution. Gel beads resulted with diameters ranging from 800 to 950  $\mu\text{m}$  (Figure 5.6-A). For islet encapsulation in polysulphone hollow fibres, alginate solution was inserted into them (490  $\mu\text{m}$  inner diameter and 70  $\mu\text{m}$  membrane thickness, Fresenius Medical Care, Bad Hamburg, Germany) using a perfusion system, to allow uniform loading of islet solution among the fibres at a concentration of 50 IEQ/ $\mu\text{l}$  (Figure 5.6-B). After perfusion, fibres were sealed and immersed into 100 mM  $\text{CaCl}_2$  solution for 10 minutes to allow alginate gelification, and then the loaded fibres were immersed in culture medium.

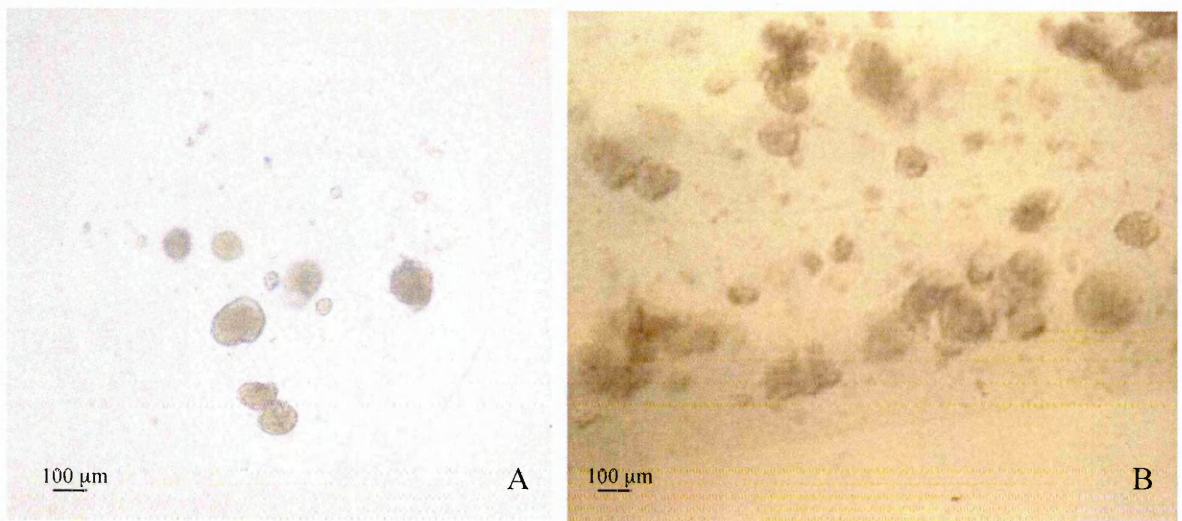


Figure 5.6 Islets encapsulated in microcapsules (A) or in hollow fibres (B).



Oxygen consumption measurements.

For these measurements, islets from four different preparations were used. The number of islets in each sample was calculated on the basis of total islet number *per* isolation, using a dilution of islet suspension. Each sample contained on average 997 IEQ (650-1200 IEQ). Islets were centrifuged for 2 min at 800 rpm, supernatant was removed and the pellet was suspended in 200  $\mu$ l of pre-warmed (37°C) M199 serum-free medium (glucose concentration = 5.5 mM). The islet suspension was added to the chamber and after sealing, thermal equilibration at 37°C was allowed for around 30 seconds; each measurement lasted in the region of 30 minutes. For OCR determination at high glucose, a glucose concentration of 25 mM was used, adding concentrated glucose solution in the same preparation. OCR of encapsulated islets was assessed immediately after encapsulation in microcapsules and hollow fibres (day after the isolation process) and 1 day after encapsulation. Also for this series of measurements, islets of four different preparations were used for each encapsulation technique. Each sample contained on average 1060 IEQ (670-1500 IEQ) and was placed in the chamber for OCR measurement. During all measurements the suspension was stirred, using a magnetic plate at around 50 rpm. In some experiments, after OCR measurements, free and encapsulated islets were counted and resulted to be within 96% of the value estimated before OCR measurement.

Initially the OCR was estimated of free bovine islets in suspension for a three days period after isolation. As shown in Figure 5.7, estimated mean OCR averaged  $1.39 \pm 0.38$  (pmol/IEQ/min) immediately after isolation and numerically increased to  $2.28 \pm 0.64$  (pmol/IEQ/min) at the end of the observation period (n=4).

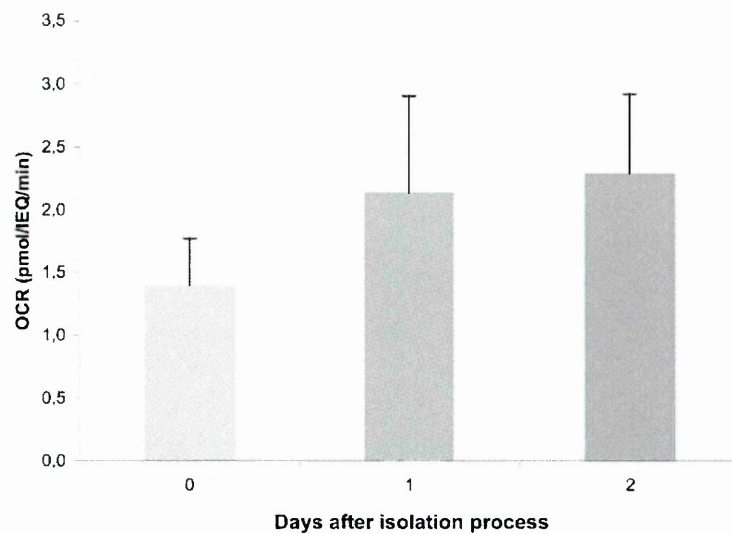


Figure 5.7 OCR of free islets measured the day of isolation (0), 24 h after the isolation process (1), and 48 h after (2).

To investigate the effect of changes in glucose concentration by OCR of free bovine islets, the day after isolation, aliquots of islet preparation were suspended either in M199 at low glucose (5.5 mM) or supplemented with high glucose (25 mM). Increase in glucose concentration significantly increased OCR as shown in the representative recording, Figure 5.8, calculated OCR averaged  $1.98 \pm 0.79$  and  $2.49 \pm 0.97$  (pmol/IEQ/min), respectively at low and high glucose levels ( $p < 0.01$ ,  $n = 12$ ).

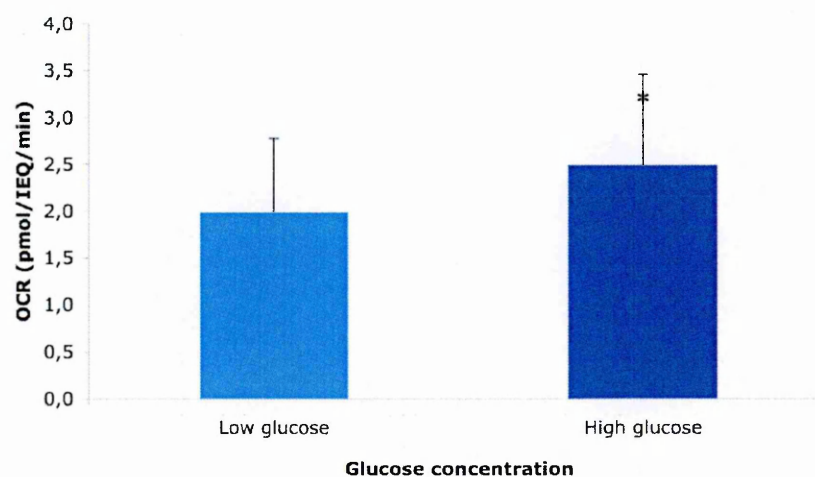


Figure 5.8 OCR in free islets measured the day after the isolation process, exposed to low or to high glucose concentration \* $p < 0.01$  low glucose vs. high glucose.

For islets encapsulated in alginate microcapsules, at a density of 3 IEQ/ $\mu$ l, the day of encapsulation OCR averaged  $2.12 \pm 0.87$  (pmol/IEQ/min) and the following day OCR averaged  $2.26 \pm 0.95$  (pmol/IEQ/min); that difference not being statistically significant. Both values were also comparable to mean OCR calculated for free islets. As shown in Figure 5.9, OCR of islets embedded in hollow fibres averaged  $1.75 \pm 0.57$  (pmol/IEQ/min) the day of encapsulation and  $2.21 \pm 0.69$  (pmol/IEQ/min) the following day (n=4), this difference not reaching statistical significance. Mean OCR of islets embedded in hollow fibres was also comparable to mean OCR measured for freely suspended islets.

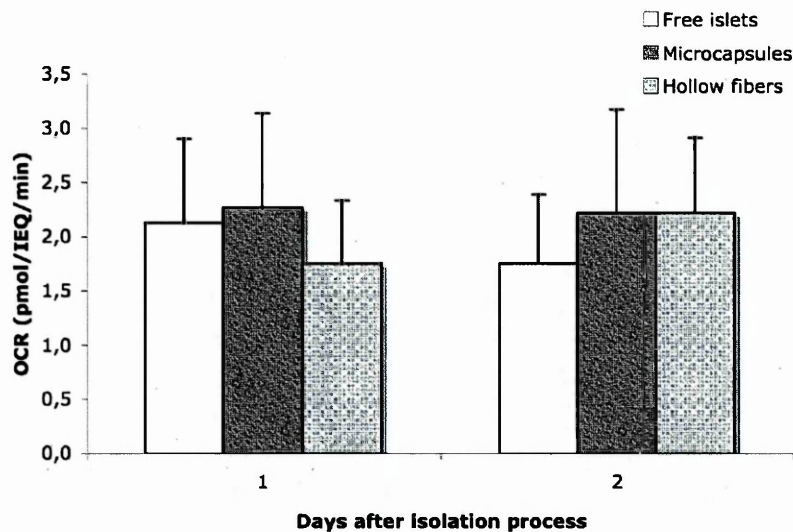


Figure 5.9 OCR for free islets, islets in microcapsules and islets in hollow fibres, measured 24 h (1) after the isolation process or 48 h (2) after.

## Conclusion

In this chapter a simple laboratory method for rapid measurement of OCR in free or encapsulated islets has been described, as a quantitative method for islet preparation and quality assessment, which allowed for measurement of OCR of bovine pancreatic islets in different experimental conditions. An average value of  $1.98 \pm 0.79$  pmol/IEQ/min was estimated for OCR in basal conditions. This is the first time that OCR of bovine islets has been determined and the values obtained are comparable to other estimates previously reported in literature for other species (6-9). The rate of oxygen consumption was found to range from 1.5 to 4.2 pmol/IEQ/min in mouse pancreatic islets, from 2 to 3 pmol/IEQ/min in rat islets and from 2.5 to 3.3 pmol/IEQ/min in human islets, these values increasing during metabolic activity induced by elevated glucose concentrations (10).

OCR of bovine islets exposed to low and high glucose concentration was also studied to assess functionality in addition to viability. Metabolism of glucose triggers insulin secretion, with acceleration of  $\beta$ -cell activity (11). Mean OCR of these bovine pancreatic islets at low glucose concentration was found to be significantly higher when exposed to high glucose concentration. It has been previously reported that static incubation with low and high glucose concentration (the same used in the present study) increased insulin production rate by bovine islets (12). Moreover, mean calculated change in OCR (see Table 5.1) of  $0.51 \pm 0.30$  pmol/IEQ/min was estimated between low and high glucose conditions (n=12), these results are in line with those reported by Sweet *et al.* for mice and human islets (13). Finally, the measured increase in OCR in response to changes in glucose concentration will provide a useful and rapid *in vitro* assay to assess functionality and viability of islet preparations.

Isolation	OCR ( $\mu\text{mol}/(\text{IEQ}\cdot\text{min})$ )		$\Delta\text{OCR}$ ( $\mu\text{mol}/(\text{IEQ}\cdot\text{min})$ )	% increase
	5.5mM glucose	25 mM glucose		
	1	0.85	1.01	0.16
2	1.74	2.02	0.28	16.2
3	1.55	2.33	0.77	49.6
4	0.94	1.45	0.51	54.5
5	1.72	2.58	0.86	50.2
6	1.99	2.12	0.13	6.6
7	2.66	3.18	0.52	19.4
8	3.17	4.07	0.90	28.4
9	1.71	2.21	0.50	29.0
10	1.46	1.56	0.10	7.2
11	3.00	3.87	0.88	29.2
12	2.96	3.43	0.47	15.8
<b>Mean</b>	<b>1.98</b>	<b>2.49*</b>	<b>0.5</b>	<b>27.1</b>
<b>SD</b>	<b>0.79</b>	<b>0.97</b>	<b>0.30</b>	<b>16.5</b>

Table 5.1 OCR,  $\Delta\text{OCR}$  and % increase in preparation of free islets exposed to low and high glucose concentration, \* $p < 0.01$

OCR by encapsulated islets was also measured to evaluate whether immunoisolation barriers represent obstacles to diffusion of oxygen, limiting normal islet function and viability. Two types of immunoisolation device were tested: alginate microcapsules (850-900  $\mu\text{m}$  diameter) and polysulphone hollow fibres (490  $\mu\text{m}$  inner diameter, 70  $\mu\text{m}$  wall thickness). There is theoretical and experimental evidence (14) to indicate that oxygen is a limiting factor for islet viability and function under immunoisolation conditions. Even though alginate gel is highly permeable to oxygen, the distance between islets in the capsules and oxygen source outside the capsule, may more than 400  $\mu\text{m}$ . For islets in hollow fibre, the worst case distance is 315  $\mu\text{m}$  between the central part of the islet and the

outside of the device, thus this distance theoretically limits diffusion of oxygen. In these experimental conditions both immunoisolation barriers allowed recording of OCR values comparable to those measured in free islets. This demonstrates that at least for high external concentration of oxygen adequate diffusion takes place. This is consistent with frequently reported long-term function of islets in alginate capsules implanted in the peritoneal cavity of diabetic rats (15). OCR by islets encapsulated in polysulphone hollow fibre also indicated that there were no major obstacles to oxygen diffusion, and here also oxygen consumption was similar to that of free islets.

## References

1. de Vos P, Hamel AF, Tatarkiewicz K. Considerations for successful transplantation of encapsulated pancreatic islets. *Diabetologia* 2002;45:159-173.
2. Valdes-Gonzalez RA, White DJ, Dorantes LM, Teran L, Garibay-Nieto GN, Bracho-Blanchet E *et al.* Three-yr follow-up of a type 1 diabetes mellitus patient with an islet xenotransplant. *Clin Transplant* 2007;21:352-357.
3. Matschinsky FM. Banting Lecture 1995. A lesson in metabolic regulation inspired by the glucokinase glucose sensor paradigm. *Diabetes* 1996;45:223-241.
4. Severinghaus JW, Astrup PB. History of blood gas analysis. IV. Leland Clark's oxygen electrode. *J Clin Monit* 1986;2:125-139.
5. Palsson B. Tissue engineering. Pearson Prentice Hall Bioengineering, 2004.
6. Hutton JC, Malaisse WJ. Dynamics of O<sub>2</sub> consumption in rat pancreatic islets. *Diabetologia* 1980;18:395-405.
7. Jung SK, Gorski W, Aspinwall CA, Kauri LM, Kennedy RT. Oxygen microsensor and its application to single cells and mouse pancreatic islets. *Anal Chem* 1999;71:3642-3649.
8. Panten U, Klein H. O<sub>2</sub> consumption by isolated pancreatic islets, as measured in a microincubation system with a Clark-type electrode. *Endocrinology* 1982;111:1595-1600.
9. Sweet IR, Khalil G, Wallen AR, Steedman M, Schenkman KA, Reems JA *et al.* Continuous measurement of oxygen consumption by pancreatic islets. *Diabetes Technol Ther* 2002;4:661-672.

10. Sweet IR, Gilbert M, Jensen R, Sabek O, Fraga DW, Gaber AO *et al.* Glucose stimulation of cytochrome C reduction and oxygen consumption as assessment of human islet quality. *Transplantation* 2005;80:1003-1011.
11. Newgard CB, McGarry JD. Metabolic coupling factors in pancreatic beta-cell signal transduction. *Annu Rev Biochem* 1995;64:689-719.
12. Figliuzzi M, Zappella S, Morigi M, Rossi P, Marchetti P, Remuzzi A. Influence of donor age on bovine pancreatic islet isolation. *Transplantation* 2000;70:1032-1037.
13. Sweet IR, Gilbert M. Contribution of calcium influx in mediating glucose-stimulated oxygen consumption in pancreatic islets. *Diabetes* 2006;55:3509-3519.
14. Avgoustiniatos ES, Colton CK. Effect of external oxygen mass transfer resistances on viability of immunoisolated tissue. *Ann N Y Acad Sci* 1997;831:145-167.
15. Figliuzzi M, Plati T, Cornolti R, Adobati F, Fagiani A, Rossi L *et al.* Biocompatibility and function of microencapsulated pancreatic islets. *Acta Biomater* 2006;2:221-227.



## Chapter 6

*In vivo* evaluation of glycaemic control in transplanted islets using continuous glucose monitoring system (CGMS)

### 6.1 Intraperitoneal glucose tolerance test

#### 6.1.1 *Materials and methods*

#### 6.1.2 *Results*

### 6.2 Pharmacokinetic model and fitting of experimental data

#### 6.2.1 *Materials and methods*

#### 6.2.2 *Results*

Conclusion

References

## ***In vivo* evaluation glycaemic control in transplanted islets using CGMS**

Islet transplantation could be a solution for diabetic patients. Site of implantation and use of immunoisolation system have to be thoroughly explored and analyzed to evaluate which is the better solution. Several rats with syngeneic islets were transplanted into the sub-capsular space of the kidney or in the peritoneal cavity, using free or encapsulated islets. Here a method was set-up to evaluate the *in vivo* ability of the islets to respond to glucose stimulation using a new system. To measure glucose control the continuous subcutaneous glucose monitoring system was used (CGMS; Medtronic, Minneapolis, MN, USA, Figure 6.1) to calculate mean glucose concentration after glucose stimulation.

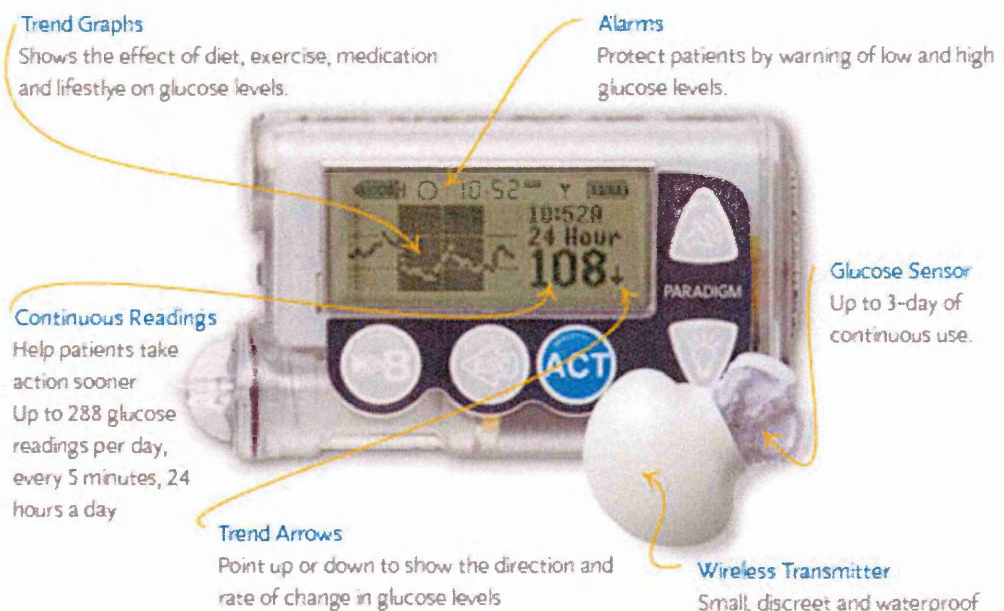


Figure 6.1 Medtronic continuous subcutaneous glucose monitoring system

CGMS has been previously used to measure glucose concentrations in subcutaneous interstitial fluid of the abdomen of human patients (1) (2) (3) and in previous studies,

CGMS levels also correlated well with capillary plasma glucose (4). This technique has been used in our laboratory as it permits a continuous monitoring of glucose concentration without continuous separate measurements of capillary plasma glucose. The primary aim of this study was to assess the value of CGMS in rats implanted with islets. A second aim was to investigate any relationships between glucose concentrations after glucose stimulation and the kind of implantation, using healthy rats as control.

## **6.1 Intraperitoneal glucose tolerance test**

The intraperitoneal glucose tolerance test (IPGTT) is a commonly used technique to measure acute, first-phase insulin release in response to glucose load and therefore represents a useful method to assess pancreatic function (5) (6). The IPGTT was established as a standardised method for assessing compounds designed to improve pancreatic islet function.

### ***6.1.1 Materials and methods***

Highly inbred male Lewis rats were used as donors and recipients. Animals were divided in three groups: n=8 healthy rats, n=8 diabetic rats transplanted with islets in microcapsules and n=8 diabetic rats transplanted with islets beneath kidney capsules. Diabetes was induced by a single injection of streptozotocin (65 mg/kg body weight; Sigma, St. Louis, MO, USA) into the tail vein, and then non-fasting blood glucose levels and body weight were measured twice a week. Blood glucose concentration was determined by tail bleedings using the Glucocard Memory 2 system (Menarini, Firenze, Italy).

#### **Islet isolation**

In this kind of experiment the automatic method was applied and it has been used to process 10-14 pancreata of Lewis rats, as shown in Chapter 2, page 54. Briefly, rats were anesthetized with an intraperitoneal injection of sodium pentobarbital (7). For each rat the same procedure was followed: after main bile duct location at its entrance in the gut, it was legated with silk suture 4.0. The duct was cannulated with polyethylene tubing (PE 50) connected to a 22-gauge cannula and the rat was sacrificed. The pancreas was distended with 10-12 ml of collagenase P solution and dissected free of small bowel,

stomach and spleen; then it was removed and then rinsed in a centrifuge tube containing cold HBSS. Distended pancreases were then loaded into the digestion chamber at 37°C with four stainless steel ball bearings. When optimum digestion time was reached, the chamber was flushed with cold HBSS (4°C). Digested tissue was collected and purified by centrifugation on Histopaque gradient. Islets, >95% purity, were counted and cultured at 37°C in a cell incubator in humidified atmosphere with 5% CO<sub>2</sub> in RPMI medium, supplemented with bovine serum.

#### *Islet encapsulation in microcapsules and transplantation*

For encapsulation and transplantation the same procedures described in Chapter 4 was applied, page 100. Briefly, after 24 hours in culture, for the production of capsules, 3000 islets were suspended in a solution of 1.7% sodium alginate at a concentration of 1 islets/μl. The islet-alginate mixture was then extruded through an air jet droplet generator into a solution of 100 mM CaCl<sub>2</sub> solution. Gel beads resulted in having a diameter ranging from 800 to 950 μm. Implantation of microcapsules was into diabetic rats weighing 200–220 g, into the peritoneal cavity through a small (1–2 cm) midline incision under Avertin anaesthesia (8).

#### *Islet transplantation under the kidney capsule*

For transplantation the same procedures described in Chapter 3 was used, page 81. Briefly, the day after isolation, 3,000 islets were resuspended in HBSS. After centrifugation, they were inserted into a polyethylene catheter with an internal diameter of 500 μm, and islets were concentrated into pellets in the final delivery tubing used to transplant them under the kidney capsule. In the experimental facility, the rat was anaesthetized with Avertin and when the anaesthetic had taken effect, the left flank of the rat was shaven. After kidney location, just beneath the spleen, a small incision in the skin permitted the peritoneum visualization. Making a small incision also into the peritoneum, the kidney was exposed.

The kidney and the abdomen of the rat were kept moist by the use of saline solution applications during the whole procedure. Using a 23 or 25 gauge needle, a small scratch on the right flank of the kidney was made, creating a nick in the kidney capsule, into which the PE50 tubing was carefully and slowly inserted, making a small pocket. Using a Hamilton syringe, islets were slowly advanced into this. The PE50 tubing was slowly removed and carefully the nick was cauterized with low heat. The kidney was then gently replaced into the peritoneum, prior to closing the rat with suture and skin staples.

*IPGTT and continuous glucose monitoring system*

Six hours before IPGTT, the rat was anesthetized with Avertin and when the anaesthetic had taken effect, its dorsal skin was shaven. A tiny glucose-sensing device (sensor, Figure 6.2) was inserted just under the skin quickly and painlessly. After calibration, the sensor began to measure glucose levels in the tissue every 10 seconds and sent the information by wire to a pager-sized device (the receiver) positioned near rat's cage.

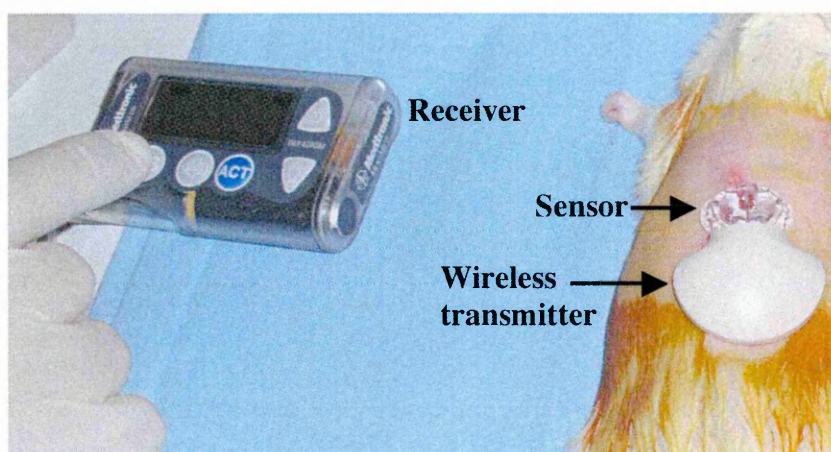


Figure 6.2 Photograph of the system inserted on the back of a rat with all the components specified

The system automatically recorded average glucose values every 5 minutes for up to 72 hours. After 6 hours, the rat was injected intraperitoneally with sterile glucose solution. After 3 days, the sensor was removed and information stored in the CGMS was

downloaded to a computer. The limit of glucose concentration measured from the system was 400 mg/dl. Over this value the system gave a reading of 400 mg/dl.

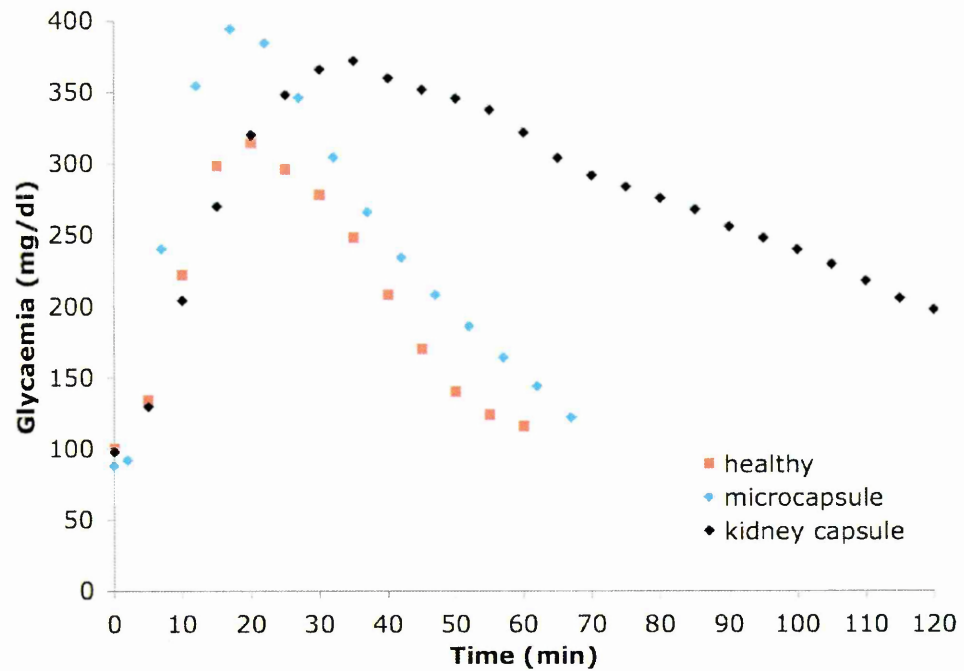
### **6.1.2 Results**

First, a homogeneous state of normoglycaemia was observed in the three groups, with no significant statistical differences over non-fasting glucose concentration, as shown in Table 6.1.

<b>Group</b>	<b>Glycaemia mg/dl (mean <math>\pm</math> SD)</b>
Healthy rats	91 $\pm$ 14
Microcapsules tx	90 $\pm$ 16
Kidney capsule tx	108 $\pm$ 22

Table 6.1 Values of non-fasting blood glucose concentration for the three experimental groups

Then values of glucose concentration were analyzed under stimulation, downloaded from each receiver, then were inserted in a Excel spreadsheet. Each group (healthy rats, diabetic rats transplanted with islets in microcapsules and diabetic rats transplanted with islets under the kidney capsules) was determined; a representative curve of values of glycaemia after glucose injection (t=0) is provided below.



From these graphic values, areas under the curve (AUC) were calculated for each experiment and values obtained were expressed as mean  $\pm$  SD in Table 6.2. Statistical significance was determined using the analysis of variance (software StatView, SAS Institute Inc. Cary, NC, USA) and specific comparisons between groups were calculated using Student's t-test and with the Bonferroni correction (9). The level of significance was taken to be  $p < 0.05$

Group	AUC mg/dl x min (mean $\pm$ SD)
Healthy rats	11055 $\pm$ 4038
Microcapsules tx	21883 $\pm$ 4560
Kidney capsule tx	48411 $\pm$ 23062 *

Table 6.2 Values of AUC for the three experimental groups. \* $p < 0.05$  vs. kidney capsule and microcapsules

These data were used to understand the process of glucose elimination for each group of animals. Then it was elaborated a pharmacokinetic model that would best fit the experimental data.



## 6.2 Pharmacokinetic model and fitting of experimental data

One of the most important outcomes in pharmacokinetic modelling is the ability to predict drug levels and dynamic types of behaviour of drugs in the body, another is the ability to deduce mechanistic insight into what events have been observed. Sometimes the question is not how realistic the models are but what is their consistency and adequacy in making predictions. Most models are simplifications of the reality, but they are easy to assemble, useful, and relevant.

Various approaches have emerged to predict blood/plasma and tissue concentration time profiles and to provide mechanistic insight into what events have occurred (10). Compartmental approaches are the simplest and most widely used. The premise is based on venous equilibration and mass transfer into and out of compartments. In recent decades, however, modelling techniques have become more sophisticated. There is some departure from the compartmental modelling approach to physiological modelling, in order to confer more significance to anatomy, flow, and discrete eliminatory and distributional organs in the body. In the case of the glucose elimination process after intraperitoneal injection a two compartments pharmacokinetic model was applied with first order absorption. The single compartment model assumes that the drug rapidly distributes throughout the homogeneous apparent distribution volume. However, the drug may distribute at different rates into different tissues of the body, and it may require an extended period of time before its concentration equilibrates between different tissue and fluid regions. Clearly, this is a complex process and a reasonable simplification is the two compartments model shown in Figure 6.3.

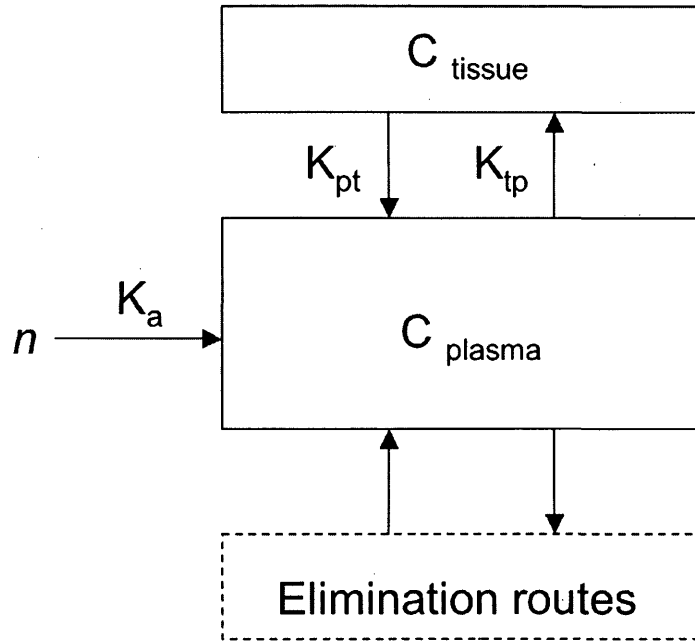


Figure 6.3 Two compartments model with first order absorption

Glucose is introduced into the central compartment (plasma) and then slowly distributes into the remaining tissue and fluid space. The constants  $k_{pt}$  and  $k_{tp}$  represent rate constants describing first order transport between the plasma and tissue compartment. In this case insulin is the “elimination route” for glucose.

### 6.2.1 Materials and methods

Values of glycaemia recorded every 5 minutes by CGMS were inserted into software for non-linear regression (EasyPlot) to fit the experimental data. For fitting was used the two compartments model for first order absorption, where concentration of glucose in the tissue  $C_{tissue}$  is determined solving the mass balance equation for glucose written for the plasma and the tissue and the concentration of glucose in the tissue compartment given by

$$C_{tissue}(t) = k_{pt} k_a n \left[ \frac{e^{-At}}{(k_a - A)(B - A)} + \frac{e^{-Bt}}{(k_a - B)(A - B)} + \frac{e^{-k_a t}}{(A - k_a)(B - k_a)} \right] \quad (6.1)$$

where  $k_{pt}$  is the rate constant describing the first order transport between the plasma (p) and the tissue (t) compartments,  $k_a$  is the rate constant describing absorption (a),  $n$  a numerical parameter dependent from on weight of the rat and the dose of glucose injected. A and B are the parameters determined by fitting. These parameters have dependence given by the following equations

$$\begin{cases} k_{tot} = \frac{AB}{k_{ip}} \\ k_{pt} = (A + B) - (k_{ip} + k_{tot}) \end{cases} \quad (6.2)$$

where  $k_{ip}$  is the rate constant describing the first order transport between the tissue and the plasma compartments and  $k_{tot}$  is the constant describing the elimination process.

### **6.2.2 Results**

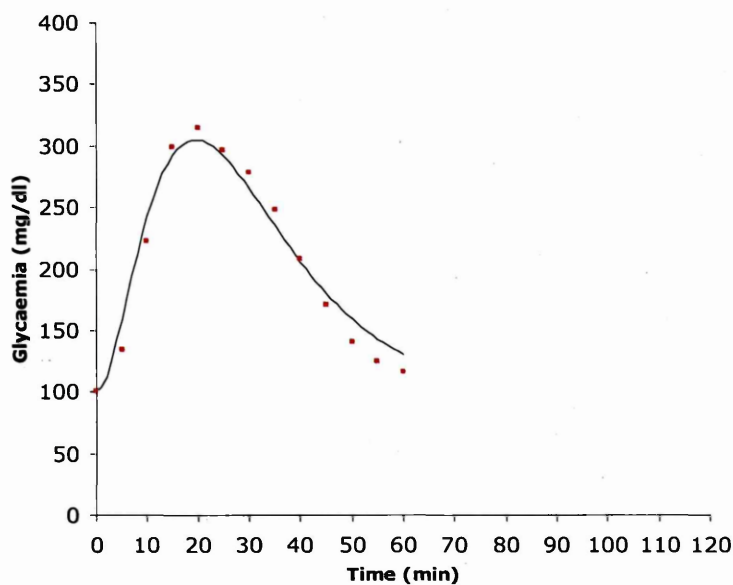
From the model applied to fit the experimental data, using EasyPlot software, the 4 unknown parameters in equation (6.1) were determined: A, B,  $k_a$  and  $k_{pt}$ . Solving the system of equations (6.2),  $k_{tot}$  was calculated, results are in Table 6.3. Also in this case, statistical significance was determined using the analysis of variance (software StatView, SAS Institute Inc. Cary, NC, USA) and specific comparisons between groups were calculated using Student's t-test and with the Bonferroni correction. The level of significance was taken to be  $p < 0.05$

Group	$k_a$ (mean $\pm$ SD) $\text{min}^{-1}$	$K_{pt}$ (mean $\pm$ SD) $\text{min}^{-1}$	$k_{tot}$ (mean $\pm$ SD) $\text{min}^{-1}$
Healthy rats	$0.104 \pm 0.018^{\Delta}$	$0.040 \pm 0.015$	$0.217 \pm 0.041^*$
Microcapsules tx	$0.083 \pm 0.031$	$0.046 \pm 0.020$	$0.156 \pm 0.026$
Kidney capsule tx	$0.051 \pm 0.038$	$0.043 \pm 0.027$	$0.110 \pm 0.041^{**}$

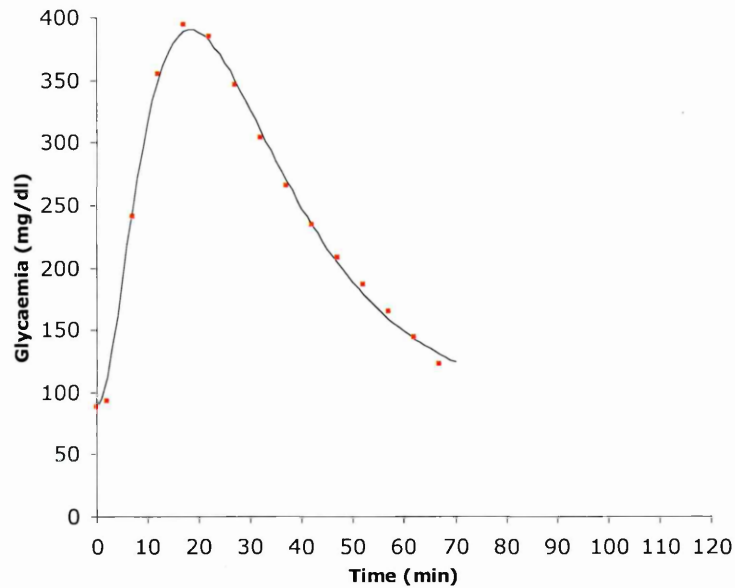
Table 6.3 Values of  $k_a$ ,  $k_{pt}$  and  $k_{tot}$  for the three experimental groups;  $^{\Delta}p < 0.05$  healthy rats vs. kidney capsule;  $*p < 0.05$  healthy rats vs. kidney capsules and microcapsules;  $**p < 0.05$  microcapsules vs. kidney capsules

An example of fitting from each group is reported in the following figures: the fitting curve being in black, the experimental points in red.

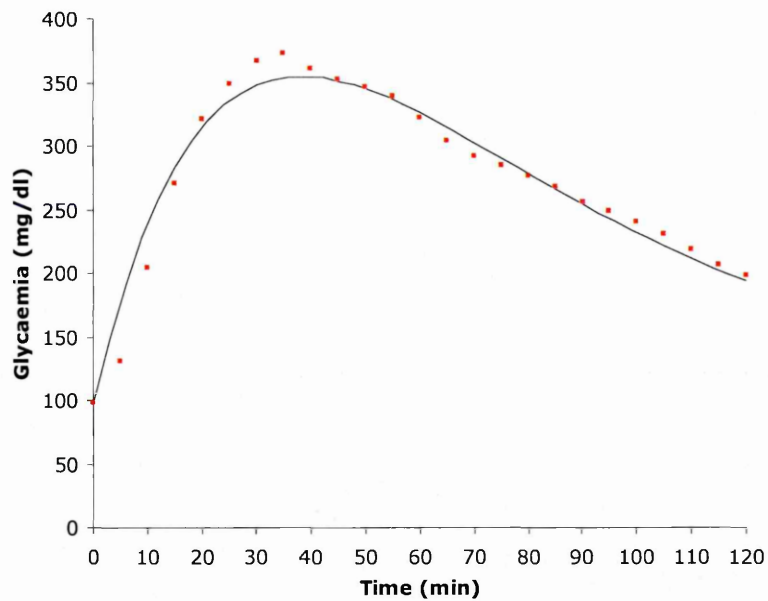
For healthy rats:



Diabetic rats transplanted with islets in microcapsules:



Diabetic rats transplanted with islets beneath the kidney capsules:



Only through a simple analysis of the graphics it can be concluded that rats implanted with microcapsules had good glycaemic control, without any statistically significant difference from healthy rats. Rats with islets implanted beneath the kidney capsule showed glycaemic control which was significantly different from healthy and microcapsule islet groups.

## Conclusion

This work was performed to evaluate the efficacy of a given system of immunoisolation on functionality of the islets involved. Periodically glucose concentration in the blood was measured to control islet functionality in terms of normoglycaemia, and it was verified for both kinds of implantation (islets in microcapsules and free islets beneath the kidney capsules). But it was necessary to explore ability of islets to respond to glucose stimulation and thus this response was examined to determine whether it would be similar to the physiological one. A new technique was applied, avoiding continuous blood sampling in the tail of rats. This system, previously used in rats only once (3), allowed monitoring glucose concentration continuously, permitting achievement of good results in terms of measurements and analysis of data.

Firstly the values downloaded from the receiver were analyzed and the results showed that the AUC of rats implanted beneath kidney capsules was seen to be statistically different from AUC of healthy rats and those implanted with islets in microcapsules. To best analyze the data obtained, a pharmacokinetic model was derived that best fitted the experimental data. Results were thoroughly analysed as administration of glucose intraperitoneally would be similar to administration of a molecule for kinetic study in pharmacological application. Moreover, values describing the glucose elimination process would be a good index of islet functionality. Values of  $k_{tot}$  were obtained for rats that were transplanted with islets beneath the kidney capsules, and these were statistically different from the other two groups, demonstrating that transplanted free islets responded to glucose stimulation but not like islets of healthy rats or like encapsulated islets. This result is

important as it demonstrates that encapsulated islets function properly, permitting optimal glucose control, also under stimulation.

## References

1. Iafusco D, Stoppoloni F, Salvia G, Verneti G, Passaro P, Petrovski G *et al.* Use of real time continuous glucose monitoring and intravenous insulin in type 1 diabetic mothers to prevent respiratory distress and hypoglycaemia in infants. *BMC Pregnancy Childbirth* 2008;8:23.
2. Stenninger E, Lindqvist A, Aman J, Ostlund I, Schvarcz E. Continuous Subcutaneous Glucose Monitoring System in diabetic mothers during labour and postnatal glucose adaptation of their infants. *Diabet Med* 2008;25:450-454.
3. Jamali R, Ludvigsson J, Mohseni S. Continuous monitoring of the subcutaneous glucose level in freely moving normal and diabetic rats and in humans with type 1 diabetes. *Diabetes Technol Ther* 2002;4:305-312.
4. Kerssen A, de Valk HW, Visser GH. The Continuous Glucose Monitoring System during pregnancy of women with type 1 diabetes mellitus: accuracy assessment. *Diabetes Technol Ther* 2004;6:645-651.
5. Li S, Sakai T, Suzuki Y, Goto T, Tanaka T, Yoshikawa T *et al.* Improved quantity and in vivo function of islets isolated by reduced pressure-controlled injection of collagenase in a rat model. *Cell Transplant* 2007;16:539-545.
6. Sharma A, Sorenby A, Wernerson A, Efendic S, Kumagai-Braesch M, Tibell A. Exendin-4 treatment improves metabolic control after rat islet transplantation to athymic mice with streptozotocin-induced diabetes. *Diabetologia* 2006;49:1247-1253.
7. Alvarez RA. Pharmacokinetics of pentobarbital and thiopental in the isolated perfused rat liver. *Arch Int Pharmacodyn Ther* 1971;189:380.



8. Papaioannou VE, Fox JG. Efficacy of tribromoethanol anesthesia in mice. *Lab Anim Sci* 1993;43:189-192.
9. Wallenstein S, Zucker CL, Fleiss JL. Some statistical methods useful in circulation research. *Circ Res* 1980;47:1-9.
10. Fournier R. Two compartment models. In: Francis T, (ed). *Basic Transport Phenomena in Biomedical Engineering*. New York, 2006.

## Chapter 7

### Design of an immunoisolation device for islet transplantation

#### 8.1 Determination of solute diffusivity

##### *8.1.1 Solute diffusivity in porous membrane*

##### *8.1.2 Solute diffusivity in alginate gel*

#### 8.2 Mathematical model of an immunoisolation device for islet transplantation

##### *8.2.1 Simulation of glucose transport*

##### *8.2.2 Simulation of insulin transport*

##### *8.2.3 Simulation of immunoglobulin (IgG) transport*

### Discussion and conclusion

### References

## **Design of an immunoisolation device for islet transplantation**

An ideal membrane for an immunoisolation device should have permeability properties that allow at the same time immunoprotection and tissue nutrition. If the pore size is too large, harmful factors such as antibodies or even immune cells may cross the membrane and damage the encapsulated graft. If the pore size is too small, this will interfere with the nutritional demands of the graft, jeopardizing graft survival (1).

Then, diffusion process of macromolecules of various molecular weights was studied through a semipermeable polycarbonate membrane designed for an immunoisolation device for pancreatic islets, designed and experimented in a European Project (BARP+, project n. NMP3-CT-2003-505614). Actually, the effective diffusivity of a solute within a porous medium (such as the alginate matrix or a polymeric membrane) is less than in bulk solution. Even if these materials have been used in several previous investigations (2) (3), quantification of hindered diffusion has not been provided yet. The objective of this work was to show the method used to estimate the solute diffusion within porous membrane, on the basis of experimental measurements of the geometrical characteristics of the membrane considered. The estimated diffusion coefficients were used in a mathematical model set-up and simulation of diffusion kinetics of glucose, insulin and antibodies within an immunoisolation device were performed.

## 7.1 Determination of solute diffusivity

### 7.1.1 Solute diffusivity in porous membrane (4)

The recent application of nanotechnology techniques in the development of porous synthetic membranes opened the possibility to generate specific membranes for different applications.

An ideal semipermeable membrane must allow adequate diffusion of oxygen and nutrients to maintain islet viability and function but, at the same time, must be selective enough to prevent the permeation of host immune proteins. As stated before, effective diffusivity coefficient of solutes, like glucose and insulin, within a porous membrane is lower than in bulk solution. This phenomenon, known as “hindered diffusion”, depends from the size of solute molecules compared to the pore dimension and density. Beck and Shultz in 1970 (5) studied solute diffusion for a variety of porous membranes. A summary of their results, for a number of neutral solutes is shown in Figure 7.1.

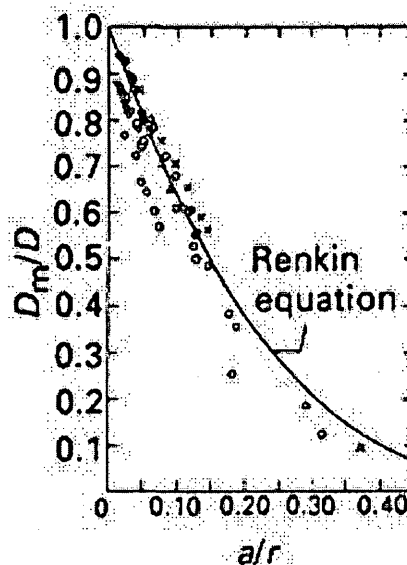


Figure 7.1 Solute diffusivity of molecules of radius ( $a$ ) in pores of a membrane with radius ( $r$ )

In this plot the ratio of solute diffusivity within the pore membrane ( $D_m$ ) and the bulk diffusivity ( $D_\infty$ ) are plotted as a function of the ratio between solute radius and pore radius ( $a/r$ ). The solid line represents the best fit of the Renkin equation (6) to their experimental data using the following expression

$$\frac{D_m}{D_\infty} = \left(1 - \frac{a}{r}\right)^2 \left[1 - 2.1 * \left(\frac{a}{r}\right) + 2.09 * \left(\frac{a}{r}\right)^3 - 0.95 * \left(\frac{a}{r}\right)^5\right] \quad (7.1)$$

The first term in this equation takes into account that only a fraction of the pore transversal area is available to the molecule. This coefficient is known as the “partition coefficient” and represents the effect of steric exclusion. The second term accounts for the increase in hydrodynamic drag as the solute diffuses through the pore. Considering the effective diffusion of a solute in the overall membrane, the following equation can be written

$$D_e = D_\infty * \frac{A_p}{S_{tot}} * \left(1 - \frac{a}{r}\right)^2 * \left[1 - 2.1 * \left(\frac{a}{r}\right) + 2.09 * \left(\frac{a}{r}\right)^3 - 0.95 * \left(\frac{a}{r}\right)^5\right] \quad (7.2)$$

where  $A_p$  is the pores area and  $S_{tot}$  is the total surface area.

The bulk diffusivity of a solute with known radius =  $a$  in a solution with viscosity =  $\mu$  can be calculated using the Stokes-Einstein equation

$$D_\infty = k * \frac{T}{6\pi\mu a} \quad (7.3)$$

where

$k = 1.38054 * 10^{-23}$	$\frac{\text{Joule}}{\text{K}}$	<i>Boltzmann constant</i>
$T = 293.15$	$^{\circ}\text{K}$	<i>temperature in Kelvin</i>

In case of islet immunoisolation, three important molecules were considered: glucose ( $a=2.47 \text{ \AA}$ , (7)), insulin ( $a=16 \text{ \AA}$ ) and immunoglobuline (IgG  $a=55 \text{ \AA}$ ) (8). The bulk diffusivity constants were then calculated at  $37^{\circ}\text{C}$  and they are:

$$D_{\infty \text{ glucose}} = 9.02 * 10^{-4} \text{ mm}^2/\text{sec}$$

$$D_{\infty \text{ insulin}} = 1.39 * 10^{-4} \text{ mm}^2/\text{sec}$$

$$D_{\infty \text{ IgG}} = 4.05 * 10^{-5} \text{ mm}^2/\text{sec}$$

Experimental determination of membrane pore diameter and density

Pore dimension and density of polycarbonate membrane were analysed using scanning electron microscopy (SEM). On digitized images a morphometrical analysis was performed. For each image, pore number and area were calculated. A representative image of the membrane surface is shown in Figure 7.2.



Figure 7.2 SEM of the nanoporous polycarbonate membrane

Using a calibrated grid, the image resolution ( $\mu\text{m}/\text{pixel}$ ) and the mean values of pore radius,  $A_p$  and  $S_{\text{tot}}$  were calculated, using standard morphometrical technique. In each image the outline of the pore area was automatically traced and surface area measured. Mean pore radius averaged 31.45 nm and pore density  $2.54 \cdot 10^9$  pores/ $\text{cm}^2$ .  $D_e$  was then calculated for each molecule considered:

$$D_{e \text{ glucose}} = 6.62 \cdot 10^{-5} \text{ mm}^2/\text{sec} = 0.241 \text{ mm}^2/\text{h}$$

$$D_{e \text{ insulin}} = 8.61 \cdot 10^{-6} \text{ mm}^2/\text{sec} = 0.031 \text{ mm}^2/\text{h}$$

$$D_{e \text{ IgG}} = 1.46 \cdot 10^{-6} \text{ mm}^2/\text{sec} = 0.005 \text{ mm}^2/\text{h}$$

### ***7.1.2 Solute diffusivity in alginate gel***

This experience, in line with previous investigations reported in literature, suggests that alginate gel is attractive as matrix for immunoisolation devices because of its ability to eliminate convective mixing and its selectivity for molecules based on size, charge, and chemical affinity. This gel is space-filling at low-volume fractions of the network material (e.g., cross-linked polymer).

About the diffusion across a gel, the driving force is usually dependent from concentration gradients and the effective diffusivity ( $D_{\text{eff}}$ ) within the gel is given by

$$D_{\text{eff}} = \Phi * D_{\infty} \quad (7.4)$$

where  $\Phi$  is the partition coefficient of a solute molecule and  $D_{\infty}$  is the free solution diffusivity.

To estimate  $\Phi$  from gel composition and solute radius ( $a_s$ ), Ogston (9) developed a model based on the probability of a rigid sphere of radius  $a_s$  to be contained in a matrix composed of long cylindrical fibres of radius  $a_f$ . This relationship predict  $\Phi$  for uncharged, spherical macromolecules within a randomly oriented array of cylindrical fibres and it's

$$\Phi = \exp\left[-\phi\left(1 + \frac{a_s}{a_f}\right)\right] * D_\infty \quad (7.5)$$

where  $\phi$  is the volume fraction of the fibres and  $a_f$  is the radius of the fibre.

Considering the three molecules of interest their effective diffusivity was calculated in gel alginate solution of 2.7% assuming fibres of the polymer gel of 5 Å radius:

$$D_{\text{eff glucose}} = 8.49 * 10^{-4} \text{ mm}^2/\text{sec} = 3.05 \text{ mm}^2/\text{h}$$

$$D_{\text{eff insulin}} = 8.65 * 10^{-5} \text{ mm}^2/\text{sec} = 0.311 \text{ mm}^2/\text{h}$$

$$D_{\text{eff IgG}} = 8.30 * 10^{-7} \text{ mm}^2/\text{sec} = 0.003 \text{ mm}^2/\text{h}$$

## 7.2 Mathematical model of an immunoisolation device for islet transplantation

Solute diffusion across porous membranes is only regulated by the concentration gradient between internal and external side. A theoretical model can be used to simulate solute trans-membrane transport using continuity equation and Fick's laws, the principal laws that regulate diffusion process. Assuming that diffusion takes place in only one dimension (10):

$$J = -D \frac{\Delta C}{\Delta x} \quad (7.6)$$

where  $\Delta C$  is the concentration gradient of the molecule in x direction, perpendicular to membrane surface, D is the diffusivity constant and J the solute flux. For the conservation of mass applied to a control volume  $dV(dx,dy,dz)$ , results

$$\frac{dC}{dt} = -\frac{dJ}{dx} \quad (7.7)$$



Combining equation (7.6) and (7.7) the second Fick's law was obtained

$$\frac{dC}{dt} = D \frac{d^2C}{dx^2} \quad (7.8)$$

In this model, solute concentration is a function only of  $x$  and  $t$  (time dependent mono-dimensional problem) and considering the membrane

$$\frac{dC_m}{dt} = D_m \frac{d^2C_m}{dx^2} \quad (7.9)$$

where  $C_m$  is the solute concentration and  $D_m$  the effective diffusivity in the membrane. For the inner part of the device

$$\frac{dC_i}{dt} = D_a \frac{d^2C_i}{dx^2} \quad (7.10)$$

where  $D_a$  is the effective diffusivity in alginate gel.

Each part of the device was divided in small volumes, one near the other, and mass balance equation for each volume was solved, considering initial and boundary conditions.

The model represented in Figure 7.3 is one dimensional symmetric model.

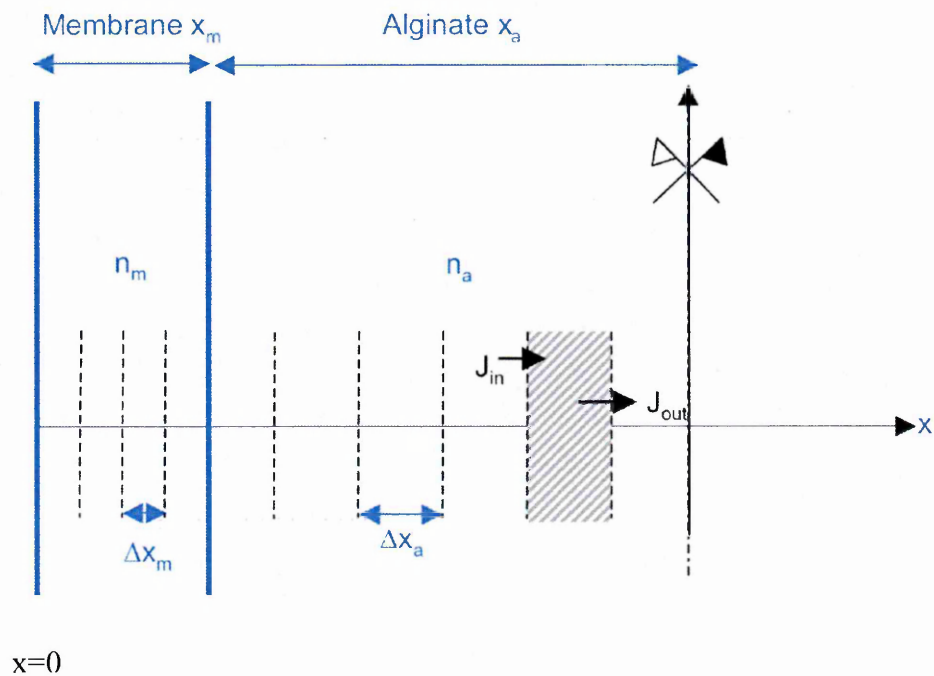


Figure 7.3 One-dimension model of the device

Where the geometrical parameters are:

$n_a$  = number of elements in the alginate

$$\Delta x_a = x_a / n_a$$

$n_m$  = number of elements in the membrane

$$\Delta x_m = x_m / n_m$$

$J_{in}$  = mass flux in

$J_{out}$  = mass flux out

A numerical solution of equation (7.9) and (7.10) can be obtained using the finite differential method. Since the device was divided in a finite number elements ( $n_a+n_m$ ), the differential equations were transformed into a linear system of equations. To this purpose, the membrane ( $x_m$ ), the alginate ( $x_a$ ) and time ( $t$ ) were divided into equal intervals, so that an  $x$ - $t$  region covered by a grid of rectangles was create, as shown in Figure 7.4. Coordinates of a representative grid points can be written as  $(idx, jdt)$  where  $i$  and  $j$  are integer. The value of  $C$  at the point  $(idx, jdt)$  was denoted by  $C_{ij}$  with corresponding values at neighbouring points.

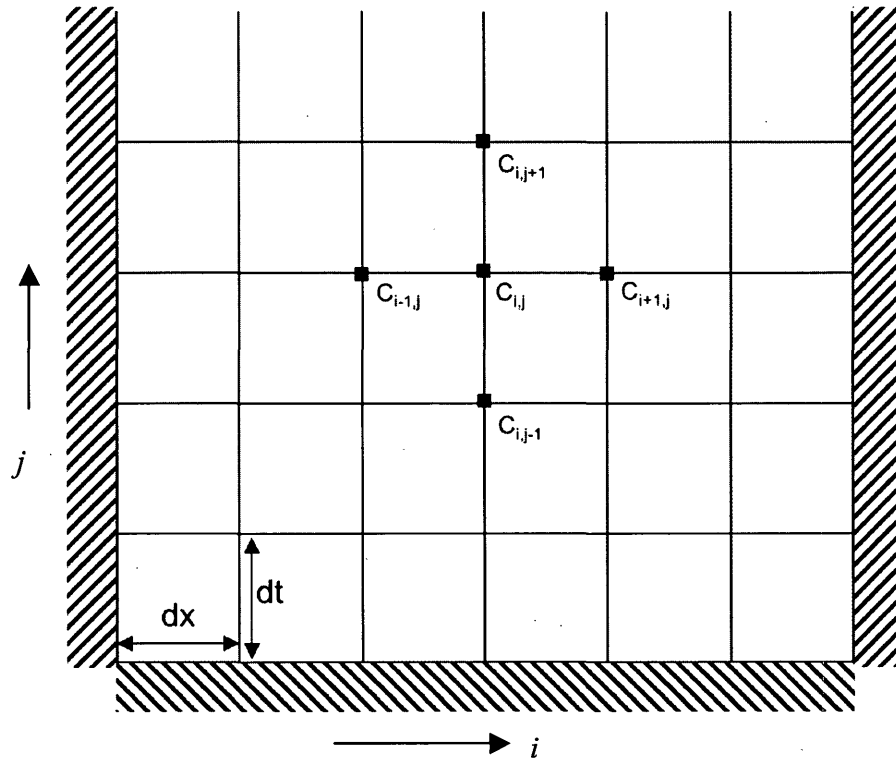


Figure 7.4 x-t region covered by a grid of rectangles of side  $dx$ ,  $dt$ .

The value of  $C$  at the point  $(idx, jdt)$  is denoted  $C_{i,j}$

By using Taylor's series in the  $t$  direction, keeping  $x$  constant, it can be written

$$C_{i,j} = C_{i,j-1} + dt \left( \frac{dC}{dt} \right)_{i,j-1} + \frac{1}{2} (dt)^2 \left( \frac{d^2C}{dt^2} \right)_{i,j-1} + \dots \quad (7.11)$$

from which it follows that

$$\left( \frac{dC}{dt} \right)_{i,j-1} = \frac{C_{i,j} - C_{i,j-1}}{dt} + O(dt) \quad (7.12)$$

where  $O(dt)$  represents the major term neglected that is of the order of  $dt$ . Similarly by

applying Taylor's series in the  $x$  direction, keeping  $t$  constant, it results

$$C_{i+1,j} = C_{i,j} + dx \left( \frac{dC}{dx} \right)_{i,j} + \frac{1}{2} (dx)^2 \left( \frac{d^2C}{dx^2} \right)_{i,j} + \dots \quad (7.13)$$

$$C_{i-1,j} = C_{i,j} - dx \left( \frac{dC}{dx} \right)_{i,j} + \frac{1}{2} (dx)^2 \left( \frac{d^2C}{dx^2} \right)_{i,j} - \dots \quad (7.14)$$

on adding, it was obtained

$$\left(\frac{d^2C}{dx^2}\right)_{i,j} = \frac{C_{i+1,j} - 2C_{i,j} + C_{i-1,j}}{(dx)^2} + O(dx)^2 \quad (7.15)$$

By substituting eq. (7.12) and (7.15) in the second Fick's law and neglecting the error terms, after re-arrangements, it was found that

$$C_{i,j} = C_{i,j-1} + D \frac{dt}{dx^2} (C_{i-1,j-1} - 2C_{i,j-1} + C_{i+1,j-1}) \quad (7.16)$$

For a given value of  $\frac{dt}{dx^2}$ , using eq. (7.12) values of C at all points of the grid can be calculated, providing initial starting values of C at  $t=0$  and conditions on each of the boundaries. A formula such as (7.16) which enables unknown value to be expressed directly in terms of known values is called an "explicit finite difference formula". To obtain C(x,t) for different times or in different x, a computer code in MatLab was developed and described in details in the Appendix A.

Determination of numerical analysis parameters:

Finite-difference methods provide reasonable approximation to the solution of partial differential equations. For code implementation, the right choice of parameters has to be done. There are serious limitations on the assumption of the value of the parameter

$r = D \frac{dt}{dx^2}$  since equation (7.16) is based on approximations and neglected error terms.

Smith et al. in 1965 (11) demonstrated that  $r = \frac{1}{2}$  is a critical value, as shown in Figure

7.5.

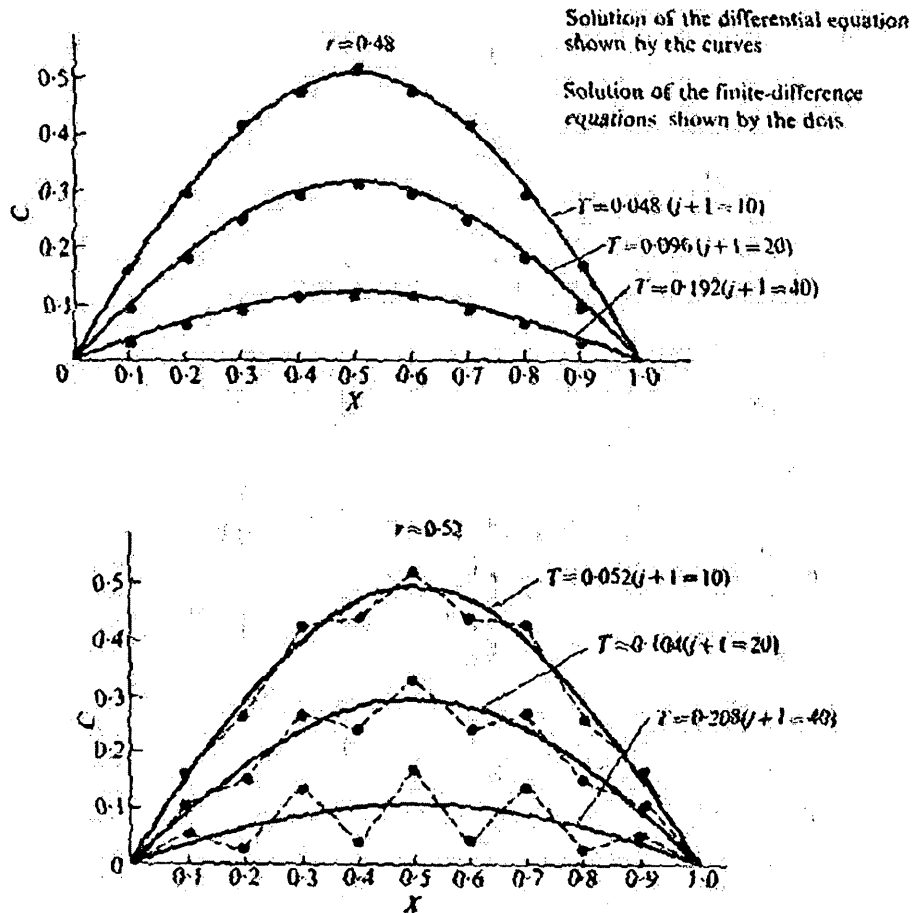


Figure 7.5 Demonstration that  $r > 0.5$  is a critical point

In fact, for  $r=0.48$  the finite difference solutions well agree with the analytical solution, but for  $r=0.52$  oscillations develop and solution becomes unstable (errors increase without limit). For this reason, at the beginning of the code, was imposed a limitation on the value of  $r$ ; if it's  $>0.4$ , a warning message to the user is visualized. The following input parameters have been defined.

Assumed input parameters:

- tmax: time of observation
- xmax: thickness of the alginate gel=0.5 mm ( $x_a$ )
- Lm: thickness of the membrane=0.03 mm
- Lmstep: number of the elements in the membrane=30

- xstep: total number of the elements ( $Lmstep \times 5$ ) = 150
- tstep: number of the intervals in which the time period is divided

The value of  $dt$  is given by  $tmax/tstep$ . Inside the membrane  $dx=Lm/Lmstep$ , within the alginate gel  $dx=xmax/(xstep-Lmstep)$ .

### 7.2.1 Simulation of glucose transport

A basal level of glucose equal 0 inside the entire device and a value of external concentration equal to 100 and constant in time were assumed. At  $t=0$  a concentration gradient is present between intern part ( $C_i$ ) and external part of the device ( $C_e$ ). Assuming constant glucose concentration outside the device, an increase of glucose concentration inside was reached with time. Then it was assumed :

$$\text{For } t < 0 \quad C_i = C_e = 0$$

$$\text{For } t = 0 \quad C_i = 0$$

$$C_e = 100$$

The aim of the study was to calculate the time required for glucose to reach all the points internal to the device, diffusing through the immunoisolation membrane into alginate gel.

Boundary conditions for this case (glucose diffusion) have been defined as follows:

$$- \frac{dC_i(x,t)}{dx} = 0 \text{ in } x = (x_a + x_m) \text{ for the assumption of a symmetry plane,}$$

no flow in the centre of the device

$$- D_m \frac{dC_i(x,t)}{dx} \Big|_{x=x_a} = D_a \frac{dC_i(x,t)}{dx} \Big|_{x=x_a} \text{ for continuity of mass flow at the alginate}$$

membrane interface

Assumed input parameters for simulation:

- tmax: 1200 seconds
- xmax: 0.5 mm
- Lm: 0.03 mm
- tstep: 600000

The values calculated using MatLab code for different times at the centre of the device ( $x=x_{step}$ ) are reported in Figure 7.6.

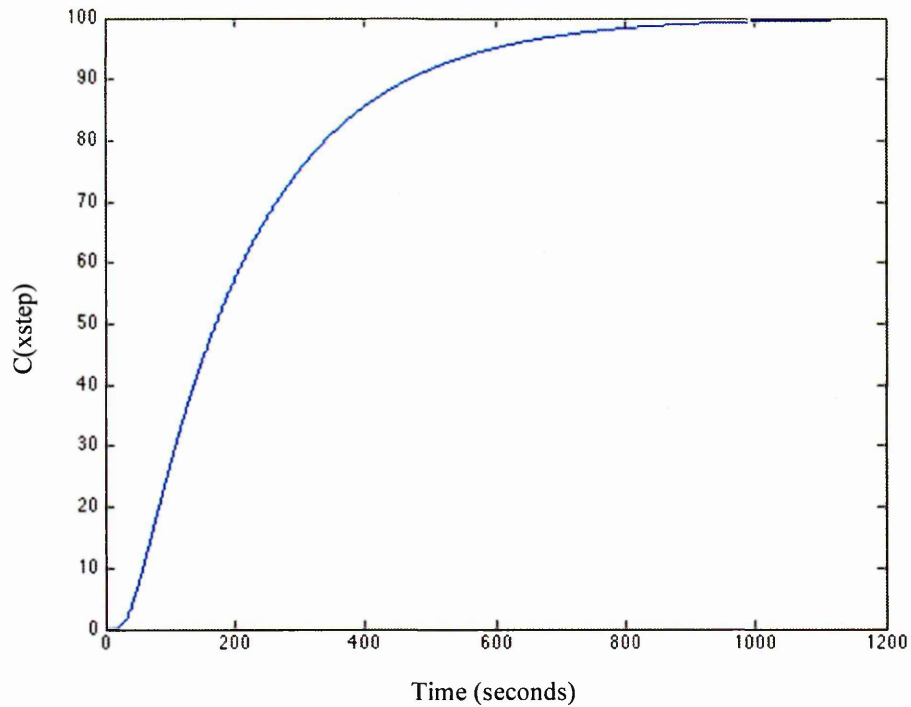


Figure 7.6 Glucose concentrations in  $x=x_{step}$

The values of glucose concentration  $C(x,t)$  as a function of  $x$  and  $t$  are reported in Figure 7.7, each line every 30 seconds. The diffusion process of glucose ends in about 1200 seconds with a uniform concentration equal to the external one, obtaining a dynamic balance.



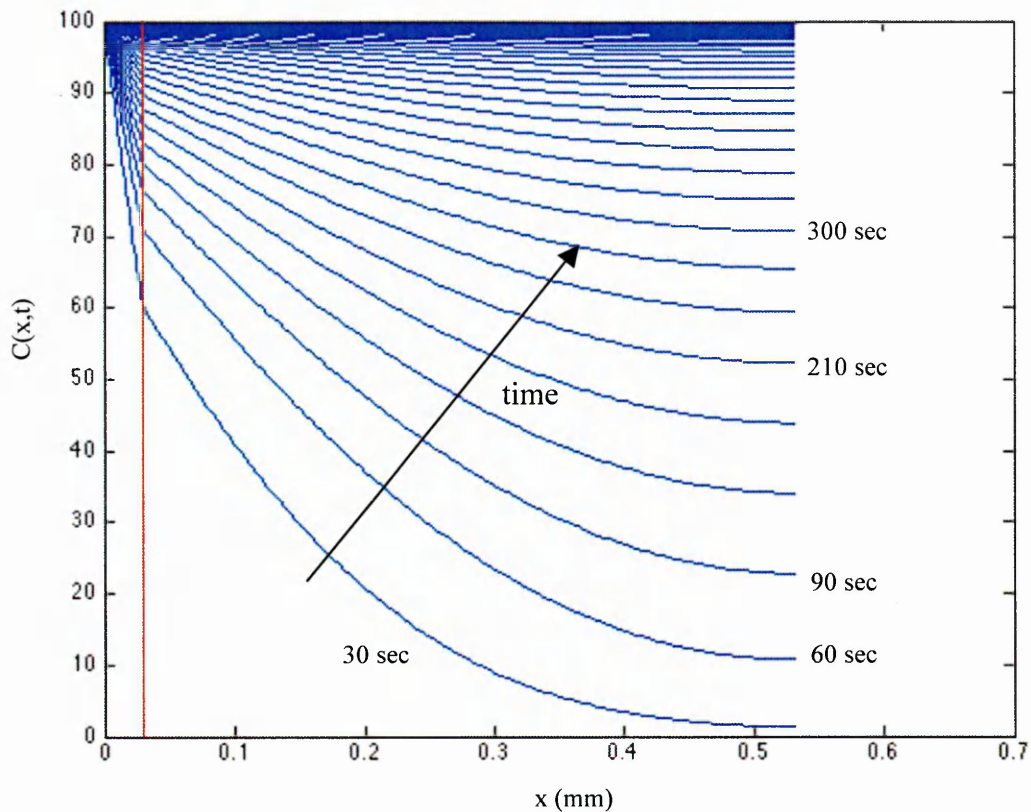


Figure 7.7 Family of curves  $C(x,t)$  in function of  $x$  at different times

The time at which the centre of the device reached 90% of glucose concentration was 467 seconds (less than 8 minutes).

### 7.2.2 Simulation of insulin transport

When the concentration of glucose arises, islets inside the device begin to produce insulin that as per diffusion will go to the external part of the device. A basal level of insulin equal 0 was assumed outside the device and constant with time and a value of internal concentration equal to 100.

It was assumed that:

$$\text{For } t < 0 \quad C_i = C_e = 0$$

$$\begin{aligned} \text{For } t=0 \quad C_i &= 100 \\ C_e &= 0 \end{aligned}$$

The aim of the study was to evaluate insulin kinetic, if insulin diffusion was rapid to obtain a good glycaemic control and if the membrane was an obstacle for insulin diffusion. Boundary conditions were defined for this case (insulin diffusion) as follows:

$$- \frac{dC_i(x,t)}{dx} = 0 \text{ in } x=x_a+x_m \text{ for the assumption of a symmetric model, no flow in the}$$

centre of the device

$$- D_m \frac{dC_i(x,t)}{dx} \Big|_{x=x_a} = D_a \frac{dC_i(x,t)}{dx} \Big|_{x=x_a} \text{ for continuity of mass flow at the alginate-}$$

membrane interface

Input parameters:

- tmax: 2 hours
- xmax: 0.5 mm
- Lm: 0.03 mm
- tstep: 600000

The values calculated using MatLab code of insulin concentration  $c(x,t)$  as a function of  $x$  and  $t$  are reported in Figure 7.8, each curve every 5 minutes. The diffusion process of insulin ends in about 2 hours, obtaining a dynamic balance with the external compartment.

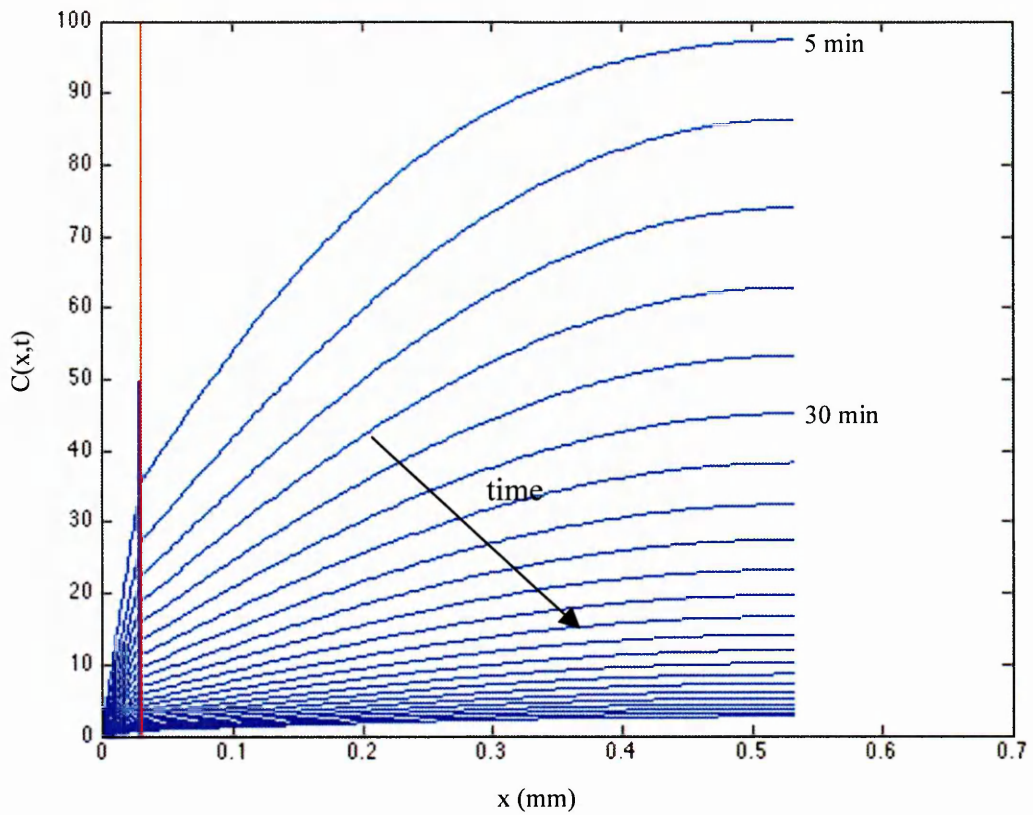


Figure 7.8 Family of curves  $C(x,t)$  in function of  $x$  at different times

To study if this kinetic is acceptable for a glycaemic control, the code returns in output the value of the mass of insulin inside the device and then the time in which the quantity of mass reach the maximum value as reported in Figure 7.9.

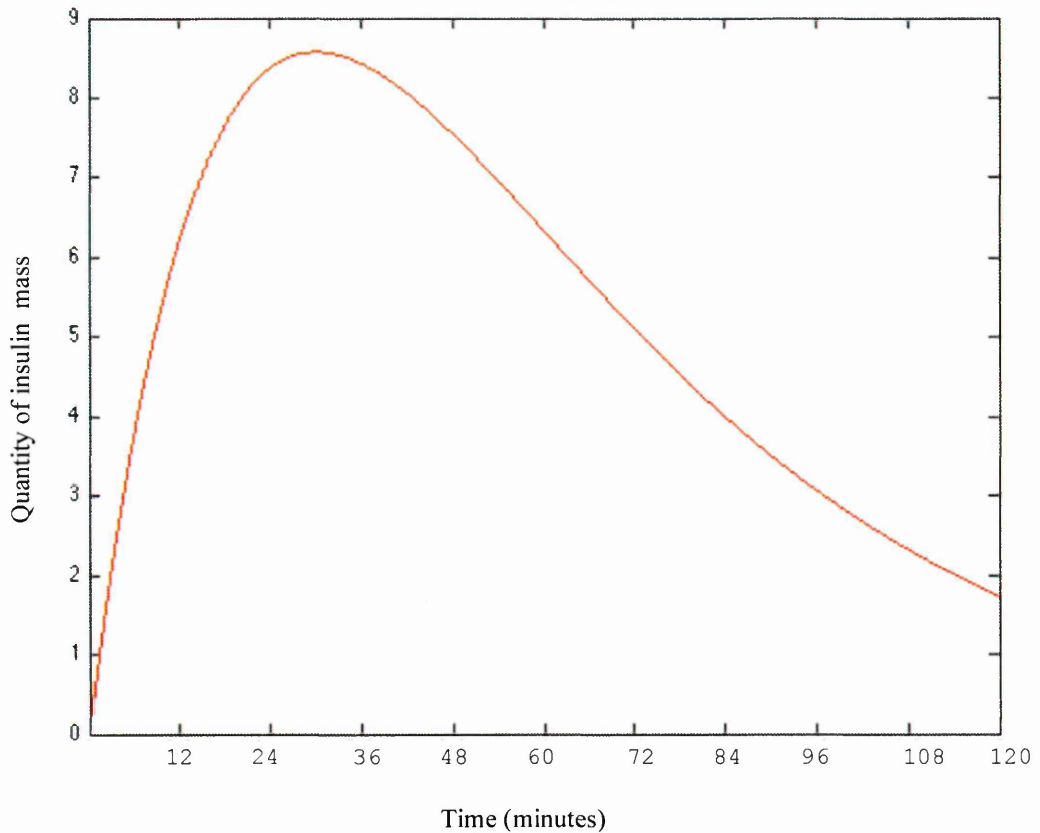


Figure 7.9 Quantity of mass insulin mass in function of time

This curve represents the mass of insulin outbound from the device and the time in which it is greatest was estimate and resulted 30.06 minutes, which is quite acceptable. Kinetic of diffusion for insulin is slower than glucose. This is due to the difference between the dimensions of the molecules.

### ***7.2.3 Simulation of immunoglobulin (IgG) transport***

As stated before, an ideal immunoisolation membrane must prevent the passage of cytotoxic cells, macrophages, antibodies and complement to remain effective. Previous studies indicated that immunoisolation could be attained if C1q and IgG were completely retained (1). Moreover, if the cells implanted are xenogeneic, it seems that immunoisolation will require membranes that not only provide protection of the

encapsulated tissue from the host immune system, but also have properties that diminish the release of xenogeneic antigens through reduced pore size. Evaluation of this membrane in terms of desired IgG diffusion kinetics was performed.

For the model we assumed that:

$$\text{For } t < 0 \quad C_i = C_e = 0$$

$$\text{For } t = 0 \quad C_i = 0$$

$$C_e = 100$$

The aim of this study was to estimate if the membrane is an obstacle for IgG diffusion.

Also in this case boundary conditions as follows were defined:

$$- \frac{dC_i(x,t)}{dx} = 0 \text{ in } x = x_a + x_m \text{ for the assumption of a symmetric model, no flow in the}$$

centre of the device

$$- D_m \frac{dC_i(x,t)}{dx} \Big|_{x=x_a} = D_a \frac{dC_i(x,t)}{dx} \Big|_{x=x_a} \text{ for continuity of mass flow at the alginate-}$$

membrane interface

Input parameters:

- tmax: 24 hours
- xmax: 0.5 mm
- Lm: 0.03 mm
- tstep: 600000

The values of IgG concentration  $C(x,t)$  calculated using MatLab code as a function of  $x$  and  $t$  are reported in Figure 7.10, each lines every 1/2 hour.

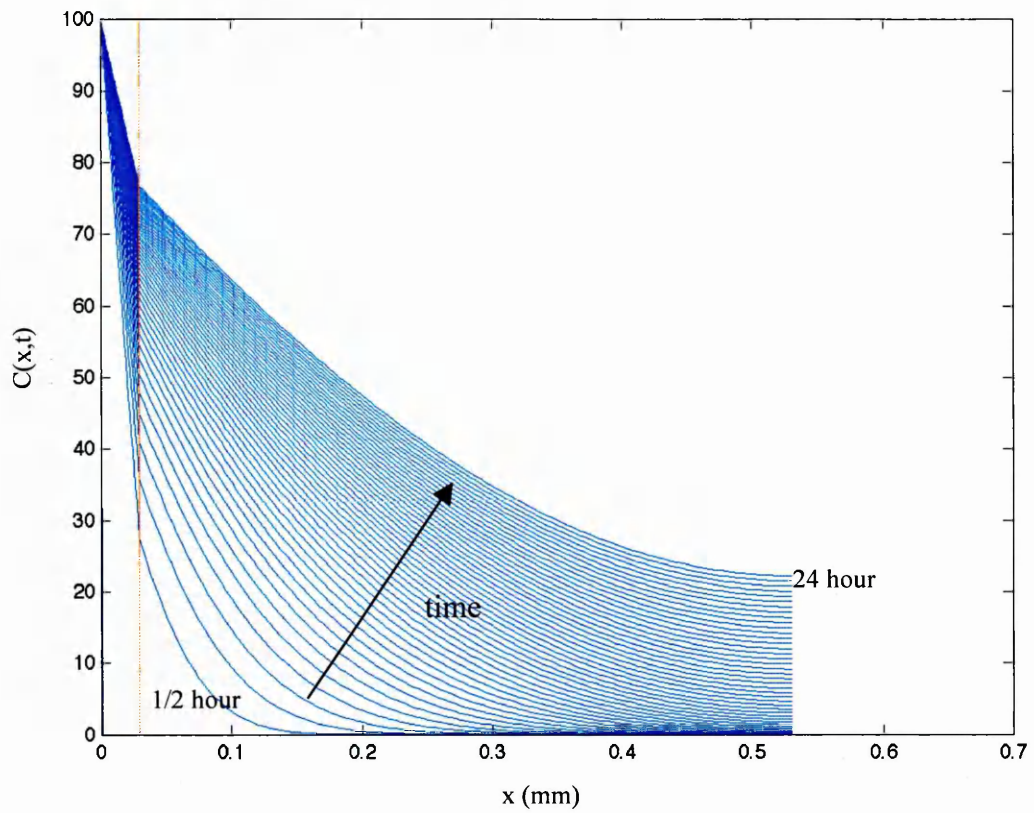


Figure 7.10 Family of curves  $C(x,t)$  in function of  $x$  at different times

To study if this kinetic is acceptable for an immunoisolation membrane, the code calculated the value of IgG concentration just after the membrane (in  $x=Lmstep+1$ ) and the time at which in this point 10% of IgG concentration was reached (Figure 7.11).

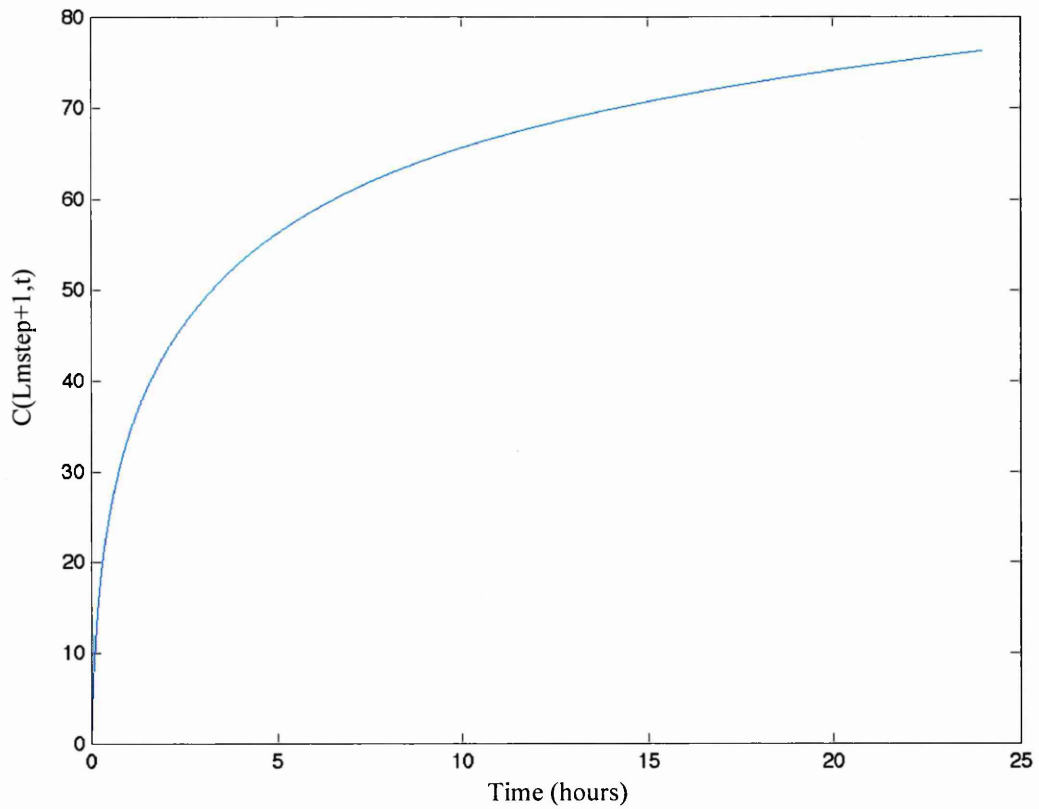


Figure 7.11 IgG concentrations in  $x=Lmstep+1$

After 24 hours it was found that the percent of IgG diffusion near the membrane was about 75%. This value couldn't be acceptable for an immunoisolation membrane. For this reason, in order to maintain glucose and insulin kinetics acceptable (in terms of time of diffusion) and to obtain complete antibodies obstruction MatLab analysis changing pore diameter and density were performed.

## Discussion and conclusion

An ideal immunoisolation membrane must have specific characteristics in order to allow good diffusivity of glucose and insulin and ability to retain antibodies to prevent islet destruction. The mathematical model and the numerical solution code developed in this investigation allowed to analyse the dynamic of diffusivity of these molecules, giving us useful determinations that permit to evaluate a membrane performance before effective use in experimental setting, i.e. with animal studies.

Polycarbonate membrane designed for the European Project BARP+ was not ideal for immunoisolation purposes because it permits a good kinetic of diffusion to insulin and glucose, but it is too permeable to IgG and the cells implanted (allogeneic or xenogeneic) would be expected to be rejected. Then, it was tried to define the properties that an hypothetical membrane must have, on the bases of the simulation tools developed. Different pore radius and density were adopted and the indexes of functionality were compared in order to identify an adequate membrane to be used for immunoisolation devices.

The following values of pore radius were adopted:

- 30 nm (like polycarbonate)
- 20 nm
- 10 nm
- 5 nm

with different pore density:

- $2.5 \times 10^9$  pores/cm<sup>2</sup>
- $5 \times 10^9$  pores/cm<sup>2</sup>



–  $7.5 \times 10^9$  pores/cm<sup>2</sup>

–  $10 \times 10^9$  pores/cm<sup>2</sup>

For these different combinations, diffusion simulation were performed with the device using MatLab code for each molecule.

### Glucose diffusion

Firstly, effective diffusivity ( $D_e$ ) was calculated in each case and results are shown in

Table 7.1

<b>Radius</b> <b>Density</b>	<b>30 nm</b>	<b>20 nm</b>	<b>10 nm</b>	<b>5 nm</b>
<b><math>2.5 \times 10^9</math></b>	6.16E-05	2.69E-05	6.39E-06	1.60E-06
<b><math>5 \times 10^9</math></b>	1.23E-04	5.38E-05	1.28E-05	3.20E-06
<b><math>7.5 \times 10^9</math></b>	1.85E-04	8.08E-05	1.92E-05	4.80E-06
<b><math>10 \times 10^9</math></b>	2.46E-04	1.08E-04	2.56E-05	6.40E-06

Table 7.1 Glucose diffusivity in different cases (mm<sup>2</sup>/sec)

For each case the value of time at which the centre of the device was reached by 90% of glucose ( $T_{90\%}$ ) was determined and results obtained are shown in table 7.2 and plotted in Figure 7.12.

<b>Radius</b> <b>Density</b>	<b>30 nm</b>	<b>20 nm</b>	<b>10 nm</b>	<b>5 nm</b>
<b><math>2.5 \times 10^9</math></b>	467	479	555	967
<b><math>5 \times 10^9</math></b>	462	468	504	692
<b><math>7.5 \times 10^9</math></b>	461	465	488	607
<b><math>10 \times 10^9</math></b>	460	463	480	567

Table 7.2 Time at which 90% of glucose reach the centre of device (in seconds)

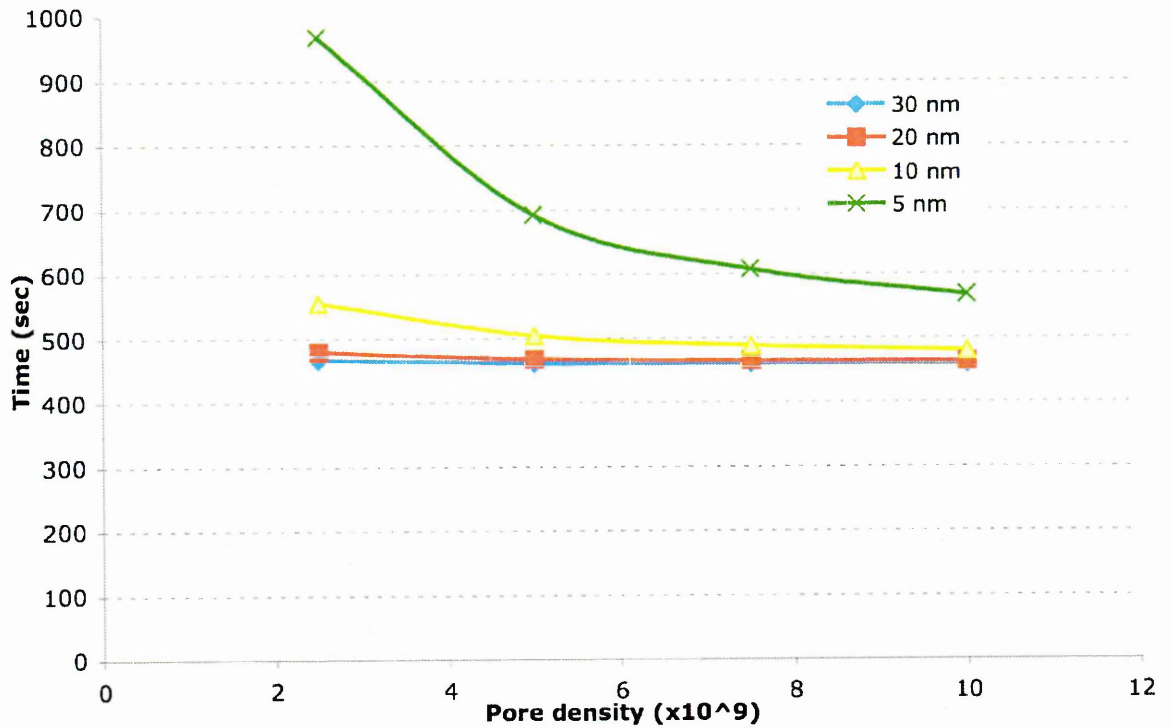


Figure 7.12 Time at which 90% of glucose reach the centre of device in function of pore density

It can be easily conclude that if pore radius is 10-30 nm, pore density didn't influence glucose kinetics. If pore radius is 5 nm, only with high density of pores acceptable values of glucose diffusion were obtained.

Insulin diffusion

Also in this case, effective diffusivity ( $D_e$ ) was calculated in each case and results are shown in Table 7.3

<b>Radius</b> <b>Density</b>	<b>30 nm</b>	<b>20 nm</b>	<b>10 nm</b>	<b>5 nm</b>
<b>2.5 x 10<sup>9</sup></b>	2.84E-02	1.13E-02	1.99E-03	2.45E-04
<b>5 x 10<sup>9</sup></b>	5.68E-02	2.25E-02	3.98E-03	4.90E-04
<b>7.5 x 10<sup>9</sup></b>	8.51E-02	3.38E-02	5.98E-03	7.35E-04
<b>10 x 10<sup>9</sup></b>	1.14E-01	4.51E-02	7.97E-03	9.81E-04

Table 7.3 Insulin diffusivity in different cases (mm<sup>2</sup>/h)

For each case with MatLab code the time in which the mass flow reaches the maximum value ( $T_{max}$ ) was determined and results were shown in table 7.4 and represented in Figure 7.13.

<b>Radius</b> <b>Density</b>	<b>30 nm</b>	<b>20 nm</b>	<b>10 nm</b>	<b>5 nm</b>
<b>2.5 x 10<sup>9</sup></b>	30.06	30.42	33.72	47.40
<b>5 x 10<sup>9</sup></b>	29.94	30.12	31.62	42.78
<b>7.5 x 10<sup>9</sup></b>	29.88	30.00	30.96	39.72
<b>10 x 10<sup>9</sup></b>	29.82	29.94	30.66	37.68

Table 7.4 Time at which quantity of mass reach the maximum value (in minutes)

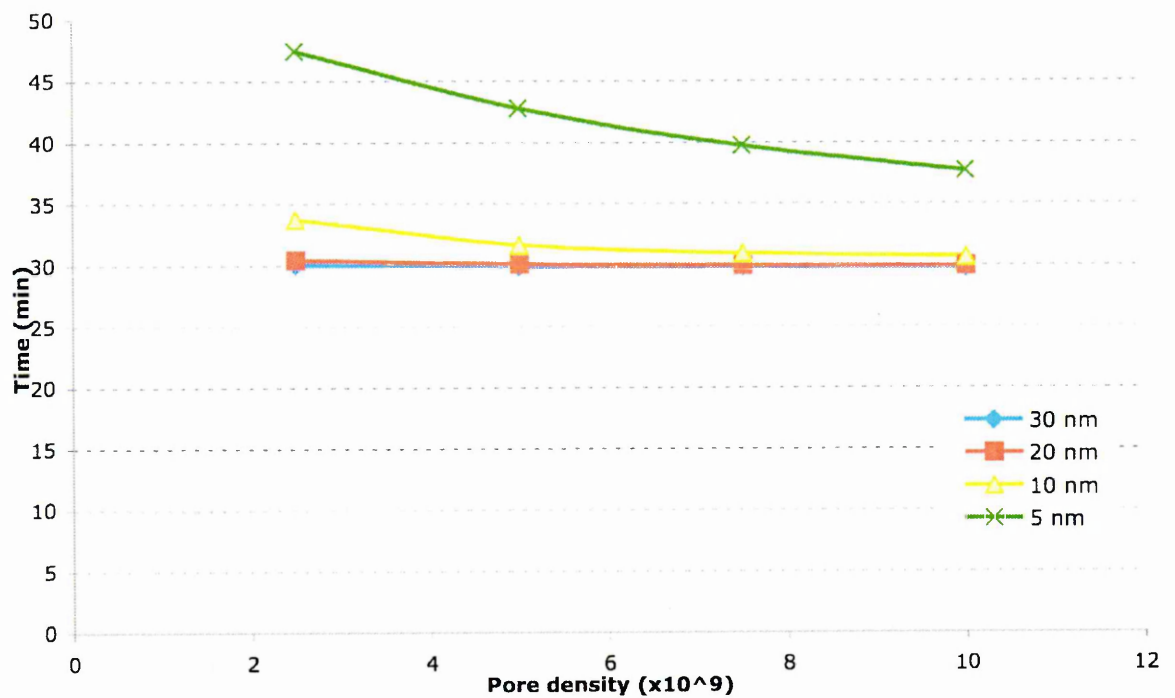


Figure 7.13 Time at which quantity of mass reach the maximum value (in minutes) in function of pore density

It can be concluded that also in this case if pore radius is 10-30 nm, pore density didn't influence insulin kinetics and the maximum value of mass quantity is reached after 30-35 minutes. If pore radius is 5 nm, only with high density of pores acceptable values of insulin diffusion were obtained, even if they are about 20% higher than the others.

Immunoglobulin (IgG) diffusion:

First of all, in the membrane effective diffusivity ( $D_e$ ) was calculated in each case and results are shown in Table 7.5. Since IgG radius is more than 5 nm, no value of diffusivity for membrane with these pores was determined.

<b>Radius</b> <b>Density</b>	<b>30 nm</b>	<b>20 nm</b>	<b>10 nm</b>	<b>5 nm</b>
<b>2.5 x 10<sup>9</sup></b>	4.71E-03	1.39E-03	9.96E-05	no
<b>5 x 10<sup>9</sup></b>	9.42E-03	2.79E-03	1.99E-04	no
<b>7.5 x 10<sup>9</sup></b>	1.41E-02	4.18E-03	2.99E-04	no
<b>10 x 10<sup>9</sup></b>	1.88E-02	5.58E-03	3.98E-04	no

Table 7.5 IgG diffusivity in different cases (mm<sup>2</sup>/h)

For each case MatLab code returns in output the time at which the value of IgG concentration just after the membrane (in  $x=Lmstep+1$ ) reached 10%. Results were shown in table 7.6 and represented in Figure 7.14.

<b>Radius</b> <b>Density</b>	<b>30 nm</b>	<b>20 nm</b>	<b>10 nm</b>	<b>5 nm</b>
<b>2.5 x 10<sup>9</sup></b>	10	16	99	never
<b>5 x 10<sup>9</sup></b>	8.8	12	57	never
<b>7.5 x 10<sup>9</sup></b>	8.3	10	42	never
<b>10 x 10<sup>9</sup></b>	8.1	9.6	34	never

Table 7.5 Time at which the value of IgG concentration just after the membrane (in  $x=Lmstep+1$ ) reached 10% (in minutes)

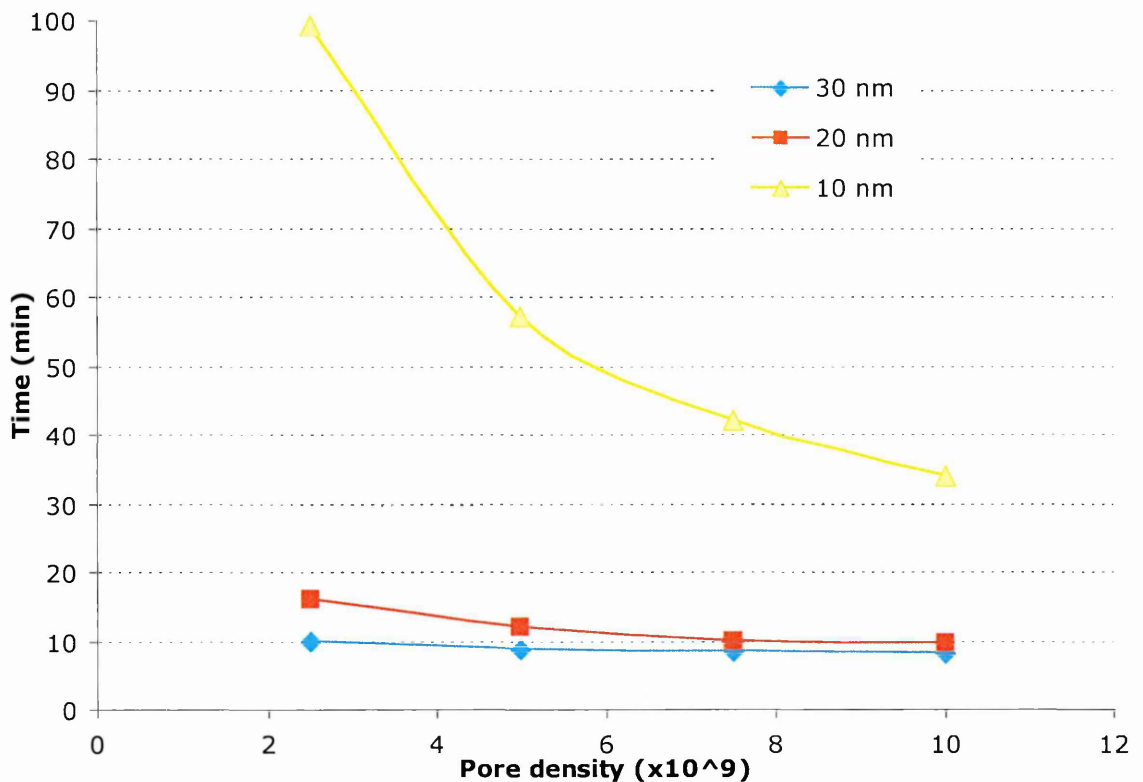


Figure 7.14 Time at which the value of IgG concentration just after the membrane (in  $x=Lmstep+1$ ) reached 10% in function of pore density

It can be concluded that, if pore radius is ranging from 20-30 nm, pore density does not influence IgG kinetics and the 10% of IgG quantity passes the membrane after 10-20 minutes. If pore radius is reduced to 10 nm, with low density of pores acceptable values of IgG transport obstruction are obtained, and the transport of IgG with the entire alginate volume is expected to be very long, thus protecting the implanted material.

The results of these calculations allow to derive some interesting conclusions.

- 1) The actual pore-size adopted in previous studies, around 30 nm, is too large for immunoprotection. More efficient size-selectivity must be obtained with pore-size less than 20 nm.

- 2) From the values of IgG diffusivity within the pore membrane and within the alginate matrix, it is evident that a more efficient blockade of large macromolecule movement can be obtained both in alginate than in the pore membrane. Thus, using more selective matrix material, dependently from the membrane pore dimension, would give more effective results in making macromolecule diffusion more slow with the possibility for small molecules to show adequate diffusion.

In general this approach showed that more careful determination of the performance of an immunoisolation device can help a lot in performing less but more successful experimental evaluations.

## References

1. Colton CK. Implantable biohybrid artificial organs. *Cell Transplant* 1995;4:415-436.
2. Deen WM, Bohrer MP, Epstein NB. Effects of molecular size and configuration on diffusion in microporous membranes. *AIChE Journal* 1981;27:7.
3. Yashonath S, Ghorai PK. Diffusion in nanoporous phases: size dependence and levitation effect. *J Phys Chem B* 2008;112(3):665-686.
4. Fournier R. Two compartment models. In: Francis T, (ed). *Basic Transport Phenomena in Biomedical Engineering*. New York, 2006.
5. Beck RE, Schultz JS. Hindered Diffusion in Microporous Membranes with Known Pore Geometry. *Science* 1970;170:1302-1305.
6. Renkin EM. Filtration, diffusion, and molecular sieving through porous cellulose membranes. *J Gen Physiol* 1954;3:225-243.
7. Shachar-Hill B, Hill AE. Convective fluid flow through the paracellular system of *Necturus* gall-bladder epithelium as revealed by dextran probes. *J Physiol* 1993;468:463-486.
8. Desai TA, West T, Cohen M, Boiarski T, Rampersaud A. Nanoporous microsystems for islet cell replacement. *Adv Drug Deliv Rev* 2004;56:1661-1673.
9. Ogston AG. The space in a uniform random suspension of fibers. *Trans Faraday Soc* 1958;54:3.
10. Crank J. *The mathematics of diffusion*. Glasgow, 1956.
11. Smith EA, Williams GS, Mohlman HT. Goniophotometer to measure diffusion characteristics of rear projection screens. AMRL-TR-65-207. AMRL TR 1965:1-20.



## Chapter 8

### Conclusions and future work

#### 8.1 Goals achieved

##### *8.1.1 Islet isolation*

##### *8.1.2 Islet transplantation by immunoisolation*

#### 8.2 Future perspective

### References

## Conclusions

The current conventional approaches for treating type I diabetes are based on exogenous insulin therapy and intensive glucose monitoring. Only in exceptional cases pancreas transplantation is performed. Although daily glucose monitoring and exogenous insulin administration are the standard therapy since the discovery of insulin, the non optimal control of blood glucose with important fluctuations leads to many severe complications including neuropathy, nephropathy, retinopathy, heart disease, and atherosclerosis (1) (2) (3). In 1993, the Diabetes Control and Complications Trial showed that strict control of blood glucose levels reduced the risk of developing diabetes-related complications (4).

Within the past 20 years, pancreatic islet transplantation has become a clinical reality and an option in the treatment of diabetes. Islet transplantation has a distinct advantage over whole pancreas transplantation in regards to reduce peri-procedure morbidity. Islet transplantation involves the isolation of pancreatic islets from cadaveric, multiorgan donors. These islets are then injected into the liver of the diabetic patient by the portal vein, from where they get deposited in liver sinuses. Islet transplantation, beside being less invasive than whole pancreas transplantation, can provide certain advantages that are not available with pancreas transplantation, including the potential for modifying tissue immunogenicity through in vitro culture or gene therapy approaches, tissue encapsulation for immunoisolation, potential for engraftment in immunoprivileged sites, and the possibility of using alternative tissue sources including xenogenic islets or stem cell derived  $\beta$ -cell lines. Widespread clinical application of this procedure, however, is currently limited by the need for lifelong immunosuppression and the need for two to four donor pancreases per recipient. Additional drawbacks include complications of

immunosuppression such as nephrotoxicity with chronic treatment with Sirolimus and Tacrolimus. The need for relatively large masses of insulin-producing cells to achieve insulin independence has led to the use of multiple donors (sequential or pooled islet preparations) per recipient. This may increase the risk for allosensitization to multiple anti-human leukocyte antigen (HLA) antibodies, limiting the possibility of future solid organ transplantation (5). Then, immunoisolation of islet was deeply explored to open the possibility of allo- or xeno- islet transplantation without the use of pharmacological immunosuppression and avoiding allosensitization of the patient (6).

The present work reports the results of scientific research activity performed with the aim of improving technical and biological aspects of islet transplantation using immunoisolation device.

## 8.1 Goals achieved

### 8.1.1 Islet isolation

The challenges to successful transplantation of islets include improvements in isolation process, islet culture, characterization and preservation. The results obtained and their relevance are presented in the following.

Automatic method for islet isolation: an islet isolation process that is automated was set up and validated. It provides most of the advantages of an automated system. It provides ease of operation with minimum number of process operating personnel. With the introduction of a newly designed digestion chamber, in different phases of the procedure a single operator can control various components of the process. Moreover, after the application of the automatic procedure, the number of the islets obtained from each isolation significantly increased.

Process Standardization: The application of this automated islet isolation protocol ensured that each pancreas goes through a similar process environment. The process has been standardized and the results were comparable and can be easily analysed.

Data collection: The automated process allows collection of large data contained in a single file for each islet isolation being carried out. These files contain several informations like type and amount of enzyme used, time of digestion, time for purification, type and quantity of solutions used. This large pool of data can further be analyzed to find out how the process was run during isolation and to possible correlation between the isolation parameters and the final outcome of the process.

In vitro and in vivo tests of functionality: The application of the automated method allows large numbers of islets to be obtained used to perform different type of tests to evaluate islet functionality and viability. A method for the in vitro evaluation of each islet preparation was set up, measuring the oxygen consumption rate of free islets under

different experiment conditions (i.e. at low and high glucose concentrations). Moreover, in vivo tests of free islet transplantation were performed under the kidney capsule. These transplantation experiments indicate that, to obtain normalization of hyperglycaemic state using allogeneic or xenogeneic islets, a barrier must be created to avoid tissue rejection but allowing diffusivity of glucose, insulin, oxygen and other metabolically active products, to insure islet functionality and therapeutic effectiveness. For this reason two types of immunoisolation devices were examined, as described in the following paragraphs.

### ***8.1.2 Islet transplantation by immunoisolation***

Applications for biomaterials in improving islet engraftment by immunoisolation of the transplanted tissue through semipermeable membranes are increasing. Immunoisolation of transplanted islet tissue is an attractive strategy that aims to solve the problem of host immune destruction of transplanted tissue by blocking access of the host immune system.

*Solute permeability of membrane for cell immunoisolation:* To select an appropriate membrane for device construction, membrane permeability properties were characterized and a computational model was developed. This theoretical provided for investigation of solute transport through different membranes on the basis of the diffusivity constant being experimentally determined. On the basis of the geometrical parameter obtained for real membranes, the best combination of pores density and pore radii of an hypothetical suitable membrane were estimated to obtain immunoisolation function. Theoretically increasing molecular weight cut-offs (7) would eliminate the escape of shed antigens, however, using smaller pore size would most probably limit the diffusion of essential nutrients to the encapsulated cells below the survival threshold. As Desai et al. suggest (8) the control of pore size down to tens nanometers can prevent protein binding and

overcome some of immunological challenges, at least hinder the passage of small cytokines and cell-secreted antigens. The results presented, in line with suggestion by other groups, indicate that control of membrane pore parameters is the only way to achieve functional immunoisolation (9) (10). Moreover, production of new membranes with more calibrated pore dimensions and density could allow to development of efficient immunoisolation devices, opening the possibility of clinical applications.

*Design of immunoisolation device:* In the present work two types of immunoisolation systems were studied, one for subcutaneous implantation (hollow fibres device) and one for the implantation in the peritoneal cavity (gel microcapsules). The hollow fibres device is compact and thin enough to be used for a subcutaneous implantation in the rat. An advantage of this site is that it requires a minimally invasive surgery and allows easy recovery in case of failure. Hollow fibre devices were tested in xenogeneic and syngeneic protocols, showing that the formation of a non-specific fibrotic capsule *in vivo* hinders the diffusion of metabolites like oxygen, causing the central necrosis of the islet cells. Then *in vitro* the permeability of these immunoisolation devices to oxygen was tested, showing that both polysulphone hollow fibers and alginate were not actually reducing oxygen diffusion and consumption within the devices. Through glucose tolerance test *in vivo* functional response of transplanted encapsulated or free islet was also studied. Continuous glucose monitoring was performed in diabetic animals receiving islet immobilized in alginate gel or inserted under the kidney capsule or in normal animals for control. In animals with islets in alginate capsules the glycaemic profile upon glucose challenge was comparable to that of normal controls while, in animals receiving islet under the kidney capsule, the metabolic control was delayed. This result is important because it demonstrates that islet encapsulation allows adequate function and optimal glucose control, also under stimulation.

Overall these experimental results indicate that islet transplantation using alginate gel microcapsules in the peritoneal cavity successfully control glycaemia in diabetic animals. This positive result, however, is not possible to translate in human application for the implantation site. Then an alternative strategy was developed based on membrane device to be used in the subcutaneous space. Despite permeability properties of the device have been proved to be adequate, the functional response of transplanted islet in hollow fibre device was only temporary. The reason of this lack of sustained function is likely dependent on the cellular response of the recipient and the development of fibrotic tissue around the device.

## 8.2 Future perspective

The research activity described in this thesis was focused on development of techniques to improve pancreatic islet isolation and to set up a device for immunoisolation of islets for transplantation without immunosuppression. In both tasks improvements have been accomplished and significant advancements have been obtained over previously reported results. There is, however, necessity to further improve this immunoisolation device to obtain final proof of function in experimental animals and to open the possibility for human experimentation.

The use of a theoretical model allows evaluation and selection of new membrane materials for islet immunoisolation. In future studies these new membranes could be further investigated. The next step is then to design experimental protocols that, in great detail, study membrane biocompatibility and effective permeability properties. After the selection of such new membranes, device function can be studied *in vitro*, maintaining device containing islets in culture for different periods of time and with different density of islets and investigating islet function, tested at different glucose concentrations. The *in vivo* efficacy of these new devices would need to be determined by performing allo- or xeno-transplantations into diabetic recipients. Finally, another issue to investigate is exploring new sites of implantation that minimize surgical procedures and reduce implant failure.



---

## Reference

1. Bailes BK. Diabetes mellitus and its chronic complications. *AORN J* 2002;76:266-276, 278-282; 283-266.
2. Bloomgarden ZT. Diabetes complications. *Diabetes Care* 2004;27:1506-1514.
3. Hill J. Identifying and managing the complications of diabetes. *Nurs Times* 2004;100:40-44.
4. The effect of intensive treatment of diabetes on the development and progression of long-term complications in insulin-dependent diabetes mellitus. The Diabetes Control and Complications Trial Research Group. *N Engl J Med* 1993;329:977-986.
5. Cardani R, Pileggi A, Ricordi C, Gomez C, Baidal DA, Ponte GG *et al.* Allosensitization of islet allograft recipients. *Transplantation* 2007;84:1413-1427.
6. Narang AS, Mahato RI. Biological and biomaterial approaches for improved islet transplantation. *Pharmacol Rev* 2006;58:194-243.
7. Gray DW. Pancreatic islet transplantation future prospects. *Immunol Lett* 1991;29:153-156.
8. Desai TA, West T, Cohen M, Boiarski T, Rampersaud A. Nanoporous microsystems for islet cell replacement. *Adv Drug Deliv Rev* 2004;56:1661-1673.
9. Brissova M, Lacik I, Powers AC, Anilkumar AV, Wang T. Control and measurement of permeability for design of microcapsule cell delivery system. *J Biomed Mater Res* 1998;39:61-70.
10. Lacik I, Brissova M, Anilkumar AV, Powers AC, Wang T. New capsule with tailored properties for the encapsulation of living cells. *J Biomed Mater Res* 1998;39:52-60.

```

        1)))/((Lm/Lmstep)^2);
    end
    for i=Lmstep+1:xstep-1
        C(i,j)=C(i,j-1)+(Dalginato*T*(C(i-1,j-1)-2*C(i,j-1)+C(i+1,j-1)))/(X^2);
    end
        C(xstep,j)=C(xstep,j-1)+(Dalginato*T*(C(xstep-1,j-1)-C(xstep,j-1))-
0)/(X^2);
        disp(sprintf('tstep %d su %d',j,tstep));
    end
% vectors for data analysis on concentration
CFref=zeros([tstep/100,1]);
for k=1:tstep/100
    CFref(k)=C(xstep,100*k-99);
end
Ci=zeros([tstep/15,1]);
for k=1:tstep/15
    Ci(k)=C(2,15*k-14);
end

% vectors for plot
xa = linspace(0,Lm,Lmstep);
xm = linspace(Lm,xmax+Lm,xstep-Lmstep+1);

xg = zeros([1,xstep]);
xg(1,1:Lmstep)=xa;
xg(1,Lmstep:xstep)=xm;
t = linspace(0,tmax,tstep);

for nplot=1:15000:600000
    plot(xg,C(:,nplot),'b-');
    hold on;
end
plot([Lm Lm],[0 100],'r-');

xlabel('Axis x');
ylabel('C(x,t)');
print('-dtiff','Cfunzdix')

figure;
plot(t,C(xstep,:), 'b-');
xlabel('tempo (ore)');
ylabel('C(xstep,t)');
print('-dtiff','C(x=xstep)')

figure;
plot(t,C(Lmstep,:), 'b-');
xlabel('tempo (ore)');
ylabel('C(Lmstep,t)');
print('-dtiff','C(x=Lmstep)')

figure;
plot(t,C(Lmstep-2,:), 'b-');
xlabel('tempo (ore)');
ylabel('C(Lmstep-2,t)');
print('-dtiff','C(x=Lmstep-2)')

```

**Insulin**

```

clear all;
close all;

% Parameters
xmax=0.5;           % alginate in millimetres
Lm=0.03;           % membrane thickness in millimetres
tmax=2;            % time in hours
Lmstep=30;         % elements in the membrane
xstep=5*Lmstep;    % elements in total (space)
tstep=600000;     % elements in which time is divided

% Code
T=tmax/tstep;      % dt
X=xmax/(xstep-Lmstep); % dx

D=0.028375;        % mm^2/h, membrane diffusivity
                    % mm^2/h, alginate diffusivity
Dalginato=0.3114;

% Stability conditions
rmem=D*T/((Lm/Lmstep)^2);
if (rmem>0.4)
    disp('rmem troppo grande!!!');
    disp(rmem);
    return;
end
ralg=Dalginato*T/X^2;
if (ralg>0.4)
    disp('ralg troppo grande!!!');
    return;
end

% definition of matrix C(x,t) in which there are
% concentration values in x and t
C=zeros(xstep,tstep);
% premise and boundary conditions
C(1:Lmstep,1)=0;
C(Lmstep:xstep,1)=100;
C(1,:)=0;
% insulin diffusion
for j=2:tstep
    for i=2:Lmstep
        C(i,j)=C(i,j-1)+(D*T*(C(i-1,j-1)-2*C(i,j-1)+C(i+1,j-1)))/((Lm/Lmstep)^2);
    end
    for i=Lmstep+1:xstep-1
        C(i,j)=C(i,j-1)+(Dalginato*T*(C(i-1,j-1)-2*C(i,j-1)+C(i+1,j-1)))/(X^2);
    end
    C(xstep,j)=C(xstep,j-1)+(Dalginato*T*(C(xstep-1,j-1)-C(xstep,j-1)))/X^2;
    disp(sprintf('tstep %d su %d',j,tstep));
end
% vectors for data analysis on concentration
CFref=zeros([tstep/100,1]);
for k=1:tstep/100
    CFref(k)=C(xstep,100*k-99);
end
Ci=zeros([tstep/15,1]);
for k=1:tstep/15
    Ci(k)=C(2,15*k-14);
end

```

```

% vectors for data analysis on insulin mass
Massa=zeros([tstep,1]);
QMassa=zeros([tstep,1]);
MaxQmassa=0.00;
Kmassa=0;
TMaxmassa=0.00;

for j=1:tstep
    Massa(j)=Massa(j)+C(1,j)*0.5*Lm/Lmstep;
    for i=2:Lmstep
        Massa(j)=Massa(j)+C(i,j)*Lm/Lmstep;
    end
    for i=Lmstep+1:xstep-1
        Massa(j)=Massa(j)+C(i,j)*X;
    end
    Massa(j)=Massa(j)+C(xstep,j)*0.5*X;
end

for k=1:tstep
    QMassa(k)=Massa(k)*(k-1)*T;
end

for k=1:tstep
    if (MaxQmassa<QMassa(k))
        MaxQmassa=QMassa(k);
        Kmassa=k;
    end
end

TMaxmassa=Kmassa*T;
disp(sprintf('max Qmassa= %i in t= %i ore',MaxQmassa,TMaxmassa));

% vectors for plot
xa = linspace(0,Lm,Lmstep);
xm = linspace(Lm,xmax+Lm,xstep-Lmstep+1);

xg = zeros([1,xstep]);
xg(1,1:Lmstep)=xa;
xg(1,Lmstep:xstep)=xm;
t = linspace(0,tmax,tstep);

for nplot=1:25000:600000
    plot(xg,C(:,nplot),'b-');
    hold on;
end
plot([Lm Lm],[0 100],'r-');

xlabel('Axis x');
ylabel('C(x,t)');
print('-dtiff','Cfunzdix')

figure;
plot(t,C(xstep,:), 'b-');
xlabel('tempo (ore)');
ylabel('C(xstep,t)');
print('-dtiff','C(x=xstep)')

figure;
plot(t,C(Lmstep,:), 'b-');
xlabel('tempo (ore)');
ylabel('C(Lmstep,t)');
print('-dtiff','C(x=Lmstep)')

figure;
plot(t,C(Lmstep-2,:), 'b-');

```

```
xlabel('tempo (ore)');
ylabel('C(Lmstep-2,t)');
print('-dtiff','C(x=Lmstep-2)')
```

```
figure;
plot(t,C(2,:), 'b-');
xlabel('tempo (ore)');
ylabel('C(2,t)');
print('-dtiff','C(x=2)')
```

```
figure;
plot(t,Massa(:), 'r-');
```

```
figure;
plot(t,QMassa(:), 'r-');
```

### **IgG**

```
clear all;
close all;

% Parameters
xmax=0.5;           % alginate in millimetres
Lm=0.03;            % membrane thickness in millimetres
tmax=24;            % time in hours
Lmstep=30;          % elements in the membrane
xstep=5*Lmstep;    % elements in total (space)
tstep=600000;      % elements in which time is divided

% Code
T=tmax/tstep;      % dt
X=xmax/(xstep-Lmstep); % dx

D=0.005;           % mm^2/h, membrane diffusivity
Dalginato=0.003;  % mm^2/h, alginate diffusivity

% Stability conditions
rmem=D*T/((Lm/Lmstep)^2);
if (rmem>0.4)
    disp('rmem troppo grande!!!');
    disp(rmem);
    return;
end
ralg=Dalginato*T/X^2;
if (ralg>0.4)
    disp('ralg troppo grande!!!');
    return;
end

% definition of matrix C(x,t) in which there are
% concentration values in x and t
C=zeros(xstep,tstep);
% premise and boundary conditions
C(1:Lmstep,1)=0;
C(Lmstep:xstep,1)=0;
C(1,:)=100;
% IgG diffusion
for j=2:tstep
    for i=2:Lmstep
        C(i,j)=C(i,j-1)+(D*T*(C(i-1,j-1)-2*C(i,j-1)+C(i+1,j-1)))/((Lm/Lmstep)^2);
    end
end
```

```

    for i=Lmstep+1:xstep-1
        C(i,j)=C(i,j-1)+(Dalginato*T*(C(i-1,j-1)-2*C(i,j-1)+C(i+1,j-1)))/(X^2);
    end
    C(xstep,j)=C(xstep,j-1)+(Dalginato*T*(C(xstep-1,j-1)-C(xstep,j-1))-
0)/(X^2);
    disp(sprintf('tstep %d su %d',j,tstep));
end
% vectors for data analysis on concentration
CFref=zeros([tstep/100,1]);
for k=1:tstep/100
    CFref(k)=C(xstep,100*k-99);
end
Ci=zeros([tstep/15,1]);
for k=1:tstep/15
    Ci(k)=C(2,15*k-14);
end

% vectors for plot
xa = linspace(0,Lm,Lmstep);
xm = linspace(Lm,xmax+Lm,xstep-Lmstep+1);

xg = zeros([1,xstep]);
xg(1,1:Lmstep)=xa;
xg(1,Lmstep:xstep)=xm;
t = linspace(0,tmax,tstep);

for nplot=1:12500:600000
    plot(xg,C(:,nplot),'b-');
    hold on;
end
plot([Lm Lm],[0 100],'r-');

xlabel('Axis x');
ylabel('C(x,t)');
print('-dtiff','Cfunzdix')

figure;
plot(t,C(xstep,:), 'b-');
xlabel('tempo (ore)');
ylabel('C(xstep,t)');
print('-dtiff','C(x=xstep)')

figure;
plot(t,C(Lmstep,:), 'b-');
xlabel('tempo (ore)');
ylabel('C(Lmstep,t)');
print('-dtiff','C(x=Lmstep)')

figure;
plot(t,C(Lmstep-2,:), 'b-');
xlabel('tempo (ore)');
ylabel('C(Lmstep-2,t)');
print('-dtiff','C(x=Lmstep-2)')

```

## **B. Standard Operating Procedure for Human Islet Isolation**

### **HUMAN PANCREATIC ISLET ISOLATION**

**PURPOSE:** To outline the process for the isolation of islet cells from a human pancreas for clinical transplantation

**RESPONSABILITY:** Cell Transplant Supervisor or designee.

**SCOPE:** All trained personnel working in the Clinical Cell Transplant Islet Laboratory.

## I. INTRODUCTION:

- A. This procedure must be performed under the strictest sterile conditions possible.
- B. Frequent changing of sterile gloves will be necessary to maintain sterility. At least two people are needed throughout this procedure - one will remain sterile at all times and work within the hood ("sterile person"). The other ("Non-Sterile person") will pass and receive all necessary materials, reagents and supplies to the sterile person and document all necessary information throughout the procedure.
- C. Utilizing sterile technique while opening sterile packaging involves removing the outer cover and placing the item inside the hood without touching the inside packaging.
- D. The manufacturer, lot number and expiration dates of all media, reagents, enzymes or solutions used in this procedure must be documented. Throughout the procedure, this is best accomplished by placing all bottles or containers before use in one designated location, then recording the lot numbers at the beginning and throughout the procedure.
- E. Record the manufacturer, lot number and expiration dates of all disposables (if not previously done) and record the autoclave cycle number, autoclave dates and chemical control results of all autoclaved non disposables .
- F. Note that additional ingredients are needed to supplement CMRL and they must be added at the time of use. CMRL without additives cannot be used to culture the islets.
- G. Pancreas will be delivered to NIT at the local procurement laboratory (Villa Camozzi, 1 floor). The on-call person will be notified when the organ has arrived. The on-call person or designee must pick up the pancreas. When the pancreas is from the local procurement laboratory, request and obtain a copy of the donor chart (also referred to as the coordinator' s chart) and bring back with the pancreas.



## II. MATERIALS & EQUIPMENT

### A. Reagents & Media

- CMRL 1066, Supplemented, MediaTech or equivalent
- Human Serum Albumin (HAS) Kedrion S.p.A or equivalent
- Hanks Balanced Salt Solution (HBSS), MediaTech or equivalent
- University of Wisconsin Solution
- Biocoll Gradients (1.100 and 1.077 densities), Biochrom or equivalent
- Dithizone (DTZ) Sigma or equivalent
- Dimethyl Sulphoxide (DMSO) Sigma or equivalent
- Liberase HI Enzyme by Roche (Boeingerher-Mannheim)
- Sterile commercially prepared water for injection, SALF or equivalent

### B. Instruments, Equipment & Non Disposables

- Instruments
  - Portable pipet-aid
  - Micropipettor for 50 ml
  - Timer
  - 3 peristaltic pumps
  - Heated water bath (37°C and 45°C)
  - 1 refrigerated floor centrifuge
  - 1 microscope
  - 1 temperature monitor with attached temperature sensor holder
  - Trip balance
  - Biological Safety Cabinets/Hoods: #1 and #2
  - Vacuum pump
  - Holders for red biohazard bags
  - 1 refrigerated COBE 2991 Cell Washer
- Sterile Human Islet Isolation Pack
  - Large stainless steel tray
  - Medium stainless steel tray

- Small stainless steel tray containing surgical instruments:
  - 1 large scissors with blunt ends
  - 1 small scissors with blunt ends
  - 2 large sharp scissors
  - 4 klemmer or mosquito clamps
  - 1 large clamp
  - 1 small clamp
- 2 beaker of 1 L
- 2 beaker of 400 ml
- 2 beaker of 250 ml
- Sterile catheters
- Sterile 4.0 silk suture
- Sterile Human Chamber Isolation Pack
  - 1 screen (500 mm)
  - 500 ml stainless steel isolation chamber with lid
  - 2 rubber ring
  - 7 stainless steel beads
  - 1 heating coil
  - silicone tubing
    - 3 size 1/4" -3/8"
- Sterile Human Purification Pack
  - silicone tubing
  - Sterile Cobe couplers and processing sets
  - Teflon coated magnetic bar
- Disposables I (into a drawer in the Islet Lab)
  - Sterile wide mouth pipettes: 1, 2, 5, 10 and 25 ml
  - Sterile syringes: 10ml and 60ml
  - Sterile 3.5 ml plastic transfer pipettes
  - Sterile 10 X 35 counting and petri dishes & 100 X 15 petri dishes
  - Sterile 18G needles

- Sterile 150 ml and 600 ml transfer bags
- Sterile disposable sheets
- Disposables II
  - 2 Freeze packs
  - Sterile 250 ml conical centrifuge tubes
  - Sterile tissue culture flasks, vented: T-75 Sarsted
  - Sterile disposable gloves, gown, shoe covers, head cover and mask
  - Large and small red biohazard bags
  - Large and small sharps containers

### III. PROCEDURE

#### A. Islet Laboratory Set Up

1. Enter the hand-washing room and wash hands
2. Remove the outer plastic bags from a packaged sterile gown and sterile gloves without touching the inner packaging.
3. Put shoe covers, sterile gown and sterile gloves in that order. Street clothes cannot be worn under the green scrubs.
4. Enter the clean room (Islet lab) and put on eye protection.
5. Perform the following tasks:
  - a) Ensure that blower is on in the #1 hood and that ultraviolet (UV) light is off. Turn on light and thoroughly wipe interior with 10% bleach or Lachisan using a disposable yellow dusters. Repeat this for the other hood.
  - b) After cleaning, allow blower to run for at least 10 minutes before using the hood.
  - c) Turn on the power for the refrigerated centrifuge, wipe interior with 10% bleach or Lachisan using a disposable yellow dusters. Ensure that the temperature is set to 4°C, close the lids and run them (empty) for 5 minutes. This will allow the temperature to reach 4°C.
  - d) Wipe down all counters with 10% bleach or Lachisan.

- e) Ensure that fresh empty red bags (double bagged) are in bag holders and that several new sharps containers are in place.
- f) Assemble the vacuum collection system near the #2 hood by attaching one end of the vacuum tubing to the pump and the other end to the sterile 2 ml pipette without cotton.
- g) Fill the water bath with distilled sterile water, turn on water bath and warm to 45° C.
- h) Obtain the following and place all on a desk in the islet lab:
  - o Sterile Islet Isolation Pack
  - o All items listed in "Disposables II".

#### **B. Hood and Chamber Apparatus Set Up & Reagent Preparation**

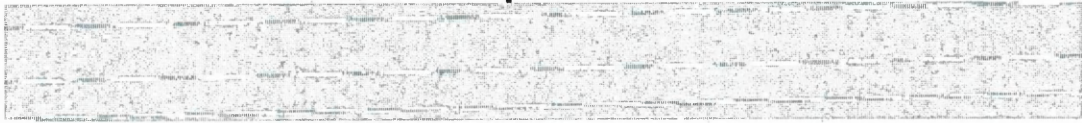
1. All individuals performing the procedure must scrub and gown but one will be designated as "sterile" and the others as "non-sterile".

##### **5. Sterile Person:**

- a) Open to completely cover the sterile surface of the hood while avoiding the non-sterile vented areas.
- b) Accept the chamber.
- c) Put the rubber ring on the chamber and on the lid
- d) Connect one silicone tube to the inlet port of the chamber and to the outlet port of the chamber lid.
- e) Connect the free end of the silicone tube connected to the inner port to the outlet port of the glass coil. Connect the last tube to the inner port of the glass coil.

##### **6. Non-Sterile Person:**

- a) Remove packaging from sterile half sheet in #1 hood
- b) Open the wrap of the chamber pack
- c) Open the wrap of the rubber ring pack
- d) Open the wrap of three silicone tube packs
- e) Open the wrap of the coil pack
- f) Open the wrap of 400 ml beaker pack

- 
- f) Bring the coil out of the hood.
- g) Place the tube that enter in the pump in a 400 ml glass beaker
- h) When tubing circuit is complete, place the temperature probe into the side port of the chamber. Insert and screw the probe into the port on the bottom of the chamber. The other flat end of the probe is inserted into the temperature sensor .
- i) Instruct the non-sterile person to adjust the pump speed to 320 ml/min (range of 200-350 ml/min acceptable), and start filling the circuit.
- j) The chamber must be filled from the bottom, via the silicone tubing through the inlet port at the bottom of the chamber.
- k) Make sure that the circuit doesn't lose.
- g) Place the coil in the water bath filled with distilled autoclaved water warmed to 45°C
- h) Place the silicone tube connected to the inlet port of the coil in the pump head and secure.
- i) Fill the 400 ml beaker with 300 ml 2% Hanks when requested by the sterile person.
- j) Adjust the pump speed to 320 ml/min (range of 200-350 ml/min acceptable), and start filling the circuit at the sterile person's request
- k) Prepare dithizone (DTZ) solution
- l) Prepare enzyme (see section D, "Enzyme Preparation"). **Do not warm the enzyme until instructed to do so by the sterile person.**
- 

**C. Pancreas Cleaning & Cannulation****1. Sterile person:**

- a) All processes performed by the sterile person must be performed in the #1 hood.
- b) Open to completely cover the freeze packs and sterile surface of the hood while avoiding the non-sterile vented areas
- c) Place the large tray inside the larger tray with the slush and instruct the non-sterile person to add approximately 500 ml of cold UW solution to the medium tray.
- d) Using sterile technique, open the pancreas container and remove 2-3 ml of the UW-1 solution (which the pancreas is transported in) from the pancreas transport container using a sterile plastic 3.5 ml pipette. Pass this to the non-sterile person for sterility tests.
- e) Instruct the non-sterile person to heat the enzyme approximately 10 minutes before completion of cleaning and cannulation.
- f) Move the pancreas to the tray with the UW solution and clean off the fat and connective tissue using sterile scissors and forceps:
  - Spread the scissors in a “spreading, closing” motion to separate the connective tissue from the pancreas.
  - Remove fat and connective tissue using a blunt dissection technique.

**2. Non-Sterile person:**

- a) Remove packaging from sterile half sheet in #1 hood
- b) Put the freeze packs on the working plate of the #1 hood
- c) Open the small stainless steel tray containing surgical instruments on the working plate of the #1 hood
- d) Remove packaging from the large tray
- e) Accept plastic pipette with the sample for sterility testing and aseptically place in the #2 hood.
- f) Open the outside wrap of the pancreas container and pass the inside sterile container inside the hood to the sterile person.
- g) Accept transport container from the sterile person, open it, measure the temperature of UW solution in which

- Do not trim the pancreas too closely as leaks may develop.
  - Note that the fat floats while the pancreatic tissue does not.
  - During cleaning locate ducts exiting the pancreas from the non-dissected end and clamp with mosquito clamps to facilitate distention.
- g) Place the cleaned pancreas in the sterile 250 ml beaker (included in the isolation pack), cover with foil and pass to the non-sterile person for weighing.
- h) Note the amount of fat, presence of edema, whether pancreas is flushed, and the texture of the pancreas by gently examining it. Communicate this information to the non-sterile person so that it can be documented
- i) Use a No. 10 scalpel to cut the pancreas at the neck, just below the head.
- the pancreas is transported using the second temperature probe and record the temperature.
- h) When instructed by the sterile person, place the enzyme in the waterbath warmed to 45°C and slide the end of the probe hanging out of the bottle (flat end) into the temperature sensor attached to the temperature monitor and clip it in place. Note that the side with the 2 holes is placed facing the sensor wires.
- i) Allow the enzyme to warm to 30°C. Gently swirl bottle before reading the temperature registered on the temperature monitor and ensure that the monitor is not reading "room temperature".
- j) Weigh the cleaned pancreas when instructed to do so by the sterile person as follows:
- Accept the empty foil covered beaker and use to tare the scale.
  - Weigh beaker and pancreas.
  - Hold the beaker under hood #1 so that sterile person can retrieve the pancreas and then remove beaker from hood.

- j) Remove the needle from the 18 G catheters before cannulation to prevent the catheters from falling out after cannulation.
- k) Locate the large pancreatic duct and cannulate both the head and tail portions with the catheters.
- l) Secure the catheter in the duct of the pancreas body as follows:
- Insert the straight needle (2.0 black silk attached) on one side, close to surface of the cut, but not too close to the cannula.
  - Pull the needle through leaving a length of silk adequate to tie several knots.
  - Reinsert the needle on the other side in the same manner and cut the needle off from the silk.
  - Use both ends of the silk to tie the catheter in place.
  - Before tightening, reinsert the needles into the catheters to avoid crushing the plastic cannula and bend the needle (at the top) to prevent it from coming out of the tip of the catheter.
  - Repeat the tying three times and place an additional tie after twice wrapping the silk around the catheter. Tie the loose ends of the silk into a loop and use this to pick up and transport the pancreas.
- k) Record this and all other required information. Communicate with the sterile person for verbal assessment of the pancreas and document this information.



- The catheter is secure when it does not slide out of the duct even after gently trying to pull it out.
- m) Repeat this procedure (outlined in section n, above) for the head of the pancreas.
- n) Once both catheters are in place and tied in, wait for the collagenase solution to be heated then pass the large tray with the iced saline to the non-sterile person for removal from the hood. The gland is now ready to be distended.

#### D. Enzyme Preparation

1. The Non-Sterile person performs this activity and all processes are to be performed under the #2 hood.
2. Place a bottle of plain Hanks and a bottle of commercially prepared sterile water for injection in the #2 hood.
3. Remove the enzyme package from the -70° C freezer in the Islet lab, remove and discard the package and let bottle stand in the #2 hood at room temperature for a few minutes.
4. Record the enzyme lot number and expiration date.
5. Remove the rubber lid from the enzyme bottle by inserting a sterile needle through one side of the rubber lid to the other side then gently lifting the cap off using the needle as an anchor.
6. Avoiding bubbles, add 15 ml of sterile water for injection to the contents of the enzyme bottle (0.5 g lyophilized pellet) and do not shake the bottle. Let the bottle sit at 4°C for 30 minutes. Avoid any introduction of bubbles that will affect the action of the enzyme.

7. After the enzyme pellet has dissolved, transfer the contents of the bottle to the upper chamber of the 500 ml filter (0.2  $\mu$ m size) system. Wash the enzyme bottle several times with plain Hanks and add to the upper chamber of the filter system.
8. Add plain Hanks to the upper chamber to reach a total volume of 350 ml (bottle has measurement markings on the side). This will result in a final enzyme concentration of 1.4 mg/ml (0.5 g / 350 ml).
9. Connect the free end of the vacuum tubing to the filter bottle inside the hood and turn the vacuum pump on (on the ground nearby) using your foot. Once the vacuum is on, filtering will be automatic.
10. Immediately after sterile filtering, remove the upper chamber from the bottle, remove the clear cap from one end of the probe and aseptically place the probe inside the bottle while allowing the flat end of the probe to hang outside. Tightly cap the bottle without breaking the wire of the probe and place it in the refrigerator until ready for warming.

**E. Pancreas Distention****1. Sterile Person:**

2.

- a) Perform all activities in this section in hood #1.
- b) Pour out the UW solution from the medium sized tray (used to clean the pancreas) into the large saline bath tray and pass to the non-sterile person.
- c) Distend the head of the pancreas with ~150 ml of collagenase solution using a 60 cc syringe connected to the catheter – forcefully push the plunger of the syringe to force the enzyme into the pancreas and avoid creating bubbles. The pancreas will enlarge if there are no leaks or cuts.
- d) When leaks are observed, use a sterile hemostat to clamp off the area, preventing the enzyme from leaking.
- e) The tail of the pancreas is distended next using ~200 ml of enzyme solution. It may again be necessary to check for leaks and to close them off with hemostats.
- f) Occasionally, a portion of the pancreas does not distend well. This may be due to the presence of an accessory duct or to technical problems. The poorly distended region may be injected intraparenchymally (using an 18 or 20 Gauge needle attached to a 60 cc syringe) to

**3. Non-Sterile Person:**

- a) Accept the large tray from the sterile person and discard contents.
- b) When the temperature of the enzyme solution reaches 30°C, remove the bottle of enzyme from the water bath.
- c) Open the bottle containing the enzyme solution under hood #1 and aseptically pour its contents into a 400 ml beaker supplied in the pack without touching anything under the hood.

achieve proper distention.

- g) While the pancreas is being distended, drain the solution from the chamber system into a 1L beaker as follows:
- Instruct non-sterile person to stop the pump and reverse the direction of the flow.
  - Remove the end of the large tubing to a 250 ml beaker and start the pump again. The solution will flow in a different direction; the chamber will empty via two ports at the bottom of the chamber and small tubing connected to the ports.
  - Discard the recirculating fluid from the chamber system.
- h) Continue cleaning the pancreas. Remove as much "non-pancreatic" tissue as possible as well as cannulas and sutures. Do not discard these.
- d) After the system has drained, stop the pump and reverse direction of the flow.
- e) Weigh removed tissue, sutures and cannulas in order to determine true weight of the pancreas during the digestion. Calculate weight and record it.

**F. Pancreas Digestion****1. Sterile Person:**

- a) Open the chamber. Place distended pancreas cut in 7 pieces inside the chamber and fill the chamber with collagenase solution up to the filter level.
- b) Put screen (430  $\mu\text{m}$ ) in the chamber and the top of the chamber and tighten securely.
- c) Pour all the remaining collagenase solution into the 250 ml beaker placed in the ring stand and instruct non-sterile person to begin pumping solution through the system at a rate of 225 ml/min while the circuit is filling.

**2. Non-Sterile Person:**

- a) Begin pumping solution through the system at a rate of 225 ml/min while the circuit is filling.
- b) Add more 2% Hanks to the beaker (without touching anything under hood #1) in order to fill the system completely and to eliminate air from the circuit.
- c) As soon as circuit is complete and no air bubbles are observed in the system, adjust the pump speed to 150 ml/min (100-150 ml/min range is acceptable).
- d) Begin recording the temperature in the chamber. The desired rate of heating is  $2^{\circ}/\text{min}$  until  $37^{\circ}\text{C}$  is reached.

- d) After 8 minutes of digestion, take a 3 ml sample from the end of the large Tubing (one minute before the sample is taken, the chamber must be shaken vigorously to assure that a representative sample is collected).
- e) Place a few drops of digest in a small, 10 x 35 mm petri dish and pass to the Non-Sterile person.
- e) Pull the tubing extending from the top and bottom of the chamber through the plastic rings attached to the hood to make sure that the tubing does not interfere with the machine.
- f) Swirl the collection flask gently during the collection of the first 100 ml.
- g) Temperature should not increase above 37° C during the digestion.
- h) The length of digestion time varies but in general, once the temperature has reached 37° C inside the chamber, the digestion is continued for about 20-25 minutes. Regulate the temperature in the chamber by taking the heating coil partially or completely out of the water bath when the temperature reaches 37°C.
- i) Add a few drops of dithizone (DTZ) solution to the digest and observe under the microscope. DTZ stains the islets a red color by the binding of zinc to insulin granules. Conversely, the acinar tissue appears unstained. Record all observations. Normally, fat cells are seen first, followed by acinar and an occasional islet fragment.

- f) Accept and unwrap the flasks and place them on either side of the ring stand.
- g) As the digestion nears completion, instruct the non-sterile person to fill one of the flasks with 3 L of 10% RPMI (uptake flask) and pour 1L of 10% RPMI in the other flask which will be used to collect the digest (collection flask) without touching anything in Hood #1.
- j) There is an increase in the amount of acinar tissue as digestion proceeds. The digestion is considered complete when an increase in the amount of tissue liberated from the chamber is observed, most or all of the islets are free of the surrounding acinar tissue, intact islets are observed, and the acinar tissue becomes finer (smaller cell clusters).
- k) While the digestion is in progress, aseptically pass 2 chilled sterile 4L flasks to the sterile person.
- l) When instructed by the sterile person, pour 3 L of 10% RPMI in the uptake flask without touching anything in the #1 hood.
- m) Pour 1 liter of 10% RPMI to the collection flask in the same manner when instructed to do so by the sterile person.
- n) Place a sterile tray with sterile ice in the #2 hood.

- h) Stop the digestion process (switch to dilution), regardless of the number of free islets in the sample when most islets are free, even if lightly embedded. In the case of heavily embedded or mantled islets, the digestion can be prolonged to the point before the islets become irregular in shape, before small irregular islet fragments are seen, and/or before acinar tissue becomes too fine (overdigestion).

#### G. Dilution and Collection of the Digest

##### 1. Sterile Person:

- a) When digestion is judged complete, the dilution phase. This is carried out in hood #1.
- b) At this time, instruct the non-sterile person to turn the pump off and simultaneously place the end of the smaller tubing into the flask containing 3 L of 10% RPMI (uptake flask) and place the end of the large tubing into the collection flask which contains 1 L of 10% RPMI.
- c) Pour the contents of the 250 ml beaker containing the digest into the collection flask, rinse this beaker with 100 ml of FBS and add to the collection flask to help inactivate the enzyme in the digest.

##### 2. Non-Sterile Person:

- a) Turn the pump off when instructed to do so by the sterile person.



- d) Instruct the non-sterile person to turn the pump back on, adjust the speed to provide a flow of 320 ml/min (200-350 ml/min range is acceptable), remove heating coil from the water bath to allow the chamber to be cooled, and start to shake the chamber vigorously
- e) Begin collecting digest solution into the collection flask until 2-3 L of fluid is obtained.
- f) Replenish the uptake flask (flask with large tubing) continuously with more 10% RPMI as and when needed.
- g) Once the flask has 3 liters, cover with aluminum foil and pass it to the Non-Sterile person who will transfer it to the #2 hood, where tissue can be collected by centrifugation.
- h) Move the end of the large tubing to a labeled 1 L sterile bottle and continue collecting the tissue. Once a bottle is full, cap it tightly and pass it to the Non-Sterile person to place in the refrigerator. Repeat this as many times as there is still digest to be collected.
- i) The dilution phase lasts 15-45 minutes or until islets are no longer detected in a sample.
- j) Weigh and record the weight of the undigested pancreas. Do not subtract the weight of the undigested pancreas from the total weight of the pancreas!
- b) When instructed by the sterile person, turn the pump back on, adjust the speed to provide a flow of 320 ml/min (200-350 ml/min range is acceptable), remove heating coil from the water bath to allow the chamber to be cooled, and start to shake the chamber vigorously
- c) Take out 4-6L of 10% RPMI from the refrigerator when needed by the sterile person and replenish the uptake flask without touching anything in hood #1.
- d) In the #2 hood, mix well and then pour digest solution from the collection flask into sterile 1 L beakers and cover with foil. Pour digest from beakers into 250 ml conical centrifuge tubes, cap and close tightly. Fill as many tubes as possible – 4 conicals can be centrifuged at the same time
- e) Balance the tubes and centrifuge them at 1000 rpm for 2 minutes at 4°C.
- f) When the spin is over, remove tubes from centrifuge and place in #2 hood.
- g) In the #2 hood, add 180 ml cold UW solution and 20 ml FBS to a sterile flat bottomed jar or beaker and place this on sterile ice located in the hood. UW solution prevents the acinar from

- k) Proceed to Section H, Separation of Islets Using Discontinuous Gradients and perform steps 1-16.
- h) Discard supernatant with a single smooth motion (progressing slowly to a 135° angle between conical and flask and without creating air bubbles that could disrupt the pellet) into the empty collection flask now labeled as "waste". Leave a small amount of liquid in the lip of the conical to resuspend the pellet.
- i) Detach the pellet from the bottom of the conical tube using a quick circular motion, pour pellet into the jar or beaker containing 20 ml of FBS and 180 ml of UW solution on ice.
- j) Repeat steps d-i, above, using all of the digest (from the 4L flask and all bottles placed in the refrigerator) until all the tissue is centrifuged and collected using fresh sterile 250 conicals each time.
- k) If there is a large amount of tissue, use a second jar or beaker for collection containing 20 ml FBS and 180 ml UW solution.
- l) Keep resuspending the tissue as more is added to the tube by slowly aspirating up and down using a 25 ml pipette.
- becoming edematous.

- m) Once all of the tissue has been collected, take a 100 $\mu$ l sample for pre-purification count from 100 ml of tissue suspension using a micropipette with extender (see section I on "Counting of Islets")
- n) Centrifuge tubes at 1000 rpm for 5 minutes.  
Record the comments on the condition of the acinar tissue and percentage of free islets.
- o) Resuspend the tissue in 250 ml stock Biocoll solution, combining pellets if more than one conical was used.
- p) After gentle resuspension of the tissue, divide the suspension in 2 or more 250 ml conicals depending on the size of the digest pellet (20 ml per conical).

#### **H. Separation of Islets Using Discontinuous Gradients**

1. Face shield must be worn at all times when operating the Cobe. Position Cobe and turn power on. Open the Plexiglas cover by removing the metal latch. Remove the locking glass bowl cover and remove Plexiglas cover and underlying foam ring from the bowl area.
2. Place centrifuge Cobe bag inside the bowl. This is done by carefully rolling the bag around the rotating seal into a cigar shape and sliding it through the opening in the glass bowl cover. Care must be taken not to damage the rotating seal.

3. Position the bag over the four central posts in the bowl. Tuck the perimeter of the bag into the bowl so that the bag lies smoothly on the bottom of the bowl with the edge curving up the sides of the bowl. Position the sampling port so that the stem lies flat and parallel to the side of the bowl.
4. Place plastic collar (around tubing at the center of the bag) below the rotating seal. Lower the locking glass cover and lock it in place. Take care not to catch any part of the bag in the slots at the edge of the bowl which holds the bowl cover. This could result in damage to the bag.
5. Close the sliding Plexiglas cover and place the metal latch over the posts and the rotating seal. The rotating seal may require minor manipulation in order to position it to slide into the slot in the weight. Let it use its own weight to lock the cover and hold the rotating seal. Do not push down on the weight as this could damage the seal.
6. Turn the locking rod to the down position.
7. Place the tubing into the valve slots on the Cobe (but outside the pinch valves), using the color-coding to determine position. The tubing is not loaded into the pinch valves, but merely held in place in the tubing guides.
8. Clamp each tube using hemostats.
9. Place sterilized silicon tubing (size 16) into the Masterflex pump heads located inside the #2 hood.
10. Label 4 sterile conicals for each Cobe run as "1" for top, "2" for second layer, "3" for third layer and "S" for supernatant layer and place in rack(s) in the #2 hood.
11. Aseptically spike the silicone tubing by placing the plastic end of the green or red tubing from the Cobe into the end of the silicone tubing. Place the other end of the sterile silicone tubing into a sterile 250 ml conical.
12. Heat-seal the purple, blue and yellow lines between the T-junction and valve slots.
13. In the #2 hood, place a 60cc wide mouth syringe in a ring stand clamp.

14. Handle only the barrel of the syringe, as this will be used to load the suspended tissue into a 600 ml transfer bag.
15. Remove the plunger and place upright with the barrel touching the flat surface of the hood. Remove the tip cover of the syringe.
16. Attach a sterile piece of tubing to the tip of the syringe. Connect the other end of the tubing to the non-spiked end of the Cobe coupler. Spike the other end of the Cobe coupler/adaptor into a 600 ml transfer bag labeled with the HP #.  
Use the side port of the 600 ml transfer bag.
17. Tie a loose knot in the tubing of the 600 ml transfer bag.
18. If more than 20 ml of tissue was collected, two syringe set ups, two Cobe set ups, and two sets of the solutions below are necessary.
19. Remove the solutions for the discontinuous gradients from the refrigerator. Biocoll gradients are pre prepared in 75 ml aliquots. Solutions needed for each Cobe run are listed below:

Bottom layer:	75 ml of Biocoll (1.100)
Middle layer:	75 ml of Biocoll (1.096)
Top layer:	75 ml of Biocoll (1.037)
Plain Hanks:	50 ml
20. Remove aliquot(s) of 300 ml Biocoll stock solution from the refrigerator.
21. Remove all but approximately 20 ml of supernatant from the centrifuged tissue using a bacteriological pipette (no cotton) connected to the vacuum system. Use caution so that the pellet is not disturbed while most of the supernatant is removed at the same time.
22. The last 20 ml of supernatant should be removed using a manual pipet aid to minimize the risk of pellet aspiration.
23. Mix well together the digest in the conical with a small amount of stock Biocoll (so that mixing can be thorough) in a sideways or upright circular motion to avoid creating bubbles.
24. Thoroughly resuspend tissue in conical(s) using, if necessary, a sterile disposable 10 ml pipette to break up any clumps.

25. Pour the above suspension(s) into the 60cc syringe connected to the 600 ml transfer bag(s) and allow to flow by gravity via the set-up described above.
26. Add Biocoll stock from each bottle to each conical to rinse conical(s) and then pour into respective syringes after the pellet mixture containing islets have all entered the solution. The total volume of stock Biocoll should be 300 ml.
27. Plunger may be used to force the stock Biocoll into the bag once all of the tissue has entered the transfer bag.
28. Tighten the loose knot in the line of the bag and heat seal bag.
29. Immediately attach the filled transfer bag(s) to the red or green Cobe tubing and hang on the metal rail of the Cobe, with red and green color tubing clamped with hemostats.
30. Release clamp on the tube attached to the transfer bag so tissue flows into the Cobe bag in the centrifuge bowl.
31. Once the tissue has entered the centrifuge bag, the tubing attached to the transfer bag is clamped, the tubing attached to the silicone tube is unclamped and the most dense of Biocoll layers (1.100) is pumped through this tubing up to the T-junction.
32. When the solution reaches the T-junction, stop the pump and clamp the tubing connected to the silicone tube.
33. Unclamp tube connected to the transfer bag.
34. Remove air in the centrifuge bag as follows:
  - Set Cobe speed at **2,000 rpm**. (the speed should be maintained at this setting throughout the whole procedure).
  - Hit "**Start**" button.
  - When centrifuge reaches **2,000 rpm**, push "**SuperOut**" button.
  - Immediately adjust **SuperOut rate to 150ml/min** (Solution will be pushed up through the tubing towards the T-junction).
  - Press "**HOLD**" button.
  - **Clamp red tubing** as solution reaches T-junction and simultaneously press "**Stop/Reset**" button.

35. When machine stops, reset dial of **SuperOut rate to "0"** but do not press SuperOut button.

36. Press "**Start**" button again.

37. When the centrifuge has attained speed, unclamp tubing connected to the silicone tube, start the pump and begin pumping the Biocoll solutions of varying density at a rate of approximately 90 ml/min. This is accomplished by placing the end of the masterflex tubing in the designated conicals and moving the tubing to the next designated conical (stop the pump while moving the tubing between conicals to avoid the introduction of air into the Cobe).

Sequence for solution movement is as indicated below:

- Pump in 75 ml of 1.108 Biocoll on top of the 300 ml pellet layer, which contains tissue, resuspended in Ficoll stock.
- Pump in 75 ml of 1.096 Biocoll on top of the 75 ml preceding 1.108 layer.
- Pump in 75 ml of 1.037 Biocoll on top of the 75 ml preceding 1.108 layer.
- Pump in 50 ml of plain Hanks until the fluid/air interface reaches midway down the tubing leading to the rotating seal. Plain Hanks is necessary to remove proteins from the rotating seal. In the presence of proteins, the seal would break during the high speed rotation phase.

38. Turn off the pump and clamp the tubing connected to the silicone tube.

39. Adjust SuperOut valve to "0" ,

40. Press "**SuperOut**" and **immediately** open the red or green tube to relieve the excess pressure, then reclamp the tubing.

41. Let spin for 5 min.

42. **Before collection, make sure that the pump head is open and tubing inside it is completely released.**

43. Collect fractions through the tubing connected to the silicone tube using the 4 sterile conicals labeled 1, 2, 3 and S.

44. Unclamp the tubing connected to the silicone tube and adjust the dial of the SuperOut rate up to about 175 – **do not press the SuperOut button!**

45. Normally, 4 fractions are collected:

- Between fractions the machine is put on Hold while the green tubing is moved to the next 250 ml conical bottle to prevent spillage and tissue loss.
  - The first layer has a volume of 100-125 ml and it should be visible. Collect 75 ml of this layer in the conical labeled "S". When the distinct layer reaches the inside metal rim, wait 3 seconds, press "HOLD" and then switch tubing to the next conical labeled "1".
  - Fractions 1, 2 and 3 are approximately 75 ml each and the layers should be visible. When 75 ml is collected or the visible layer reaches the inside metal rim, wait 3 seconds, press "HOLD" and then switch tubing to the next conical labeled "2".
  - When 75 ml are collected or the visible layer reaches the inside metal rim, wait 3 seconds, press "HOLD" and transfer the tubing to the conical labeled "3".
  - Collect 100 ml of the "3" fraction and press "STOP/RESET" on the machine.
  - Discard the "S" fraction after taking a sample to confirm that it does not contain islets and keep fractions labeled as "1", "2", and "3".
46. Once the fractions are collected, stop the machine. Dilute fractions with 10% RPMI (fill conical to the top) and spin at 1500 rpm for 5 minutes at 4°C.
47. Heat seal tubing leading to centrifuge bag, cut tubing and take bag out of the bowl. Take a sample of the pellet through the port on the centrifuge bag (using sterile technique) using a Cobe coupler.
48. Place this sample in petri dish, add a few drops of DTZ solution and some saline in order to estimate if there are any islets in the pellet.
49. If a significant number of free islets are observed in the pellet, collect the entire pellet by using the Cobe coupler inserted it into the port of the Cobe bag. Collect pellet in a 250 ml conical and centrifuge at 1500 rpm for 5 minutes at 4°C. Aspirate supernatant and purify islets in the pellet by using Cobe.
50. Use a micropipettor with extender to take 3, 100  $\mu$ l samples of each fraction ("1", "2", and "3") from 100 ml of tissue suspension and place in counting



dishes (see section I, "Counting of Islet Cells"). Add DTZ and saline and observe under the microscope for the presence of islets. Discard fraction "3" if there are no islets detected.

51. Aspirate the supernatant and resuspend the pellets in 10% RPMI for a second wash and spin at 1000 rpm for 5 minutes at 4°C.
52. Resuspend the final pellet in 250 ml of CMRL-1066 (supplemented) and mix well. At this time, islets can be counted.

### I. Counting of Islet Cells

1. Mix the final islet suspension well before taking a sample.
2. Add a small volume of saline to cover the bottom of the counting dishes before taking triplicate 100 µl samples, using a micropipettor with a sterile pipet tip extender attached to a wide mouth pipet tip, from the final islet preparation and place each sample in the 10x35 mm counting dish containing saline.
3. Add a few drops of DTZ solution to the 100 µl sample contained in the counting dish and count the islets under the microscope following the steps below.
4. After staining the islets, it is possible to count the islets, which will appear red. Count the islet sample using the 10X eyepiece and the 4X objective to give a total magnification of 40X. Use the calibrated grid in the left eyepiece of the phase contrast microscope.
5. Since islet volume is approximately proportional to the cube of the islet radius, it is crucial that the islets are divided into diameter (size) classes. 50 µm diameter range increments are used, without considering particles smaller than 50 µm since their contribution to the total volume of the preparation is insignificant.

6. The distance between two lines on the calibrated grid in the eyepiece will equal 50  $\mu\text{m}$ . Using the eyepiece (40X total magnification), use the chart below as a guide:

<u>Number of Lines</u>	<u>Size of Islets</u>
2	50 $\mu\text{m}$
4	100 $\mu\text{m}$
6	150 $\mu\text{m}$
8	200 $\mu\text{m}$
10	250 $\mu\text{m}$

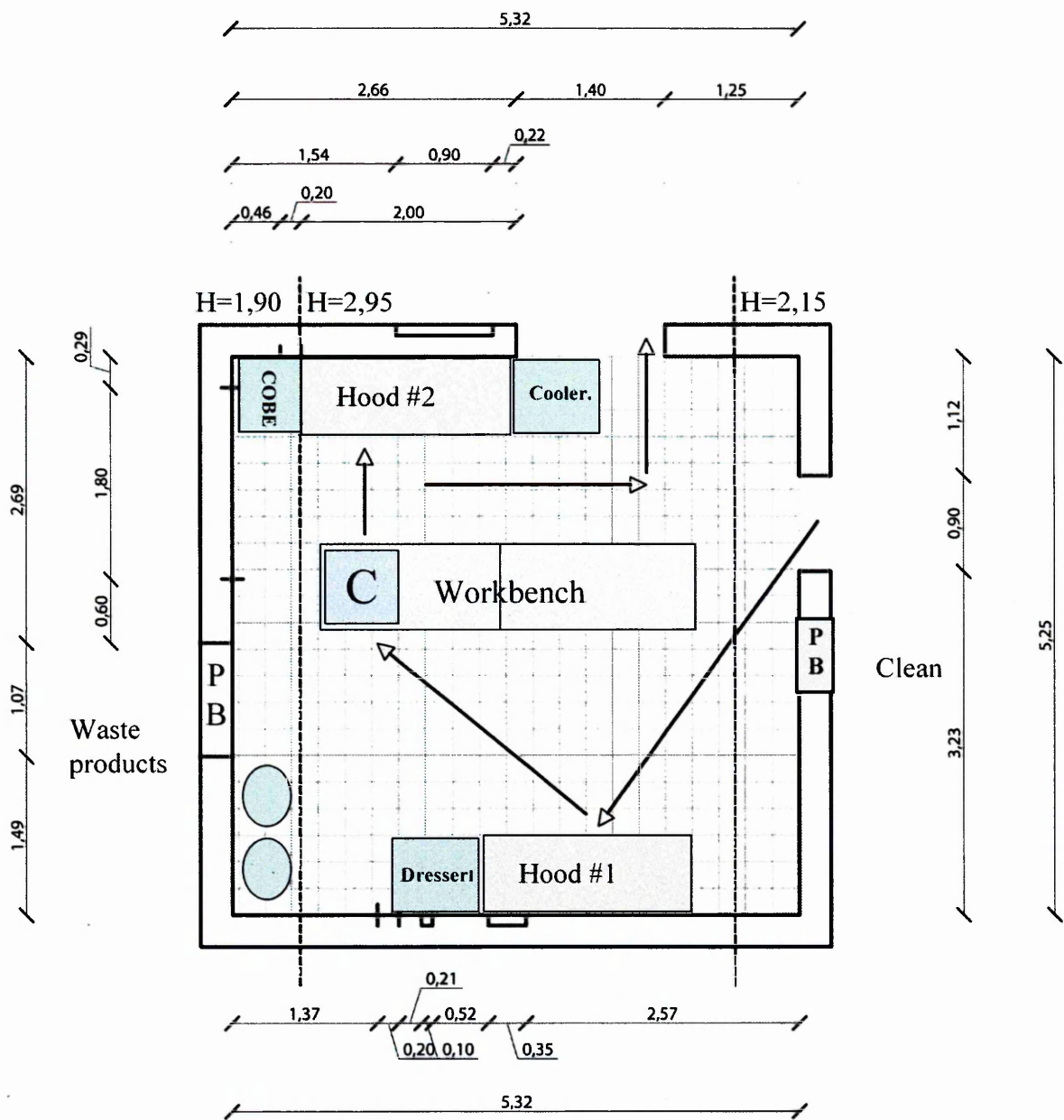
7. Count the number in each group using the manual cell counter, and record numbers as well as the purity and conversion to islet equivalents.

8. Calculates the actual islet number (IN) as well as the islet equivalent (IEQ).

9. Islet number (IN) and islet equivalent (IEQ) calculations can be done manually as well. The table below indicates the mean volume for each diameter class and the relative conversion factor into islets of 150  $\mu\text{m}$  diameter. These factors make it possible to convert the total islet number from any preparation into islet equivalent (IEQ). In place of IEQ, the total islet volume of the final preparation can be also estimated.

<b>islet diameter</b>	<b>conversion into islets</b>
<b>range (<math>\mu\text{m}</math>)</b>	<b>of 150 <math>\mu\text{m}</math> diameter (IEQ conversion factor)</b>
50-100	$n/6.00$
100-150	$n/1.50$
150-200	$n \times 1.7$
200-250	$n \times 3.5$
250-300	$n \times 6.3$
300-350	$n \times 10.4$
>350	$n \times 15.8$

C. Project of Islet Laboratory



Legend: PB Pass Box  
C Centrifuge